EMEP Report 1/2003
Date: July 2003

METEOROLOGISK INSTITUTT
Norwegian Meteorological Institute

Transboundary Acidification, Eutrophication and Ground Level Ozone in Europe

PART II

Unified EMEP Model Performance


EMEP/MSC-W: Hilde Fagerli, David Simpson and Svetlana Tsyro

EMEP/CCC: Sverre Solberg and Wenche Aas

Editted by Leonor Tarrasón

EMEP Status Report 2003

ISSN 0806-4520

Contents

Executive Summary

This report presents the performance of the Unified EMEP Eulerian model for 9 different years (1980, 1985, 1990, 1995, 1996, 1997, 1998, 1999 and 2000). The performance of the model has been assessed by comparison with observations of air and precipitation data compiled in the EMEP network. The same model version has been used in all simulations and a complete description of the model can be found in EMEP 1/2003 Part I: Unified EMEP model description.

Despite the use of different years, no attempt has been made here to derive trends in air and precipitation concentrations. The analysis identifies instead problem areas in model behaviour and proposed further work to improve the performance of the model. Not all years have been analysed for all compounds, mostly because limitations in the availability of measurement data. This has been particularly the case for ozone, PM and formaldehyde where the analysis of model performance has focused in year 2000.

Variations in the extent and quality from EMEP measurement sites, variability in emission input data and meteorological conditions contribute to the year to year variations in the presented model performance. These variations imply however small changes in the performance of the model, so that the model performance is rather homogenous over the analysed years. The only exception is for sulphur dioxide, where the model bias systematically increases over the 1990s. For all other cases, differences in model performance are more significant across compounds than for the different years. This implies that the conclusions drawn here by compound are representative and provide a realistic overview on the performance of the present version of the Unified EMEP model against observations.

The best performance of the model is for ozone daily maximum concentrations where daily correlation coefficients are generally above 0.8 across Europe. For most years, the modelled and observed frequency distributions agree rather well, although the model shows a tendency to produce narrower distributions, with under-prediction of high ozone values and over-prediction of low ozone. In any case, the average bias for daily ozone maximum concentrations is below 12%. The worse performance of the model in eastern Mediterranean regions may be related to the choice of boundary conditions. For NO_2, results are more mixed, the better results are found in northern and western Europe. In general model performance is satisfactory, with high (0.7) spatial correlations and the averaged

bias of around 17% (in 2000). Formaldehyde is only measured at few selected stations, so results are only indicative but the model manages to reproduce daily concentrations with daily correlations between (0.5-0.7) for most sites and with relative bias below 50%.

For sulphur and nitrogen compounds, the model generally shows high spatial correlation coefficients for all years (0.7 to 0.9) and good daily correlation coefficients (0.5 to 0.7). Daily correlations are higher for components in air than for concentrations in precipitation as it might be expected because of the dependence of wet scavenging in the modelisation of precipitation occurrence.

The relative bias of modelled results against observations varies from compound to compound and it is generally around 30% and below for most sulphur and nitrogen components. Sulphate concentrations in air and precipitation are reproduced by the model very well, with relative bias below 10% and reproducing both the seasonal and spatial variations across Europe in the different years. This is despite the fact that the model has problems reproducing sulphur dioxide levels over the years. For the meteorological and emission regimes prevailing during the 1980s the model reproduces SO_2concentration in air with systematic bias around 5% at the end of the 1990s the model bias systematically increases and reaches up to 40% for year 2000.

The systematic increase in the model overestimation of sulphur dioxide concentrations is probably a result of changes in the relative importance of processes dominating sulphur atmospheric chemistry over the last 20 years. It is interesting that the model oxidant capacity of the atmosphere has increased in the 1990s as a consequence of the pronounced decrease of sulphur emissions in Europe. This has implied changes in the chemical and removal processes for sulphur that the model manages to catch but only to a limited extent. For instance, the ratio between $NH_3$and SO_2in air has changed so that the inclusion of co-deposition processes has become increasingly more important for a correct description of the concentrations in air of sulphur dioxide. Still, the model continues to overestimate SO_2in air, probably because we are still missing important processes like e.g. the dependence on pH . Further work in this area is foreseen.

For nitrogen compounds, the models performance is again satisfactory at most European sites, although there are identified short comes in the model, in particular concerning nitrate. For the yearly average, the model generally overestimates nitrate in air (average 35% bias) and underestimates nitrate in precipitation (average - 22% bias). However, the performance of the model is significantly better in the summer season because the overestimation of air concentrations occurs mainly during winter. There seem to be a bias in the equilibrium equations in the model that tends to produce too little nitric acid at low temperatures. This affects particularly the production of nitrate and ammonium aerosols which are both overestimated in winter. In addition to the revision of the equilibrium equations at low temperatures, there are indications for the need of a revision of the wet scavenging coefficients.

The overestimation of ammonium in winter is related to the overestimation of nitrate (27% bias, 22% in precipitation). However, the sum of ammonium and ammonia in air are generally better reproduced by the model (8% bias), also because filter pack measurements are more reliable for the sum of $NH_3$and NH_4^+. The seasonal variation of ammonium and ammonia in air varies across Europe, also as a consequence of the seasonal cycle of ammonia emissions. The model seems to perform better in western Europe than in other European areas. In Nordic countries, for instance, the model doesn't manage to capture the peak concentrations in spring and summer. This seasonal behaviour is probably related to maximum ammonia emissions in connection with agricultural practices. The seasonal variations in agricultural emissions are at present very similarly modelled over Europe and further work should be addressed to improve the description of these sources in order to catch the seasonal variations of ammonia and ammonium concentrations.

For particulate matter PM_{10}, the model shows the lowest correlations (0.4-0.5) and general underestimation by 40-50%. This is not surprising as the Unified model is still missing some important sources like sea salt, wind blown dust, resuspension and secondary organic aerosols and basic information on the chemical composition of the primary aerosol emissions is still not available. Since PM_{10} is the sum of very different contributions, the analysis of model performance for particulate matter requires the study of the individual chemical speciation.

PM_{10} underestimation is larger in summer than in winter time, mostly because the model overestimates concentrations of nitrate and ammonium in winter. It has been shown that the introduction of sea salt improves the model performance during winter, when sea salt production is at its maximum. It is also expected that the introduction of wind blown sources will improve the model description of PM during summer and improve the model underestimate of mineral dust component. Comparison with phenomenological measurement data shows also that the model underestimates organic carbon concentrations and black carbon. This is probably related to assumption used for the chemical composition of primary emissions in the model and also to the lacking contribution of secondary organic aerosol which can be considerable in urban areas. The model validation is however hampered by lack of chemical speciation data in different European areas and given the complexity of the aerosol composition is difficult to extrapolate these results over other European regions.

For all components, the analysis of model performance across Europe is dependent on the availability, geographical coverage and quality of the measurement data. No effort has been made to qualify model performance depending on the distribution and quality of the measurement sites. Under these conditions, model performance is comparable in northern, western and eastern Europe. The performance of the model in Mediterranean areas is systematically worse than in any other European area. To a large degree this is due to the lack of measurement stations in the area and the poor quality of monitored air concentration data

compiled in the area. However, this argument is not valid for measured concentrations in precipitation, where the quality of measurements is more stable. The model systematic underestimation of concentration in precipitation in Mediterranean stations may indicate the need to review the description of convective processes in the model.

On the basis of this study, we qualify the performance of the Unified EMEP model as satisfactory and the model is to our view fit for its purpose of evaluating regional transport of photo-oxidants and particles across Europe.

Acknowledgements

The validation work presented here is dependent on the availability of good quality monitoring data and therefore relies on the contribution and effort from the Parties to the Convention on Long-Range Transboundary Air Pollution that support the EMEP network. Thanks are also due to our colleagues at NILU/CCC, Anne-Gunn Hjellbrekke and Michael Kahnert that provided us with measurement data from the EMEP and the AIRBASE networks. HC Hansson and Peter Tunved from the University of Stockholm have been most inspiring in our discussions on aerosol characterisation and are specially thanked for sharing their monitoring Swedish aerosol data for this work. The Austrian Academy of Science is also thanked for the AUPHEP project meausurement data, that was kindly forwarded to us by our colleague at IIASA, Chris Heyes.

Thanks are due to Dave Fowler, Ron Smith, Mark Sutton and colleagues from CEH, Edinburgh, for valuable and stimulating discussions which have improved the EMEP model's deposition routines over the last year. Thanks are also due to Lisa Emberson, Steve Cinderby (SEI, York), Mike Ashmore (Univ. Bradford) and Juha-Pekka Tuovinen (FMI, Helsinki) for continued help and advice on the ozone deposition modelling.

We would like to thank Sonja Vidic (MHSC in Zagreb) for providing information on effective stack heights. Vigdis Vestreng and Anna Benedictow at met.no are thanked for providing emissions and meteorological data-bases which make the modelling work possible.

We would like to thank our colleagues within the NMR Aerosol project for inspiring cooperation and constructive discussions on aerosol characterisation and modelling. In particular, we appreciate close cooperation with Markku Kulmula and Liisa Pirjola from the University of Helsinki, resulting in developing the aerosol dynamics module MM32. We are grateful to Swen Metzger (Max Planck Institute for Chemistry) for providing the gas/aerosol equilibrium model EQSAM.

Last, not least, we would like to thank our colleague Heiko Klein for the development of flexible and most useful validation programs to facilitate the visuslisation and interpretation of our results.

The work documented here has been partly funded by the EU projects CARBOSOL and MERLIN and the NMR project on the long-range transport of particulate matter.

Chapter 1

Model Performance for Sulphur and Nitrogen Compounds for the period 1980 to 2000

Hilde Fagerli, David Simpson and Wenche Aas

In this chapter we present model results for acidifying and euthrophying pollutants in Europe for the period 1980 to 2000 using the Unified EMEP Eulerian model, with full photo-oxidant chemistry (rv1.7, see (Simpson et al.(2003))). Model calculations for 9 years (1980, 1985, 1990, 1995, 1996, 1997, 1998, 1999, 2000) are analysed and compared with monitored air and precipitation data. The performance of the Unified EMEP model in different geographical parts of Europe is evaluated. Both photo oxidants and acidifying and euthrophying compounds are calculated in the model runs discussed here, but a separate chapter is devoted to the discussion of the results for the photo chemical pollutants.

1.1 Introduction

In order to obtain data that are characteristic for long-range transport, measurements in the EMEP network are collected at background stations that is representative of a larger area. The size of this area is determined by the variability of the air and precipitation quality and the desired spatial resolution in the concentrations and deposition fields. For the particular purpose of the model validation, measurements should also be representative of the EMEP 50×50 km^2 grid square average. However, the recommendation for the site not to be influenced by local pollution implies that their location is chosen to ensure representativeness of the minimum concentration in the grid, not the grid average. It should also be noted that the EMEP monitoring network is not homogeneous, neither with respect to quality of sampling methods or laboratory analyses, background representativeness or geographical coverage. Conclusions drawn from comparison of modelled

and measured values based on a limited number of stations are then direct consequences of the distribution and quality of these measurement sites. For later years, a greater number of measurement sites and in general a better data quality makes the EMEP network more suitable for analysis of model performance.

The agreement between model predicted and observed air and precipitation data also depend upon an adequate description of emissions. This includes both a reasonable estimates of national totals, gridded (source sector) data and temporal distribution of emissions.

Emissions reported by the Parties for the 1990s have both a better completeness with respect to time-series and to sources included in the emissions relative to the 1980s (V. Vestreng and H. Klein(2002))For instance, very few countries have reported data at all for ammonia emissions prior to 1990. In addition, quality control efforts both from the countries and from MSC-W have continually increased. We therefore believe that emission inventories for recent years are more reliable.

From the reasoning above it is clear that the agreement between model results and observations depend on a combination of several elements; the quality and representativeness of the measurement sites, the adequacy of emissions and the model performance. Therefore, the following discussion on model *underestimation* and *overestimation* simply imply that the calculated values are lower or higher than the observations and does not refer to model deficiency only.

1.2 Methodology of the Analysis

Data from all monitoring EMEP stations have been used in the analysis of model results. For information on the EMEP monitoring data, we refer to the EMEP web page, www.emep.int. We are aware that some of the sites have been classified by CCC as less reliable and that e.g. change in sampling techniques and chemical analysis methods employed at the stations during the period of interest may influence the analysis of the performance of the model over time. However, at the time when these analysis were carried out, no consistent system for quality labelling of the data for all years were available. CCC has now presented a new data quality flagging system for the EMEP data, and work is underway to implement this in our model verification system.

The analysis is based on the following material;

Scatter-plots and corresponding tables

Scatter-plots are based on yearly averages for stations that have at least 75% data coverage for each year for components in air, and at least 25% data coverage for each year for components in precipitation (for days with modelled precipitation). This was done to ensure that only stations with some continuity in their mea-

surements were taken into account. Besides this, no criteria have been imposed on the data. The lines on the scatter-plots display deviations in the scatter of 30% ('30% line') and 50% ('50% line') relative bias, respectively. Relative bias is defined here as

$$\text{Relative bias} = \frac{M-O}{M+O} \times 100\%$$

where M and O are yearly averaged modelled and measured concentrations.

The tables show number of stations where measurements were available and data coverage criteria was satisfied (Ns), percent of the data points (station yearly averages) that were within 50% relative bias(pc<50%), percent within 30% relative bias (pc<30%), measured yearly average over all stations (Obs), modelled yearly average over all stations (Mod), Bias ($\frac{Model-Observation}{Observation} \times 100\%$), correlation between observation and model for station yearly averages (Corr), number of stations where measurements were available and data coverage criteria was not imposed (Ns(d)) and daily correlation between all daily data for all stations for the actual year (Corr(d)). Note that in the following sections we use the terms 'Relative Bias' and 'Bias' as defined above.

Monthly time-series

Monthly time-series of model predicted versus observed data are valuable for assessing how well observed seasonal trends are captured by the model. In addition, long-term monthly time-series may help to interpret nonlinearities in e.g decrease of summer relative to winter concentrations. We have divided the measurements into groups depending on the geographic locations for the sites and plotted time-series for averages of these groups. In this way, we average out single site peculiarities and get an idea of the 'bulk performance'. However, when few measurements are available for some regions one should be very careful with drawing conclusions.

In general, we present two sets of monthly time-series; 1) time-series where all data are required to fulfil the data coverage criteria for *all* the years of interest and 2) time-series where data are required to fulfil the data coverage criteria for each year, but not necessarily all the years in the time-series. Obviously, it is an advantage to use only data from stations that cover the whole period under study. However, this would leave us with very little data to analyse. Therefore, we have presented time-series of type 1) as far as possible, and in addition, or when nothing else was possible, time-series of type 2).

Maps of relative bias and correlations

In order to visualise the geographic distribution of differences between values predicted by the Unified EMEP model and data measured in the EMEP network,

Table 1.1: Results for SO_2 in air (μg(S) m^{-3}) for 9 years from 1980-2000. Ns; the number of stations where measurements were available for at least 75% of the days in a year , $pc < 50\%$; the percent of the data points (station yearly averages) with relative bias less than 50%, $pc < 30\%$; the percent with relative bias less than 30%. Obs; the measured yearly average over Ns stations, Mod; the modelled yearly average over Ns stations, $Bias$; the bias ($\frac{Model-Observation}{Observation} \times 100\%$), $Corr$; the correlation between observation and model for station yearly averages, $Ns(d)$; the number of stations where measurements were available for at least one day and $Corr(d)$; the daily correlation between all daily data for all stations for the actual year.

Period	Ns	pc<30%	pc<50%	Obs	Mod	Bias	Corr	Ns(d)	Corr(d)
1980	44	82	98	5.46	5.70	4	0.84	52	0.61
1985	51	67	90	6.04	5.48	-8	0.76	65	0.56
1990	60	58	83	2.82	3.03	7	0.42	70	0.36
1995	77	66	87	1.42	1.75	24	0.60	86	0.46
1996	77	84	92	1.53	1.77	16	0.81	87	0.46
1997	76	75	93	1.15	1.50	30	0.80	84	0.57
1998	75	72	95	1.01	1.24	23	0.71	83	0.53
1999	80	73	94	0.84	1.04	25	0.81	90	0.53
2000	81	59	89	0.72	1.00	39	0.73	90	0.47

we present so-called dot-maps. We have chosen to present these for 1997, which represent a 'typical' year with respect to model performance. The dot-maps display relative biases and temporal correlation coefficient for each EMEP site. The relative bias is calculated in the same way as defined above.

In addition to the interpretation tools mentioned above, we also present frequency analysis and daily time-series when we find this valuable for the evaluation of the results.

1.3 Sulphur Dioxide in Air

In figure 1.1 and 1.2 scatter-plots for observed versus modelled SO_2 concentrations in air for the years 1980, 1985, 1990 and 1995 to 2000 are presented. Table 1.1 show relevant statistics for the same years.

In general, the correlation between the yearly averaged observed and modelled data at EMEP stations is high, showing that the model captures reasonably well the spatial distribution of the high and low concentration areas – though this is mainly a reflection of emissions distribution. The results for 1990 show a somewhat worse spatial correlation between the monitored data and model results, but an inspection of the scatter plot for 1990 in figure 1.1 (c) reveals that this is due to an overestimation of the SO_2 concentrations for German stations

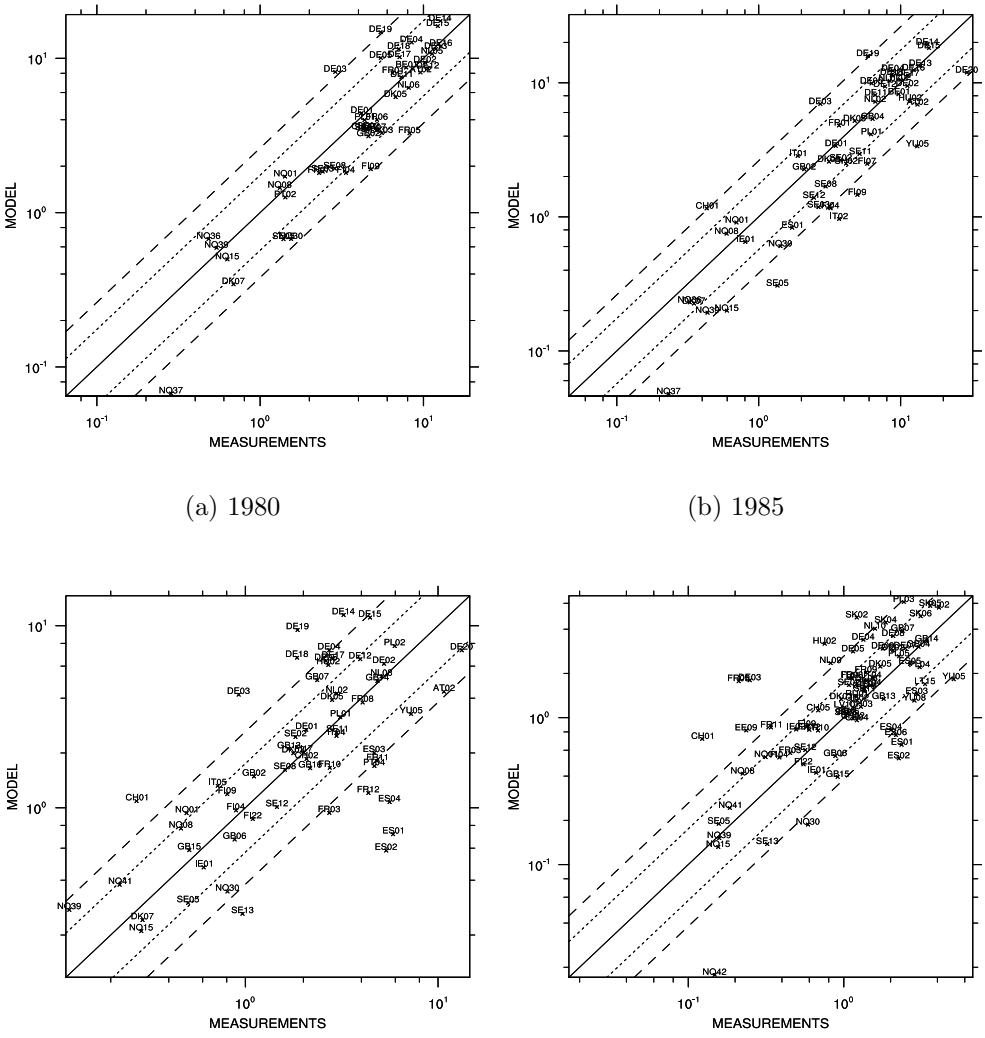

(a) 1980

(b) 1985

(c) 1990

(d) 1995

Figure 1.1: Scatter-plots of modelled versus observed SO_2 concentrations (μg(S) m^{-3}), 1980, 1985, 1990, 1995. Note that no quality criteria have been applied to determine which measurements to include in the comparison.

and an underestimation for Spanish sites.

Both German and Spanish SO_2 measurement data are however quite uncertain. In Germany they use the TCM absorption technique and it has shown to give systematically too low values both in an EMEP field inter-comparison study (Aas et al.(1999)) and in an internal German evaluation (M. Wallasch, pers. comm.). Germany has suggestion to use a correction factor of 1.46 for all their SO_2 measurements; this will be discussed in more details in this years data quality report (Aas et al.(2003))). The Spanish SO_2 data before 2000 was mea-

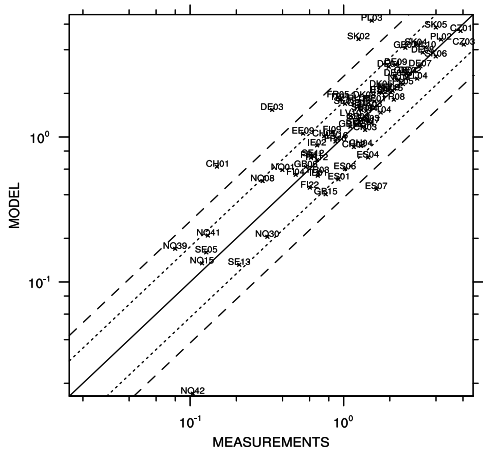

(a) 1996

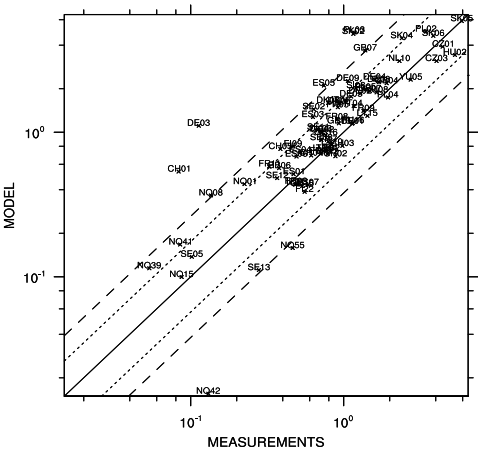

(b) 1997

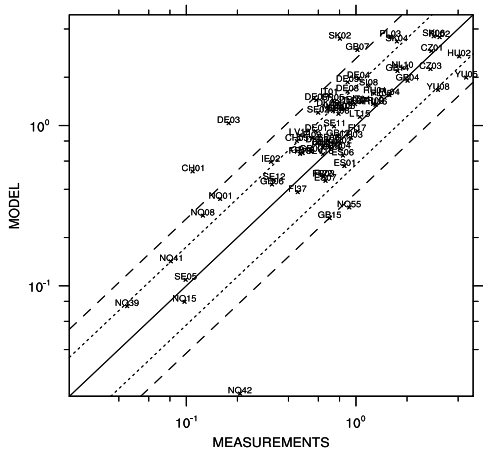

(c) 1998

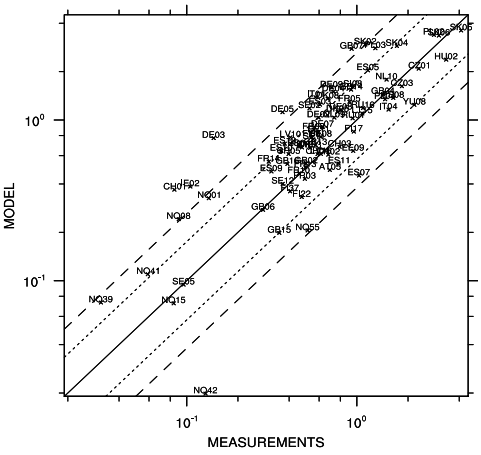

(d) 1999

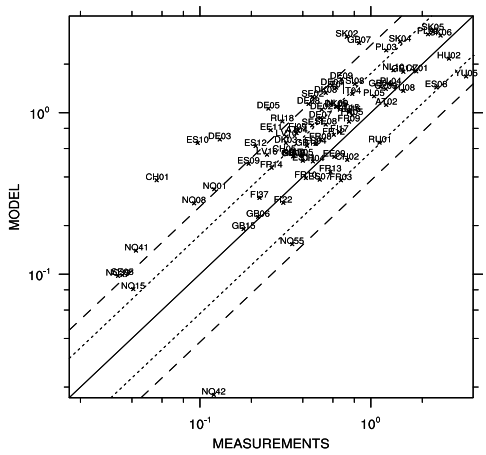

(e) 2000

Figure 1.2: scatter-plots of modelled versus observed SO_2 concentrations (μg(S) m^{-3}), 1996, 1997, 1998, 1999 and 2000. Note that no quality criteria have been applied to determine which measurements to include in the comparison.

sured using H_2O_2 absorption solution. In a field comparison in Zarra (ES12) in 2000 (Aas et al.(2002b)) it was demonstrated that this method function poorly in Spain, it was hardly any correlation with the reference method (NaOH impregnated filters). Much of the data were below the detection limit, but in the addition it showed peak values that did not correlate. For some years the average values may accidentally fall within the expected concentration, but for other years not, obviously the case for 1990. From 2000, Spain has parallel measurements with a UV fluorescence monitor at all their background sites, and these are now regarded as the official Spanish EMEP data; however this method is not either perfect, it was about 15% bias in Zarra (ES12), but this might be different at other sites depending on calibration routines etc.

The daily correlation coefficients for the different years are similar and relatively small (around 0.5). However, it should be kept in mind that the model is designed to capture the long range transport and not the variation at short time scales.

Sulphur dioxide dry deposits relatively fast (especially on wet surfaces), thus the concentrations at the ground largely depend on the modelled atmospheric stability, which is a rather uncertain model parameter. Further, since sulphur dioxide is a primary pollutant, the quality of the model results to a large extent depend on an adequate description of emissions. A large part of SO_2 emissions originates from combustion in energy and transformation industries, with emissions from high stacks. Little detailed information on the height of the emission sources in Europe is available. Moreover, since plume rise is not treated explicitly in our model, we assume effective emission heights.

It is clear that these factors and assumptions necessarily introduce uncertainties in the results (see e.g (Fagerli(2002))).

1.3.1 Model performance in different geographic areas

The majority of observation sites in the EMEP network are located in the north and west of Europe, especially in years prior to 1995. Therefore, it is difficult to study the performance of the EMEP model in the different parts of Europe for the earlier years. In the following we have therefore concentrated on 1995 to 2000.

Altogether 54 stations have measured SO_2 at least 75% of the days each year from 1995 to 2000. These stations have been divided into different groups depending on geographical location: North European stations (13), West European stations (21), East European stations (10) and South European stations (3). Monthly time-series for these groups are presented in figure 1.3 and 1.4.

The seasonal cycle for the SO_2 concentrations is determined by 1) emissions (with a peak in winter), 2) availability of oxidants (minimum in winter) and 3) dry and wet deposition. Both 1) and 2) go in direction of higher winter concentrations. However, wet deposition is in general larger in the cold (and wet) season and

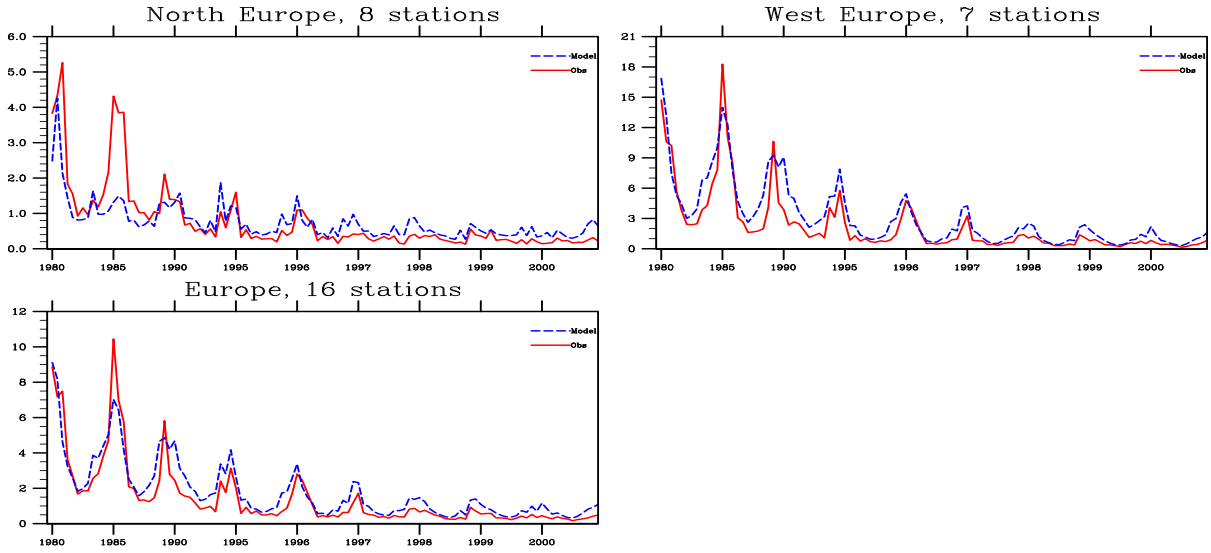

Figure 1.3: Modelled versus observed time-series (monthly) for SO_2 in air (μg(S) m^{-3}) for collections of stations that have measured SO_2 continuously from 1980 to 2000.

SO_2 is efficiently dry deposited on wet surfaces. In contrast, higher atmospheric stability in the cold season direct to lower dry deposition. In total, the overall seasonal cycle show a peak in winter time and a summer minimum. The modelled seasonal cycle for the SO_2 concentrations is well captured by the model in North, South and West Europe. For the group of South European stations, consisting of ES04, IT01 and IT04, it is difficult to evaluate the model performance. At the Spanish site Logrono (ES04) most of the SO_2 measurement data before 1999 are below the detection limit and can thereby only be considered as an estimate of the upper concentration limit. In addition, this site is influenced by local sources being situated close to a dense traffic road and it is only 1 km from a Logrono town with 130 thousand inhabitants. For Montelibretti (IT01) the data capture up to 1995 is rather low and data from 1990 to 1993 are lacking.

In general, the magnitude of the modelled summer concentrations agree very well with the observations, whereas winter concentrations are overestimated everywhere.

The dot-maps of the relative bias and the correlation coefficients in figure 1.5 show that for most stations, the EMEP model predict concentrations higher than measurements. The greatest overestimations are seen on high mountain sites as e.g. CH1 and CH5 in Czech Republic, DE3 in Germany and CZ2 and CZ4 in Switzerland. For a long-term run, these site will often be above the boundary layer (especially in the winter). With the coarse topography in the regional scale model, this cannot be well captured by the model. The correlation between measurements and modelled values are highest in west and east Europe

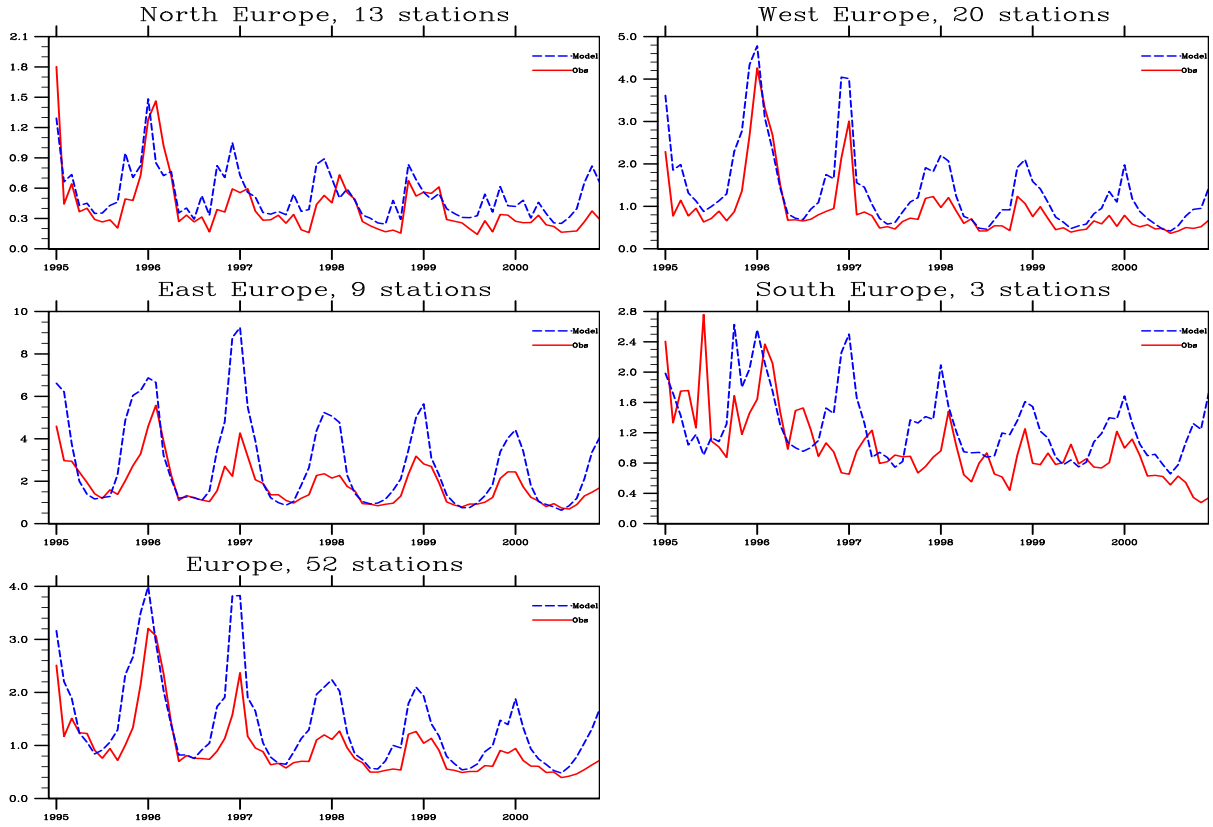

Figure 1.4: Modelled versus observed time-series (monthly) for SO_2 in air (μg(S) m^{-3}) for collections of stations that have measured SO_2 continuously from 1995 to 2000.

(often 0.6-0.8) (except Switzerland, probably due to the mountain influence and stations located at high elevations) and lowest in southern Europe and north in Scandinavia (<0.2). For the South European region the deviations can to some extent be explained by problems with the data quality at some of these sites. In the northernmost part of Europe, concentrations are very low and often below the detection limit. Fluctuations in very low values are difficult to capture both for the model and the measurements.

1.3.2 Performance of the model over different years

Table 1.1 presents the bias of the model results with respect to the observations for the years 1980-2000. In 1980 and 1985 the bias is small and the model tends to underestimate the low SO_2 concentrations. From 1990 and onwards, the model increasingly over-predicts concentrations.

In order to avoid bias in these results caused by differences in the stations that are included for the different years, we extracted a set of stations with

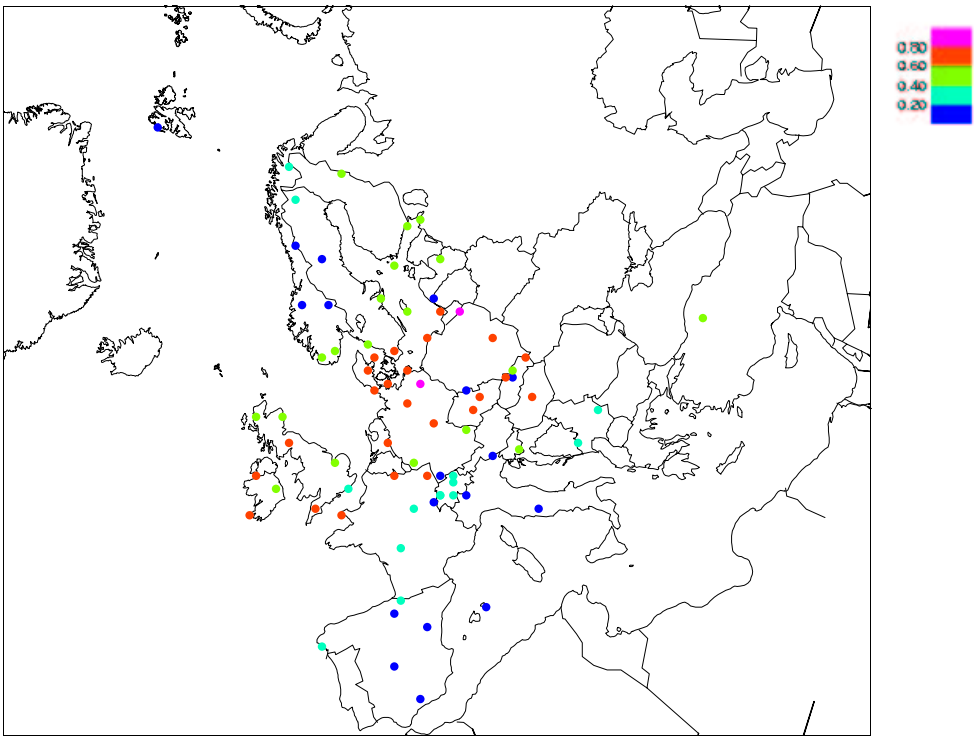

(a) Correlation

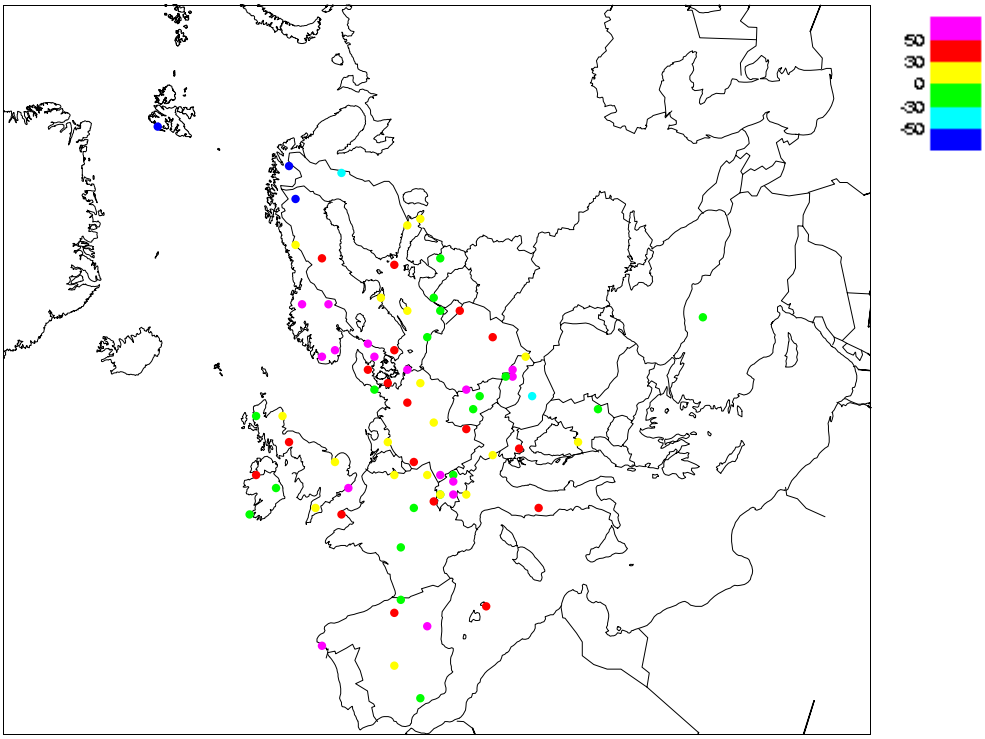

(b) Relative Bias

Figure 1.5: Correlation coefficient and relative bias in concentration of SO_2 in air, 1997.

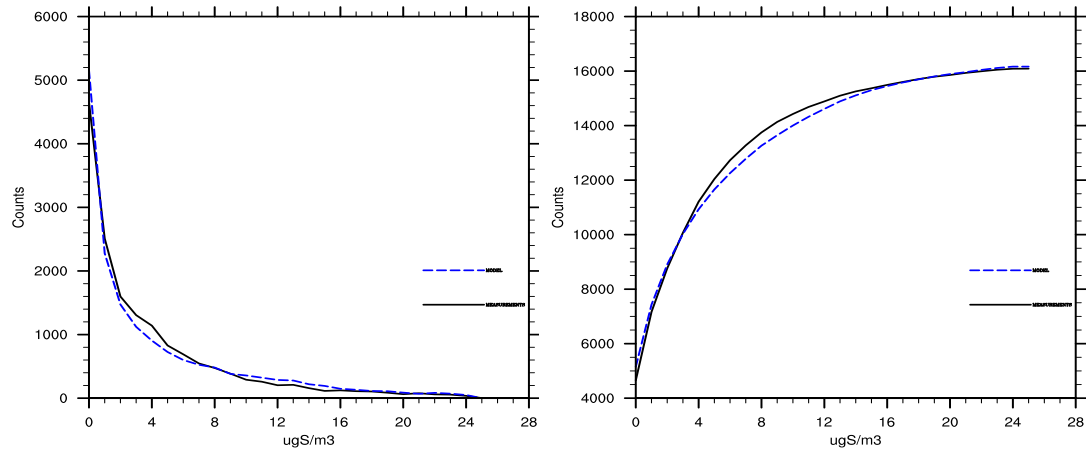

(a) 1980

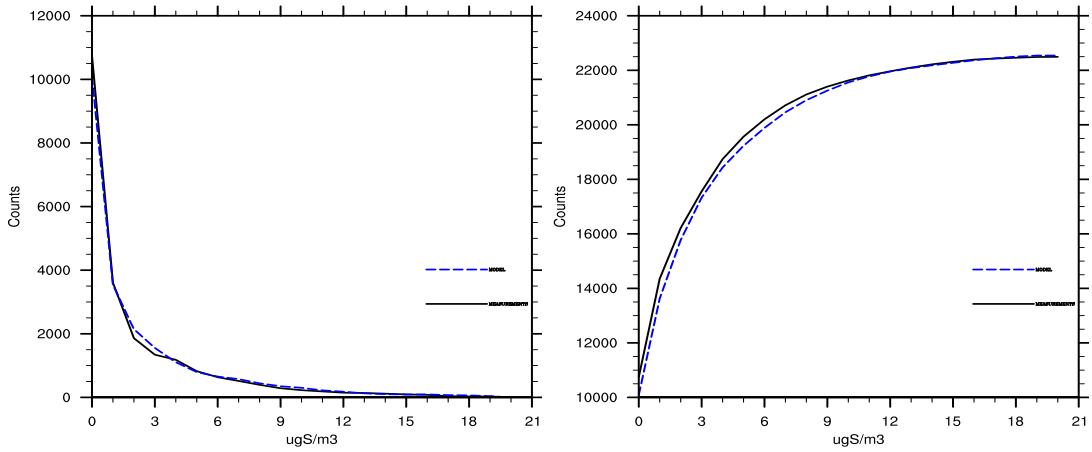

(b) 1990

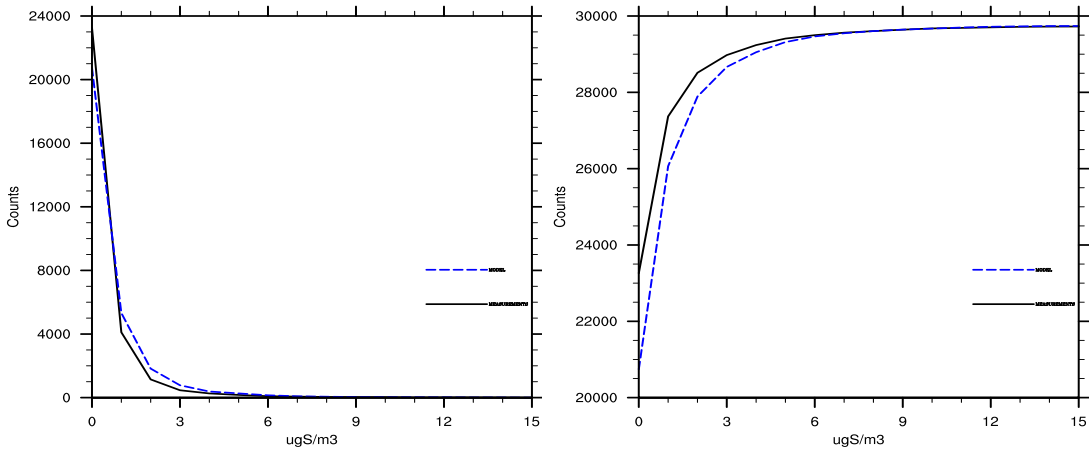

(c) 2000

Figure 1.6: Frequency analysis of Modelled (dotted line) versus Observed (full line) daily SO_2 concentrations (μg(S) m^{-3}), 1980, 1990, 2000. Note that no quality criteria have been applied to determine which measurements to include in the comparison.

measurements for the whole period.

Only 16 stations have measured SO_2 continuously since 1980. Of these, 7 are in western Europe (DE05, DK03, DE03, DE04, CH02, DK05, DE02) and 9 in Scandinavia (SE05, NO15, SE08, NO39, NO08, SE02, FI09, NO01). Even though there were several sites in the east and south of Europe in operation in 1980, many of them have either been closed down or have not been in operation continuously with an annual data capture above 75% . Since the emission regimes and climate are different in the different parts of Europe, conclusions draw for North and West Europe may not apply for the other areas.

In figure 1.3 time-series of monthly averaged data for West Europe, North Europe and the collection of all the 16 stations are presented. The figures for this long-term dataset confirm that the bias of the model versus measurements increases with time.

In the following subsections we discuss possible explanations. In order not to confuse the reader, we would like to point out that some of the processes described below (e.g oxidant limitations and co-deposition of ammonia and sulphur dioxide) have already been parametrised and implemented in the current model (revision 1.7) and thus cannot explain the remaining bias. However, uncertainty still remains as to the relative importance of these various processes.

Changes in the oxidising capacity of the atmosphere

The bulk production of SO_4^{2-} results from the oxidation of SO_2 to sulphuric acid in liquid clouds, primarily by H_2O_2 and O_3. Of these two, H_2O_2 is by far the most important oxidant. As a first approximation, the production of sulphate will be limited by the lesser of the quantities; SO_2 or H_2O_2. In the early 1980's, with SO_2 peak emissions, oxidant limitations were important, especially in the winter. At present, lower SO_2 concentrations generally lead to higher oxidation rates and thereby a relatively greater conversion of SO_2 to SO_4^{2-}. In the photo-oxidant version of the EMEP model used here (revision 1.7), the sulphur chemistry and the photo chemistry are coupled. In order to investigate how important the changes in oxidant capacity are for the model results, we have performed two sets of calculations. The first set of calculations is performed with the 'base-case' version (revision 1.7) where H_2O_2 is consumed in the reaction with SO_2. In the second 'test-case' set, H_2O_2 enters into the aqueous reaction with SO_2, but the reaction is not included as a loss reaction for H_2O_2. Thus, the availability of H_2O_2 does not depend on the amount that has already been consumed by SO_2. The difference between these two sets indicates how important the oxidant limitations (in this case only H_2O_2) is for the model predicted SO_2 and sulphate concentrations.

In figure 1.7 we present monthly time-series (average over all stations with data for the three years) for 1980, 1990 and 2000 for SO_2 and sulphate. The figures show that the model predicted SO_2 and SO_4^{2-} concentrations compare better with

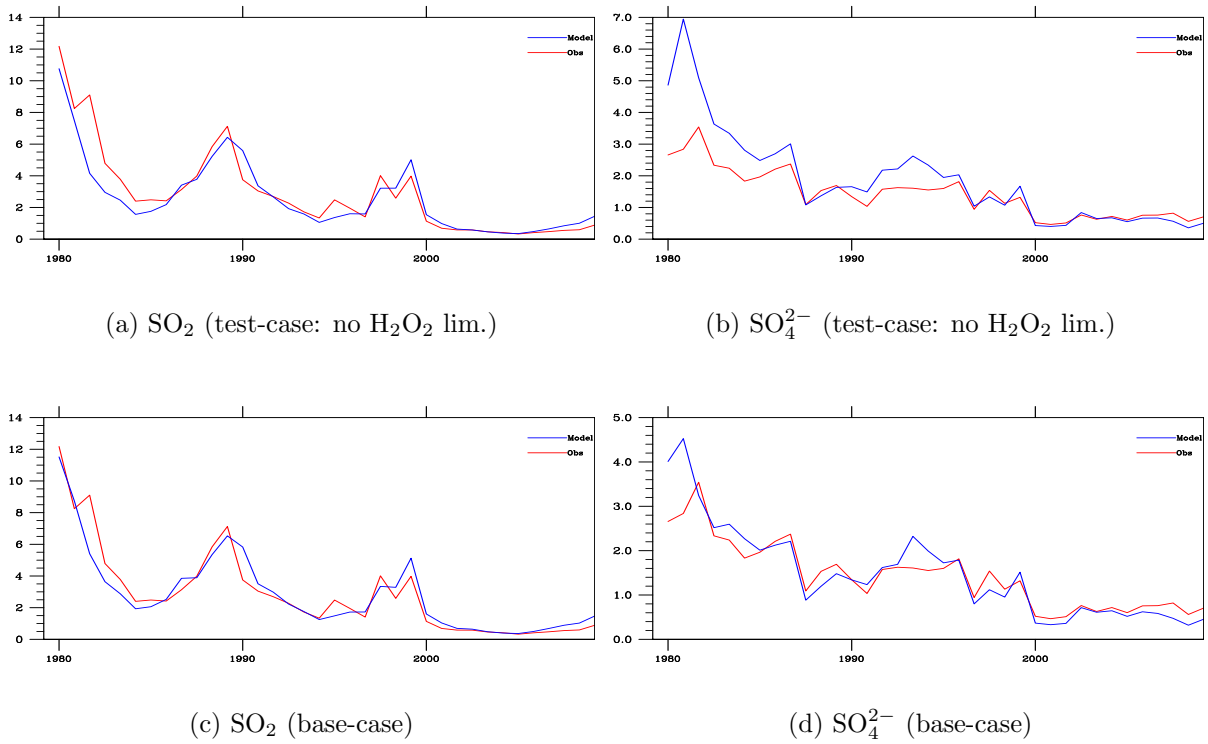

(a) SO_2 (test-case: no H_2O_2 lim.)

(b) SO_4^{2-} (test-case: no H_2O_2 lim.)

(c) SO_2 (base-case)

(d) SO_4^{2-} (base-case)

Figure 1.7: Monthly time-series for the average of all EMEP stations (1980,1990,2000) concentrations of SO_2 in air (μg(S) m^{-3}) and concentrations of SO_4^{2-} in air (μg(S) m^{-3}) . Model runs with (base-case) and without (test-case: no H_2O_2 lim.) loss reaction of H_2O_2 due to oxidation of SO_2.

observations in our base-case model where the H_2O_2 loss reaction due to oxidation of SO_2 is taken into account. Further, it indicates that oxidant limitations were far more important in 1980 than in 2000. These limited tests indicate that in order to predict changes over time for sulphur dioxide and sulphate concentrations, the coupling of sulphur and the oxidant chemistry has to be included in the chemical scheme.

The large decrease in sulphur emissions during the last twenty years has also lead to changes in the pH in the cloud liquid water. The oxidation rate for the $SO_2 + O_3$ aqueous reaction grows with increasing pH, and this pathway therefore becomes increasingly important. In the current model version, pH is assumed to have the same value for all the years (pH 4.5). Thus, we do not take into account changes in the SO_2+O_3 oxidation rate.

As will be shown in section 1.4, the nonlinearities in the sulphate concentrations are very well simulated by the model. If the increase in SO_2 to SO_4^{2-} oxidation rate was too low, a corresponding underestimation of sulphate increasing with time is expected. Thus, there are no strong indications that the increasing

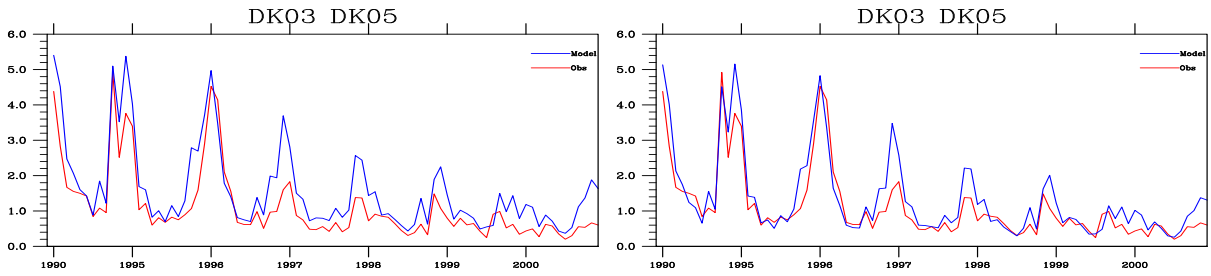

(a) test-case: without co-deposition

(b) base-case: with co-deposition

Figure 1.8: Monthly time-series for the average of two Danish stations (DK03 and DK05) concentrations of SO_2 in air (μg(S) m^{-3}). Model runs with and without parametrisation of co-deposition effects in the SO_2 dry deposition.

discrepancy between model and measurements for SO_2 concentrations is caused by deficiency in the model's ability to simulate changes in the oxidation rate of H_2O_2 plus SO_2, at least in the limited tests conducted here. However, further work is needed to understand e.g. the consequences of the increase of pH in clouds.

Co-deposition of NH_3 and SO_2

It has been discussed for some time that dry deposition of SO_2 increases in the presence of NH_3 gas and vice versa (e.g. (Fowler et al.(2001))). This so-called co-deposition effect has been parametrised in the Unified EMEP model (Simpson et al.(2003),) based on measurements from the LIFE sites and discussion with the Centre for Ecology and Hydrology, Edinburgh (Smith et al.(2003),), and depending on the relative SO_2 to NH_3 concentrations at the surface. We have performed two sets of calculations using the so-called 'acid' version of the Unified EMEP model: 'base-case' – using the parametrisation of co-deposition as it is in the current model; and 'test-case' – no parametrisation for co-deposition. (The acid version has identical chemistry for SO_2 and NH_3 to the full photo-oxidant version, but is much faster to run). Figure 1.8 shows monthly time-series for the average of two Danish stations for concentrations of SO_2 in air 1990, 1995-2000 with the base and test case, respectively. It is clear that the trend for SO_2 concentrations agree better with the observed trend for the base-case model runs when the dry deposition is allowed to vary with the relative amount of SO_2/NH_3, even though this does not fully account for the nonlinear decrease in concentrations. Further investigations, both with respect to measurements and parametrisations of the process, are necessary in order to understand the implications for modelling.

From the reasoning in the previous subsections, it is clear that the answer to

Table 1.2: Results for total sulphate in air (μg(S) m^{-3}). Ns; the number of stations where measurements were available for at least 75% of the days in a year , $pc < 50\%$; the percent of the data points (station yearly averages) with relative bias less than 50%, $pc < 30\%$; the percent with relative bias less than 30%. Obs; the measured yearly average over Ns stations, Mod; the modelled yearly average over Ns stations, $Bias$; the bias ($\frac{Model-Observation}{Observation} \times 100\%$), $Corr$; the correlation between observation and model for station yearly averages, $Ns(d)$; the number of stations where measurements were available for at least one day and $Corr(d)$; the daily correlation between all daily data for all stations for the actual year.

Period	Ns	pc<30%	pc<50%	Obs	Mod	Bias	Corr	Ns(d)	Corr(d)
1980	27	96	100	1.70	1.81	6	0.94	38	0.61
1985	34	82	97	1.57	1.52	-3	0.86	47	0.60
1990	47	87	96	1.23	1.19	-3	0.72	57	0.47
1995	67	91	97	0.95	0.94	0	0.79	75	0.53
1996	67	93	99	1.03	1.05	2	0.79	75	0.42
1997	67	93	99	0.83	0.82	0	0.77	74	0.57
1998	67	93	97	0.77	0.72	-5	0.77	73	0.61
1999	68	91	100	0.73	0.65	-10	0.74	76	0.31
2000	70	89	96	0.63	0.60	-4	0.71	78	0.56

why overestimation of SO_2 concentrations in the later years is higher than for previous periods may consist of several factors. In the current model version, we take into account the effect of H_2O_2 limitations due to SO_2 oxidation and co-deposition of SO_2 and NH_3, but over time these effects work in opposite directions and there might be a unbalance between them. In addition to the processes described, changes in wet scavenging due to increasing pH may also be important Further work, both theoretical and experimental, is likely needed. before the relative importance of these various factors are understood.

1.4 Sulphate in Air

scatter-plots for modelled versus measured sulphate concentrations in air for 1980, 1985, 1990 and 1995-2000 are presented in figure 1.9 and 1.10.

In general, the model reproduces the observed concentrations rather well. More than 96% of the annual mean concentrations for the different sites are within a relative bias of 50% for all the years studied, and approximately 90% within relative bias of 30%. The daily correlation between model and measurements is high, the correlation coefficient for North and West European sites is often between 0.6 and 0.8 (see e.g figure 1.11). The data quality of concentrations of SO_4^{2-} in air measurements is in general quite good.

Figure 1.13 present monthly time-series 1995 to 2000 of sulphate in air for

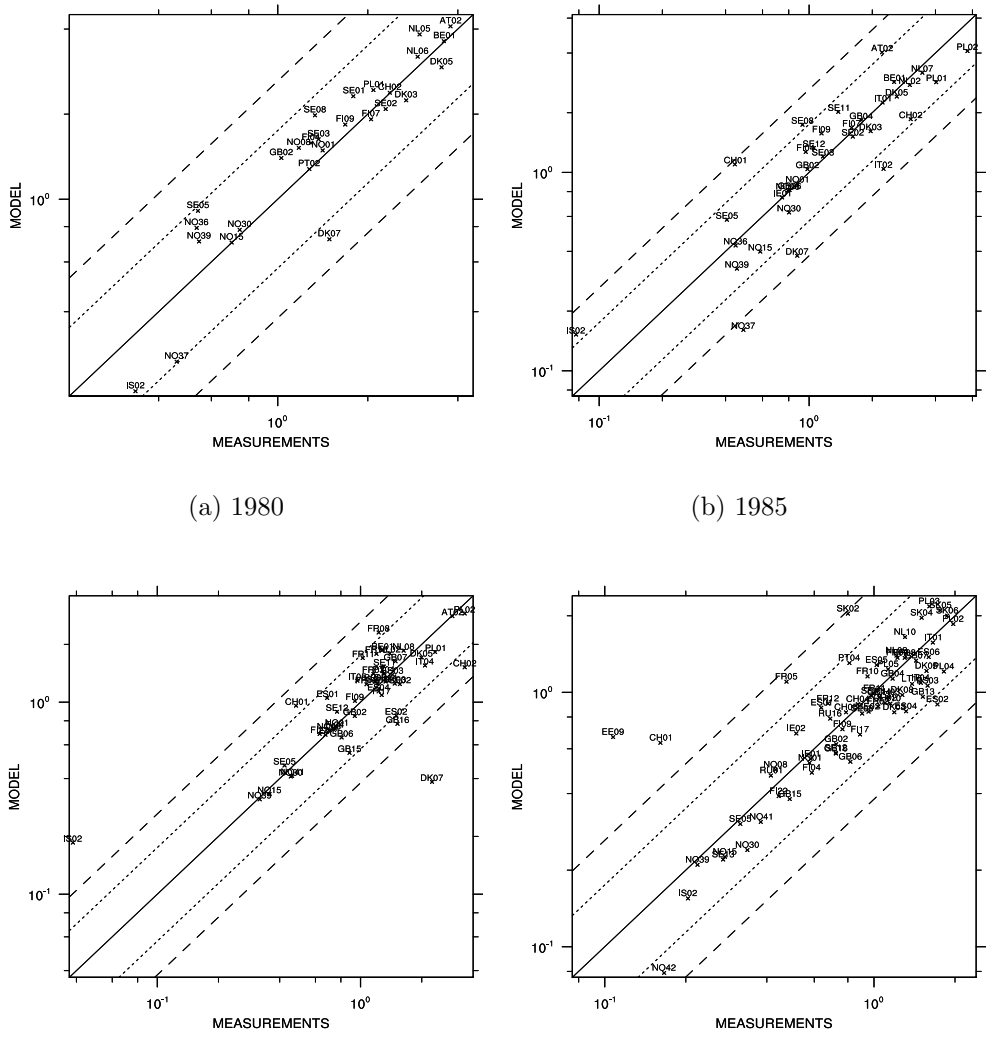

(a) 1980

(b) 1985

(c) 1990

(d) 1995

Figure 1.9: scatter-plots of modelled versus observed sulphate concentrations (μg(S) m^{-3}), 1980, 1985, 1990, 1995. Note that no quality criteria have been applied to determine which measurements to include in the comparison.

clusters of stations in North, West, East and South Europe, respectively. Figure 1.12 present similar plots for the years 1980, 1985, 1990, 1995-2000 for West and North Europe (no East or South European sites measured sulphate continuously from 1980 to 2000).

The best agreement between model and measurements is found in West Europe and North Europe. The model overpredicts concentrations in air for East European stations, especially in winter, whereas the South European sites are somewhat underestimated. At the South European sites, an overestimation of

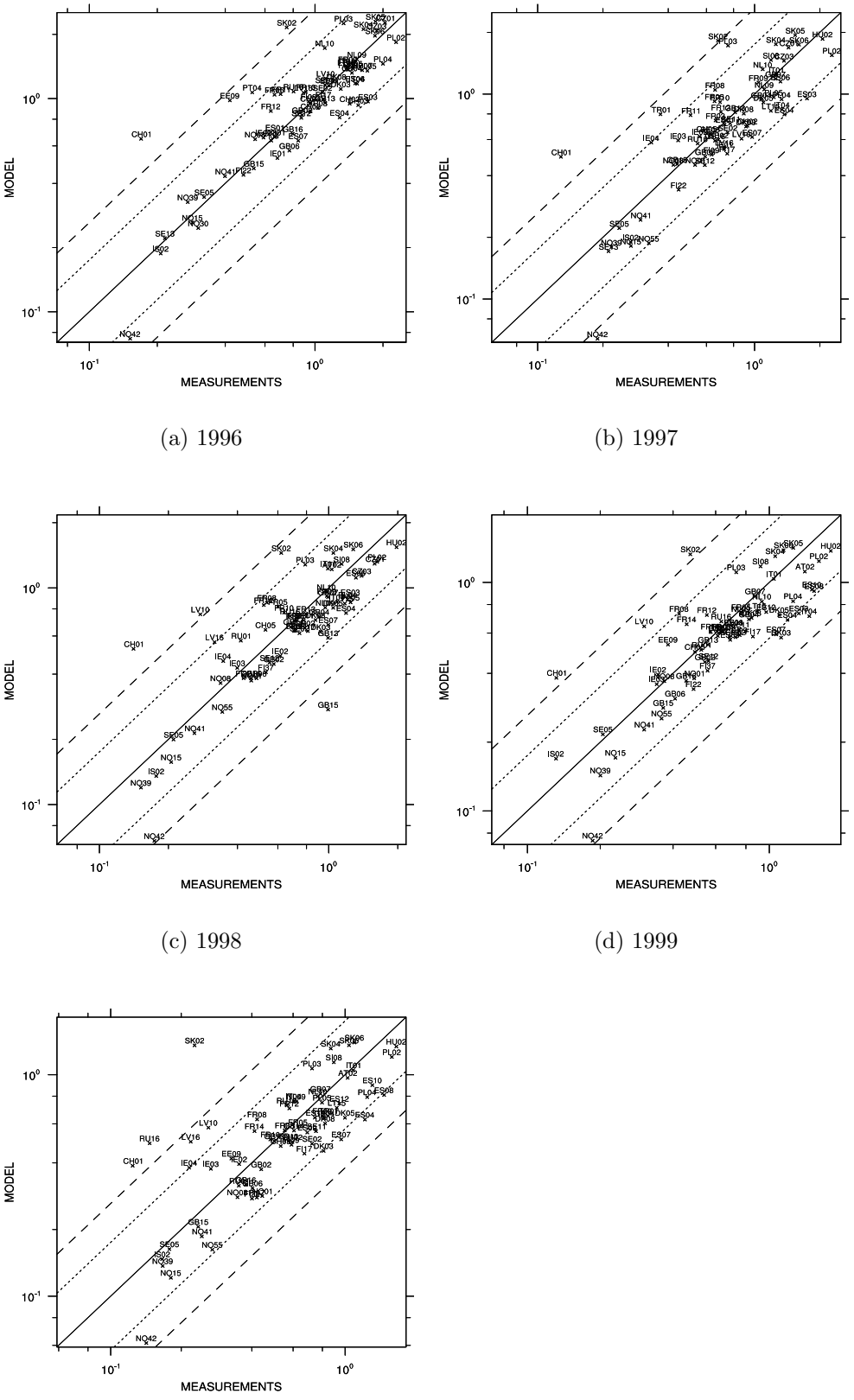

(a) 1996

(b) 1997

(c) 1998

(d) 1999

(e) 2000

Figure 1.10: scatter-plots of modelled versus observed sulphate concentrations (μg(S) m^{-3}), 1996, 1997, 1998, 1999 and 2000. Note that no quality criteria have been applied to determine which measurements to include in the comparison.

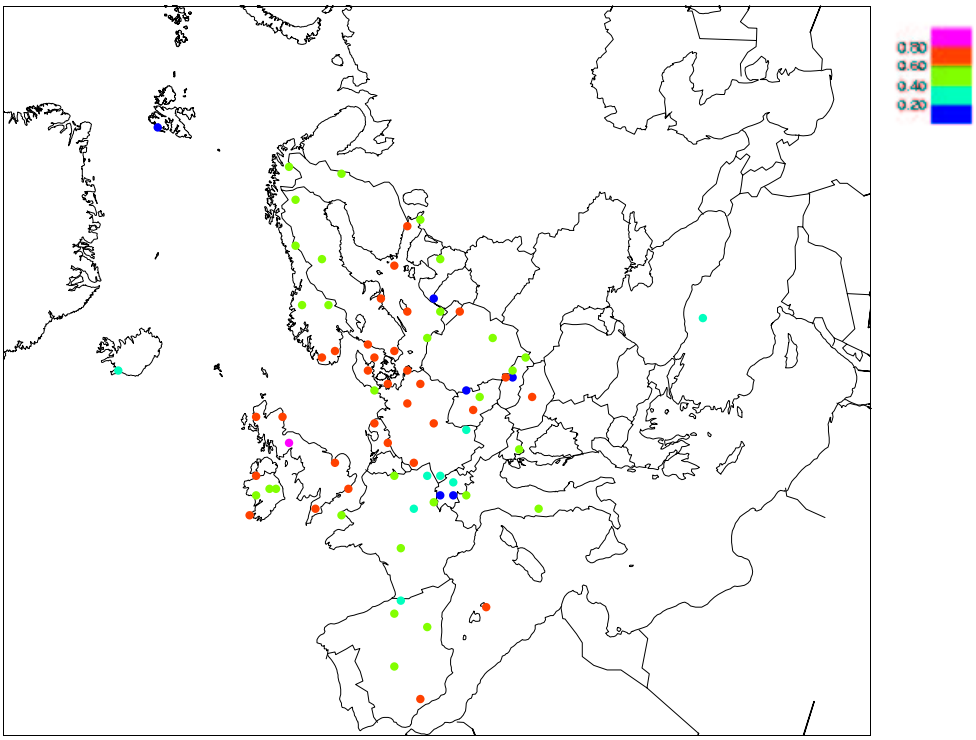

(a) Correlation

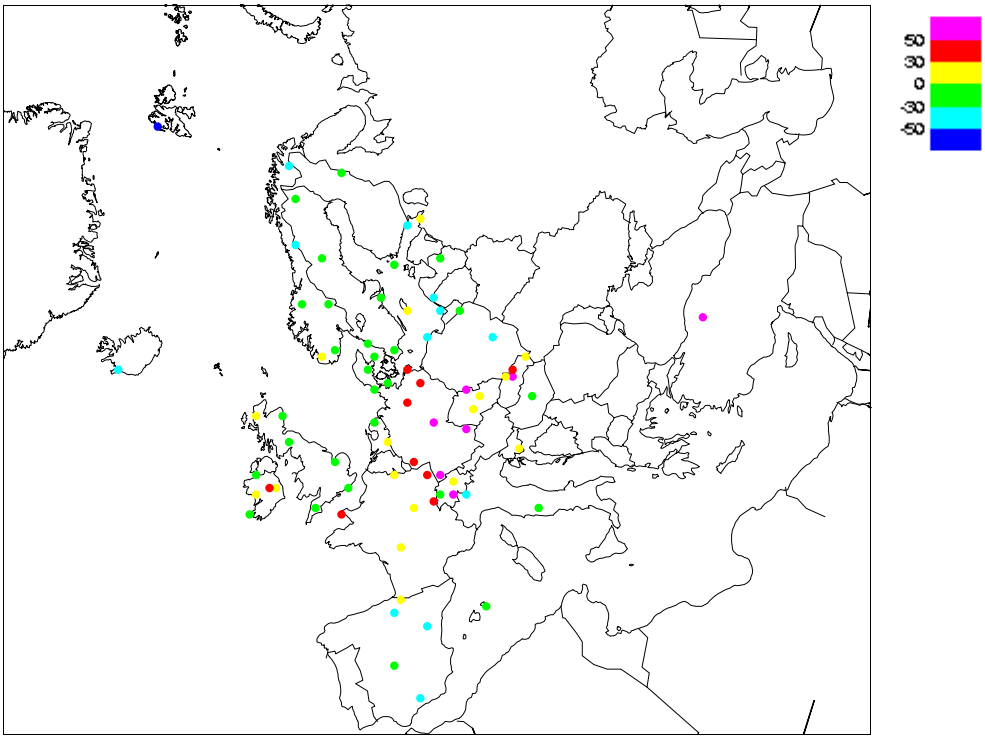

(b) Relative Bias

Figure 1.11: Correlation coefficient and relative bias in concentration of sulphate in air (μg(S) m^{-3}), 1997.

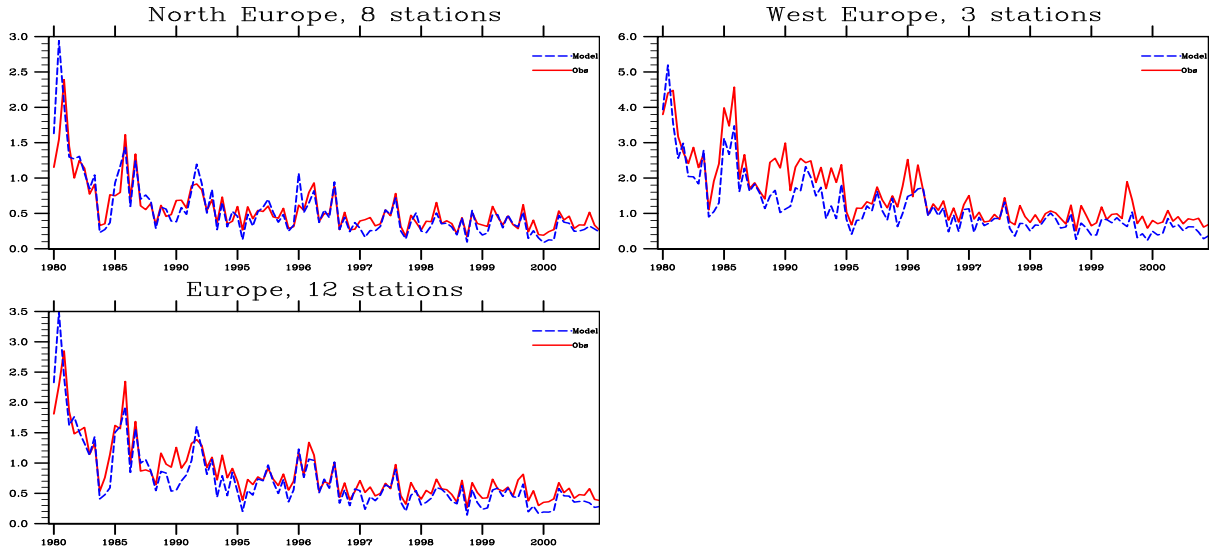

Figure 1.12: Modelled versus observed time-series (monthly) for sulphate in air (μg(S) m^{-3}) for collections of stations that have measured sulphate at least 75% of the days in a year (and every year) for 1980-2000.

SO_2 at corresponding sites indicates too little oxidation of SO_2 to sulphate.

For East Europe, the model tend to either overestimate both SO_2 and sulphate concentrations or underestimate both. The absolute values are dominated by the sites in Slovakia which overestimates both SO_2 and particulate sulphate in air as well as wet deposition of sulphur. However, many of the Slovakian stations are situated at high altitudes, e.g Chopok (SK02) at elevation of 2000m. For a long-term run, this site will often be above the boundary layer (especially in the winter). With the coarse topography in the regional scale model, this cannot be well captured by the model. Consequently, sulphur concentration are overestimated.

The seasonal cycle of sulphate is controlled by 1) the magnitude and seasonal cycle of SO_2 emissions, 2) the oxidant capacity of the atmosphere and 3) dry and wet deposition. In the southern part of Europe, where emissions are relatively high and the photochemical activity largest, sulphate exhibit a clear summer peak and a winter minimum. Despite emissions being highest in winter time, the conversion rate of SO_2 to to sulphate is so much higher in the summer half-year that sulphate concentrations are highest in this season. In the North, where emissions are lower, there is no clear seasonal pattern.

In general, the seasonal cycle seem to have flattened in the period under study (1980-2000); the summer concentrations have decreased much faster than the winter concentrations, probably due to the large decrease of SO_2 emissions leading to oxidant limitations becoming less and less important (see section 1.3).

It is reassuring that the model capture very well both the difference in the

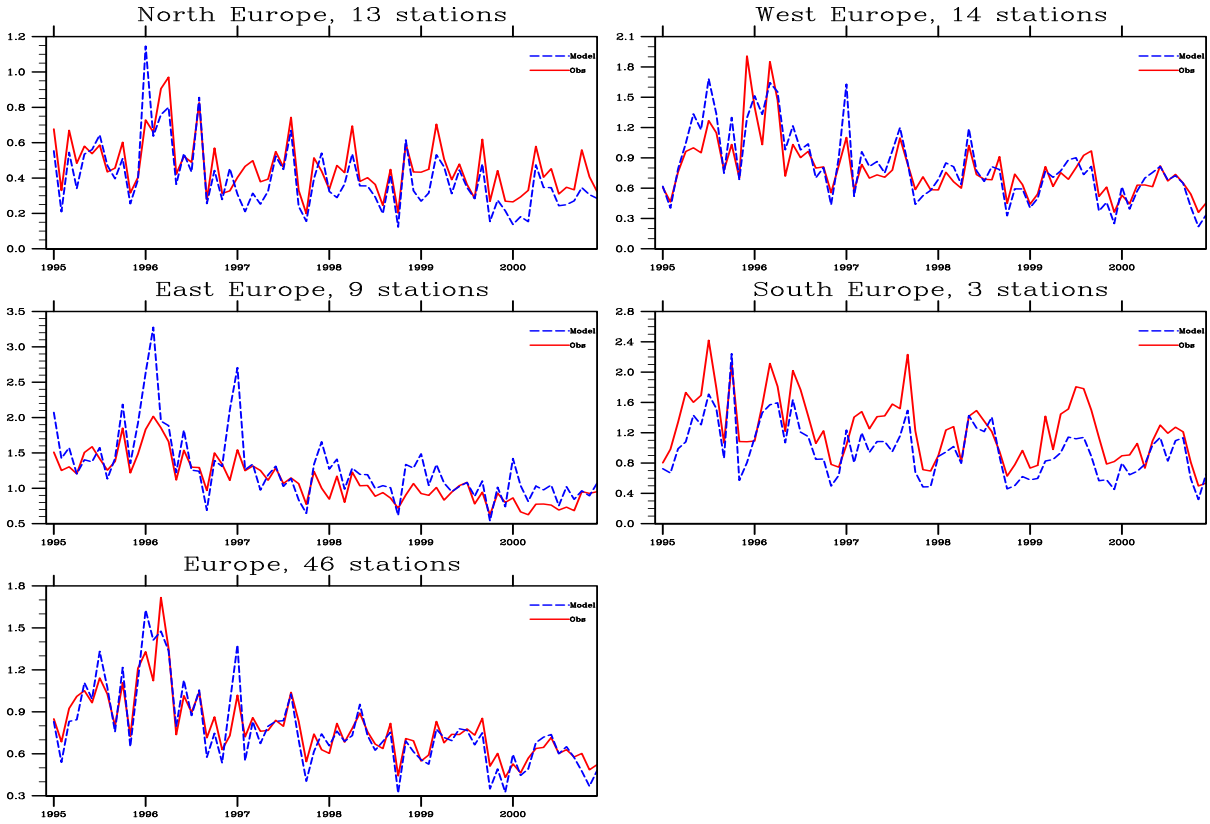

Figure 1.13: Modelled versus observed time-series (monthly) for sulphate in air (μg(S) m^{-3}) for collections of stations that have measured sulphate continuously from 1995 to 2000

seasonal cycle of SO_4^{2-} in the different parts of Europe and the (nonlinear) changes in the seasonal cycle during the last twenty years.

1.5 Nitrate and Nitric Acid in Air

Total nitrate in air was not monitored regularly in the EMEP network until the 1990's, and even at present the monitoring stations cover a very limited area, concentrated in the northern part of Europe. Furthermore, measurements of airborne nitrate are suspected to have a rather large uncertainty due to the very different physical characteristics of the compounds making up total nitrate. Whilst nitric acid is a spatially variable volatile gas with fast dry deposition, particulate nitrate dry deposits only slowly and hence concentrations are more determined by long range transport. Ammonium nitrate is mainly formed when all sulphate present is consumed by ammonia (to form ammonium sulphates) and more ammonia is present. Ammonia and nitric acid then forms ammonium nitrate in an equilibrium reaction determined by relative humidity, temperature

Table 1.3: Results for total nitrate in air (μg(N) m^{-3}). Ns; the number of stations where measurements were available for at least 75% of the days in a year , $pc < 50\%$; the percent of the data points (station yearly averages) with relative bias less than 50%, $pc < 30\%$; the percent with relative bias less than 30%. Obs; the measured yearly average over Ns stations, Mod; the modelled yearly average over Ns stations, $Bias$; the bias ($\frac{Model-Observation}{Observation} \times 100\%$), $Corr$; the correlation between observation and model for station yearly averages, $Ns(d)$; the number of stations where measurements were available for at least one day and $Corr(d)$; the daily correlation between all daily data for all stations for the actual year.

Period	Ns	pc<30%	pc<50%	Obs	Mod	Bias	Corr	Ns(d)	Corr(d)
1990	24	88	100	0.51	0.59	15	0.93	28	0.73
1995	35	80	94	0.44	0.63	42	0.92	38	0.70
1996	32	72	88	0.50	0.65	31	0.82	35	0.63
1997	35	80	89	0.46	0.62	34	0.77	38	0.62
1998	33	82	94	0.42	0.58	39	0.85	37	0.65
1999	43	74	91	0.47	0.62	33	0.79	47	0.42
2000	42	71	88	0.42	0.64	52	0.82	49	0.60

and the presence of other salts such as sea salt and base cations. Nitrate collected on samplers can break down to these volatile gases (HNO_3 and NH_3) and be lost from a filter. Thus, from a modelling perspective, nitrate is difficult.

Figure 1.14, 1.15 and 1.16 show scatter-plots for total nitrate and particulate nitrate in air, respectively. Table 1.3 and 1.4 give the relevant statistic for years when any observations has been reported. The model predict higher concentrations of both total nitrate and nitrate aerosol than observations. Both the spatial and the daily correlation coefficient between the monitored and modelled concentrations are high, in the order of 0.8-0.9 (daily r=0.6-0.7) for total nitrate and 0.7-0.8 (daily r=0.5-0.6) for particulate nitrate. An overestimation of airborne nitrate is seen for most stations.

In figure 1.17 relative bias and correlation of measurements and model results on each individual EMEP station is presented for 1997. In general, the model results compare better to observations for total nitrate than for aerosol nitrate, which also was observed for many other European regional scale models in the GLOREAM inter comparison study (Hass et al.(2003)). The reason for this is that the individual concentrations of nitrate and nitric acid are biased when using the common filter-pack method (see EMEP Manual for sampling and chemical analysis.). The sampling artifact is due to the volatile nature of ammonium nitrate, and separation of these gases and particles by a simple aerosol filter is unreliable. This can be achieved using denuders, but this is a much more demanding method which few sites in EMEP are using. The filter-pack method is however appropriate for measuring the sum of nitrate and nitric acid as well as the sum of ammonia and ammonium.

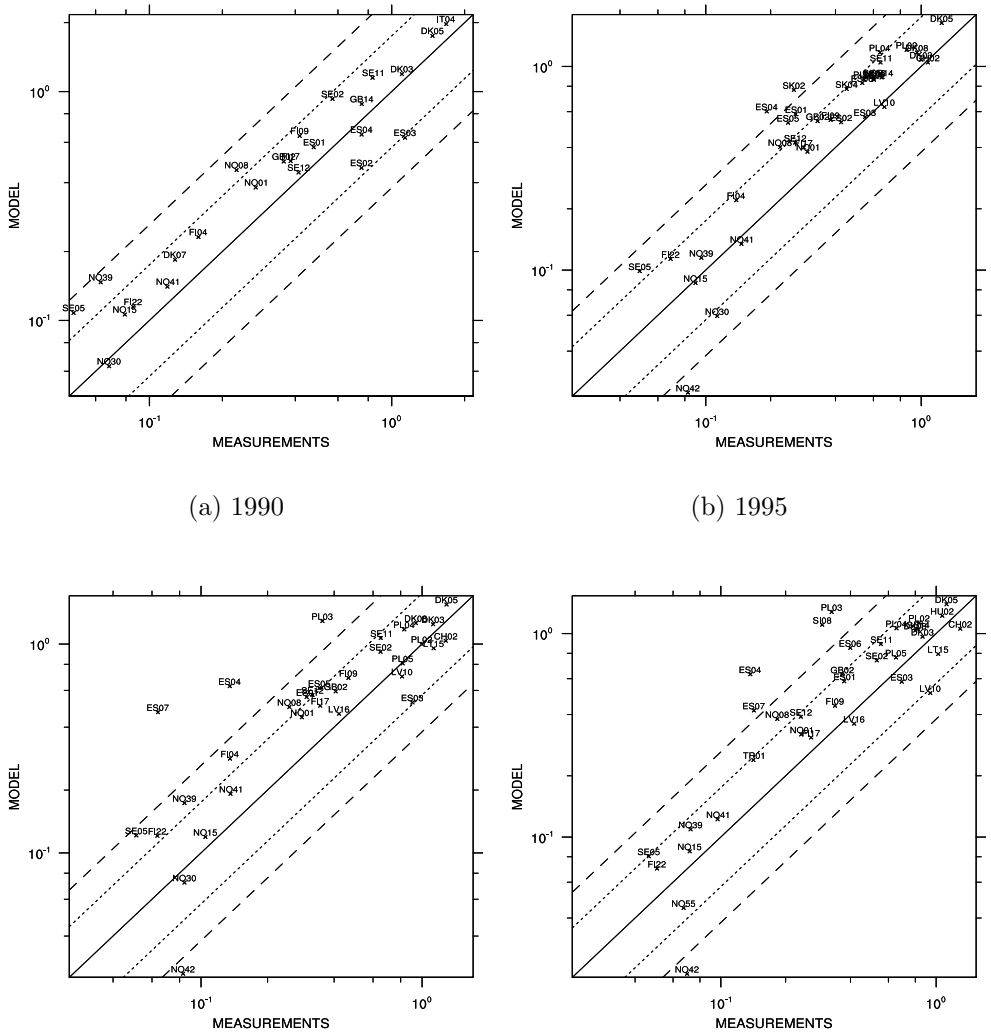

(a) 1990 (b) 1995

(c) 1996 (d) 1997

Figure 1.14: scatter-plots of modelled versus observed NO_3^-+HNO_3 concentrations (μg(N) m^{-3}). Note that no quality criteria have been applied to determine which measurements to include in the comparison.

The overestimation for nitrate aerosols are higher than for total nitrate, This may at least partly be caused by deficiencies in the sampling methods for aerosol nitrate, and possibly also indicate that nitric acid is underestimated and that the the gas-equilibrium is displaced too much towards the particulate phase. Unfortunately, it is not the same stations that measure total nitrate and particulate nitrate, which makes a station-by-station comparison difficult.

We have, however, divided the stations into groups of North, West, South

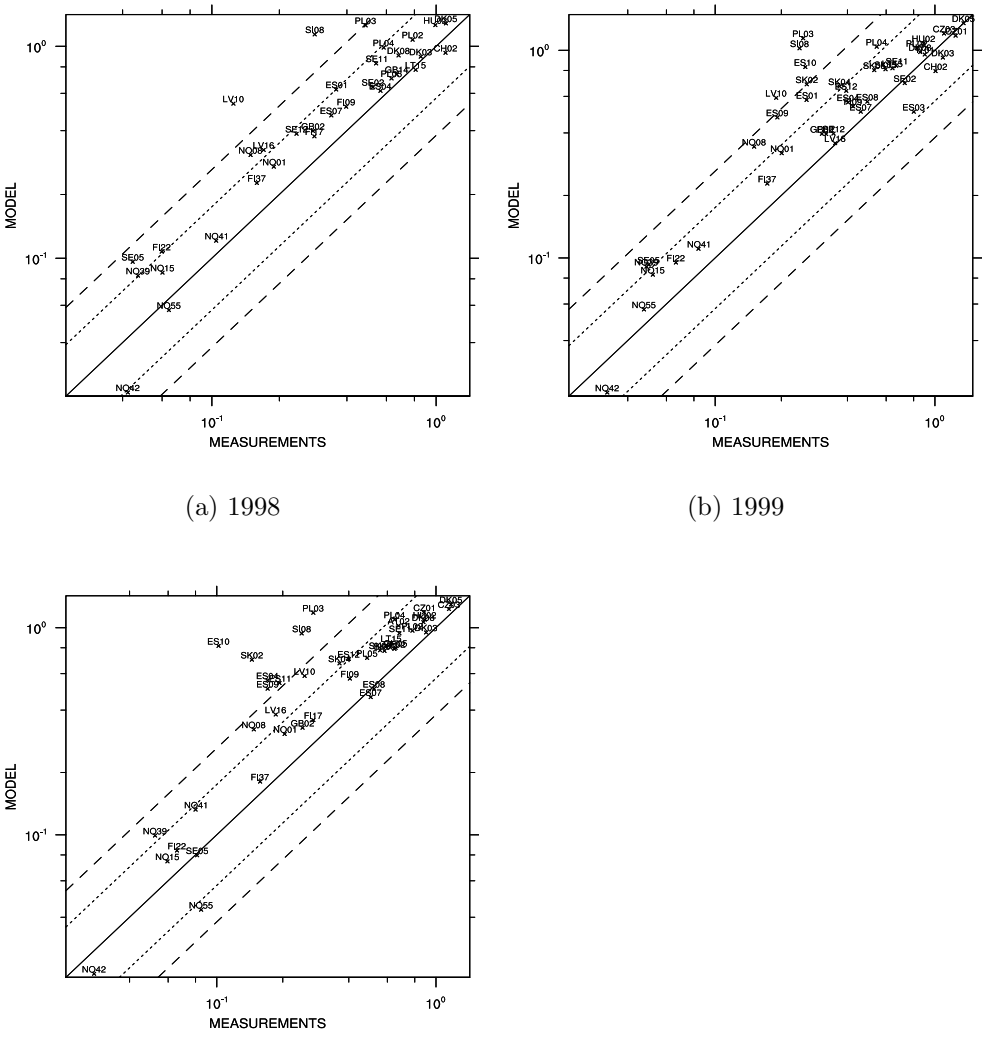

(a) 1998

(b) 1999

(c) 2000

Figure 1.15: scatter-plots of modelled versus observed NO_3^-+HNO_3 concentrations (μg(N) m^{-3}). Note that no quality criteria have been applied to determine which measurements to include in the comparison.

and East Europe and plotted monthly averaged time-series for 1995 to 2000. The stations entering into the groups were required to measure at least 75 % of the days in a year, but not necessarily each year. The result is illustrated in figure 1.19 and 1.20. Realizing that these groups consists of very few stations one should be careful about drawing conclusions. However, some indications on the performance in different emission and climate regimes can be given.

The model capture reasonably well the seasonal variation of total nitrate in air,

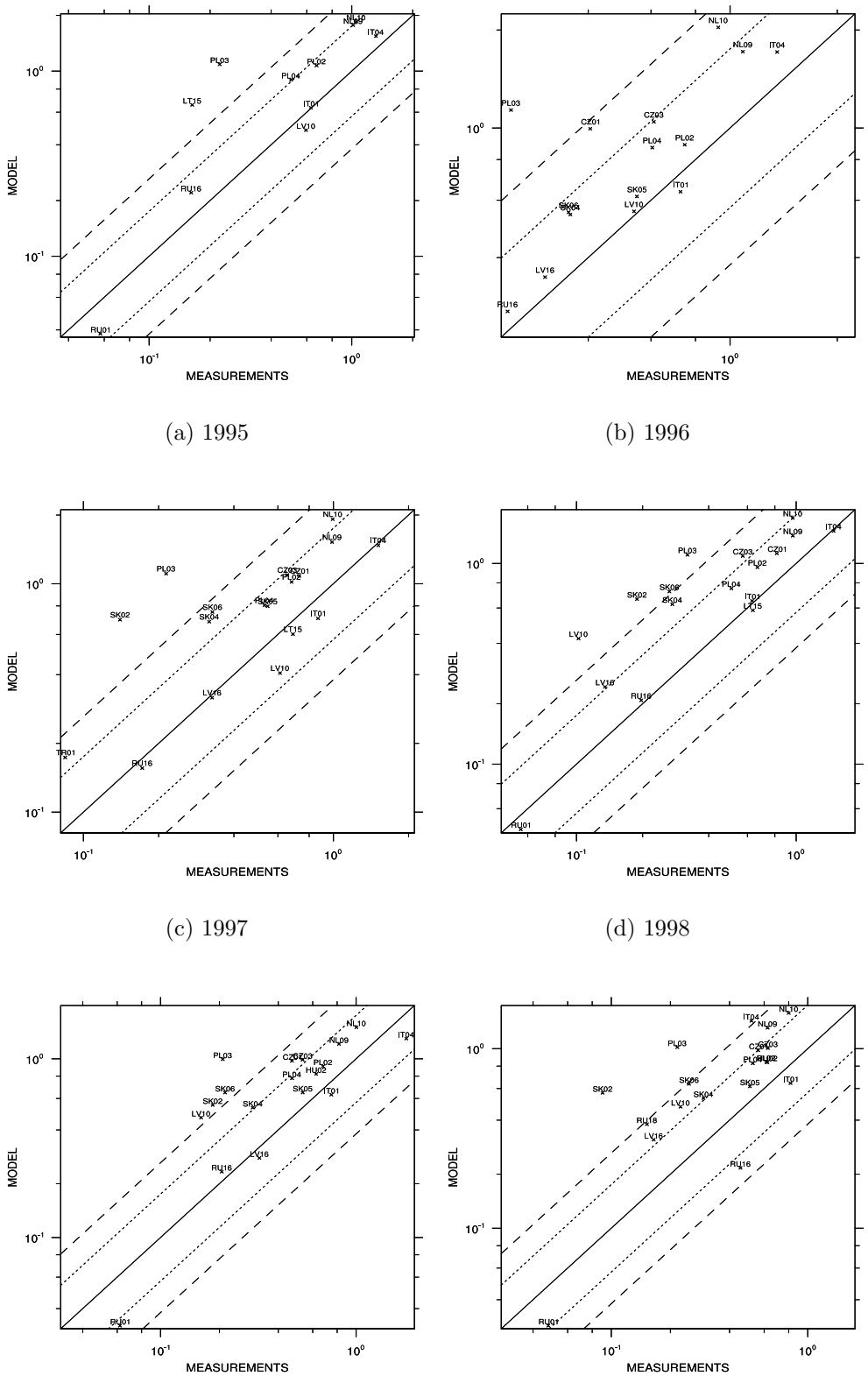

(a) 1995

(b) 1996

(c) 1997

(d) 1998

(e) 1999

(f) 2000

Figure 1.16: scatter-plots of modelled versus observed nitrate aerosol concentrations (μg(N) m^{-3}). The aerosol nitrate measurements may be biased due to inadequate method to separate gas and particles. Note that no quality criteria have been applied to determine which measurements to include in the comparison.

Table 1.4: Results for particulate nitrate in air (μg(N) m^{-3}). Note that the aerosol nitrate measurements may be biased due to inadequate method to separate gas and particles. Ns; the number of stations where measurements were available for at least 75% of the days in a year , $pc < 50\%$; the percent of the data points (station yearly averages) with relative bias less than 50%, $pc < 30\%$; the percent with relative bias less than 30%. Obs; the measured yearly average over Ns stations, Mod; the modelled yearly average over Ns stations, $Bias$; the bias ($\frac{Model-Observation}{Observation} \times 100\%$), $Corr$; the correlation between observation and model for station yearly averages, $Ns(d)$; the number of stations where measurements were available for at least one day and $Corr(d)$; the daily correlation between all daily data for all stations for the actual year.

Period	Ns	pc<30%	pc<50%	Obs	Mod	Bias	Corr	Ns(d)	Corr(d)
1995	11	82	82	0.58	0.93	61	0.83	16	0.61
1996	15	80	93	0.60	0.93	54	0.77	20	0.56
1997	18	67	89	0.58	0.85	47	0.71	20	0.57
1998	17	65	82	0.52	0.81	56	0.83	20	0.57
1999	18	67	89	0.52	0.75	45	0.73	20	0.49
2000	19	47	89	0.43	0.75	76	0.65	20	0.49

but overestimates nitrate in winter in all parts of Europe, except south Europe. Aerosol nitrate is even more overestimated in winter. For the summer period, both the nitrate sum and the aerosol phase are in much better agreement with observations. The exception is south of Europe where also summer concentrations for total nitrate are largely overestimated, whereas particulate nitrate are in reasonable agreement with the monitored data. It should be noted, however, that the southern European stations measuring total nitrate is largely dominated by the 12 Spanish stations (1 Italian), whereas only Italian stations measure particulate nitrate.

Unfortunately, very few stations measure nitric acid and particulate nitrate separately. In 2000, it was only Hungary and Italy that used the recommended denuder method to separate nitric acid and nitrate. However, those sites using the filter-pack method may (and should) report the individual concentrations, but these might be biased as described above. In figure 1.21 it is shown the correlation with the model for the two type of measurements, those using denuders (HU02, IT01) and a selection of other sites using only filter method. The best agreement between measurement and model results is found for the two sites were denuder measurements are reported.

Since the number of stations that measure gas and particulate nitrate separately is very low and most of the stations are located in the same area, it is difficult too draw conclusions from these results. However, there seem to be some indications that the conversion of HNO_3 to nitrate in the cold periods is too high. Since nitric acid is very fast dry deposited, whilst aerosol nitrate

has a much longer lifetime, this inevitably leads to too high nitrate concentrations. Preliminary results (see chapter 3) with the Unified EMEP model coupled to a more comprehensive gas-particle equilibrium chemistry (EQSAM, (Metzger et al.(2002b), Metzger et al.(2002a))) both gives a better seasonal variation of nitric acid and aerosol nitrate, respectively, and lower aerosol nitrate concentrations. There is, however, an urgent need for more measurements in different area of climate and emission regimes in order to proceed with evaluation of the gas-aerosol equilibrium chemistry.

As will be shown in section 1.9, nitrate in precipitation is underestimated. We do not have a good explanation for this discrepancy at this stage, and further work is needed to understand why airborne concentrations of nitrate are overestimated but concentrations in precipitation underestimated.

1.6 Ammonia and Ammonium in Air

As for nitrate, monitoring of the sum of ammonia and ammonium (NH_x) in air in the EMEP network did not take place to any substantial degree until the mid 1990's. In addition, very few Parties have reported ammonia emissions for years earlier than 1990 and other information available on emissions before 1990 is sparse. Therefore, an evaluation of the performance of the model for this period is less meaningful and we have concentrated on recent years (1995 to 2000). At present, the rather limited number of stations ($\sim$45) that report measurements for NH_3+NH_4^+ are concentrated in the north with a few stations scattered around in the rest of Europe. The exception is Spain that reports measurements (more or less regularly) for 10 stations.

In order to evaluate the model performance for NH_x properly, ammonia and ammonium should be studied separately. Unfortunately, very few measurements exist where the gaseous and particle phase are analysed both separately and at the same time.

As for sum of nitrate, the individual concentrations of ammonia and ammonium are biased when using the common filter-pack method due to the volatile nature of ammonium nitrate. Separation of these gases and particles by a simple aerosol filter is unreliable, and to achieve this it is necessary to use denuders. In 2000 it was only the Netherlands, Hungary and Italy (IT01) that used the recommended denuder method. However, those sites using the filter-pack method should also report the individual concentrations of ammonia and ammonium.

In figure 1.23, 1.24, 1.25 and 1.26 scatter-plots for model results versus observations for NH_x and aerosol ammonium are presented for years when measurements were available. In table 1.5 and 1.6 relevant statistics are summarised.

The modelled yearly average of the concentration of the sum of ammonia and ammonium in air are in good agreement with the monitoring data, whilst ammonium aerosols are somewhat overestimated (due to too high winter ammonium

nitrate concentrations). Both the spatial correlations and the daily correlations are among the highest for the modelled acidifying or euthrophying compounds. Unlike for the sum of gaseous nitric acid and particulate nitrate, the aerosol phase component (NH_4^+) are equally well modelled (or better) than the total sum, despite the observations for the sum probably being more reliable than the one for only the aerosol phase. This is most likely because ammonia is generally generated locally from agricultural activity, which is difficult to reflect in the model. Ammonium on the other hand is a long range pollutant and will correlated better with the model even though the measurements might be somewhat biased.

In figure 1.27 and 1.28 monthly time-series of NH_x reveals that the model has a tendency to overestimate winter concentrations (due to too much ammonium) and underestimate summer concentration. The latter is caused by an underestimation of ammonia concentrations. The underestimation in summer seem to be particularly high in North Europe. However, there is no corresponding overestimation of nitrate or sulphate in summer for these region, which indicate that too large conversion of ammonia to ammonium is not the reason.

The model performance for aerosol ammonium, being the sum of ammonium sulphates and ammonium nitrate, will roughly be the product of the model performance for sulphate and nitrate. We have already discussed that whilst the comparison between sulphate observations and model results is excellent, ammonium nitrate is overestimated in winter. Since both components are reasonably well modelled in the summer, we might expect a good comparison of model and measurements for ammonium aerosols in the summer and worse in the cold period. This is also what we see in the monthly time-series for the period 1995 to 2000 of ammonium aerosols in figure 1.29.

The daily time-series in figure 1.32 show very mixed results. The seasonal and daily concentrations are simulated very well at many sites, for example Oulanka and Bredkaelen, although some episodes are missed. At other sites, for example Virolahti and Kaarvatn, the model systematically fails to describe high peaks of emissions during the summer months when agriculture activities peak.

The reasons for this variability in performance are unclear. As has been discussed in a number of earlier EMEP reports, NH_x is difficult to model on a regional scale. Firstly, spatial and temporal emissions of ammonia are rather poorly known compared to emissions of the other pollutants in the EMEP model. Secondly, ammonia emissions are related to agriculture activities and therefore represent widely distributed (but often highly local!) sources. Further, the exchange of ammonia with the surface is a complex issue, with bi-directional exchange frequently observed (Sutton et al.(1995), Nemitz et al.(2000), Andersen et al.(1999)). Many of the local-scale processes (e.g. soil moisture, leaf wetness, pH) which control NH_3 emissions are difficult to parameterise even on a field-scale, and cannot be captured within large-scale models.

Not only is this scale issue difficult to represent in the model, but in addition measurements are very seldom characteristic for a 50×50 km^2 grid square.

Table 1.5: Results for ammonia plus ammonium in air (μg(N) m^{-3}). Ns; the number of stations where measurements were available for at least 75% of the days in a year , $pc < 50\%$; the percent of the data points (station yearly averages) with relative bias less than 50%, $pc < 30\%$; the percent with relative bias less than 30%. Obs; the measured yearly average over Ns stations, Mod; the modelled yearly average over Ns stations, $Bias$; the bias ($\frac{Model-Observation}{Observation} \times 100\%$), $Corr$; the correlation between observation and model for station yearly averages, $Ns(d)$; the number of stations where measurements were available for at least one day and $Corr(d)$; the daily correlation between all daily data for all stations for the actual year.

Period	Ns	pc<30%	pc<50%	Obs	Mod	Bias	Corr	Ns(d)	Corr(d)
1990	21	81	90	1.39	1.18	-14	0.85	27	0.64
1995	32	75	88	1.30	1.36	5	0.91	35	0.57
1996	32	78	84	1.30	1.46	13	0.84	35	0.66
1997	34	71	82	1.23	1.33	8	0.80	38	0.62
1998	34	71	88	1.04	1.20	15	0.80	37	0.60
1999	40	70	90	1.33	1.29	-2	0.78	44	0.27
2000	38	74	84	1.31	1.33	2	0.76	46	0.56

Moreover, in order to calculate the ammonia concentrations at the ground, the modelled atmospheric stability, which is rather uncertain, is of large importance. However, in areas where the SO_x and NO_x emissions dominates over the NH_3 emissions (e.g. central Europe), ammonium aerosol dominates over ammonia in NHx. This secondary pollutant deposits only slowly and is more determined by long-range transport and therefore easier to model.

Finally, the ammonia emissions presently included in the EMEP model are yearly totals officially reported by the countries to UNECE/EMEP and they are not linked to specific meteorological variations. The EMEP model imposes a temporal variation on the NH_3 emission totals derived from the results of GENEMIS project. This currently assumed seasonal variation is very similar across Europe, with a main maximum in early spring and a secondary maximum in October-November, despite very different agricultural practices over Europe. It is clear from these arguments, that the discrepancies between model predicted and observed ammonia+ammonium concentrations in Europe may at least partly be caused by deficiencies in the description of the ammonia emissions.

Table 1.6: Results for ammonium in air (μg(N) m^{-3}). Note that the aerosol ammonium measurements may be biased due to inadequate method to separate gas and particles. Ns; the number of stations where measurements were available for at least 75% of the days in a year , $pc < 50\%$; the percent of the data points (station yearly averages) with relative bias less than 50%, $pc < 30\%$; the percent with relative bias less than 30%. Obs; the measured yearly average over Ns stations, Mod; the modelled yearly average over Ns stations, $Bias$; the bias ($\frac{Model-Observation}{Observation} \times 100\%$), $Corr$; the correlation between observation and model for station yearly averages, $Ns(d)$; the number of stations where measurements were available for at least one day and $Corr(d)$; the daily correlation between all daily data for all stations for the actual year.

Period	Ns	pc<30%	pc<50%	Obs	Mod	Bias	Corr	Ns(d)	Corr(d)
1980	4	100	100	2.35	1.77	-24	0.97	5	0.71
1985	6	100	100	2.76	1.94	-29	0.99	14	0.67
1990	7	43	100	1.14	1.62	42	0.91	8	0.59
1995	16	63	94	0.95	1.30	37	0.83	22	0.63
1996	16	94	100	1.17	1.51	29	0.81	22	0.63
1997	19	84	100	1.13	1.30	15	0.80	23	0.58
1998	20	80	100	1.03	1.19	15	0.84	23	0.59
1999	22	73	100	0.89	1.04	17	0.75	25	0.48
2000	21	71	90	0.79	1.05	34	0.75	27	0.50

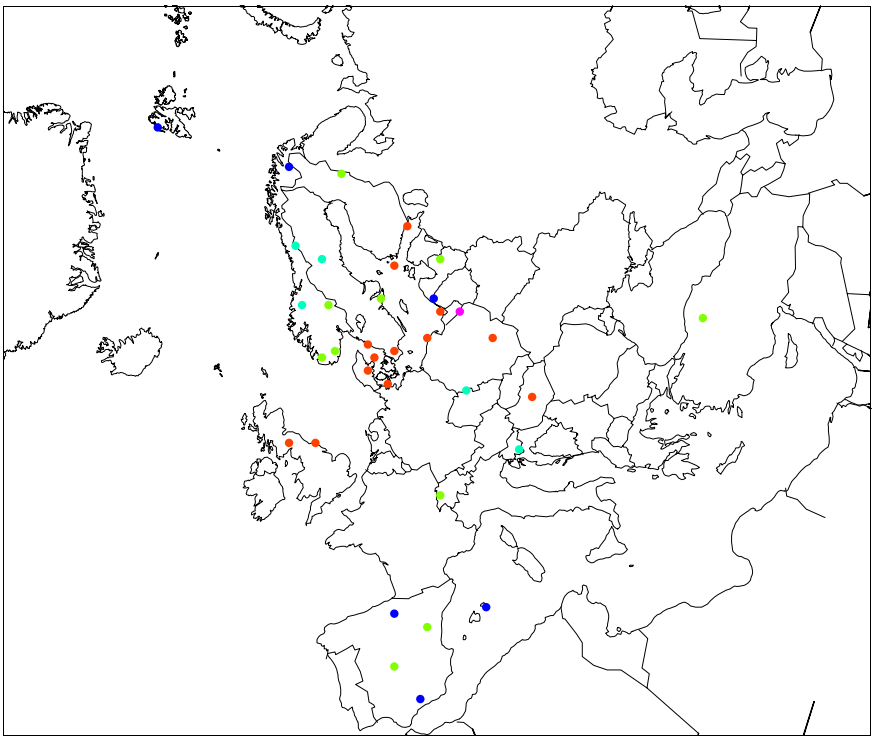

(a) Correlation

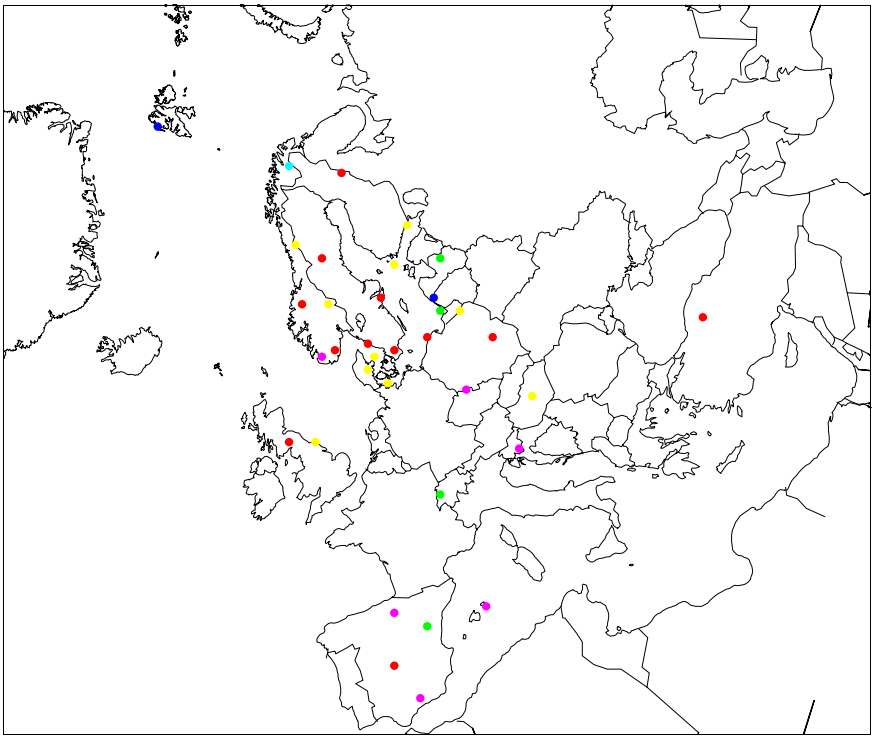

(b) Relative Bias

Figure 1.17: Correlation coefficient and relative bias in concentration of total Nitrate in air (μg(N) m^{-3}), 1997.

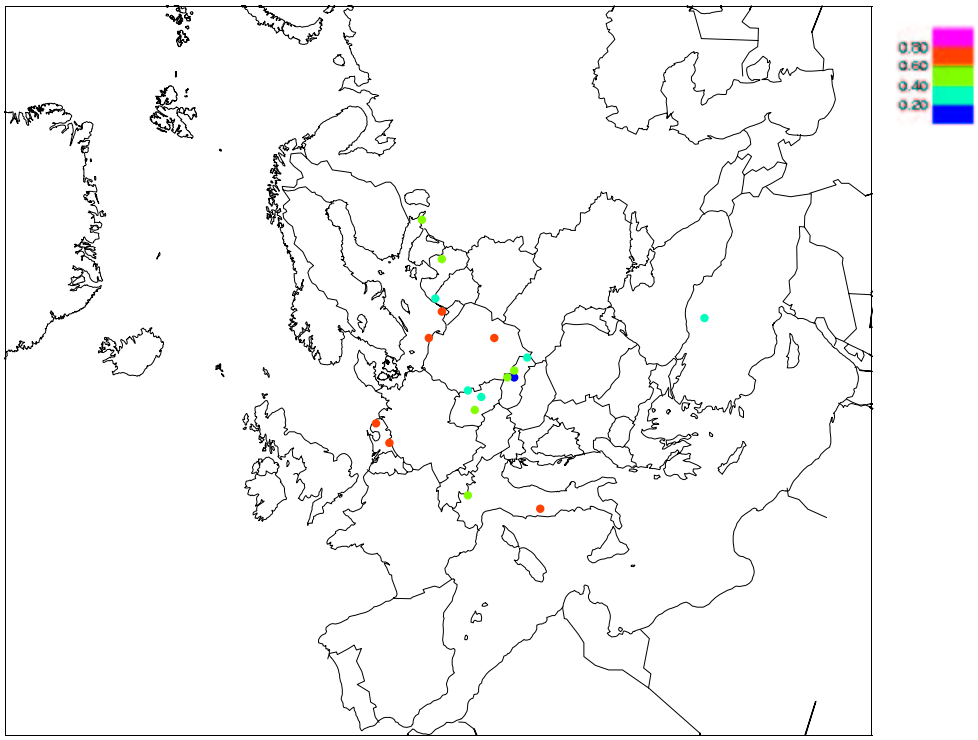

(a) Correlation

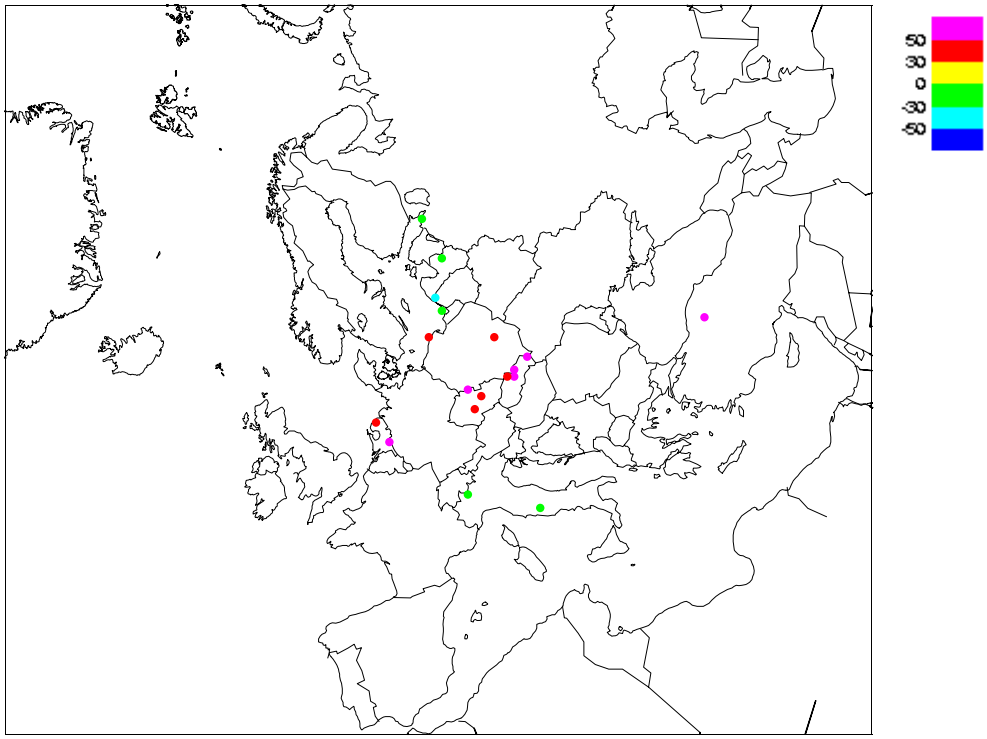

(b) Relative Bias

Figure 1.18: Correlation coefficient and relative bias in concentration of aerosol Nitrate in air (μg(N) m^{-3}), 1997. The aerosol nitrate measurements may be biased due to inadequate method to separate gas and particles.

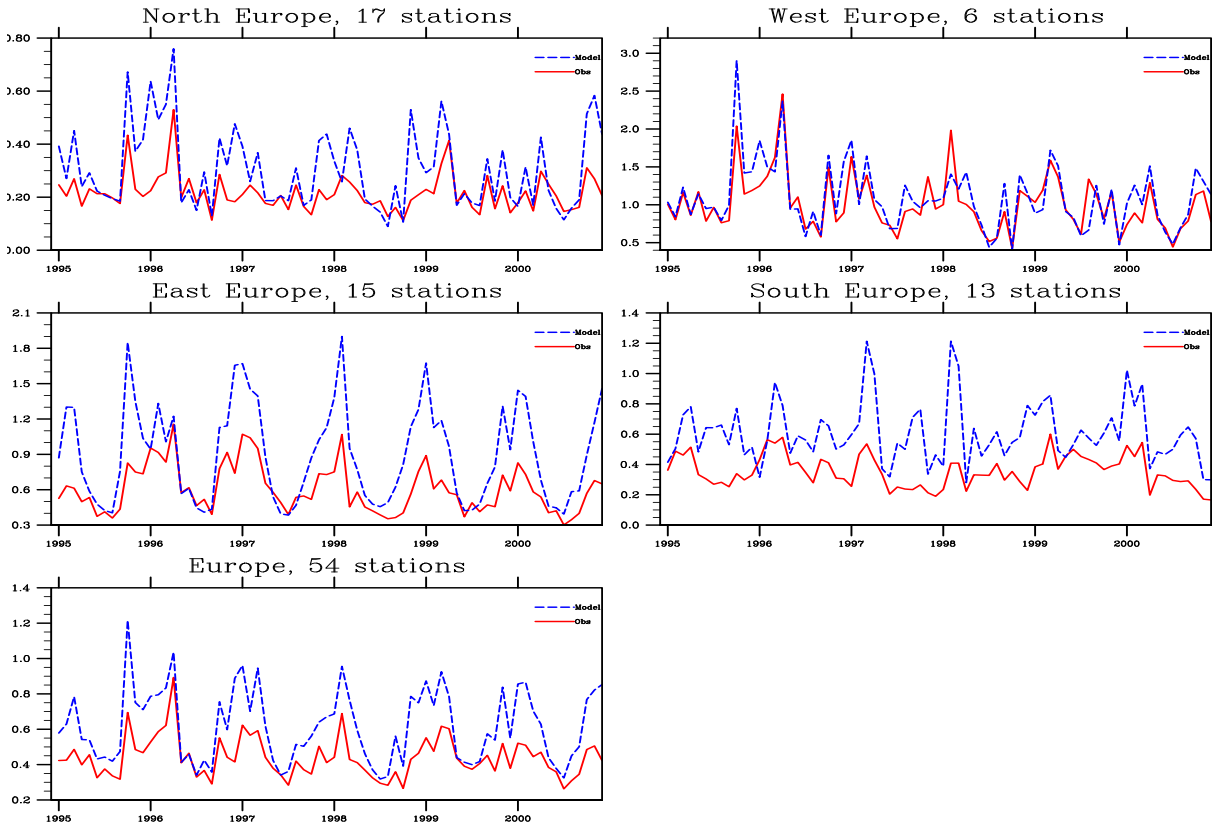

Figure 1.19: Monthly time-series of total nitrate concentrations in Air (μg(N) m^{-3}), 1995-2000. All stations with measurements more than 75% of the days per year (but not necessarily each year) have been included. Note that the number of stations included in the comparison may vary from year to year. The total number of stations is denoted at the top of the figure.

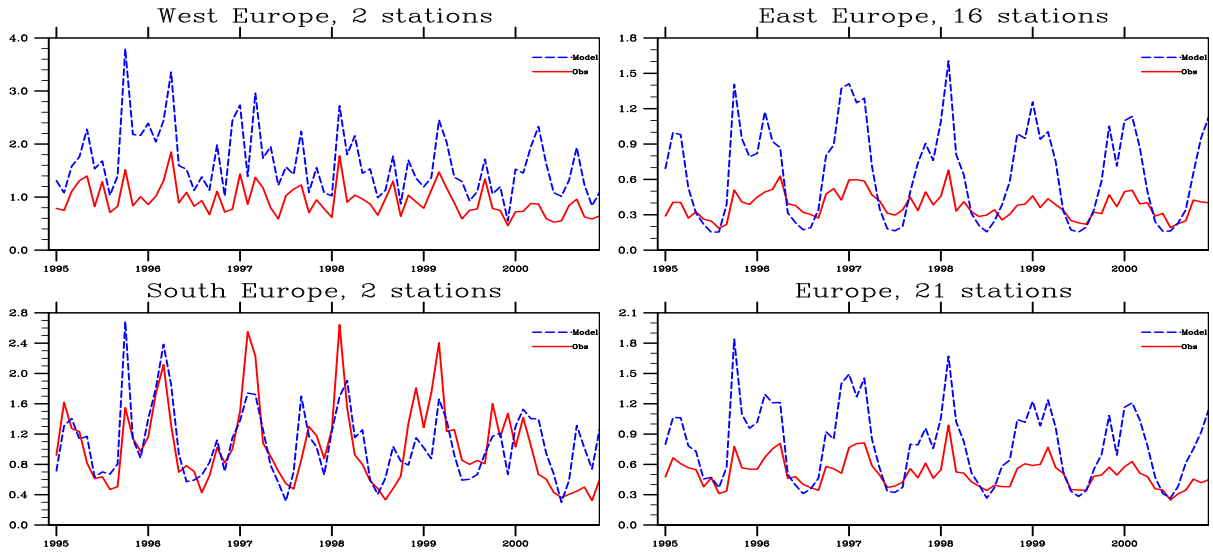

Figure 1.20: Monthly time-series of aerosol nitrate concentrations in air (μg(N) m^{-3}), 1995-2000. The aerosol nitrate measurements may be biased due to inadequate method to separate gas and particles. All stations with measurements more than 75% of the days per year (but not necessarily each year) have been included. Note that the number of stations included in the comparison may vary from year to year. The total number of stations is denoted at the top of the figure.

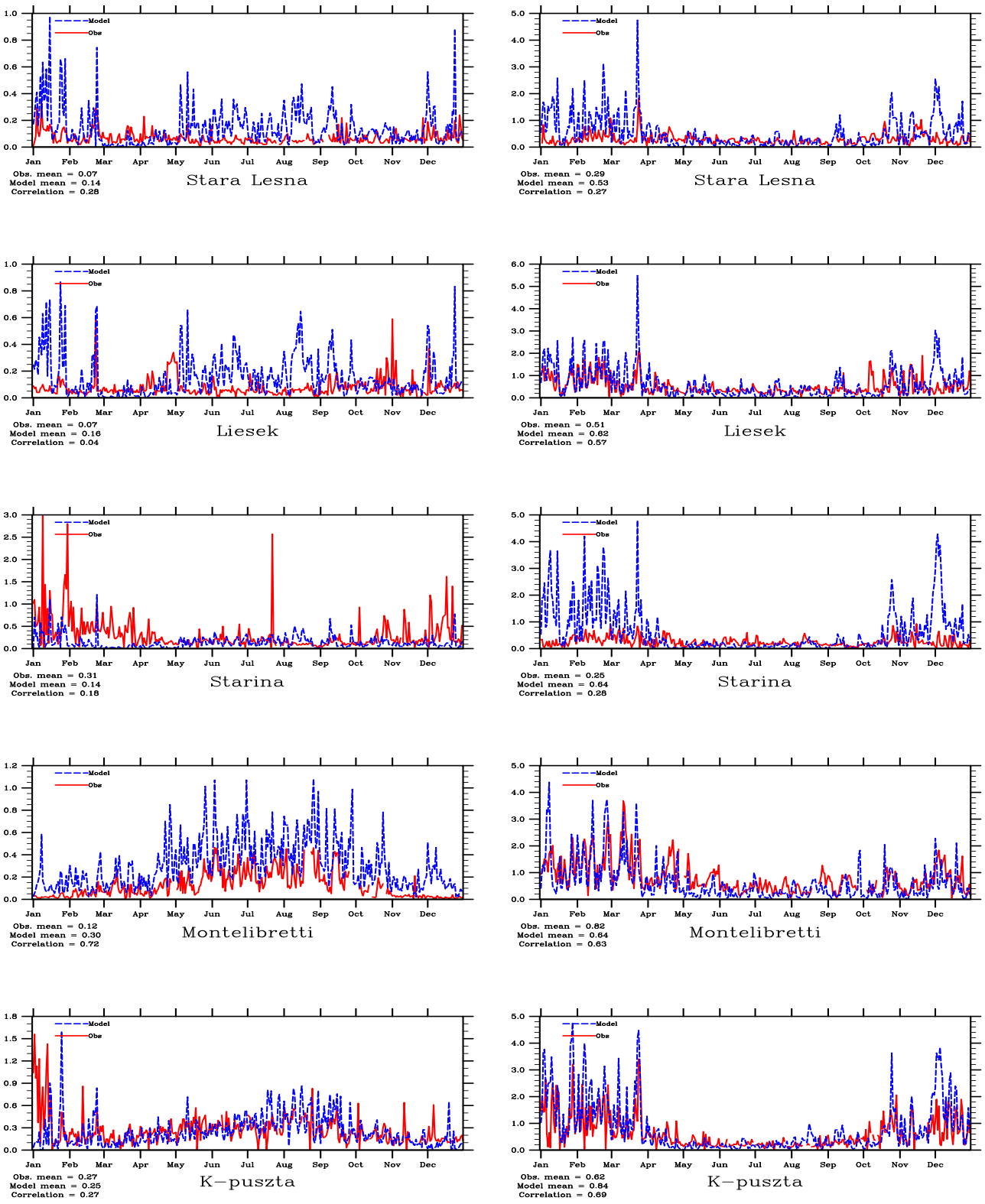

Figure 1.21: time-series (daily) of nitric acid in air (left column) and aerosol nitrate (right column), 2000. Units: (μg(N) m^{-3}).

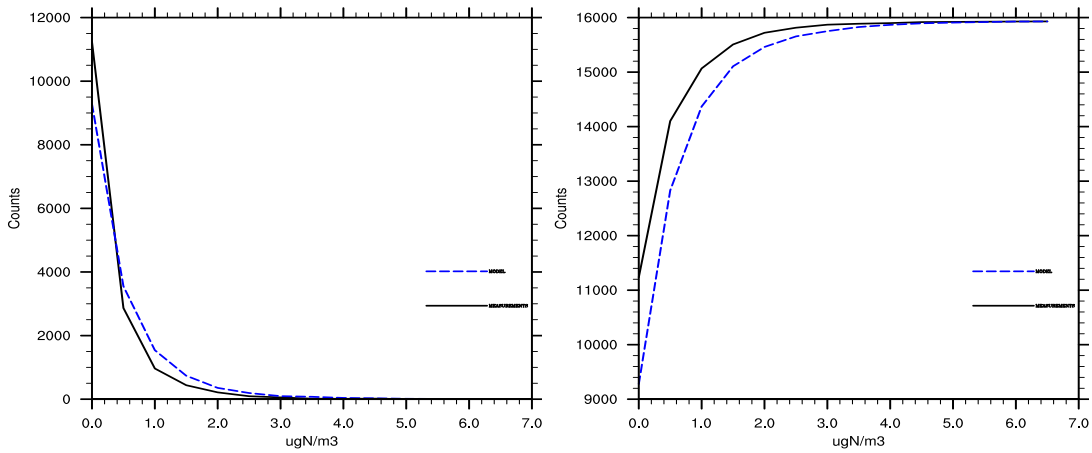

Figure 1.22: Frequency distribution (left column) and cumulative frequency distributions (right column) of model (dotted) and measurements (line), derived from all daily total nitrate concentrations, all stations, 1999. Not that no quality criteria have been applied to determine which measurements to include in the comparison.

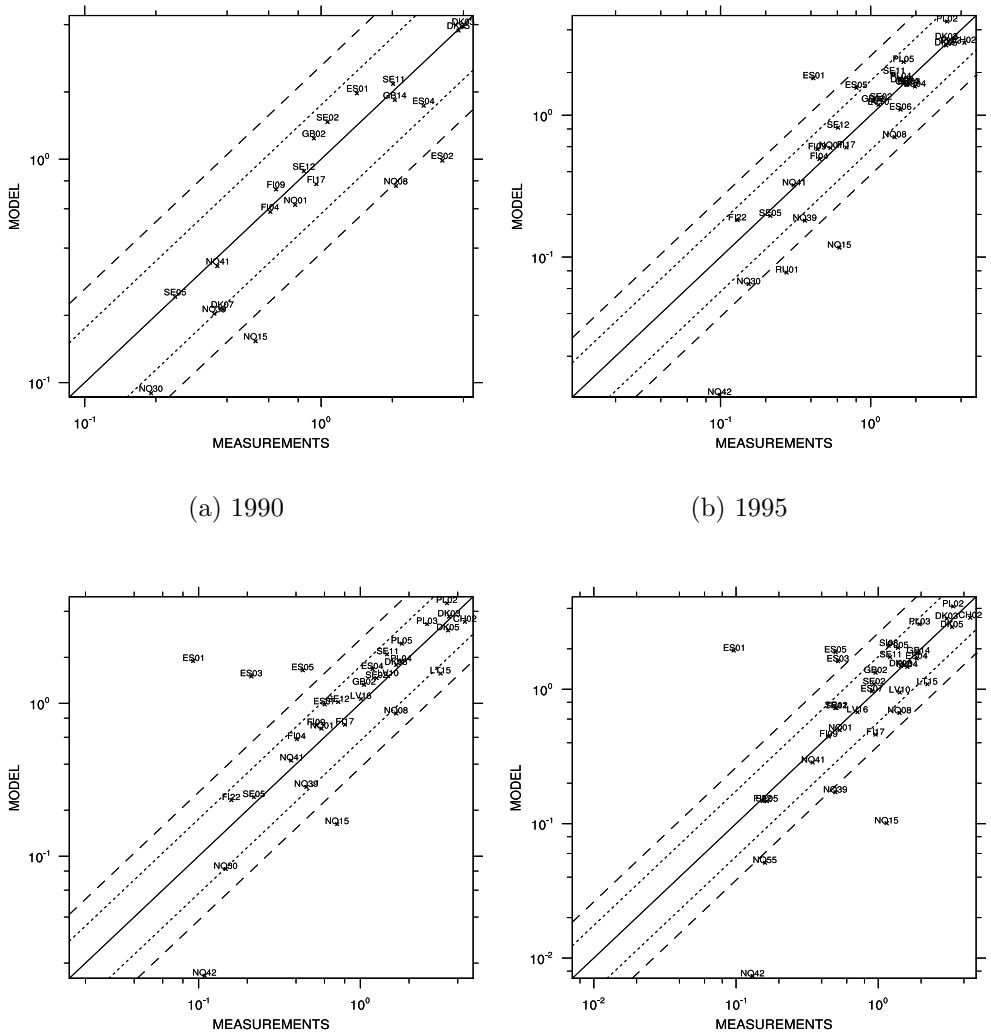

(a) 1990

(b) 1995

(c) 1996

(d) 1997

Figure 1.23: Scatter-plots of Modelled versus Observed NH_3+ NH_4^+ concentrations (μg(N) m^{-3}), 1990, 1995, 1996, 1997. Note that no quality criteria have been applied to determine which measurements to include in the comparison.

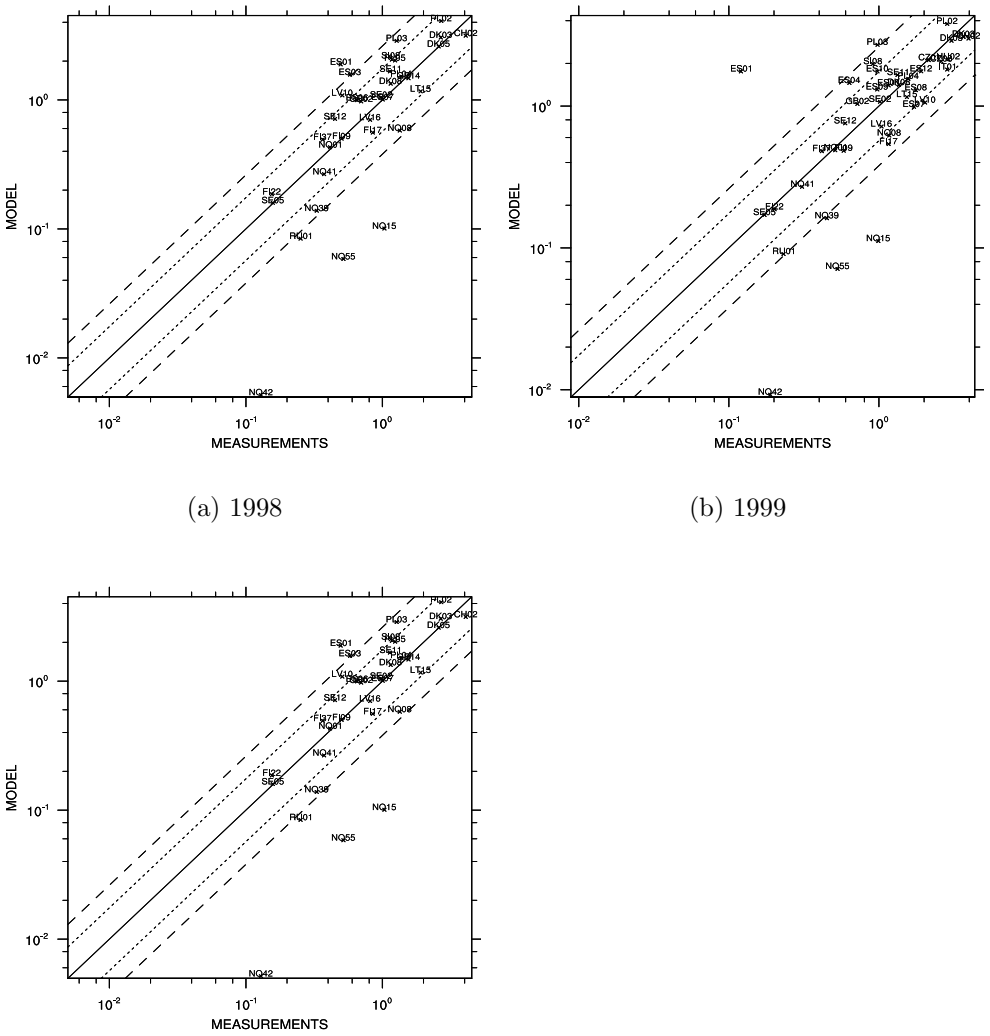

(a) 1998

(b) 1999

(c) 2000

Figure 1.24: Scatter-plots of Modelled versus Observed NH_3+ NH_4^+ concentrations (μg(N) m^{-3}), 1998, 1999, 2000. Note that no quality criteria have been applied to determine which measurements to include in the comparison.

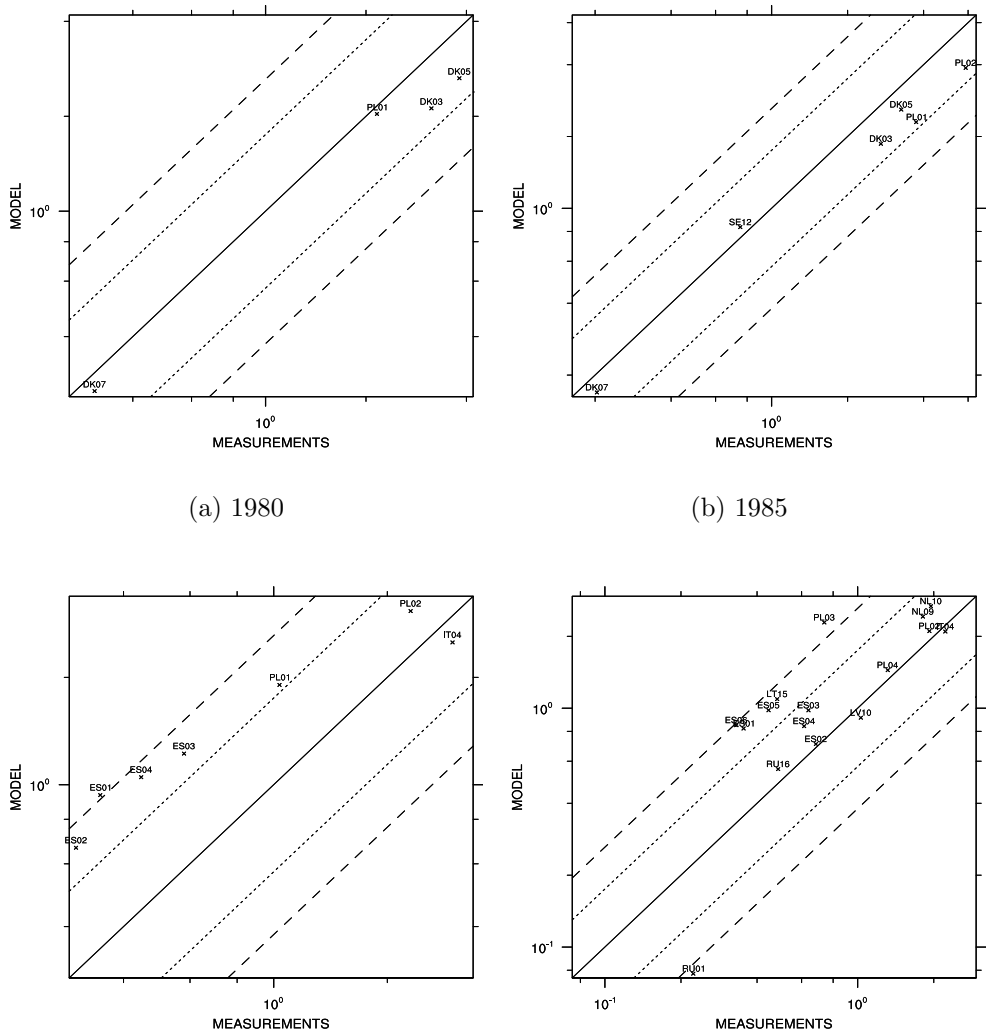

(a) 1980

(b) 1985

(c) 1990

(d) 1995

Figure 1.25: Scatter-plots of Modelled versus Observed aerosol NH_4^+ concentrations (μg(N) m^{-3}), 1980, 1985, 1990, 1995. The aerosol ammonium measurements may be biased due to inadequate method to separate gas and particles. Note that no quality criteria have been applied to determine which measurements to include in the comparison.

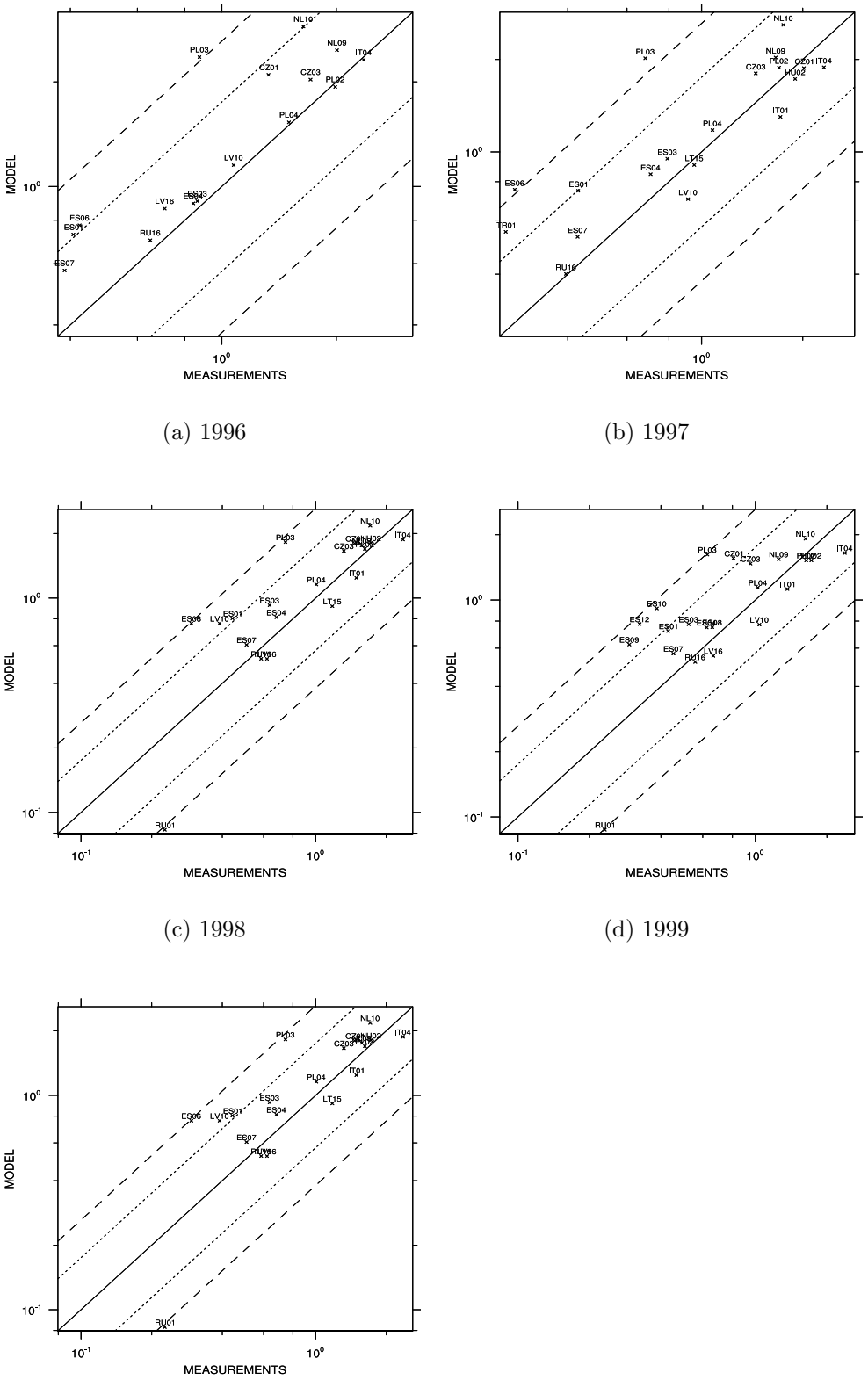

(a) 1996

(b) 1997

(c) 1998

(d) 1999

(e) 2000

Figure 1.26: Scatter-plots of Modelled versus Observed aerosol NH_4^+ concentrations (μg(N) m^{-3}), 1996-2000. The aerosol ammonium measurements may be biased due to inadequate method to separate gas and particles. Note that no quality criteria have been applied to determine which measurements to include in the comparison.

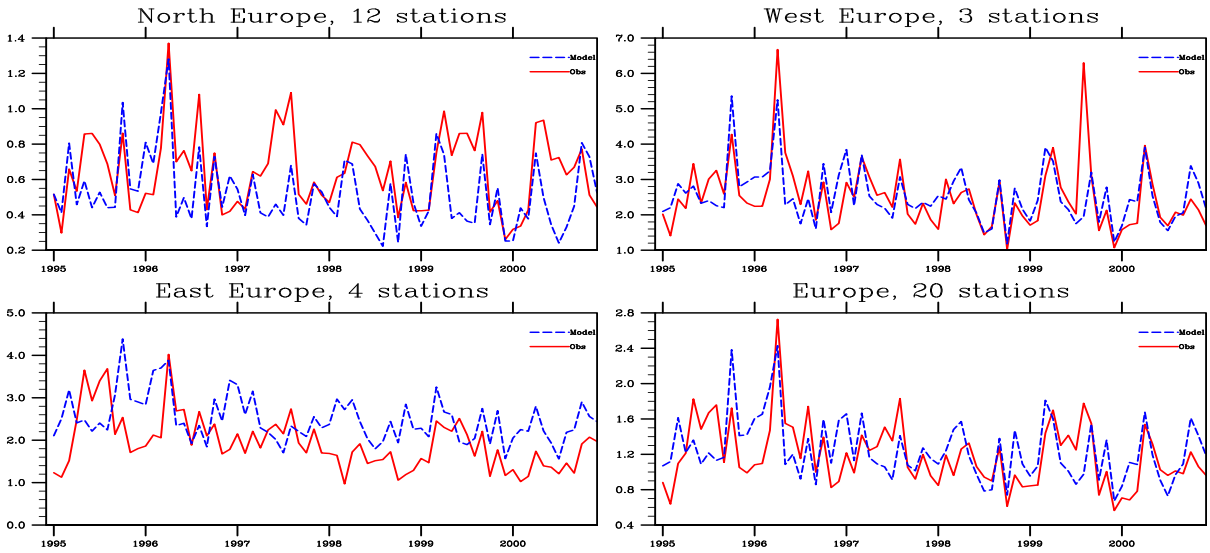

Figure 1.27: Modelled versus observed time-series (monthly) for ammonia plus ammonium in air (μg(N) m^{-3}) for collections of stations that have measured NH$_x$ continuously from 1995 to 2000

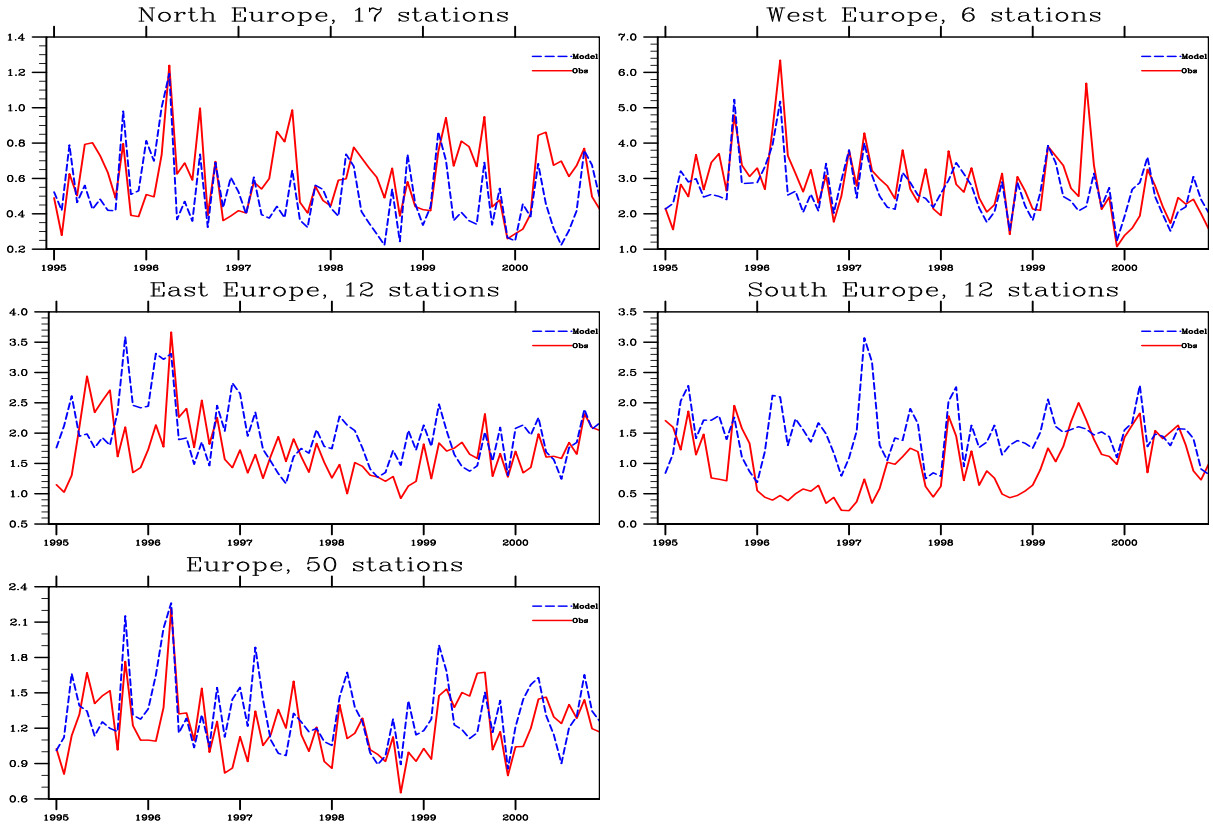

Figure 1.28: Modelled versus observed time-series (monthly) for ammonia plus ammonium in air (μg(N) m^{-3}) for collections of stations that have measured NH$_x$ at least 75% of the days each year (but not necessarily each year). Note that the number of stations included in the comparison may vary from year to year. The total number of stations is denoted at the top of the figure.

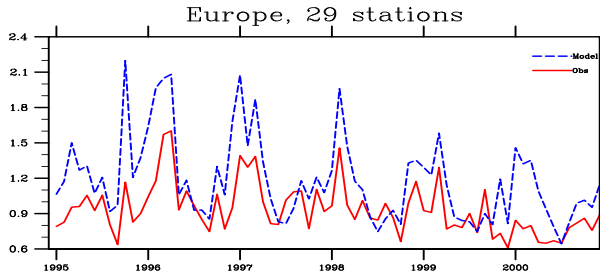

Figure 1.29: Modelled versus observed time-series (monthly) 1995-2000 for aerosol ammonium in air (μg(N) m^{-3}) for collections of stations that have measured NH$_x$ at least 75% of the days each year (but not necessarily each year).The aerosol ammonium measurements may be biased due to inadequate method to separate gas and particles. Note that the number of stations included in the comparison may vary from year to year. The total number of stations is denoted at the top of the figure.

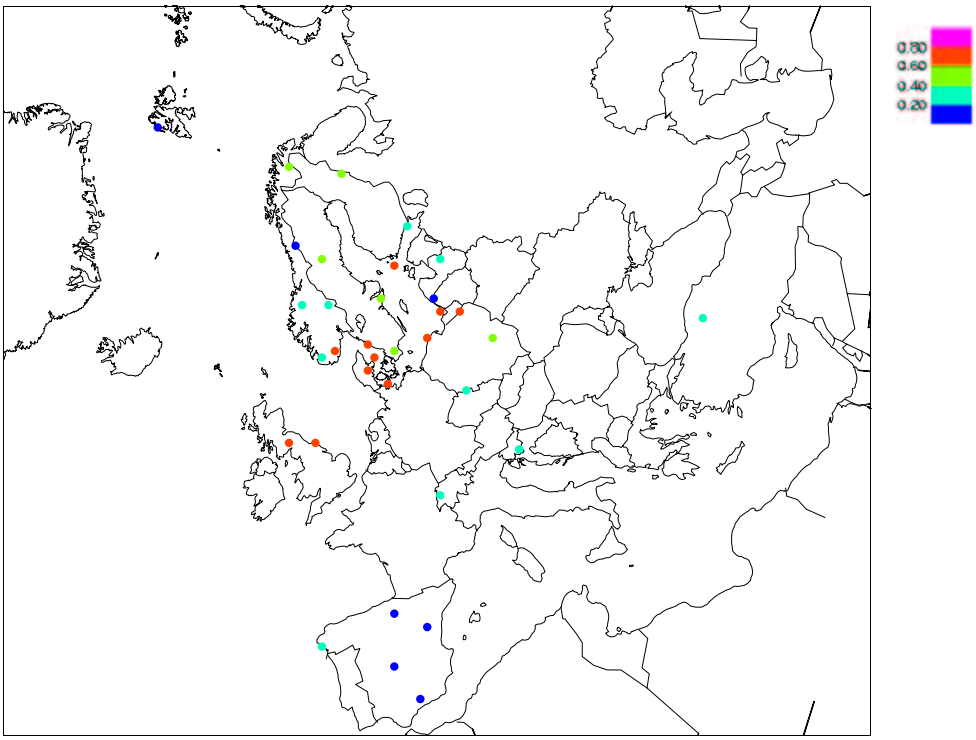

(a) Correlation

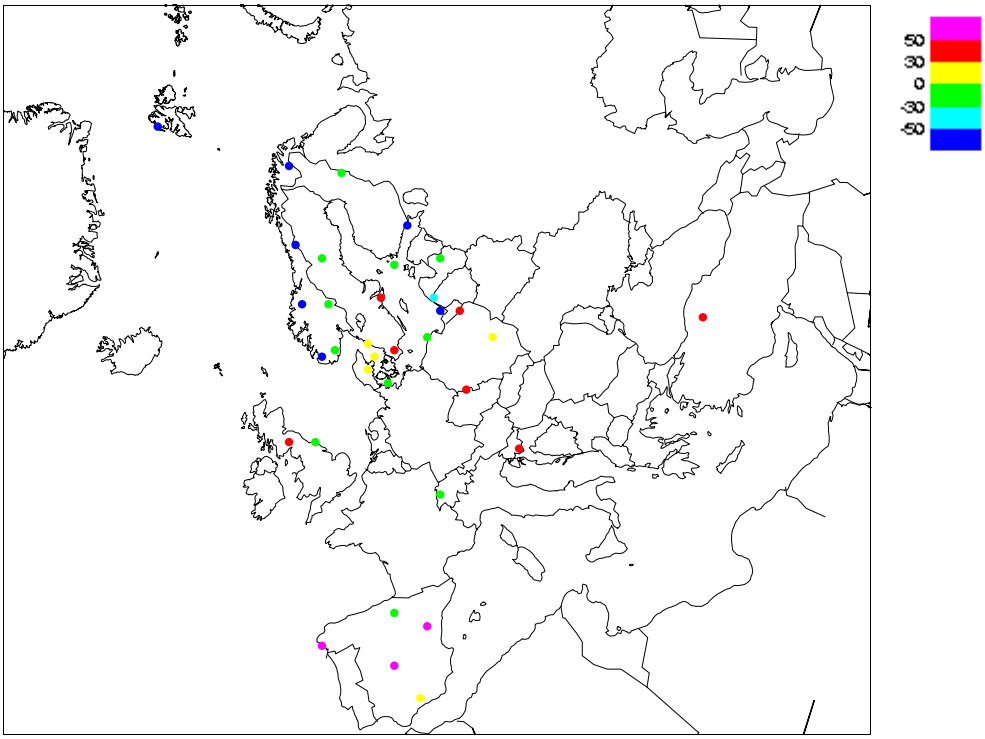

(b) Relative Bias

Figure 1.30: Correlation coefficient and relative bias in sum of NH_3 and NH_4^+ in air (μg(N) m^{-3}), 1997.

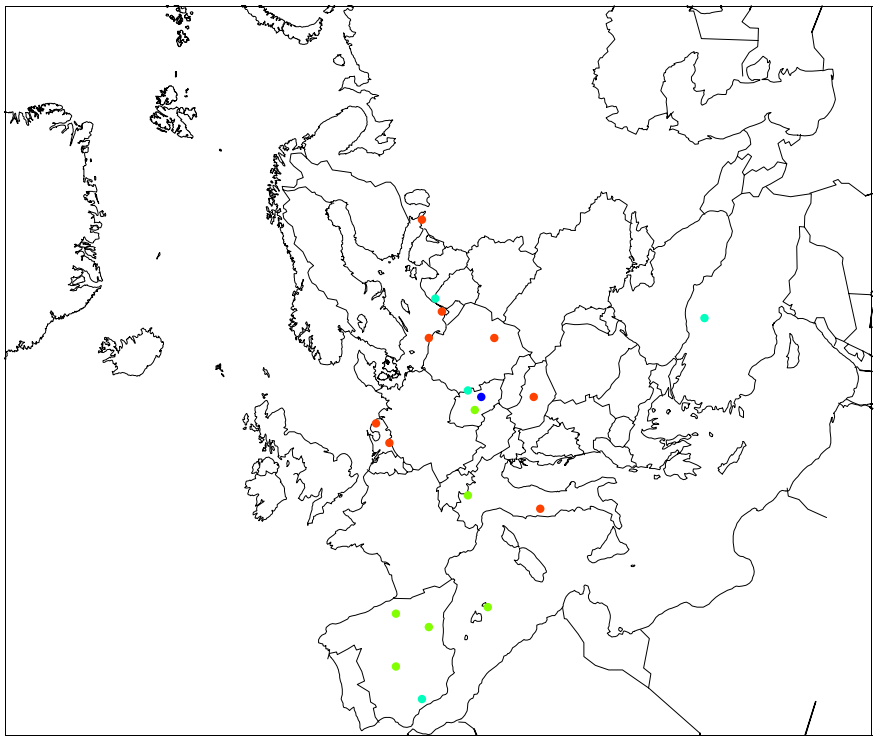

(a) Correlation

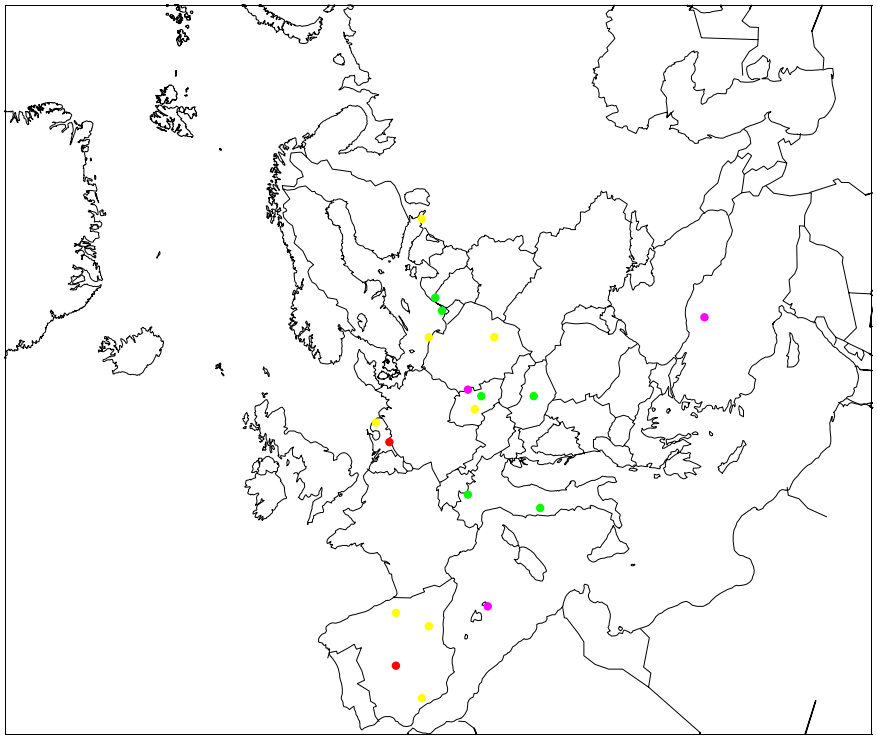

(b) Relative Bias

Figure 1.31: Correlation coefficient and relative bias for aerosol NH_4^+ in air, 1997. The aerosol ammonium measurements may be biased due to inadequate method to separate gas and particles.

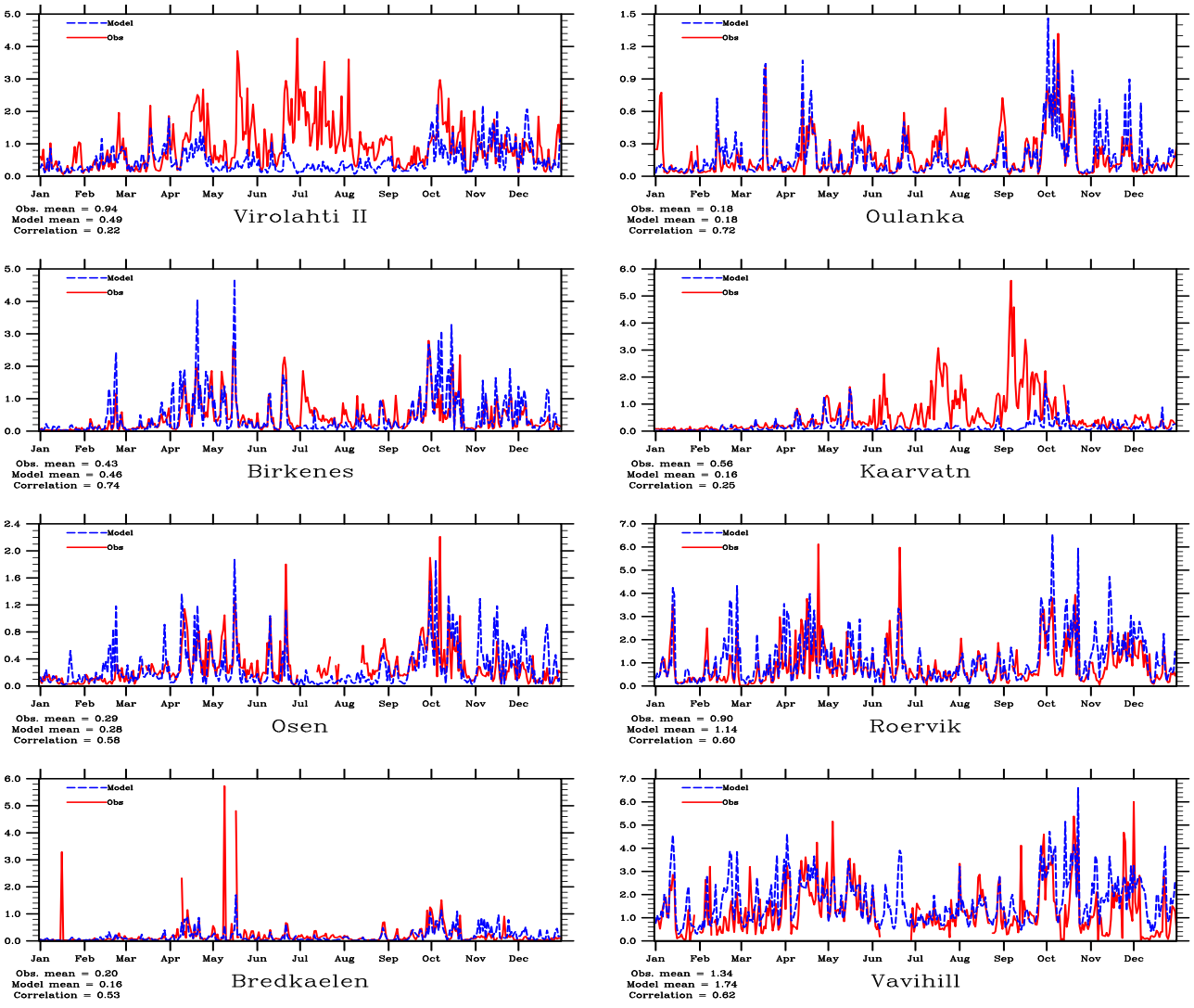

Figure 1.32: Ammonia plus Ammonium in Air (μg(N) m^{-3}), 2000

1.7 Concentrations in Precipitation and Wet Depositions

The ability of the model to predict concentrations in precipitation is limited by the accuracy of the precipitation fields used in the model. The precipitation field pattern is very patchy (e.g. influenced by local topographic effects), and the regional scale model is unable to resolve this sub grid scale distribution. A typical problem arises with small scale showers. In reality precipitation is high in a small area of a given grid, but a large fraction of the grid should remain dry. Within the model, however, this precipitation is averaged out to cover the whole grid at a lower intensity. Thus, even though average precipitation amounts may be simulated well, the model experiences precipitation more often, but in lower amounts, than occur in reality. On a shorter time scale, e.g on daily basis, this may lead to too high concentrations in precipitation for episodes when it rains only in a small part of the grid square. For a regional scale model it is more sensible to compare the bulk concentrations, i.e the sum of the wet deposited compounds divided by the sum of precipitation.

Table 1.7: Precipitation (mm). Ns; the number of stations where measurements were available for at least 25% of the days in a year , $pc < 50\%$; the percent of the data points (station yearly averages) with relative bias less than 50%, $pc < 30\%$; the percent with relative bias less than 30%. Obs; the measured yearly average over Ns stations, Mod; the modelled yearly average over Ns stations, $Bias$; the bias ($\frac{Model-Observation}{Observation} \times 100\%$), $Corr$; the correlation between observation and model for station yearly averages, $Ns(d)$; the number of stations where measurements were available for at least one day and $Corr(d)$; the daily correlation between all daily data for all stations for the actual year.

Period	Ns	pc<30%	pc<50%	Obs	Mod	Bias	Corr	Ns(d)	Corr(d)
1980	29	93	100	24475.30	23648.11	-2	0.57	43	0.31
1985	40	95	100	34827.50	34535.18	0	0.66	59	0.28
1990	60	83	92	47344.10	56734.26	20	0.49	61	0.49
1995	73	82	95	64077.14	65210.59	2	0.49	76	0.48
1996	74	84	96	60248.24	65757.76	9	0.48	80	0.51
1997	73	86	97	62200.85	70671.06	14	0.54	79	0.49
1998	75	84	95	68629.63	79209.12	15	0.48	81	0.48
1999	77	87	99	66916.71	76089.57	14	0.62	82	0.45
2000	64	83	98	54508.08	61296.83	12	0.65	77	0.46

In table 1.7 the precipitation from the model and the measured precipitation is compared. Both spatial correlation coefficients (∼0.5-0.6) and daily correlation coefficients (∼0.3-0.5) are relatively low. The model systematically underestimate precipitation for South Europe, especially for the high episodes (not shown). The

modelled precipitation in West Europe are also under predicted, whilst in East Europe the model predicts more precipitation than the observations.

The correlation between model and measurements for concentrations in precipitation and wet depositions will to a large extent depend on the model precipitation field. Thus, the results for the components in precipitation are expected to be worse than for air concentrations.

1.8 Sulphate in Precipitation

scatter-plots for wet deposition of sulphur for the years 1980, 1985, 1990, 1995-2000 are presented in figures 1.35. Figure 1.37 show corresponding plots for bulk concentrations of sulphate in precipitation. The overall agreement between measured and modelled sulphate in precipitation is found to be good. More than 95 % of the stations are within relative bias 50% for all years presented.

Nordic stations tend to be somewhat underestimated by the model. These sites also show the highest correlation between measurement and model, probably because long range transport of sulphate is the main source of wet depositions of sulphur in remote regions. The measurements for the East European stations are somewhat lower than the modelled wet depositions in winter, but overestimated in the summer. In contrast, the seasonal cycles are well reproduced for the collection of North and West European stations.

Wet deposition for the south European sites is systematically underestimated. The accumulated precipitation used in the model is lower than the measured amount. However, the underestimation of precipitation cannot explain the huge difference between modelled and observed depositions observed at these sites. In addition, there are no indications of poor quality for the measurements of concentrations in precipitation for this area. Thus, there might be a need for a review of the description of the convective process in the model.

Since data quality has been changing over the years, we cannot draw too many conclusions about model performance with respect to trend analysis from this work. Indeed, given all the difficulties and known-problems with the data-sets being used, it would seem that in broad terms, model performance has remained rather constant over this long time period. Given the large changes which have taken place in emissions over this period, the model results presented here are rather encouraging.

Table 1.8: Bulk concentrations of sulphate in precipitation (μg(S)l^{-1}). Ns; the number of stations where measurements were available for at least 25% of the days in a year , $pc < 50\%$; the percent of the data points (station yearly averages) with relative bias less than 50%, $pc < 30\%$; the percent with relative bias less than 30%. Obs; the measured yearly average over Ns stations, Mod; the modelled yearly average over Ns stations, $Bias$; the bias ($\frac{Model-Observation}{Observation} \times 100\%$), $Corr$; the correlation between observation and model for station yearly averages

Period	Ns	pc<30%	pc<50%	Obs	Mod	Bias	Corr
1980	23	78	100	0.98	1.19	21	0.85
1985	35	74	97	1.00	1.36	37	0.64
1990	38	74	97	0.77	0.97	27	0.55
1995	50	92	98	0.73	0.75	3	0.25
1996	48	94	98	0.63	0.77	22	0.78
1997	50	90	98	0.52	0.54	3	0.64
1998	58	97	100	0.44	0.48	7	0.85
1999	44	95	100	0.47	0.51	7	0.77
2000	45	96	100	0.45	0.48	6	0.86

Table 1.9: Sulphate wet deposition (μg(S)m^{-2}). Ns; the number of stations where measurements were available for at least 25% of the days in a year , $pc < 50\%$; the percent of the data points (station yearly averages) with relative bias less than 50%, $pc < 30\%$; the percent with relative bias less than 30%. Obs; the measured yearly average over Ns stations, Mod; the modelled yearly average over Ns stations, $Bias$; the bias ($\frac{Model-Observation}{Observation} \times 100\%$), $Corr$; the correlation between observation and model for station yearly averages

Period	Ns	pc<30%	pc<50%	Obs	Mod	Bias	Corr	Ns(d)	Corr(d)
1980	23	70	96	17900.49	20022.54	12	0.63	35	0.21
1985	35	60	94	24876.87	32752.52	32	0.57	54	0.08
1990	38	74	95	23306.04	26234.70	13	0.38	61	0.24
1995	50	86	96	28275.16	27691.13	-1	0.44	76	0.16
1996	48	79	96	23968.70	25421.37	6	0.71	79	0.29
1997	50	92	98	23089.41	19391.64	-15	0.29	79	0.13
1998	58	100	100	23869.89	22619.85	-4	0.82	81	0.31
1999	44	91	98	18659.32	17580.23	-5	0.73	82	0.29
2000	45	91	98	18769.39	17543.44	-6	0.62	77	0.28

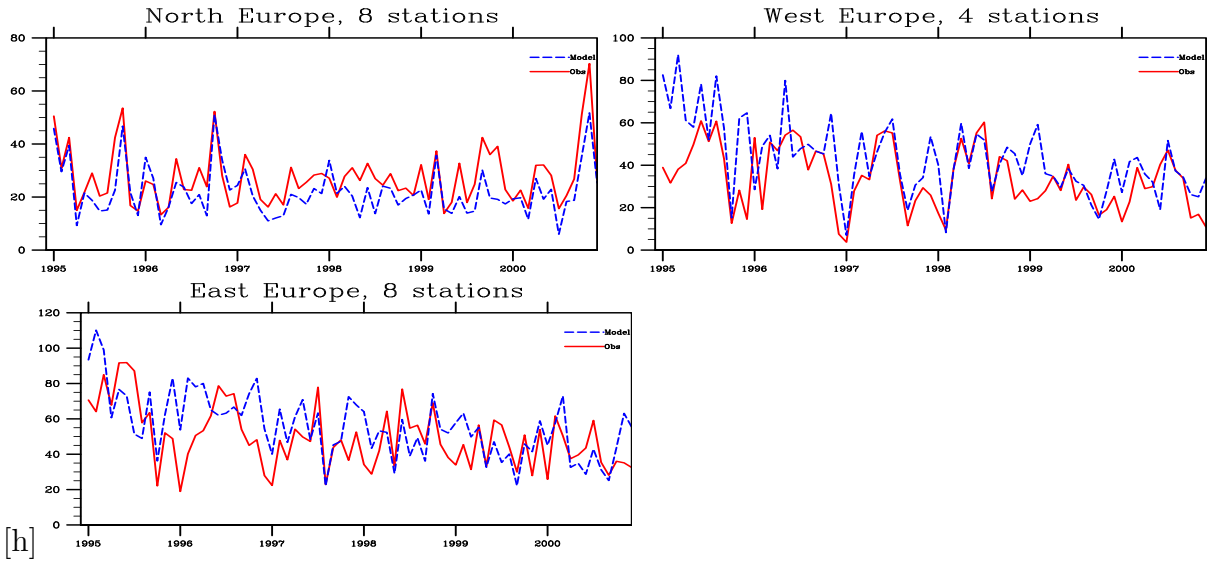

[h]

Figure 1.33: Monthly time-series of wet deposition of sulphur (μg(S)m^{-2}), 1995-2000. All stations with data more than 25% of the days per year (and every year) have been included.

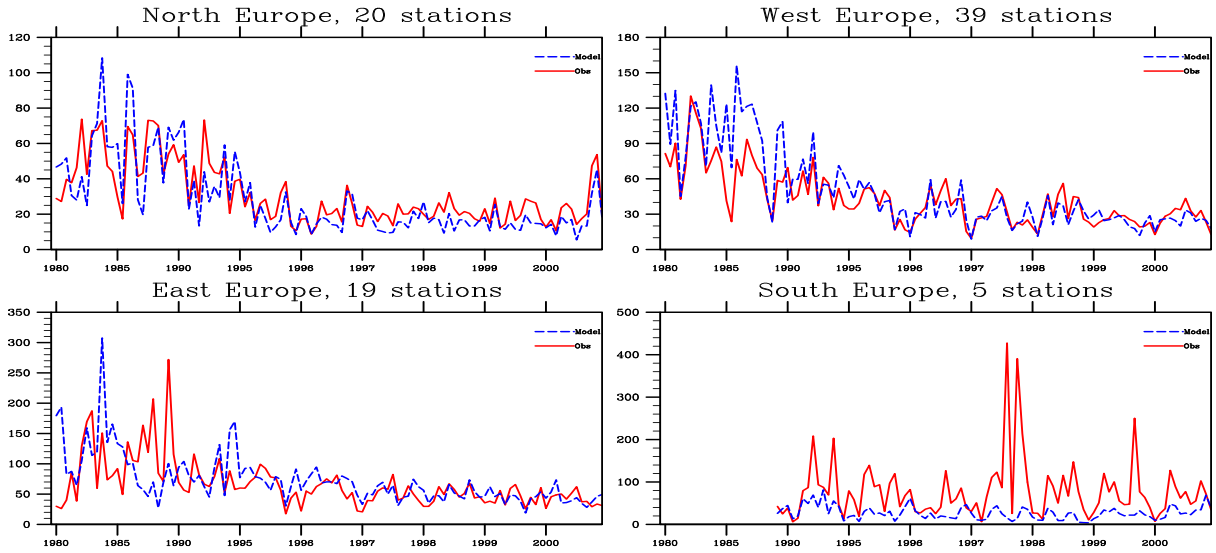

Figure 1.34: Monthly time-series of wet deposition of sulphur (μg(S)m^{-2}), 1980, 1985,1990,1995-2000. All stations with data more than 25% of the days per year (but not necessarily every year) have been included.

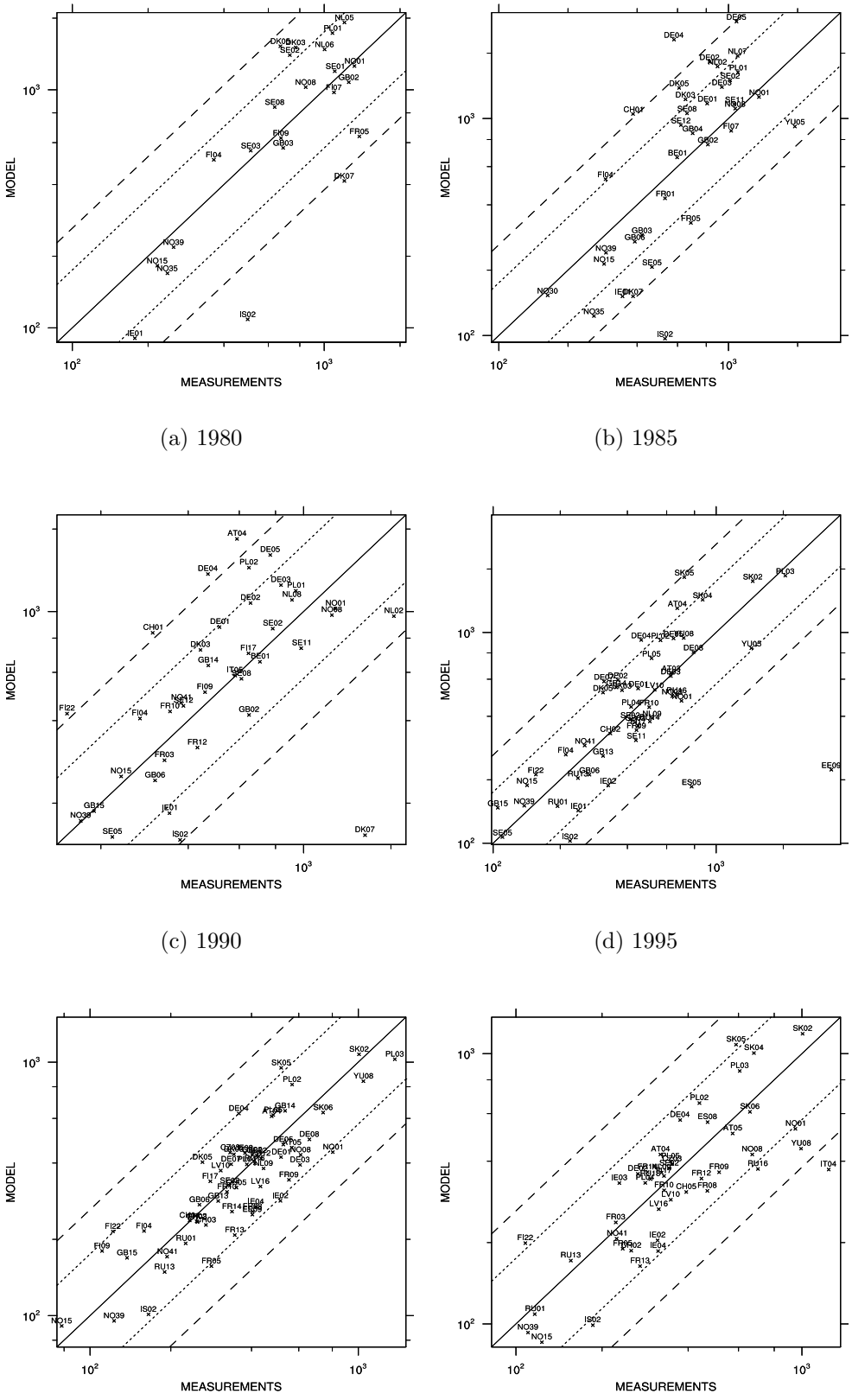

(a) 1980

(b) 1985

(c) 1990

(d) 1995

(e) 1998

(f) 2000

Figure 1.35: scatter-plots of modelled versus observed sulphur wet deposition (μg(S)m^{-2}), 1980, 1985, 1990, 1995, 1996 and 1997. Note that no quality criteria have been applied to determine which measurements to include in the comparison.

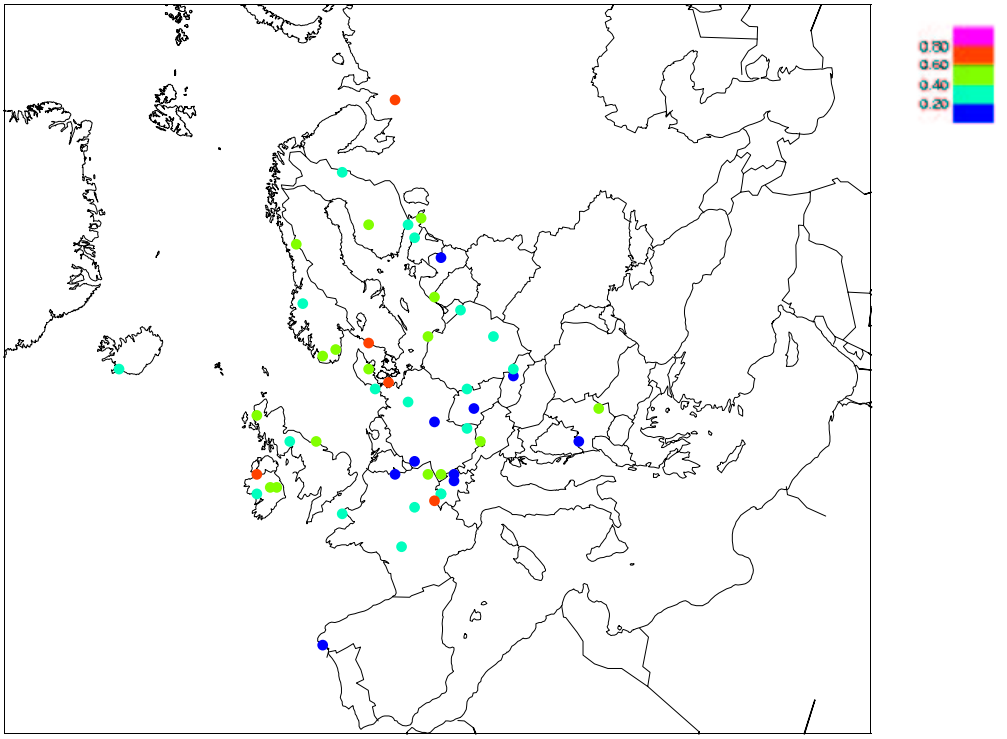

(a) Correlation

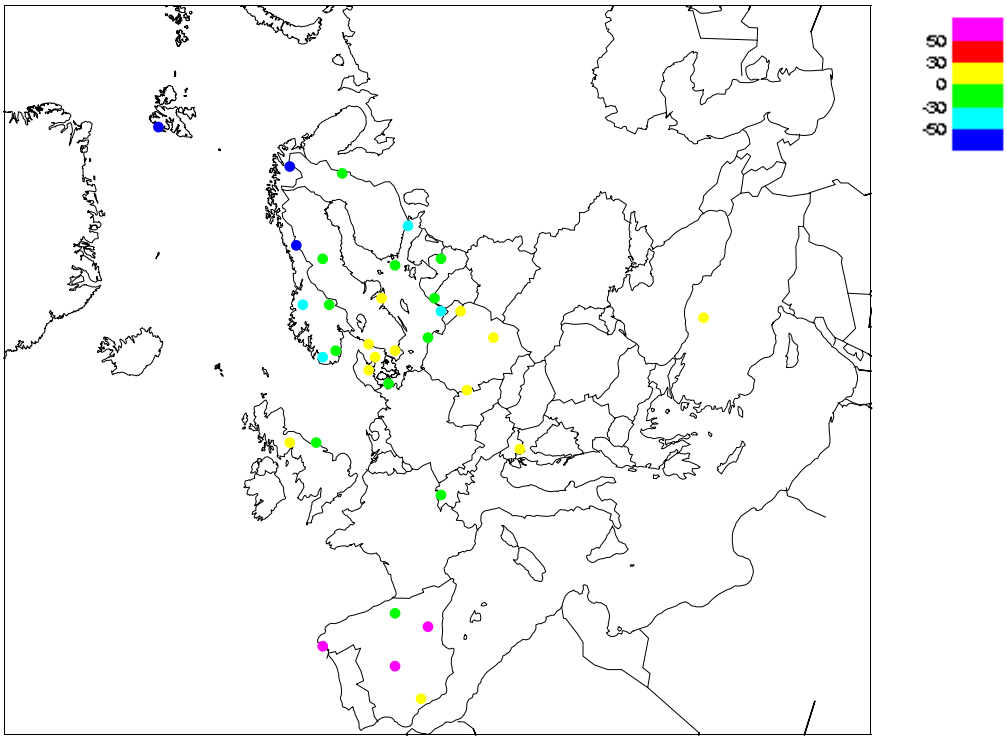

(b) Relative Bias

Figure 1.36: Correlation coefficient and relative bias for wet deposition of sulphur, 1997.

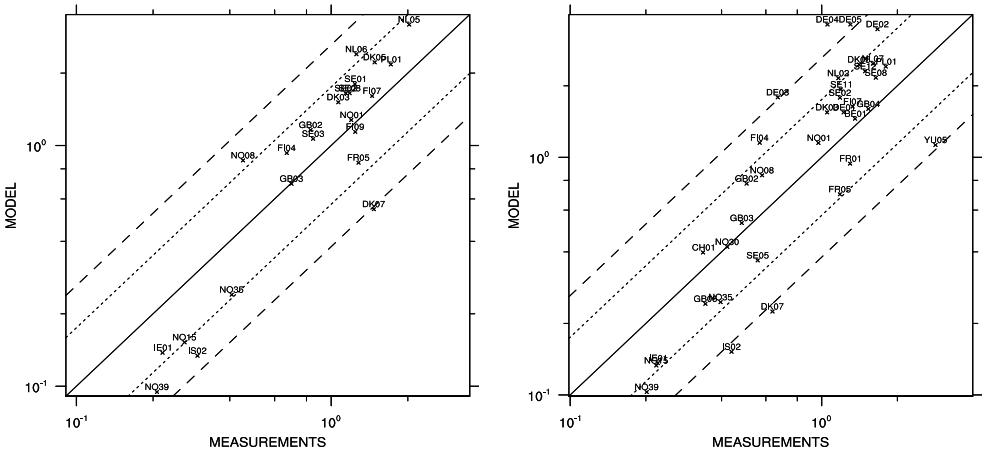

(a) 1980

(b) 1985

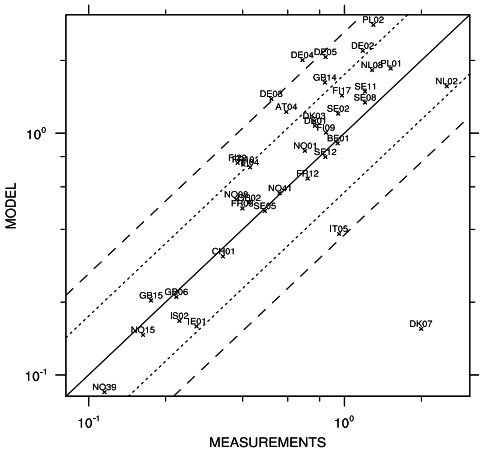

(c) 1990

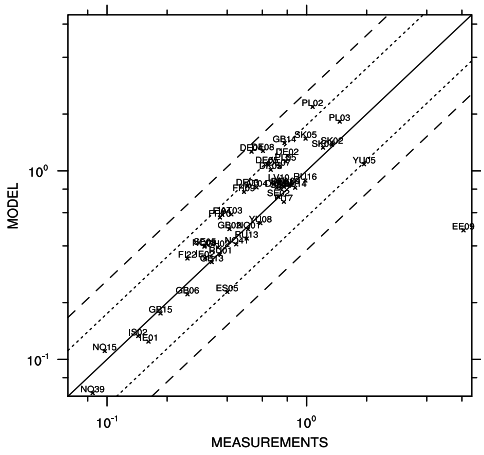

(d) 1995

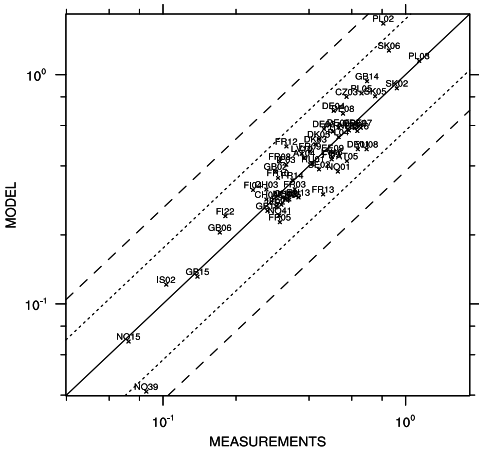

(e) 1998

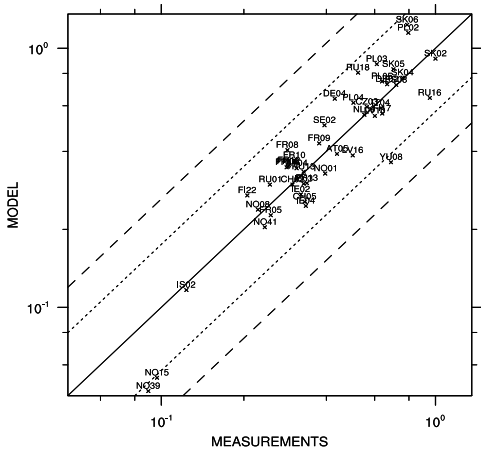

(f) 2000

Figure 1.37: scatter-plots of modelled versus observed sulphur concentration in precipitation (μg(S)l^{-1}), 1980, 1985, 1990, 1995, 1996 and 1997. Note that no quality criteria have been applied to determine which measurements to include in the comparison.

1.9 Oxidised Nitrogen in Precipitation

Calculated and measured concentrations in precipitation and wet deposition of oxidised nitrogen for 1980, 1985, 1990 and 1995-2000 for all stations in the EMEP network are compared in the figures 1.40 and 1.42. For the majority of sites, the relative bias is less than 50%, and most stations are actually within the '30%' line. In table 1.10 and 1.11 and figures 1.38 and 1.39 we present monthly time-series for oxidised nitrogen in precipitation for collections of stations in different regions in Europe. Wet deposition of nitrate is somewhat underestimated by the model for all parts of Europe. The best agreement is found in areas of West Europe, consistent with the best agreement for nitrate concentrations in air. The underestimation is particularly severe in southern Europe, where nitrate in air is largely overestimated and the amount of precipitation is underestimated. There is no indications for systematically larger underestimations in winter, which might have been suggested by the large overestimations of nitrate in air found in this period (c.f. section 1.5). However, the overestimation in winter is probably due to the nitrate equilibrium being too much shifted towards particulate nitrate. Nitric acid has a higher wet removal rate than particulate nitrate but also a faster dry deposition rate. The net result is probably a minor change in nitrate concentrations in precipitation.

Table 1.10: Bulk concentration of nitrate in precipitation (μg(N)l^{-1}). Ns; the number of stations where measurements were available for at least 75% of the days in a year , $pc < 50\%$; the percent of the data points (station yearly averages) with relative bias less than 50%, $pc < 30\%$; the percent with relative bias less than 30%. Obs; the measured yearly average over Ns stations, Mod; the modelled yearly average over Ns stations, $Bias$; the bias ($\frac{Model-Observation}{Observation} \times 100\%$), $Corr$; the correlation between observation and model for station yearly averages, $Ns(d)$; the number of stations where measurements were available for at least one day and $Corr(d)$; the daily correlation between all daily data for all stations for the actual year.

Period	Ns	pc<30%	pc<50%	Obs	Mod	Bias	Corr
1980	22	82	100	0.43	0.38	-11.00	0.86
1985	36	81	97	0.50	0.44	-11.00	0.78
1990	38	95	97	0.40	0.35	-10.00	0.84
1995	49	90	100	0.38	0.33	-12.00	0.75
1996	46	93	96	0.41	0.37	-10.00	0.70
1997	49	88	100	0.35	0.30	-13.00	0.76
1998	58	91	97	0.33	0.28	-15.00	0.78
1999	43	86	98	0.38	0.30	-19.00	0.78
2000	43	91	100	0.35	0.29	-18.00	0.86

Table 1.11: Nitrate wet deposition (μg(N)m^{-2})

Period	Ns	pc<30%	pc<50%	Obs	Mod	Bias	Corr	Ns(d)	Corr(d)
1980	22	91	100	6862	6021	-11	0.76	39	0.41
1985	36	75	97	13025	11554	-10	0.73	57	0.18
1990	38	79	100	11892	9702	-17	0.75	60	0.39
1995	49	80	96	15456	11536	-24	0.77	75	0.25
1996	46	85	93	15424	11112	-27	0.70	79	0.34
1997	49	82	96	14088	10217	-26	0.70	78	0.36
1998	58	86	97	17535	13057	-25	0.76	80	0.38
1999	43	81	95	14683	10069	-30	0.74	81	0.28
2000	43	93	98	14193	9895	-29	0.81	76	0.33

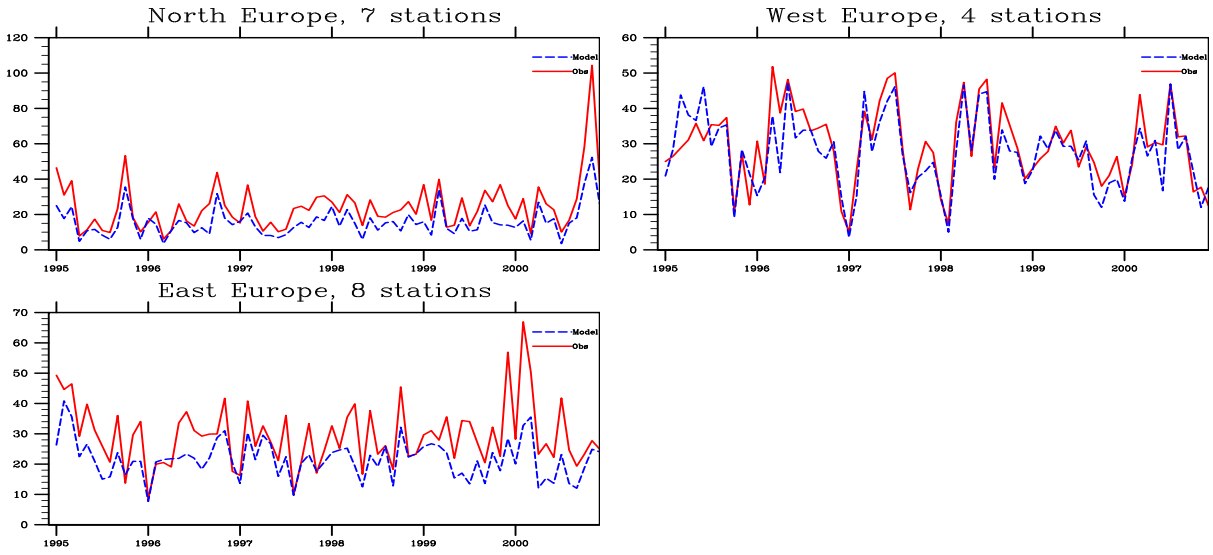

Figure 1.38: Monthly time-series of wet deposition of oxidised nitrogen (μg(N)m^{-2}), 1995-2000. All stations with data more than 25% of the days per year (and every year) have been included.

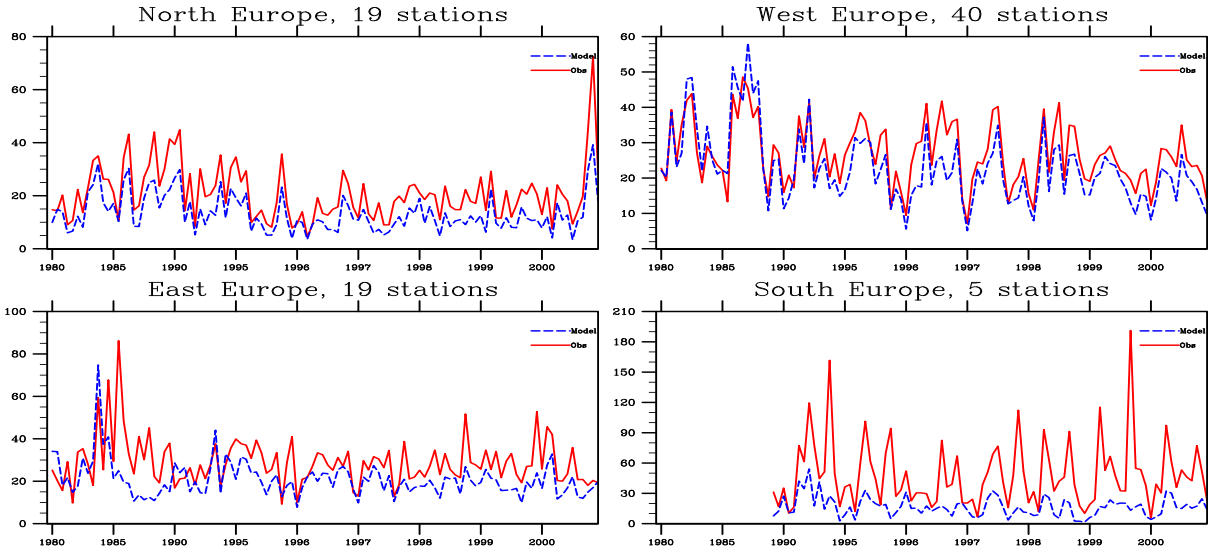

Figure 1.39: Monthly time-series of wet deposition of oxidised nitrogen (μg(N)m^{-2}), 1980, 1985,1990,1995-2000. All stations with data more than 25% of the days per year (but not necessarily every year) have been included. Note that the number of stations included in the comparison may vary from year to year. The total number of stations is denoted at the top of the figure.

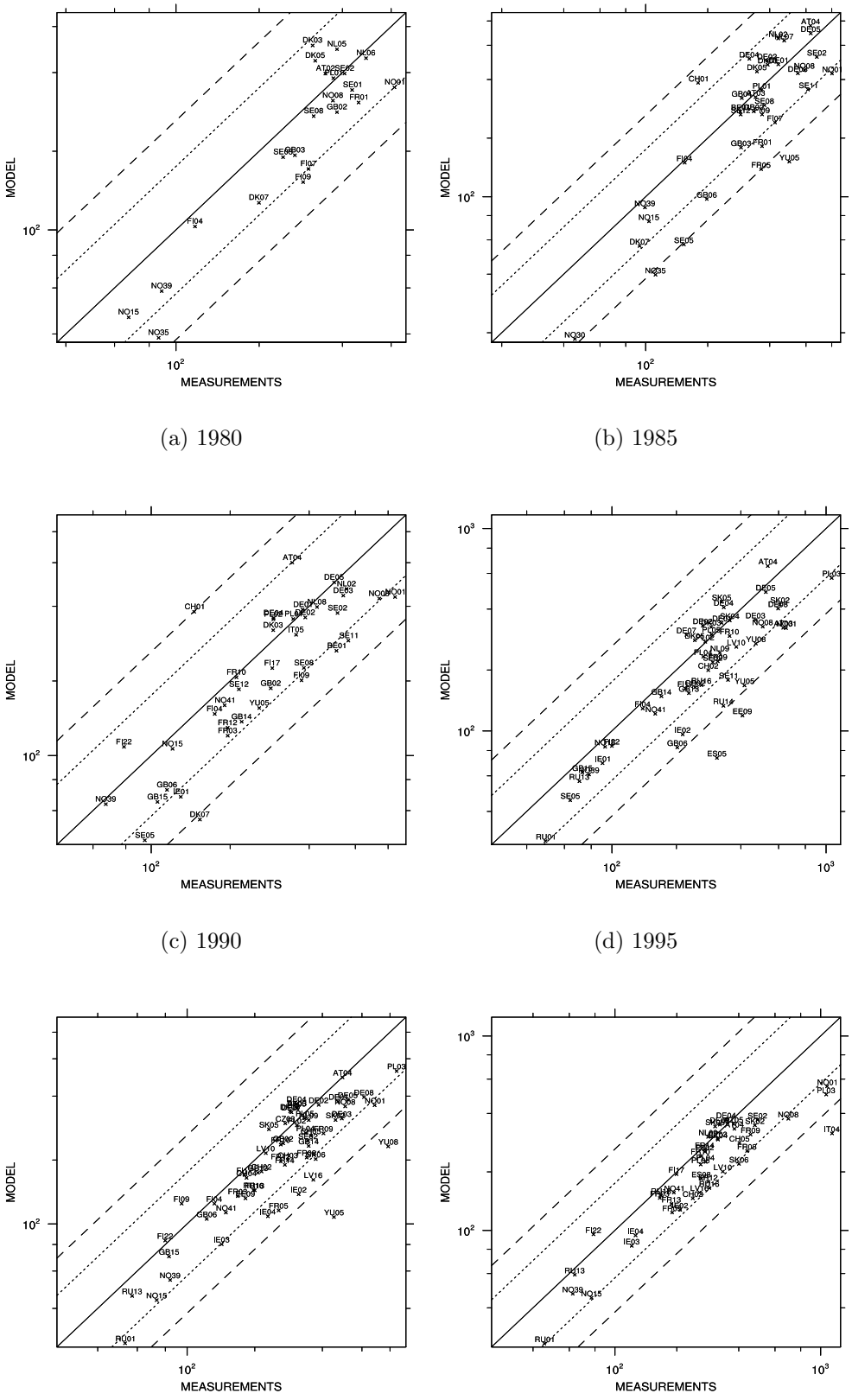

(a) 1980

(b) 1985

(c) 1990

(d) 1995

(e) 1998

(f) 2000

Figure 1.40: scatter-plots of modelled versus observed oxidised nitrogen wet deposition (μg(N)m^{-2}), 1980, 1985, 1990, 1995, 1996 and 1997. Note that no quality criteria have been applied to determine which measurements to include in the comparison.

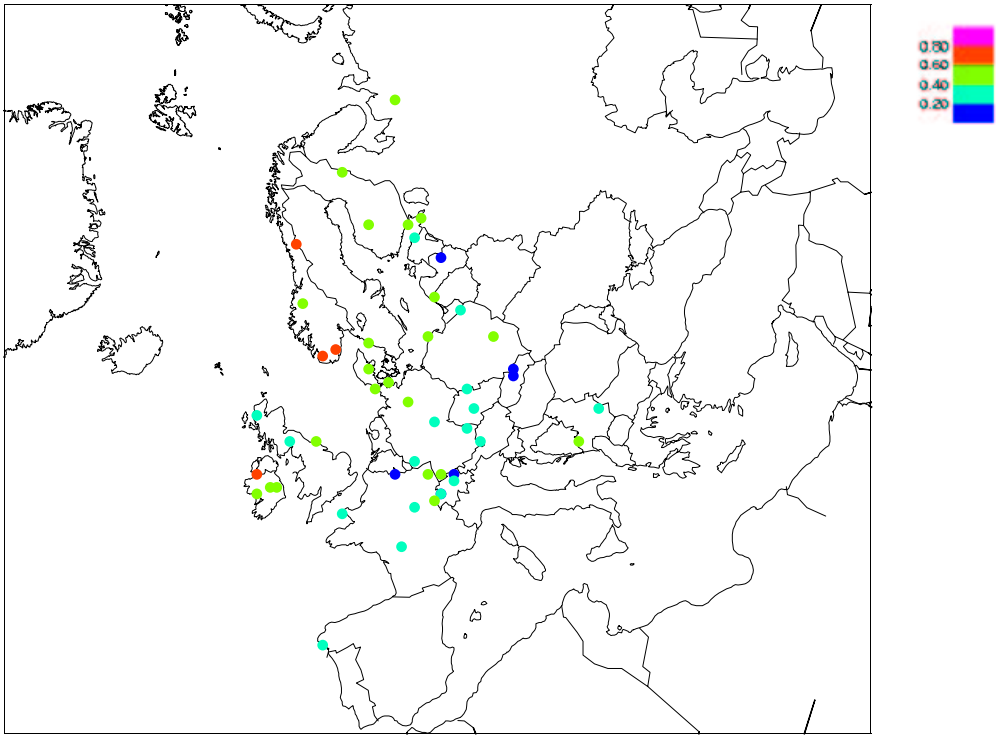

(a) Correlation

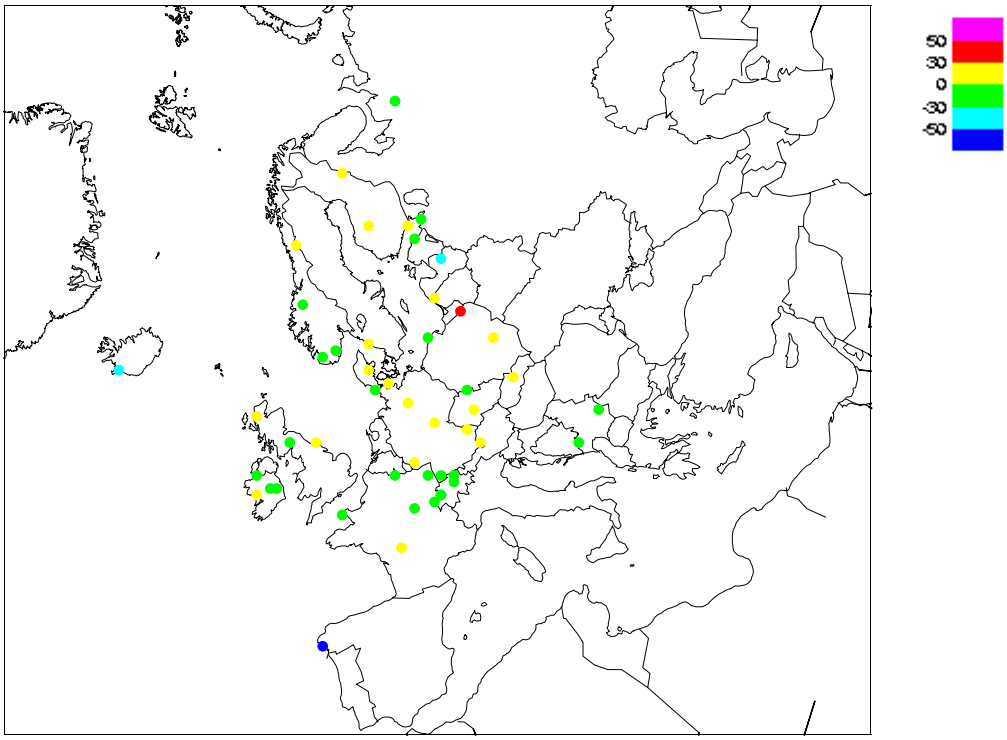

(b) Relative Bias

Figure 1.41: Correlation coefficient and relative bias for wet deposition of oxidised nitrogen , 1997.

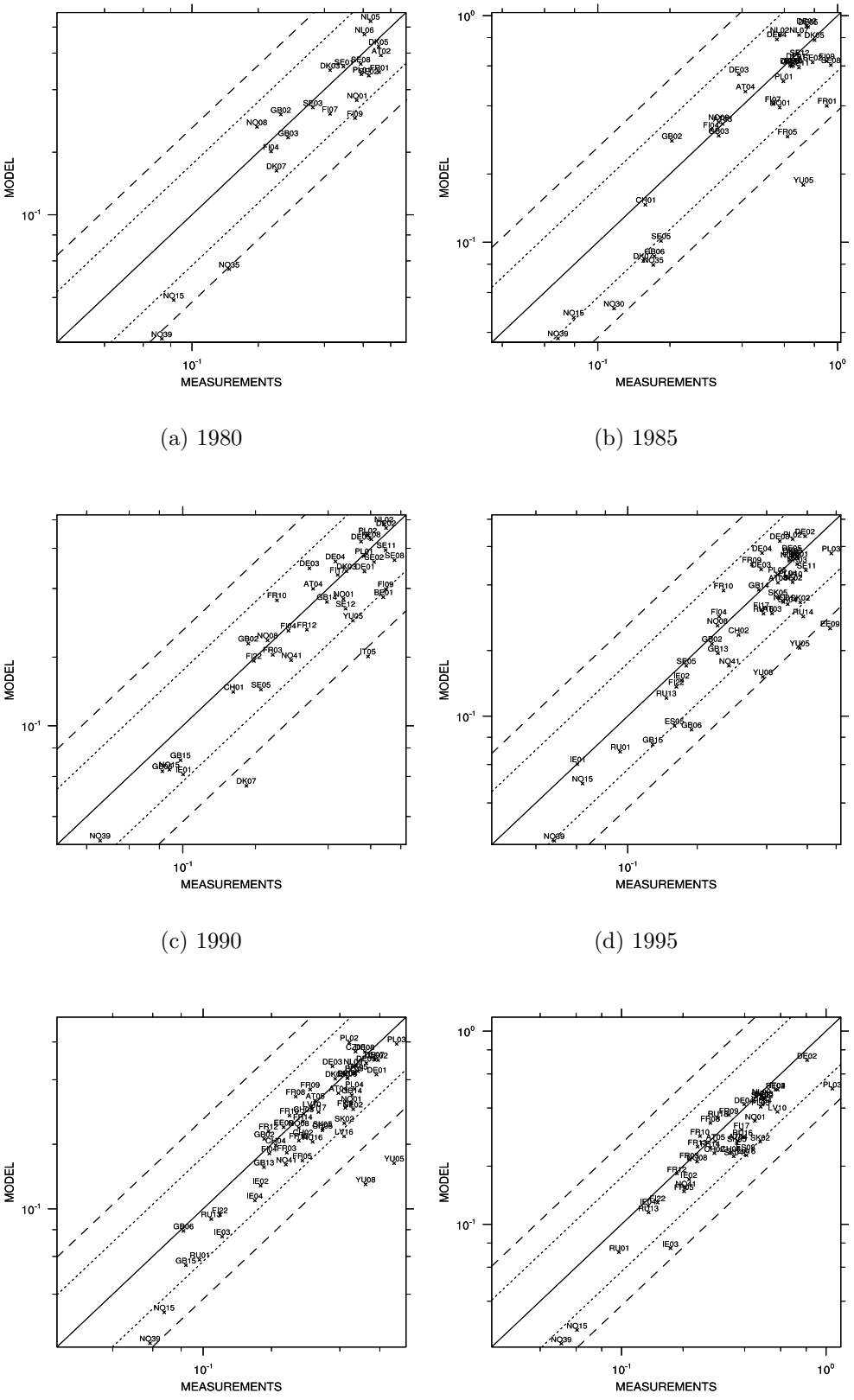

(a) 1980

(b) 1985

(c) 1990

(d) 1995

(e) 1998

(f) 2000

Figure 1.42: scatter-plots of modelled versus observed oxidised nitrogen bulk concentrations in precipitation, 1980, 1985, 1990, 1995, 1996 and 1997. Note that no quality criteria have been applied to determine which measurements to include in the comparison.

1.10 Reduced Nitrogen in Precipitation

scatter-plots for the years 1980, 1985, 1990, 1995-2000 for bulk concentrations of reduced nitrogen in precipitation and wet deposition are showed in figures 1.45 and 1.46. Similar to nitrate in precipitation, reduced nitrogen in precipitation exhibits an overall underestimation. The geographical pattern is also similar - with the best agreement in West Europe and the largest discrepancies between model and measurements in the south of Europe.

A number of nordic sites show relatively large underestimations of reduced nitrogen in precipitation, consistent with under prediction of reduced nitrogen in air. In general, central European stations show a better agreement between measurements and calculated values, also in accordance with the good agreement between observations and modelled air concentrations in this region.

A plausible explanation is that North European stations are situated in areas with low SO_x and NO_x emissions, and thus gaseous ammonia dominates the total levels of ammonia plus ammonium in air and precipitation. As discussed in section 1.6, NH_3 concentrations are difficult to model for a number of reasons. For the central European stations, a larger fraction of reduced nitrogen resides in the particulate phase, which in general is easier to model with regional scale models.

Table 1.12: Bulk concentrations of ammonium in precipitation (μg(N)l^{-1}). Ns; the number of stations where measurements were available for at least 25% of the days in a year , $pc < 50\%$; the percent of the data points (station yearly averages) with relative bias less than 50%, $pc < 30\%$; the percent with relative bias less than 30%. Obs; the measured yearly average over Ns stations, Mod; the modelled yearly average over Ns stations, $Bias$; the bias ($\frac{Model-Observation}{Observation} \times 100\%$), $Corr$; the correlation between observation and model for station yearly averages, $Ns(d)$; the number of stations where measurements were available for at least one day and $Corr(d)$; the daily correlation between all daily data for all stations for the actual year.

Period	Ns	pc<30%	pc<50%	Obs	Mod	Bias	Corr
1980	18	56	83	0.67	0.44	-34	0.87
1985	34	74	85	0.71	0.50	-29	0.77
1990	35	71	89	0.54	0.37	-31	0.69
1995	47	79	87	0.50	0.36	-27	0.62
1996	41	76	88	0.51	0.39	-23	0.62
1997	47	83	94	0.42	0.34	-18	0.68
1998	58	84	95	0.37	0.34	-9	0.78
1999	43	86	93	0.39	0.33	-14	0.84
2000	44	82	91	0.41	0.34	-15	0.64

Ammonium in precipitation results from scavenging of aerosol ammonium and

gaseous ammonia. Therefore, the model performance for ammonium in precipitation depends to some extent on the model performance for the sum of sulphate and nitrate in precipitation. As we have seen before, wet deposition of sulphur is reasonably well captured by the model (except for south Europe), whereas nitrate is overall somewhat underestimated. Thus, the underestimation of reduced nitrogen in precipitation can at least partly be a result of the corresponding underestimation of ammonium nitrate in precipitation.

Table 1.13: Wet deposition of ammonium (μg(N)l^{-1}). Ns; the number of stations where measurements were available for at least 75% of the days in a year , $pc <$ 50%; the percent of the data points (station yearly averages) with relative bias less than 50%, $pc <$ 30%; the percent with relative bias less than 30%. Obs; the measured yearly average over Ns stations, Mod; the modelled yearly average over Ns stations, $Bias$; the bias ($\frac{Model-Observation}{Observation} \times 100\%$), $Corr$; the correlation between observation and model for station yearly averages, $Ns(d)$; the number of stations where measurements were available for at least one day and $Corr(d)$; the daily correlation between all daily data for all stations for the actual year.

Period	Ns	pc<30%	pc<50%	Obs	Mod	Bias	Corr	Ns(d)	Corr(d)
1980	18	50	89	8344	5475	-33	0.76	39	0.14
1985	34	59	85	16694	12079	-27	0.82	56	0.08
1990	35	40	91	14959	9373	-36	0.51	60	0.31
1995	47	62	91	19858	12165	-38	0.72	75	0.28
1996	41	63	95	17060	11004	-34	0.72	79	0.33
1997	47	72	91	16705	11665	-29	0.71	78	0.36
1998	58	78	95	20271	15925	-20	0.72	80	0.34
1999	43	79	98	14911	11185	-24	0.80	81	0.24
2000	44	84	89	17062	12149	-28	0.53	76	0.21

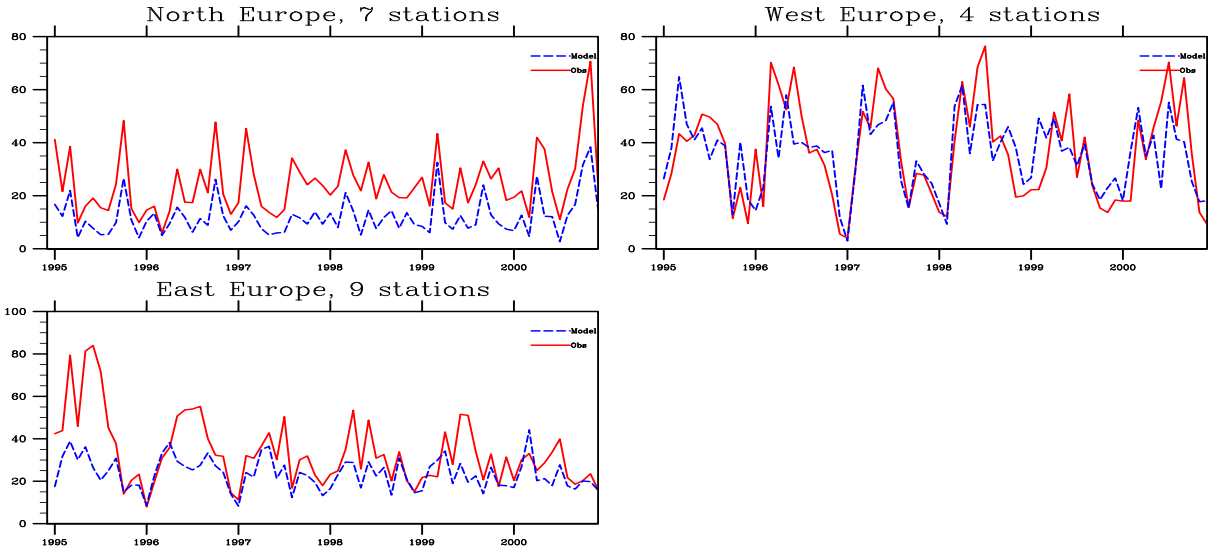

Figure 1.43: Monthly time-series of wet deposition of reduced nitrogen (μg(N)m^{-2}), 1995-2000. All stations with data more than 25% of the days per year (and every year) have been included.

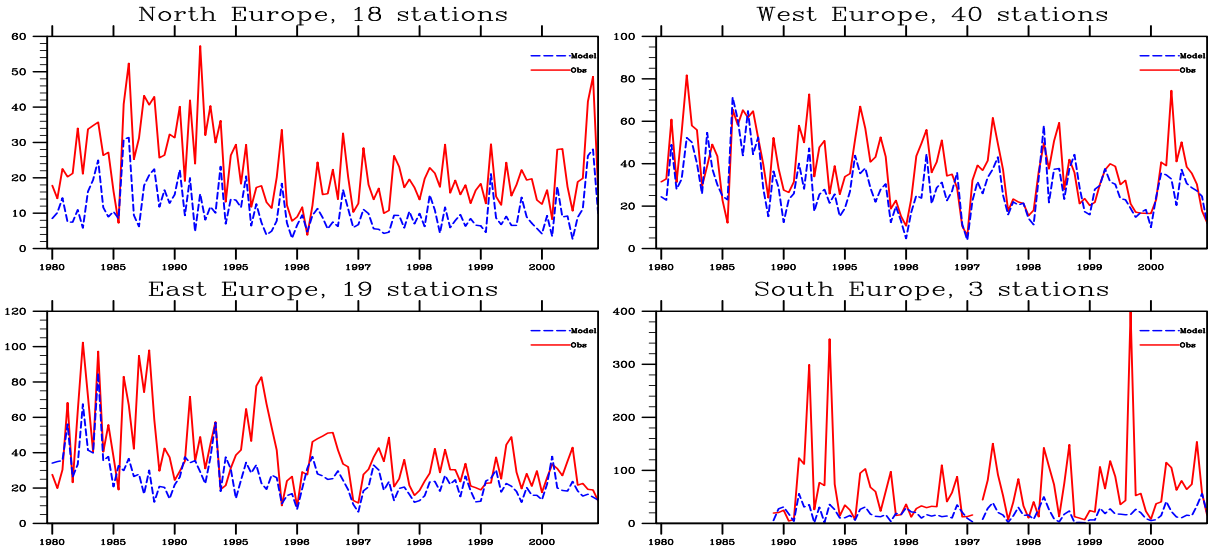

Figure 1.44: Monthly time-series of wet deposition of reduced nitrogen (μg(N)m^{-2}), 1980, 1985,1990,1995-2000. All stations with data more than 25% of the days per year (but not necessarily every year) have been included. Note that the number of stations included in the comparison may vary from year to year. The total number of stations is denoted at the top of the figure.

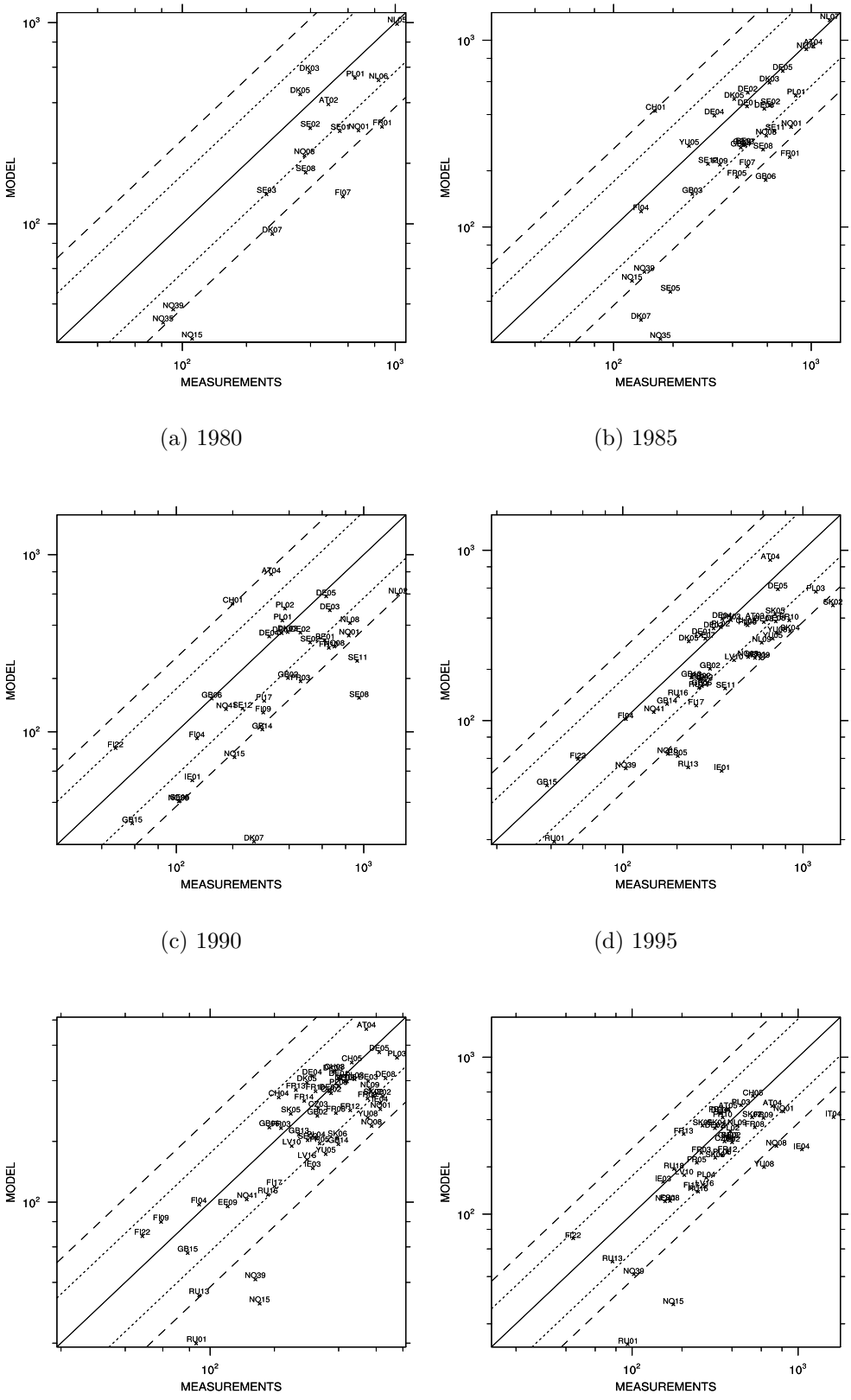

(a) 1980

(b) 1985

(c) 1990

(d) 1995

(e) 1998

(f) 2000

Figure 1.45: scatter-plots of modelled versus observed reduced nitrogen wet deposition (μg(N)m^{-2}), 1980, 1985, 1990, 1995, 1996 and 1997. Note that no quality criteria have been applied to determine which measurements to include in the comparison.

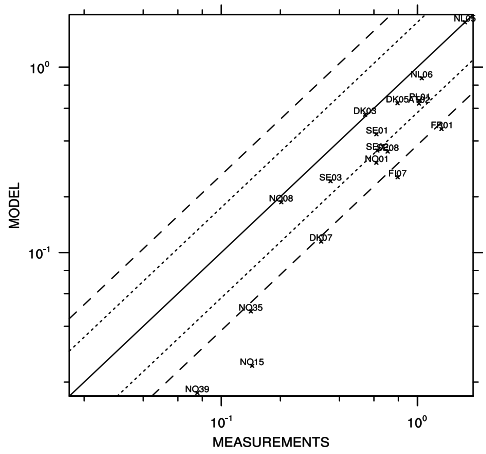

(a) 1980

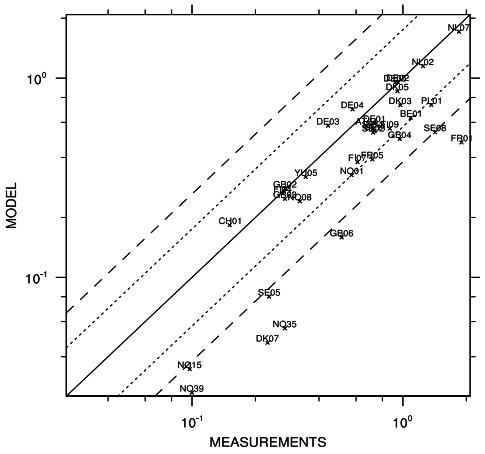

(b) 1985

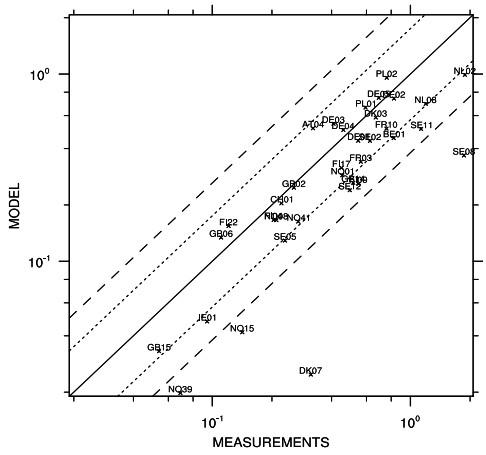

(c) 1990

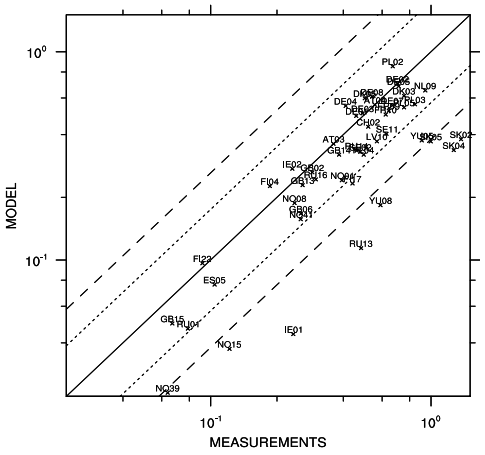

(d) 1995

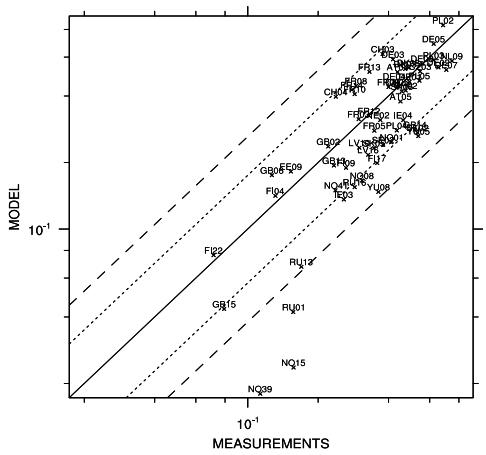

(e) 1998

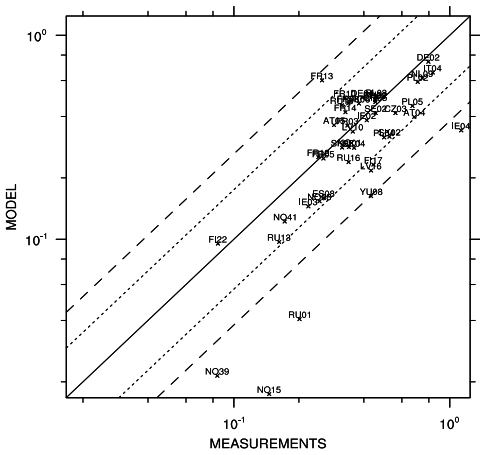

(f) 2000

Figure 1.46: scatter-plots of modelled versus observed reduced nitrogen bulk concentrations (μg(N)l^{-1}), 1980, 1985, 1990, 1995, 1996 and 1997. Note that no quality criteria have been applied to determine which measurements to include in the comparison.

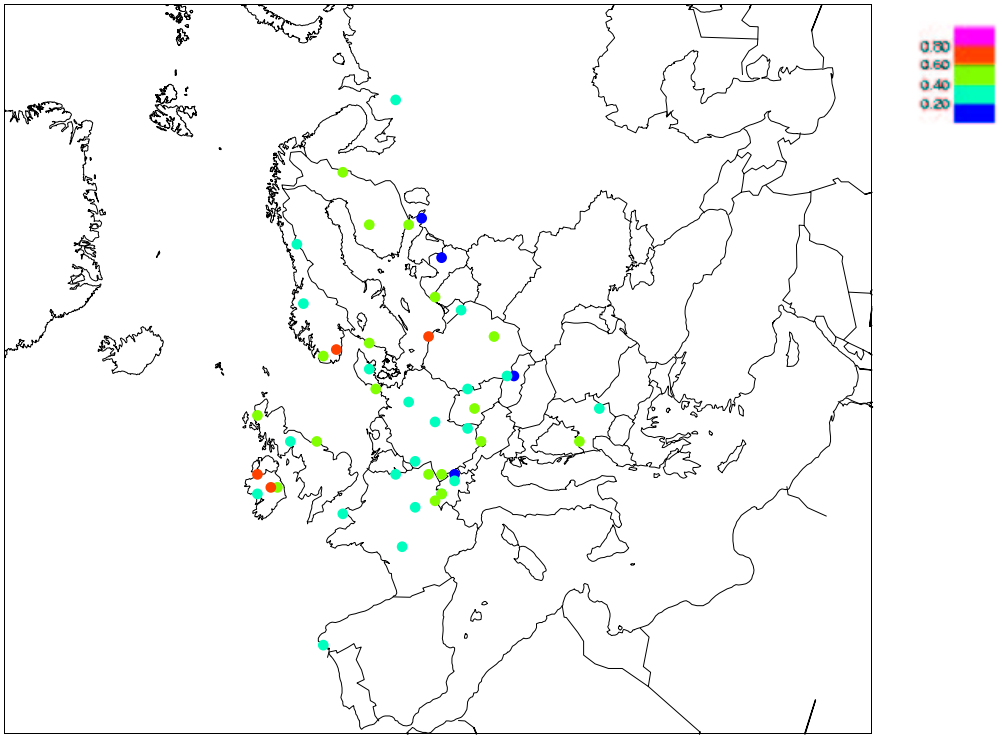

(a) Correlation

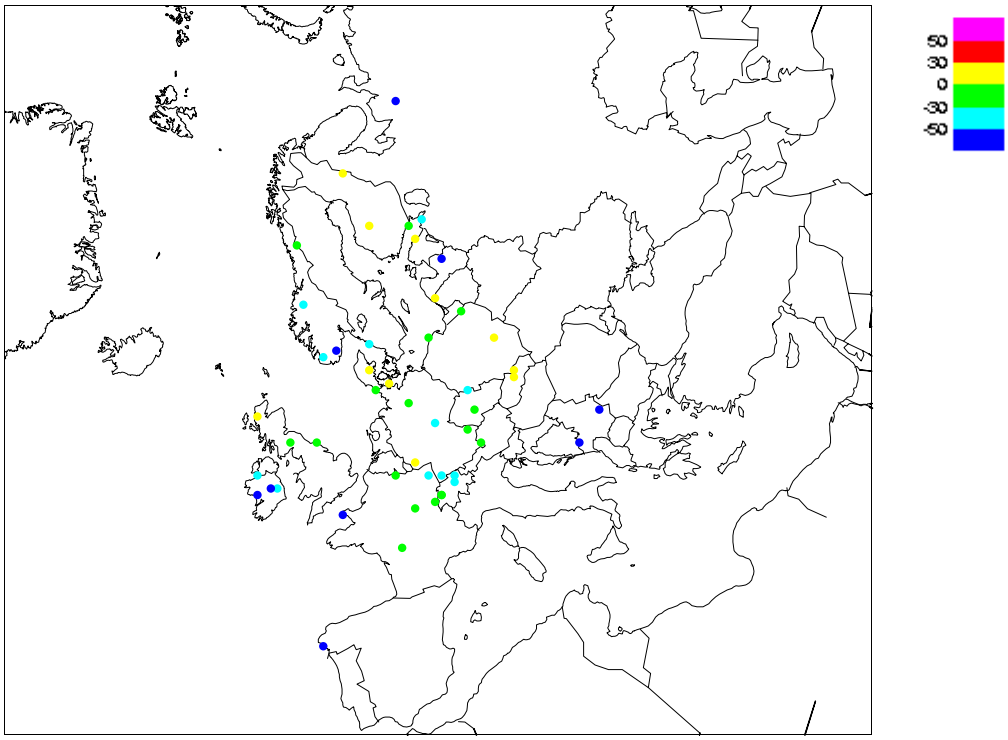

(b) Relative Bias

Figure 1.47: Correlation coefficient and relative bias for wet deposition of reduced nitrogen, 1997.

1.11 Conclusions

In this chapter, we have examined the performance of the EMEP Eulerian model (with full photo-oxidant chemistry), revision 1.7, for nitrogen and sulphur compounds using an extensive set of measurement data. The analysis has been based on comparison of model calculations and measurements for years from 1980 and onwards, focusing on the recent years.

The sulphur components (SO_2, SO_4^{2-}, SO_4^{2-} in precipitation) compares favourably with measurements. Modelled and observed seasonal cycles agree well, although some overestimation for SO_2 in cold periods is noticed for recent years. It is especially encouraging that the model reproduces the non linear changes in the seasonal cycle of sulphate during the twenty years of study (with a larger decrease in winter concentrations relative to summer concentrations).

Earlier versions of the EMEP model were found to over-predict SO_2 by more than a factor of two for the year 2000, despite good performance for 1990. We have found that a parametrisation of the co-deposition of NH_3 and SO_2 based on measurements from the LIFE sites (e.g. (Erisman et al.(2001))) give results that are in closer agreement with observations . This parametrisation, implemented in model revision 1.7, is included in all the model results shown here.

SO_2 is still found to be increasingly over predicted by the model from 1990 and onwards, although to a much lesser extent with this new revision (Bias: 39%, spatial correlation coefficient: 0.72 for 2000). However, given all the difficulties and known-problems with the data-sets being used, it would seem that in broad terms, model performance for SO_2 has remained rather constant over this long time period.

The sum of nitric acid and particulate nitrate in air is over predicted by the model ($\sim$ 50%), especially in winter. Preliminary results (see chapter 3) suggest that implementation of a more comprehensive equilibrium chemistry module (EQSAM, (Metzger et al.(2002b),Metzger et al.(2002a),)) gives total nitrate concentrations in better agreement with observations due to more correct gas-particulate partitioning. However, very few sites monitor gas and particulate nitrate simultaneously. In order to make a proper model evaluation of the equilibrium chemistry in the model there is an urgent need for more measurements!

The model results for ammonia plus ammonium in air agree well with monitoring data for West European stations, less for North and East European stations (for all stations: bias $\sim$ 10%, spatial correlation coefficient $\sim$ 0.8). In general, summer concentrations are underestimated compared to measurements, presumably due to problems in the modelling of the spatially variable ammonia gas in combination with influence of local sources on measurements.

Modelled wet deposition of sulphate agree well with observations (bias $\sim$ 10%, spatial correlation coefficient $\sim$ 0.6-0.8) , except for the South European stations. Wet depositions for reduced and oxidised nitrogen is underestimated for remote regions, whereas there is a better agreement between observations and model

results in central Europe. Both accumulated precipitation and nitrogen and sulphur wet depositions are heavily underestimated in South Europe (Bias around 30 %, spatial correlation coefficient 0.7-0.8).

It is well known (e.g (Cape and Leith(2002))) that dry deposition of NH_3 and SO_2 to open bulk precipitation collectors can account for a substantial part of the measured bulk wet deposition. Thus, the apparent under prediction of wet depositions may partly be caused by the bias in measured wet deposition. Further work is needed to fully understand the reason for the discrepancy between model and measured nitrate and ammonium wet depositions.

For all components, the analysis of model performance across Europe is dependent on the availability, geographical coverage and quality of the measurement data. No effort has been made to qualify model performance depending on the quality of the measurement sites. Under these conditions, model performance is comparable in northern, western and eastern Europe. The performance of the model in Mediterranean areas is systematically worse than in any other European area. To a large degree this is due to the poor quality of monitored air concentration data compiled in the area. However, this argument is not valid for measured concentrations in precipitation, where the quality of measurements is more stable. The model systematic underestimation of concentration in precipitation in Mediterranean stations may indicate the need to review the description of convective processes in the model.

Variations in the extent and quality from EMEP measurement sites, variability on emission input data and meteorological conditions contribute to the year to year variations in the presented model performance. These variations imply however small changes in the performance of the model and the model performance is rather homogeneous over the analysed years. In the few cases when the model performance for a specific year apparently differ significantly from other years, this is due to station measurement out-layers and often this can be traced back to e.g problems with the measurements for this year/site.

In general, differences in model performance are more significant across compounds than for the different years. This implies that the conclusions drawn here by compound are representative and provide a realistic overview on the performance of the Unified EMEP model against observations.

Chapter 2

Photo-oxidants

David Simpson, Hilde Fagerli, Sverre Solberg, Wenche Ås

2.1 Introduction

This chapter examines the performance of the EMEP photo-oxidant model (revision rv1.7) for ozone, NO_2 and aldehydes (HCHO). The analysis focuses on comparisons against recent measurements (2000), but some results will be presented for ozone as far back as 1990, and for NO_2 as far back as 1985. The later years have a much greater number of available measurements, especially for ozone. One may also expect emission inventories to be most accurate for later years so this period is most suitable for assessing performance.

2.2 Time-series for ozone

As in previous ozone model evaluations (Simpson, 1992, 1993, 1998, Simpson and Jonson, 1998, Jonson et al., 1998, 2002), , we use the daily maximum ozone as the basis of our statistical evaluation. The reason for this is that the daily maximum usually represents the time when the boundary layer is well-mixed (mid-afternoon, typically), and so modelled and observed concentrations should be most comparable.

Table 2.1 presents a summary of the model results compared against observations for all sites within the EMEP network. The correlation coefficients between the daily maximum ozone values are presented. It should be noted that no attempt has been made in this table to screen out sites which are believed to be influenced by local sources or to suffer from poor data quality, except that comparisons are only shown for those sites which had more than 274 valid days of observations. These results will be discussed region by region below, with plots presented for selected sites. Space requirements allow us to analyse only a small

proportion of these sites here, but plots for all sites and also for other years will be made available on the EMEP web-site, http://www.emep.int.

Table 2.1: Comparison of Modelled Versus Observed Ozone for Year 2000. Concentrations are 12-monthly Means of Daily Maximum Ozone Values. Correlation coefficient (r) are also between daily max values. Only sites with more than 275 valid observation days (N) are shown.

Code	Station	N (days)	Obs. (ppb)	Mod. (ppb)	r
		*N*ordic Countries			
DK31	Ulborg	351	38.41	37.82	0.79
DK32	Frederiksborg	351	33.05	37.95	0.86
FI09	Utoe	359	38.70	37.40	0.63
FI17	Virolahti II	359	36.28	35.92	0.73
FI22	Oulanka	365	35.74	33.83	0.76
FI37	Aehtaeri II	362	35.88	34.43	0.77
NO01	Birkenes	364	36.20	37.92	0.72
NO15	Tustervatn	364	38.92	37.80	0.74
NO39	Kaarvatn	365	40.11	38.24	0.64
NO41	Osen	363	35.94	36.16	0.70
NO42	Zeppelin	316	33.66	36.69	0.55
NO43	Prestebakke	360	37.40	38.35	0.77
NO45	Jeloeya	337	36.27	37.18	0.72
NO48	Voss	365	38.55	37.96	0.68
NO55	Karasjok	364	35.81	35.34	0.72
NO56	Hurdal	359	38.07	35.87	0.68
SE02	Roervik	365	39.63	37.93	0.78
SE11	Vavihill	360	37.67	37.33	0.82
SE12	Aspvreten	307	38.50	36.80	0.80
SE13	Esrange	365	36.65	35.02	0.80
SE32	Norra-Kvill	365	38.06	37.34	0.80
SE35	Vindeln	356	35.41	34.53	0.75
		*E*astern European Countries			
CZ01	Svratouch	361	43.45	41.83	0.82
CZ03	Kosetice	365	43.08	41.97	0.82
EE09	Lahemaa	363	39.49	33.23	0.68
EE11	Vilsandy	353	45.07	36.16	0.77
HU02	K-puszta	355	50.49	43.80	0.84
LT15	Preila	307	39.87	39.92	0.86

continued on next page

Code	Station	N	Obs.	Mod.	r
LV10	Rucava	343	34.35	37.07	0.76
PL02	Jarczew	324	40.93	40.92	0.81
PL03	Sniezka	365	53.28	41.84	0.81
PL04	Leba	358	39.62	38.35	0.83
PL05	Diabla Gora	354	40.75	39.40	0.85
RU18	Danki	290	30.62	39.43	0.63
SI08	Iskrba	349	50.13	46.77	0.79
SI31	Zarodnje	348	37.71	46.60	0.83
SI32	Krvavec	351	55.93	45.60	0.82
SI33	Kovk	356	47.07	45.00	0.84
SK04	Stara Lesna	337	43.84	41.87	0.71
SK06	Starina	337	43.29	43.52	0.80
SK07	Topolniky	331	42.51	44.86	0.56
	*C*entral and NW European Countries				
AT02	Illmitz	362	47.55	45.20	0.84
AT04	St. Koloman	364	48.94	45.11	0.72
AT05	Vorhegg	364	49.74	46.38	0.75
AT30	Pillersdorf	365	45.45	44.45	0.82
AT32	Sulzberg	357	49.46	46.85	0.75
AT33	Stolzalpe	351	48.18	45.27	0.71
BE01	Offagne	351	39.36	42.50	0.72
BE32	Eupen	351	38.19	38.55	0.70
BE35	Vezin	355	37.04	38.40	0.70
CH02	Payerne	354	41.97	44.11	0.78
CH03	Taenikon	361	41.76	42.59	0.78
CH04	Chaumont	350	47.51	43.85	0.79
CH05	Rigi	355	48.91	42.01	0.74
DE01	Westerl./Wenning.	360	41.23	37.20	0.68
DE02	Lang./Waldhof	355	39.39	39.37	0.83
DE03	Schauinsland	364	49.75	43.29	0.80
DE04	Deuselbach	291	44.00	43.59	0.77
DE05	Brotjacklriegel	336	47.71	43.53	0.78
DE07	Neuglobsow	355	37.26	38.45	0.83
DE08	Schmuecke	364	44.20	40.98	0.84
DE09	Zingst	363	36.75	33.88	0.76
DE12	Bassum	365	34.35	38.46	0.78
DE17	Ansbach	331	38.69	41.75	0.86
DE26	Ueckermuende	365	35.24	39.63	0.82
DE35	Lueckendorf	344	39.66	42.11	0.86
DE39	Aukrug	349	30.31	37.20	0.80
FR08	Donon	357	45.86	41.59	0.81
FR09	Revin	363	37.10	39.62	0.74

continued on next page

Code	Station	N	Obs.	Mod.	r
FR10	Morvan	344	40.01	40.98	0.73
FR12	Iraty	315	52.44	44.60	0.80
FR13	Peyrusse V.	357	35.23	40.13	0.57
FR14	Montandon	350	36.12	42.58	0.71
GB02	Eskdalemuir	362	32.54	37.21	0.77
GB06	Lough Navar	328	35.24	37.77	0.74
GB13	Yarner Wood	296	37.17	36.28	0.75
GB14	High Muffles	339	37.24	35.42	0.69
GB15	Strath Vaich	351	39.52	38.41	0.75
GB31	Aston Hill	330	38.04	37.46	0.72
GB32	Bottesford	364	34.92	34.02	0.74
GB33	Bush	340	35.54	35.10	0.67
GB34	Glazebury	274	33.51	35.04	0.73
GB36	Harwell	356	36.19	35.35	0.70
GB37	Ladybower	344	35.49	32.93	0.62
GB38	Lullington H'th	330	38.91	38.25	0.73
GB39	Sibton	332	35.50	35.84	0.73
GB44	Somerton	335	40.76	36.79	0.68
GB45	Wicken Fen	278	33.55	34.35	0.77
IE31	Mace Head	354	41.12	40.16	0.72
NL09	Kollumerwaard	360	33.53	36.00	0.81
NL10	Vreedepeel	339	30.88	36.01	0.75
	*M*editerranean Countries				
ES04	Logrono	347	43.08	44.79	0.77
ES07	Viznar	358	49.73	46.69	0.72
ES08	Niembro	361	38.13	43.76	0.68
ES09	Campisabalos	331	47.32	46.27	0.72
ES10	Cabo de Creus	357	54.71	44.09	0.80
ES11	Barcarrota	353	41.99	44.55	0.75
ES12	Zarra	364	49.27	47.50	0.85
IT01	Montelibretti	313	49.83	48.81	0.77
IT04	Ispra	356	49.61	49.78	0.73

2.2.1 Nordic Sites

Figure 2.1 presents time-series plots of modelled versus observed daily maximum ozone concentrations for a number of Nordic sites for the year 2000. Figures 2.2 presents similar plots from the years 1990 and 2000 for some of the longer-term measurements sites. In general, the model reproduces the observed concentrations rather well at these Nordic sites, and in many cases the agreement is excellent.

Seasonal variations and peaks are simulated well, over all years, especially at the Norwegian and Swedish sites. The good agreement at Tustervatn (NO15), which is located at around 66°N suggests that the procedures used for setting boundary conditions in the model (making use of obseverations from Mace Head, at only 53°N, see Simpson et al., 2003) perform well even in the far northern part of the domain.

One problem can be seen at the Finnish sites, which sometimes show episodes of high ozone in the spring months which are not picked up by the model (e.g. Oulanka, March 2000 Fig. 2.1). This behaviour is not so evident in the other Nordic countries, so cannot be ascribed to problems with boundary conditions. It seems that the model is overpredicting losses of ozone in air masses transported to Finland. A possible reason could be difficulties in defining the dry deposition characteristics of the land surface in this period of winter/spring transtion.

2.2.2 Eastern European Sites

Figure 2.3 presents time-series plots of modelled versus observed daily maximum ozone concentrations for a number of North-Eastern European sites for the year 2000. Figure 2.4 presents similar plots for one further site in Russia and for sites in South-Eastern Europe. No data are available for 1990 at any of these sites.

As for the Nordic sites, the model is able to reproduce the time-series for most of these sites rather well. Performance is poor for only two of the sites shown, Lahemaa (EE09) in Estonia and Danki in Russia. Performance is also poor for a second Estonian site (EE11, not shown), but is is not clear why these sites are poorly reproduced when compared to other sites in the Baltic region (including the Finnish site Utö and the Russian site Shepeljovo, RU16, which lies nearby). The second Russian site, Danki (RU18) lies closer to Moscow and here the discrepancy between the modelled and observed ozone values is very large.

Results for sites in SE Europe are generally good, with correlation coefficients usually exceeding 0.8. Except for the Slovakia site Starina there seems to be a tendency for the model to show lower ozone values than the observations, especially in summer-months.

2.2.3 Central and North-West European Sites

Figure 2.5 presents time-series plots of modelled versus observed daily maximum ozone concentrations for a number of central and North-West European sites for the year 2000. Figures 2.6 presents similar plots from the years 1990 and 2000. The model performs well for all of these sites, with correlation coefficients often exceeding 0.8 and with good reproduction of seasonal cycles. There seems to be some tendency to underpredict the highest ozone episodes, but the occurrence of most episodes is reproduced well.

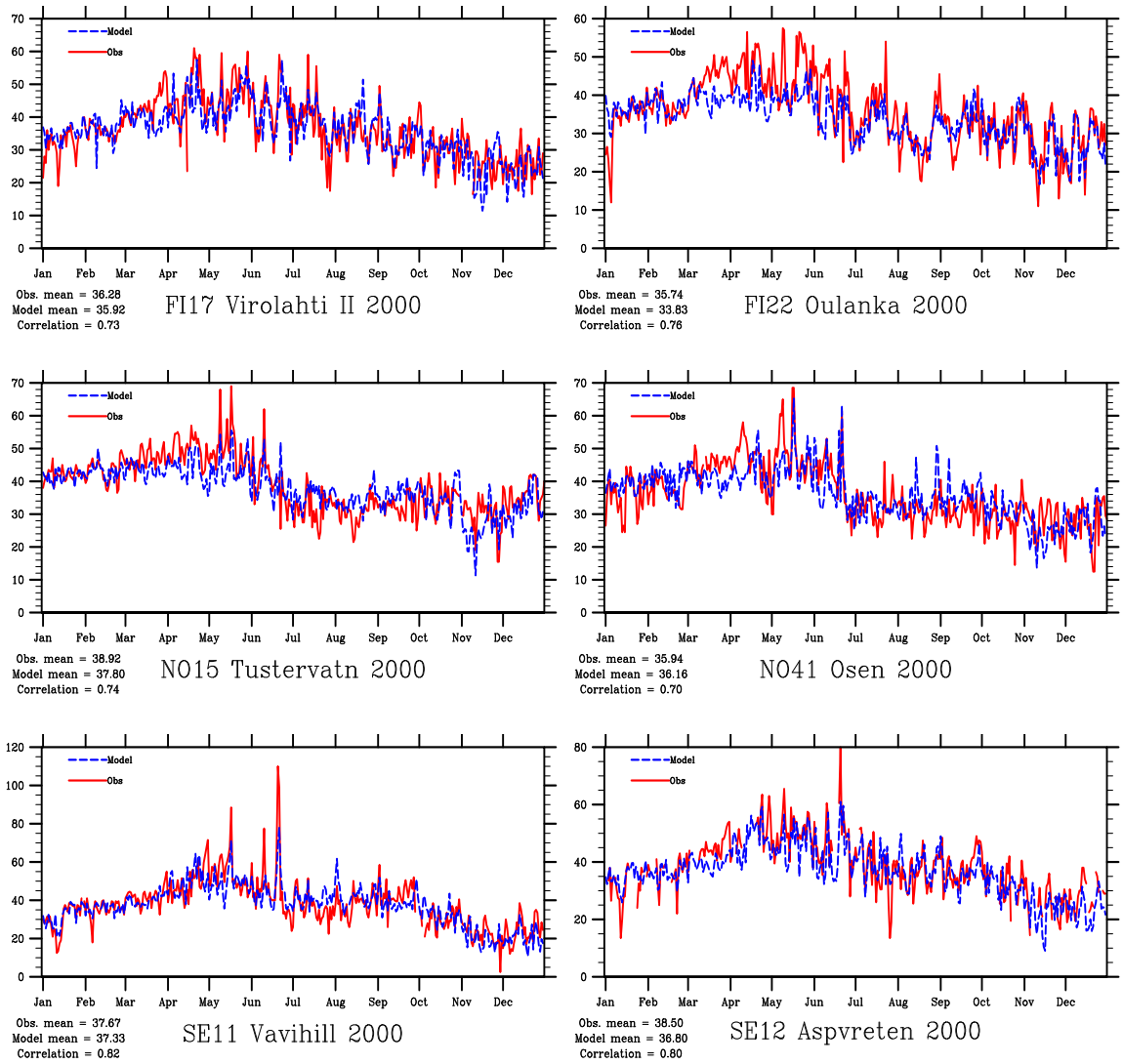

Figure 2.1: Modelled versus Observed Daily Max Ozone (ppb), Nordic Sites, 2000

It is encouraging that the model performance is so consistent across these sites, as they actually represent a large mixture of climates and ozone regimes. The remote site Mace Head (IE31) represents one extreme, being situated on the West coast of Ireland and only occasionally subject to episodes of high ozone. This sites play a strong role in setting the boundary conditions for the EMEP model (Simpson et al., 2003), so good agreement is guaranteed here for the seasonal cycle, but the ozone episodes that do occur here are well captured by the model. The seasonal cycle is also reproduced well for sites with very different concentration levels, for example DE02 (Langenbrügge/Waldhof). Furthermore,

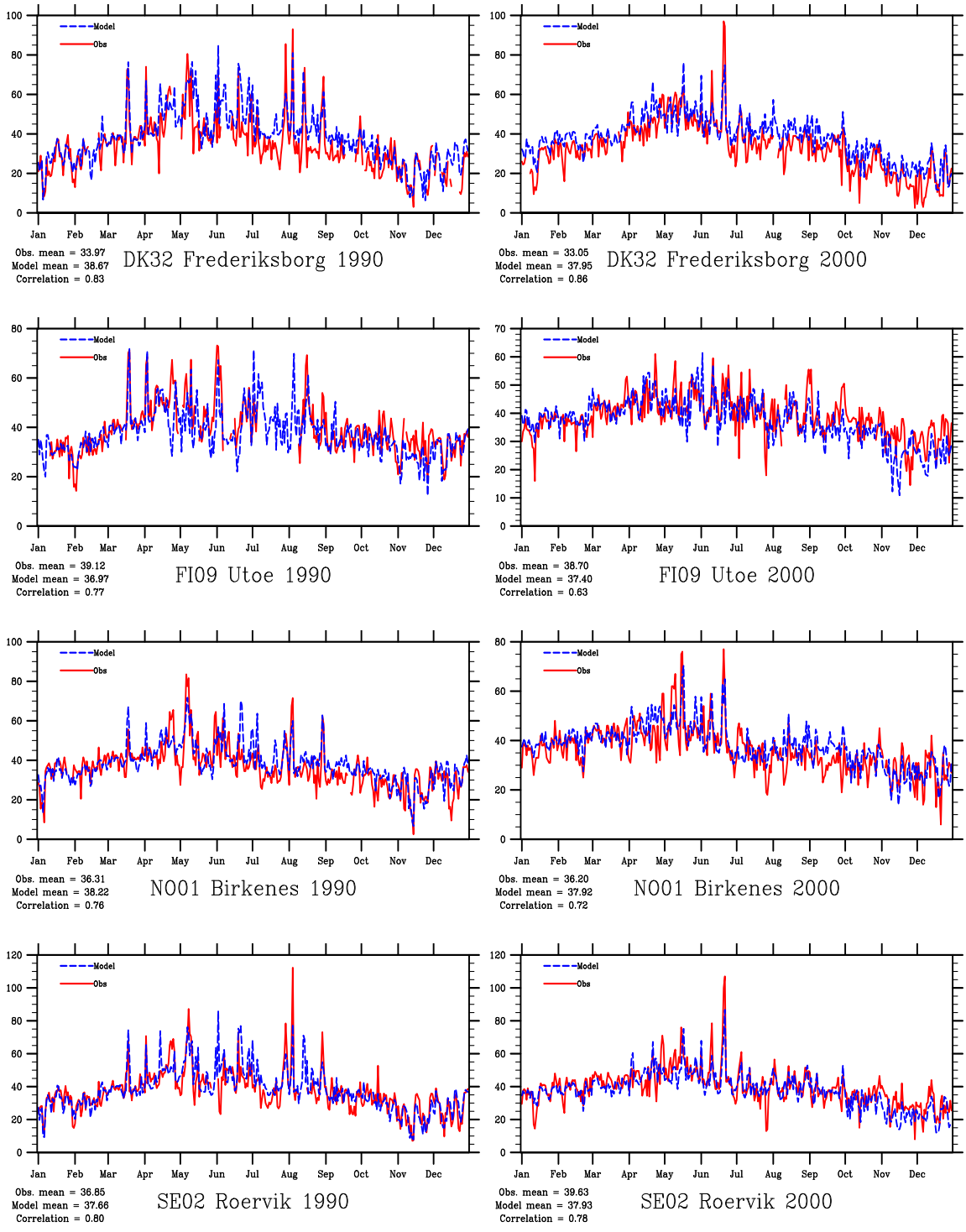

Figure 2.2: Modelled versus Observed Daily Max Ozone (ppb), Nordic Sites, 1990 and 2000

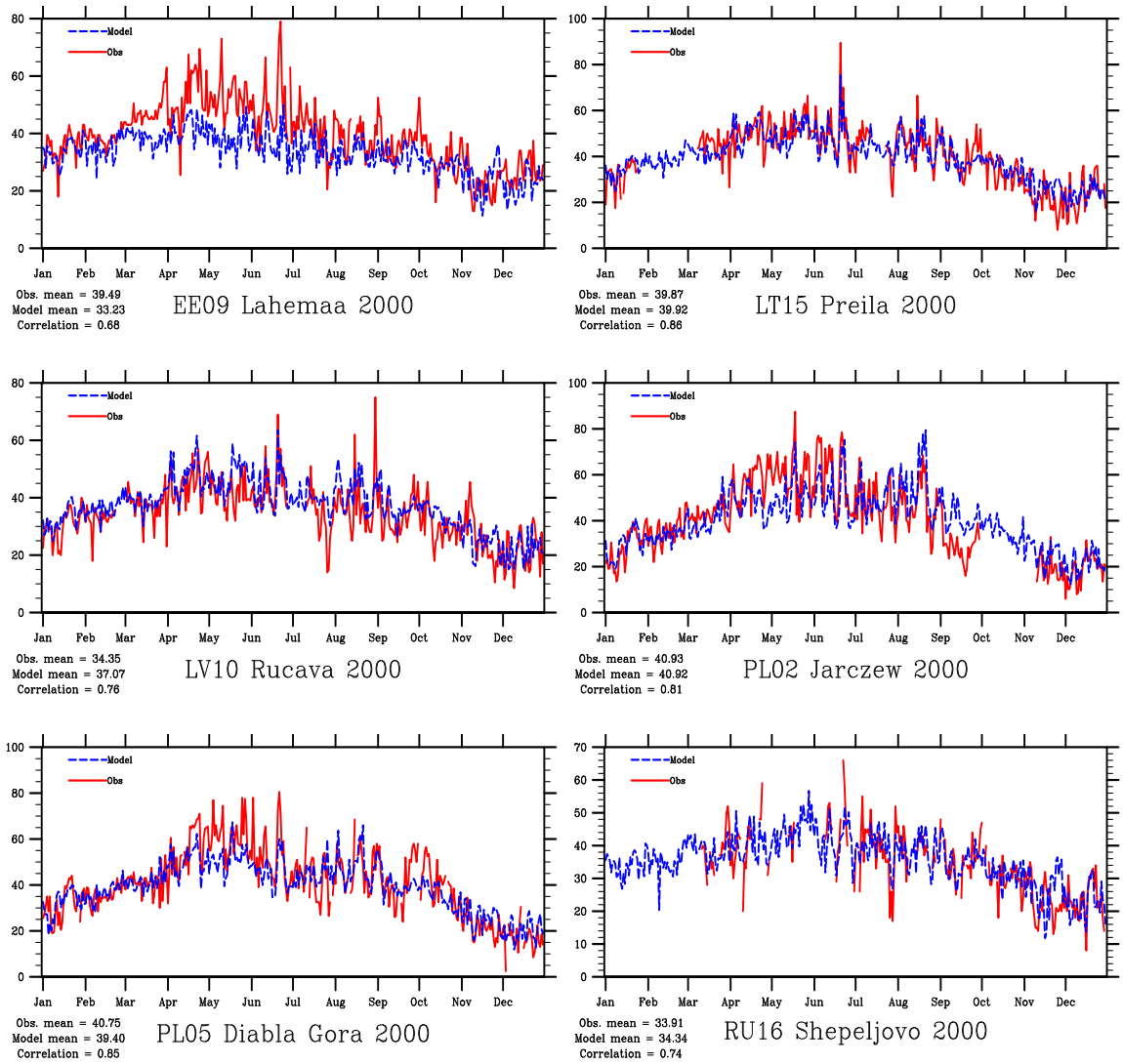

Figure 2.3: Modelled versus Observed Daily Max Ozone (ppb), North Eastern Europe, 2000

sites located in the Alps (AT02, AT04, CH02) shows similar levels of agreement across the year.

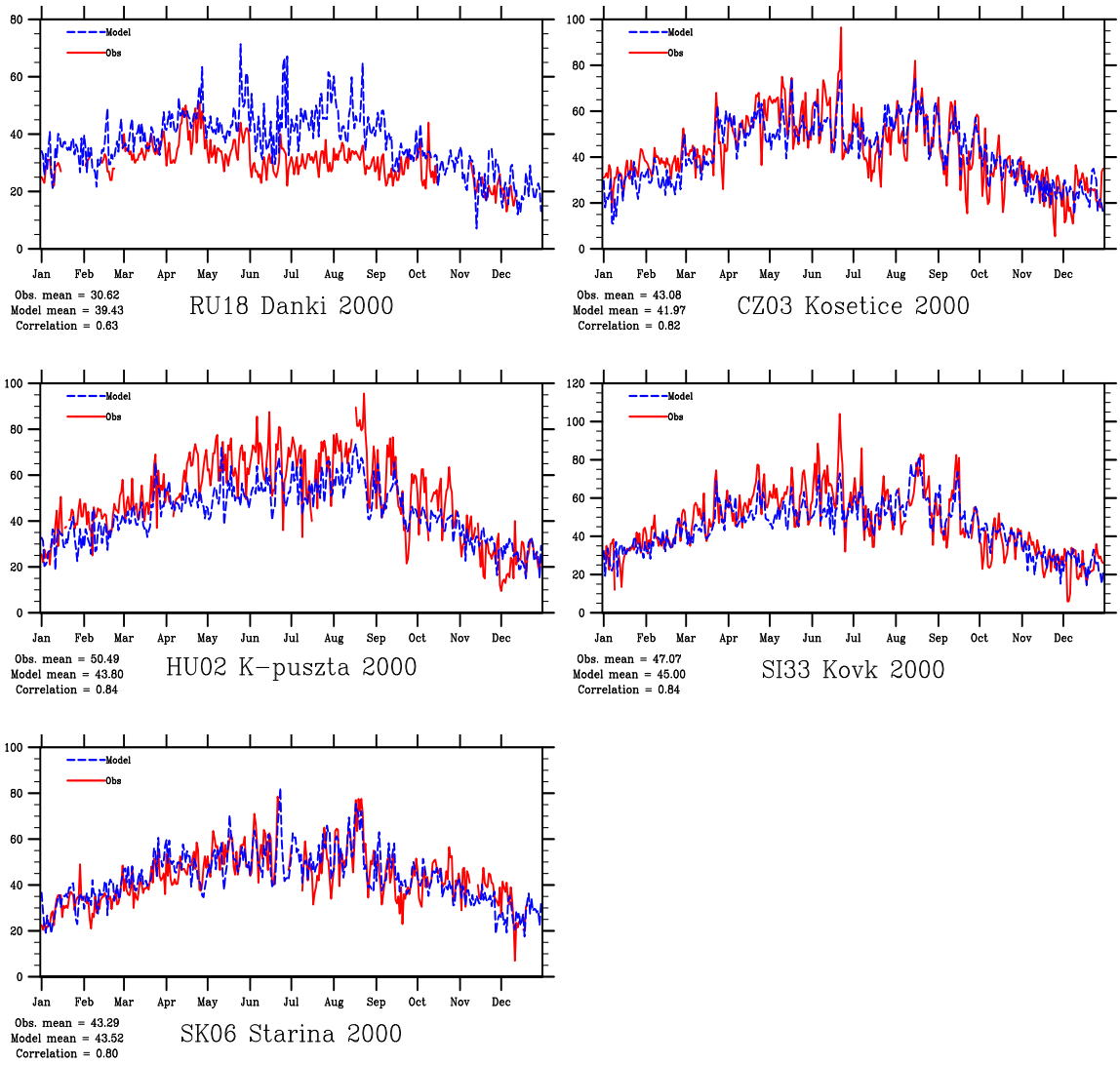

Figure 2.4: Modelled versus Observed Daily Max Ozone (ppb), East and South-East Europe, 2000

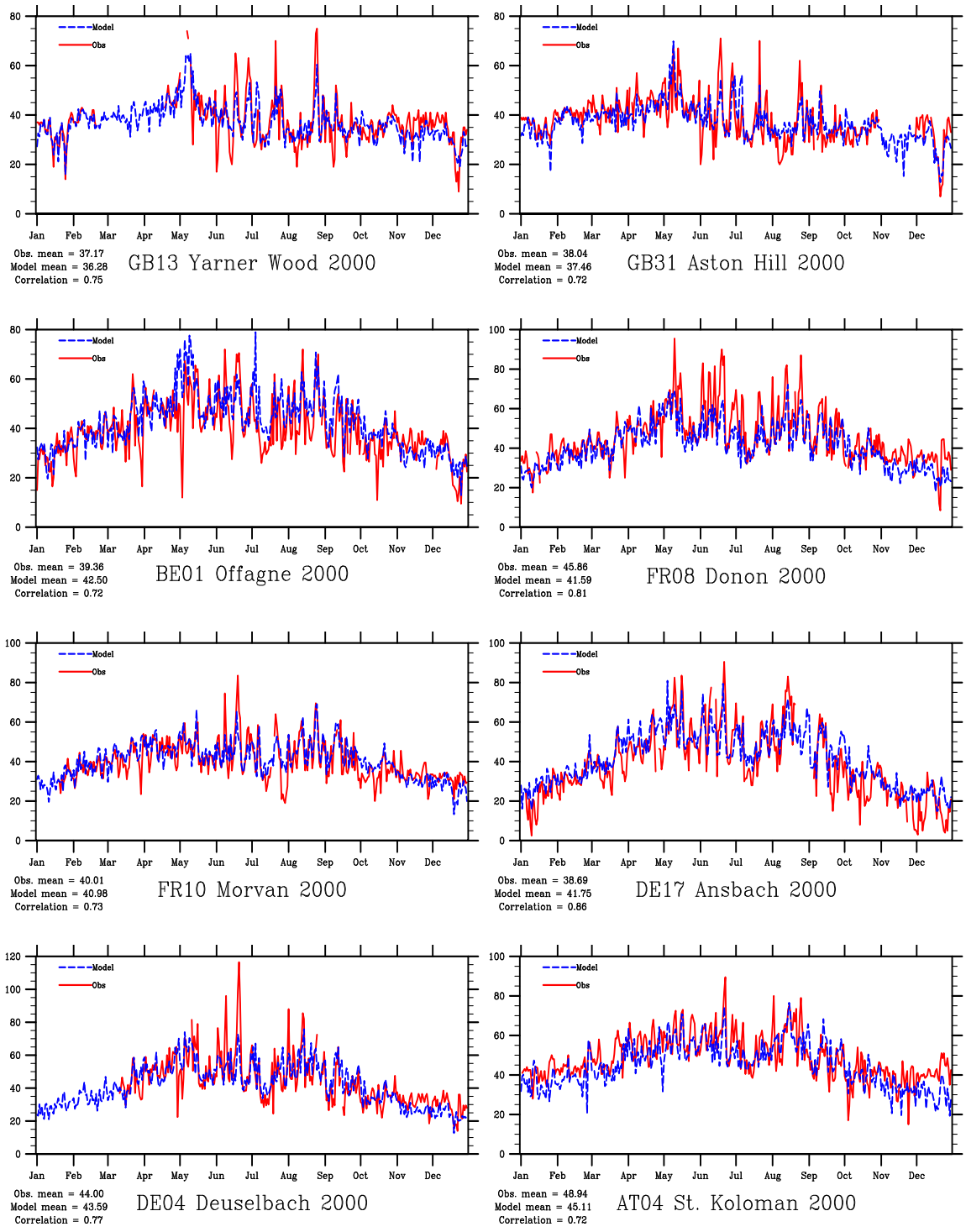

Figure 2.5: Modelled versus Observed Daily Max Ozone (ppb), Central and NW European Sites, 1999, and 2000

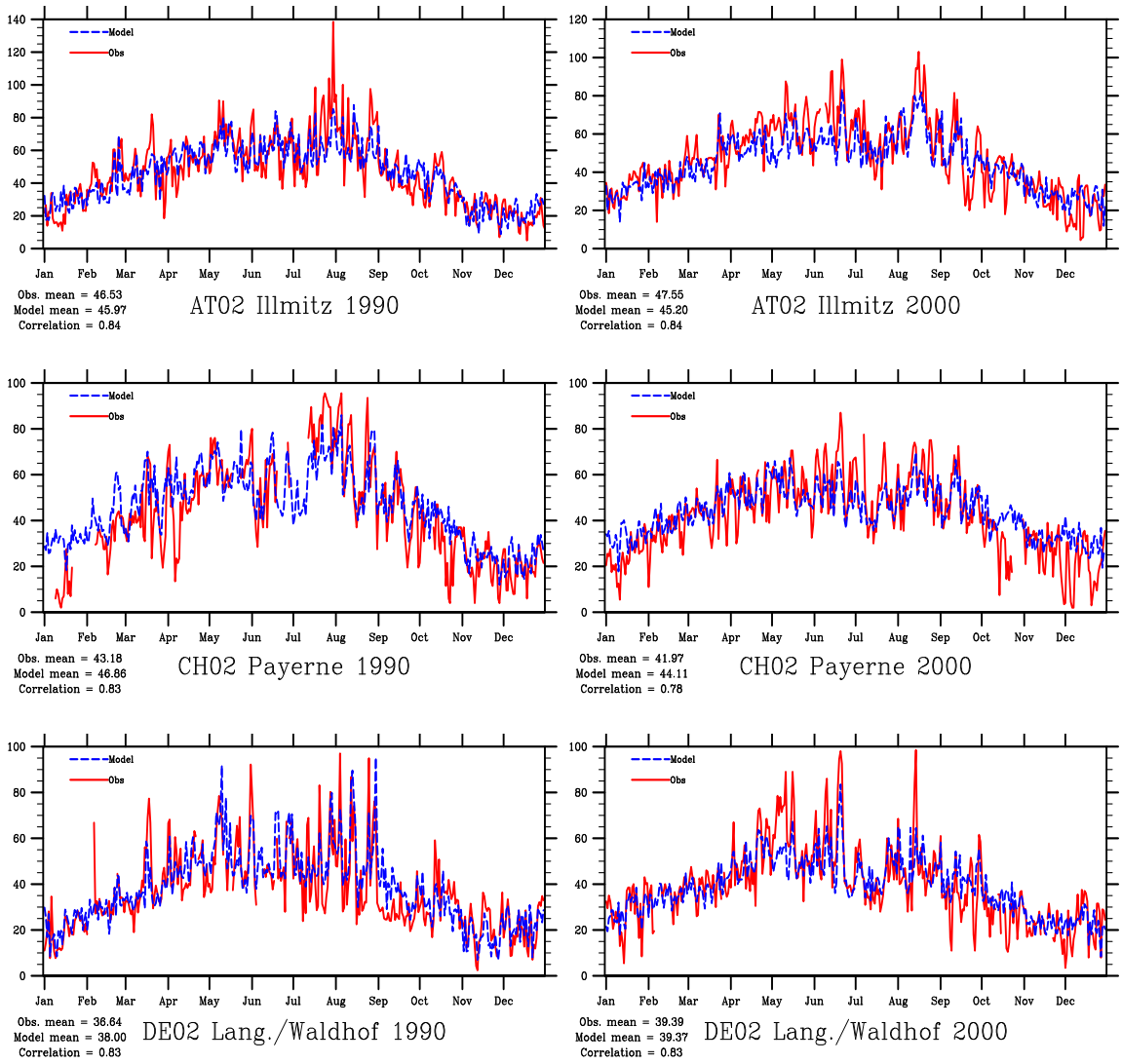

Figure 2.6: Modelled versus Observed Daily Max Ozone (ppb), Central and NW European Sites, 1990 and 2000

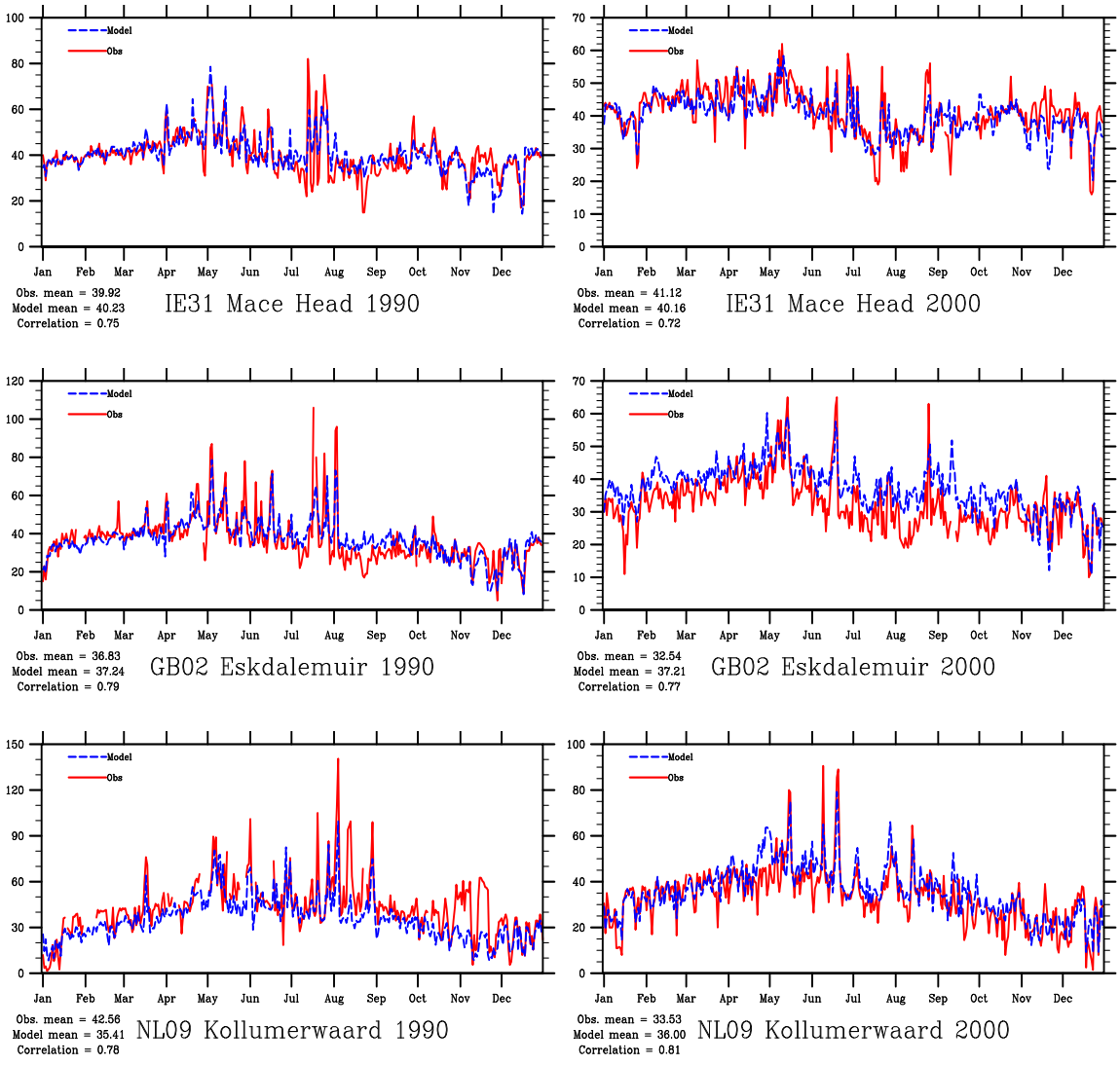

Figure 2.6: Continued

2.2.4 Mediterranean Sites

Only one site in the Mediterranean has observations for both 1990 and 2000 – the site Ispra (IT04). These results are shown in Figure 2.7. Many more sites are available for the year 2000 though, and Figure 2.8 presents time-series plots of modelled versus observed daily maximum ozone concentrations for a number of Mediterranean European sites for this year.

The model reproduces the observed concentrations at the Italian sites Ispra (IT04) and Montelibretti (IT01) rather well, although the latter suffers from some data-capture problems (and zero-ozone days) in the summer of 2000. In fact, the model seems to perform well for Ispra in all years studied, whereas results for Montelibretti are more mixed. It can be noted that Montelibretti is situated near to Rome, and often influenced by the urban plume – as is evident presumably in the frequent episodes of almost-zero ozone seen in Fig. 2.8.

The remaining site plots show a rather mixed performance. The French sites Iraty (FR12, close to the Spanish border) and Peyrusse Vieille (FR13, also southern France), and the Spanish sites shown here are reproduced reasonably well.

It should be noted that much greater disagreements are seen for several other Spanish sites (Partly included in Table 2.1, although several sites were excluded from this table because of low data-capture). However, as reported previously (Aas et al., 2000 - EMEP/CCC-Rep 6/2000) several Spanish sites established prior to 1999 were too affected by local pollution sources to be regarded as background sites, and many of these have now been closed down, including Toledo (ES01), Noia (ES05), Roquetas (ES03) and Logrono (ES04). Viznar (ES07) is situated close to Grenada with 300 000 inhabitants and so is also excluded. Spain has established a set of newer sites (from 1999 onwards) which are more suited to model evaluation for EMEP purposes, and we therefore concentrate our analyses to these sites (ES08-ES15).

Similarly, the long-term Portuguese site Monte Velho also shows clear signs of local influence, with ozone concentrations often depressed to low levels. This site is therefore excluded from our analysis.

Poorer results are obtained from a relatively new Mediterranean station, Giordan lighthouse (MT01) on Malta, and from the two Greek stations (Aliartos, GR01, and Finokalia, GR02). Although correlations are reasonable, the model systematically underpredicts observed O_3 at MT01 and GR02. Results for Aliartos are better. As these sites are relatively new to the network it is difficult to say at this stage if these problems are due to model performance, emissions, or boundary conditions for this region, or to problems with the observations.

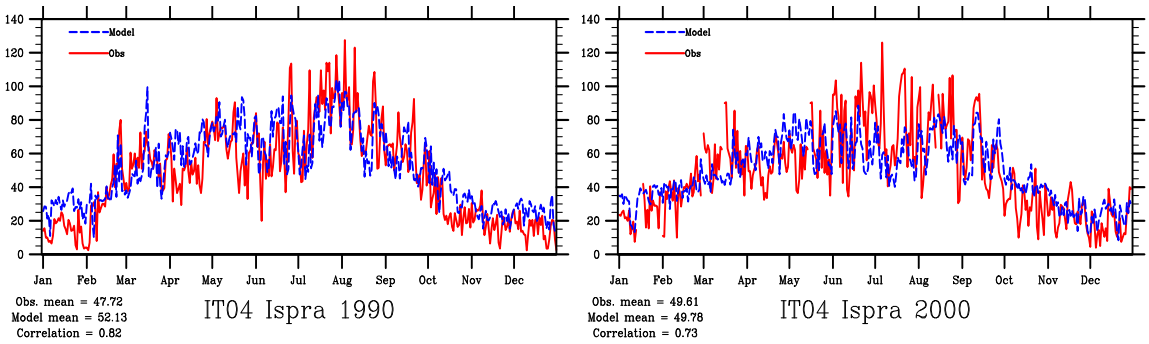

Figure 2.7: Modelled versus Observed Daily Max Ozone (ppb), Ispra (N. Italy), 1990 and 2000

2.3 Frequency Distributions for O_3

The daily maximum ozone concentrations from the model and measurements can also be displayed as frequency distributions and cumulative frequency distributions. Figure 2.9 illustrates these distributions for all years from 1990 to 2000. Data from the 17 stations which had data over this period are used, in order to compare like-with-like from year to year. Unfortunately this means that the analysis is representative mainly for North West Europe where these sites are located. In fact, only one Mediterranean site (Monte Velho, Portugal) reported data for all of these years, However, this site often shows very low ozone values, presumably due to nearby NOx sources, and is therefore excluded from the frequency analysis.

Figure 2.9 shows that for most years the modelled and observed frequency distributions match rather well. The shapes and peaks of the distributions are reproduced to a satisfactory degree, although the model has a clear tendency to a narrower distribution. The years 1997 and 1999 are the most clear examples of this, where the model underpredicts high ozone values and over-predicts low ozone values. Many reasons could be offered for such behaviour, among them the simple fact that the modelled values are averages over 50×50 km^2 grids of height $\sim$100 m, whereas the measurements are point values and hence subject to a noisier distribution. As an example, a site within a grid square is more likely to pick up local plumes of excess ozone arising from the photochemistry of nearby city emissions. On the other hand, the same site is also more likely to pick up plumes of ozone-depleted air which arise from NO_x titration, due perhaps to nearby traffic or urban area sources.

Concerning time-trends, there seems to be little change in model performance over the years. The year-to-year variation (e.g. from 1997 to 1998) is larger than the variations seem from 1990 to 2000, and it would seem that model performance is thus comparable over the 10-year period.

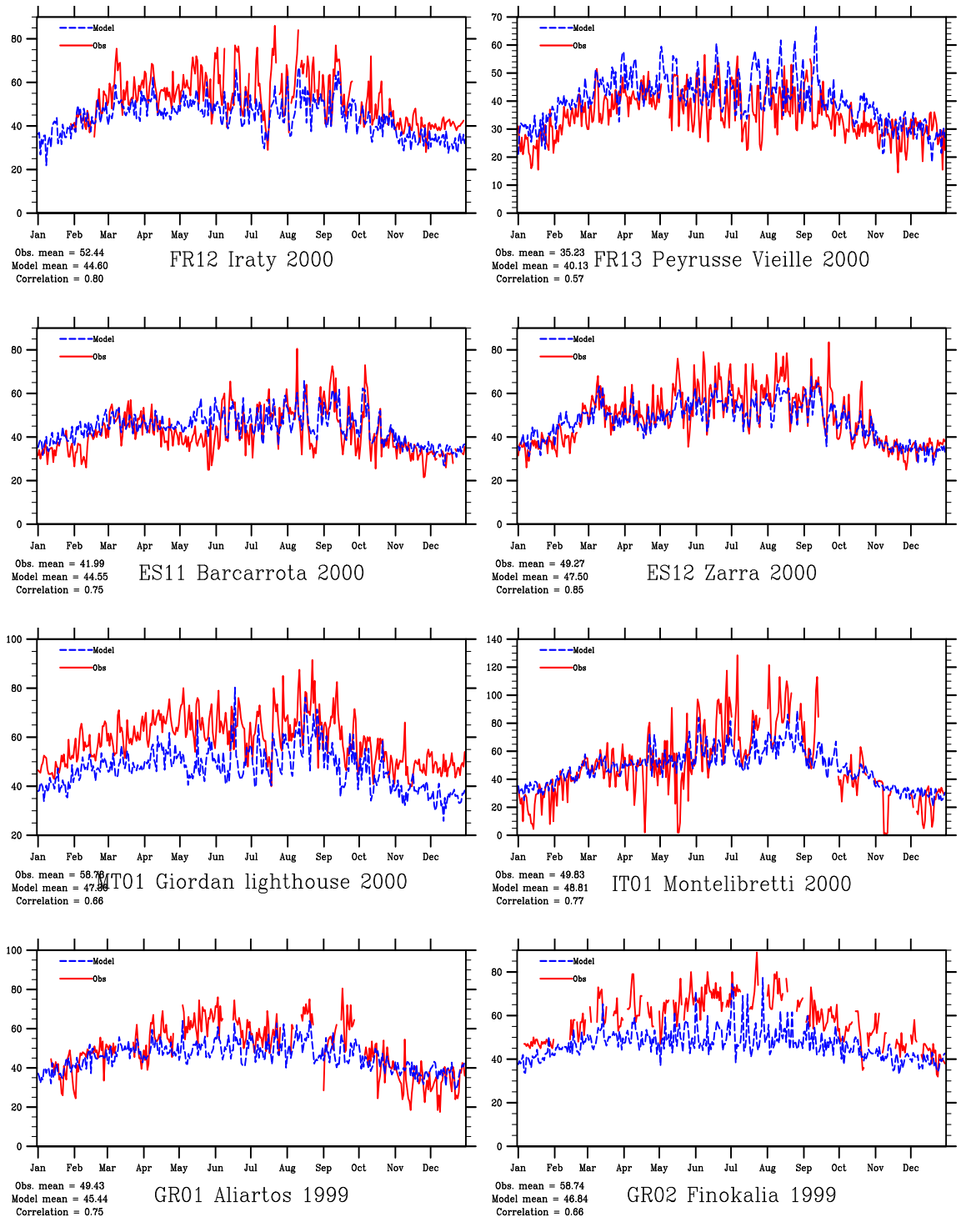

Figure 2.8: Modelled versus Observed Daily Max Ozone (ppb), Mediterranean Sites, 2000 (1999 for Greece)

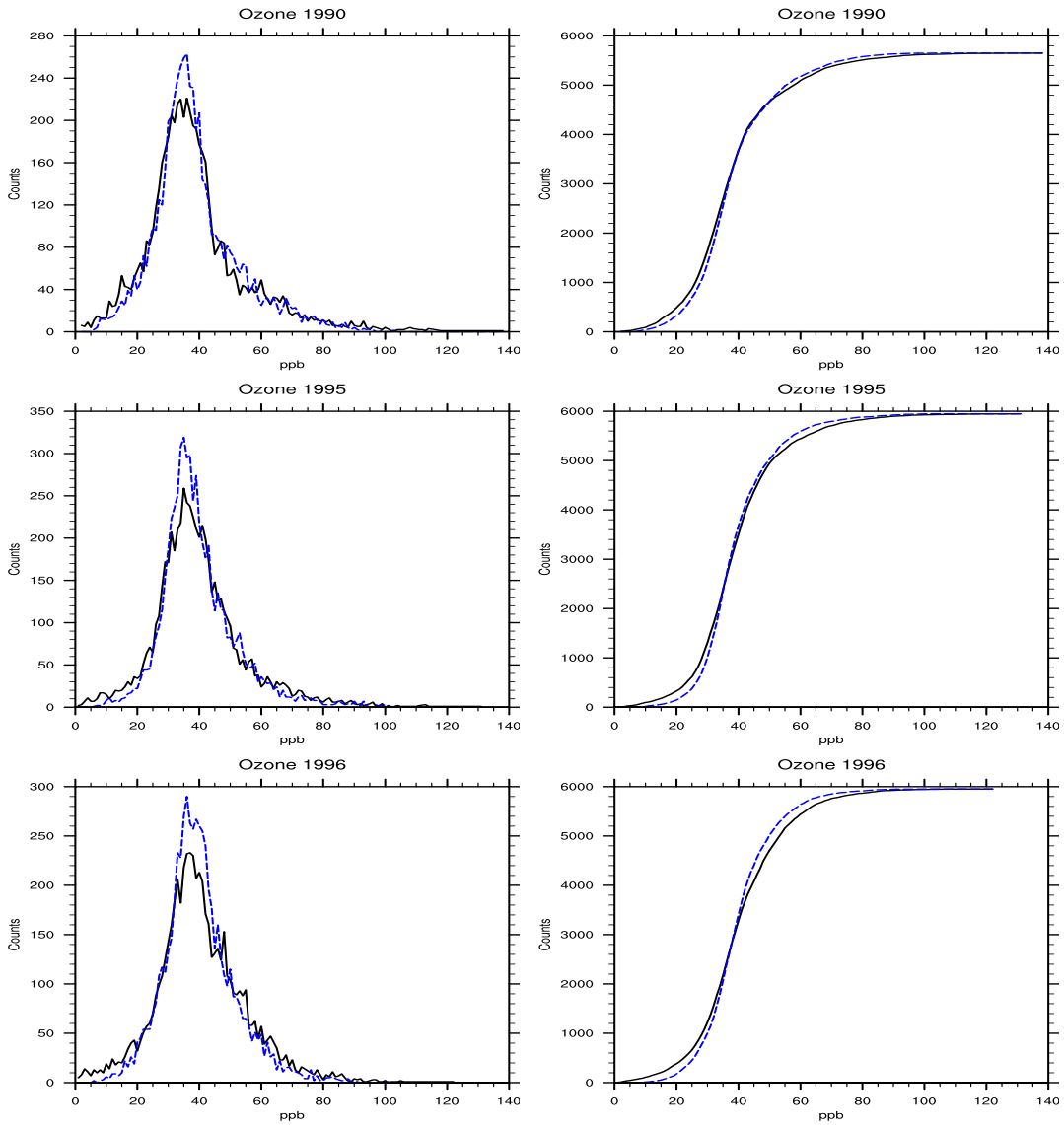

Figure 2.9: Comparison of Modelled (dashed line) versus Observed (solid line) Ozone Values, 1990, 1995-96. Frequency distribution (left column) and cumulative frequency distributions (right column), derived from all daily maximum ozone values for 17 stations.

2.4 AOT40

In recent years the so-called AOT40 index has been used as an indicator of risk to vegetation. AOT40 is the accumulated amount of ozone over a threshold value of 40 ppb, i.e..

$AOT40 = \int max(O_3 - 40 \text{ ppb}, 0.0)\, dt$

where the *max* function excludes negative values. The integral is taken over

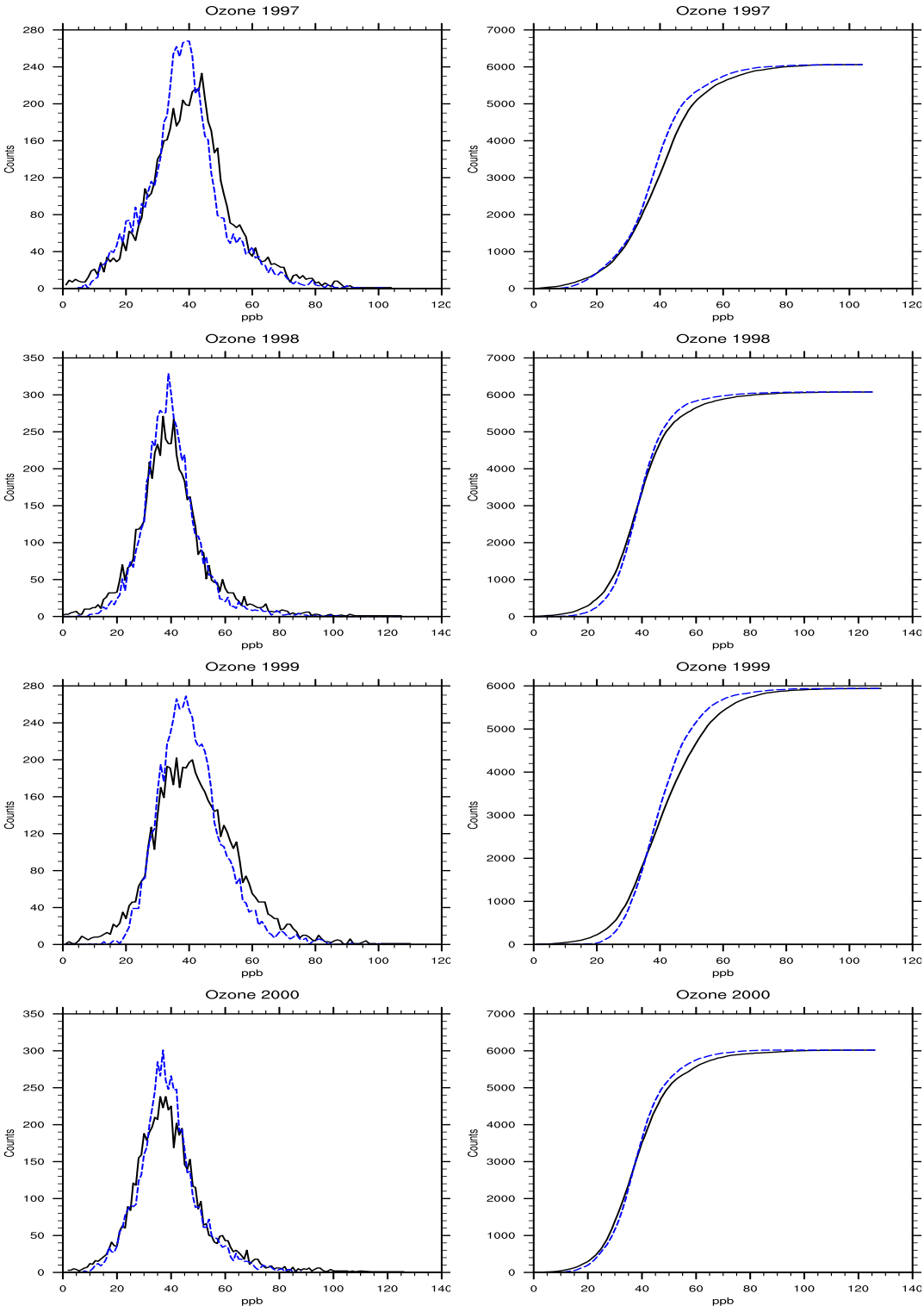

Figure 2.9: Continued, for 1997-2000

time, namely – the growing season as defined at the Bern critical levels workshop (Fuhrer and Achermann(1994),). For crops and natural vegetation AOT40 is taken over 3 months (May-July), which we denote $\mathbf{AOT40}_c$. For forests a six month period is used (April-September), denoted $\mathbf{AOT40}_f$. For UNECE AOTs should only be calculated during daylight hours, defined as period when clear-sky radiation exceeds 50 W m^{-2}. For the EU, a simpler definition is used, with AOT values calculated between 8:00 to 20:00 GMT.

As was made clear in (Simpson et al.(1998)), AOT40 and the similarly defined AOT60 have the disadvantage that they are very sensitive to small systematic errors in either the model or the measurements. Such errors are unavoidable and have many sources. Observations of ozone should usually have a good accuracy and precision with modern instruments, but calibration procedures are not uniform across the EMEP network and uncertainties of at least ±5% seem very likely. In addition, measurements are affected by site placement and local NO_x sources, so reported ozone values cannot represent the perfect regional average for an EMEP grid square. Sensitivity studies performed in both (Simpson et al.(1998)) and (Tuovinen(2000)) showed that uncertainties in AOT40 can be very significant, especially for sites where ozone levels often lie around the 40 ppb threshold value.

However, AOT40 is still an important statistic, and we present here comparisons between the modelled and observed values.

Table 2.2 shows the observed and modelled $AOT40_f$ values for the year 2000 for all stations having a summer-time data-capture of $> 90\%$. (Defined here as days with more than 18 hours of hourly observations). These data are displayed as scatter-plots in in Figure 2.10, along with similar plots for 1998 and 1999. Despite the difficulties expected for modelling this parameter, it seems that the model does a reasonable job of predicting AOT40 levels at most stations. A very large discrepancy is seen at the site Ispra (IT04), for the year 2000, but results for this site in 1998 and 1999 were much better. In general, these results are satisfactory for a statistic such as AOT40.

Table 2.2: Comparison of Observed and Modelled AOT40 (ppm h) for April-September 2000. Values given use EU-definition of AOT40, from 8-20 GMT.

Code	Station	DC† (%)	$AOT40_f$ Obs.	$AOT40_f$ Mod.
		*N*ordic Countries		
DK31	Ulborg	98.4	6.9	7.5
DK32	Frederiksborg	98.4	4.7	7.9

continued on next page

Code	Station	DC†	Obs.	Mod.
FI09	Uto	97.3	3.5	3.3
FI17	Virolahti	98.4	3.5	3.3
FI22	Oulanka	98.4	3.3	0.4
FI37	Ahtari	98.4	4.0	1.6
NO01	Birkenes	98.4	3.6	4.9
NO15	Tustervatn	97.8	4.9	1.7
NO39	Kaarvatn	100.0	7.0	2.0
NO41	Osen	98.9	4.1	2.3
NO42	Mt. Zeppelin	96.7	0.1	0.3
NO43	Prestebakke	97.8	5.5	6.5
NO45	Jeloya	99.5	2.5	5.3
NO45	Jeloya	99.5	2.5	5.3
NO48	Voss	98.9	4.5	3.5
NO55	Karasjok	100.0	2.8	0.3
NO56	Hurdal	98.4	6.2	3.0
SE02	Rorvik	99.5	7.6	7.2
SE11	Vavihill	99.5	8.3	7.4
SE13	Esrange	99.5	3.6	0.7
SE32	Norra-Kvill	100.0	7.2	4.6
SE35	Vindeln	100.0	3.5	1.2
	*E*astern European Countries			
CZ01	Svratouch	96.7	20.5	17.0
CZ03	Kosetice	100.0	19.7	17.3
EE09	Lahemaa	97.8	5.5	0.5
EE11	Vilsandy	94.5	10.1	3.0
HU02	K-puszta	96.2	31.3	18.8
LT15	Preila	94.5	6.7	9.8
LV10	Rucava	91.3	2.3	5.3
PL02	Jarczew	98.9	14.7	12.9
PL03	Sniezka	98.9	30.6	18.5
PL04	Leba	100.0	11.4	8.0
PL05	Diabla Gora	95.1	14.5	9.8
RU18	Danki	97.8	0.5	5.1
SI08	Iskrba	95.6	25.5	22.6
SI31	Zarodnje	95.1	7.2	26.5
SI32	Krvavec	97.3	34.8	23.8
SI33	Kovk	93.4	26.5	21.1
SK06	Starina	92.3	4.3	17.3
	*C*entral and NW European Countries			
AT02	Illmitz	95.1	27.8	24.4
AT04	Koloman	97.8	20.1	19.2

continued on next page

Code	Station	DC†	Obs.	Mod.
AT05	Vorhegg	98.4	24.9	21.6
AT30	Pillersdorf	98.4	25.5	22.1
AT32	Sulzberg	97.3	24.3	21.8
AT33	Stolzalpe	98.4	17.1	15.6
BE01	Offagne	94.0	8.0	15.2
BE32	Eupen	95.6	8.4	10.9
BE35	Vezin	99.5	6.0	10.4
CH02	Payerne	92.3	16.5	16.2
CH03	Taenikon	96.2	16.9	16.4
CH05	Rigi	91.3	23.7	14.4
DE01	Westerland/Wenningstedt	97.3	8.8	2.9
DE02	Waldhof	99.5	14.4	11.6
DE03	Schauinsland	99.5	23.3	18.2
DE04	Deuselbach	96.2	13.8	15.1
DE05	Brotjacklr.	94.5	20.7	18.8
DE07	Neuglobsow	94.0	13.8	11.0
DE08	Schmucke	98.4	18.5	15.4
DE09	Zingst	100.0	7.7	1.0
DE12	Bassum	98.9	6.9	11.2
DE26	Uecker.	98.4	9.4	12.3
DE35	Luck.	90.2	14.6	20.4
DE39	Aukrug	91.8	3.3	8.4
FR09	Revin	98.9	5.8	10.3
FR10	Morvan	95.6	7.3	7.9
FR12	Iraty	90.2	17.8	14.0
FR13	Peyrusse Vieille	94.0	2.2	7.3
FR14	Montandon	94.0	5.9	13.6
GB02	Eskdalemuir	98.4	1.5	9.4
GB06	Lough Navar	97.3	1.7	5.8
GB14	High Muffles	93.4	4.4	6.8
GB15	Strath Vaich Dam	95.1	3.5	7.6
GB31	Aston Hill	97.8	3.7	5.9
GB32	Bottesford	98.9	3.0	8.9
GB33	Bush	98.4	1.3	8.9
GB36	Harwell	94.5	3.4	4.9
GB37	Ladybower	94.5	2.0	6.8
GB39	Sibton	95.1	3.4	4.5
GB44	Somerton	97.3	6.4	4.1
IE31	Mace Head	92.9	3.6	10.4
NL09	Kollumerwaard	97.3	3.8	6.6
	*M*editerranean Countries			
ES08	Niembro	94.5	4.0	20.6

continued on next page

Code	Station	DC†	Obs.	Mod.
ES10	Cabo de Creus	94.0	29.9	11.8
ES11	Barcarrota	92.3	7.5	20.2
ES12	Zarra	93.4	20.7	13.7
IT04	Ispra	98.9	3.2	35.6

† Data-capture (DC) for April-September

2.5 Nitrogen Dioxide

Nitrogen oxides (NO_x = NO + NO_2) are arguably the most important precursor for photochemical oxidant formation. In rural atmospheres NO_x consists largely of nitrogen dioxide, and measurements of this compound have been conducted in the EMEP networks since 1980. These measurements consist of daily mean values, sampled from 6 GMT of one day to 6 GMT of the next, so modelled concentrations have been averaged over the same time-period.

It should be noted that NO_2 is a much more difficult pollutant to predict than ozone. Partly this is because NO_2 is a gas whose concentrations are often dominated by ground-level sources, especially traffic. Nearby roads or urban areas can therefore influence measurements in a way which a model with 50×50 km^2 resolution, and with a lowest layer of approximately 90 m depth, can never achieve. Concentrations of NO_2 are also very sensitive to uncertainties in some chemical parameters (notably the concentration of the OH radical) and to meteorology (stability, dispersion). Finally, measurements of NO_2 may be subject to interferences from other gases, especially at the very low ($\leq$ 1 ppb) concentrations often found at EMEP sites. This is not usually a problem when using the reference method, NaI impregnated glass sinters, but may affect some sites which used other methods for some years.

2.5.1 Annual Scatter Plots

Figure 2.11 presents scatter-plots of modelled versus observed NO_2 for the year 2000, and then from 1980 to 1995, in 5-year intervals. These plots show the 1:1 line (solid), the line of ±30% bias, and the lines of ±50% bias. For 1980 data were only available for seven sites. The model clearly overestimates at two of these, but performs rather well for the remaining five sites. From 1985 to 2000 the number of available sites steadily increases. Most sites fall within the ±30% lines, but there are clear outliers in these years, where observed concentrations are much higher than modelled. For a primary pollutant such as NO_2 this is probably not surprising, and can possibly be explained by nearby NO_x sources influencing the

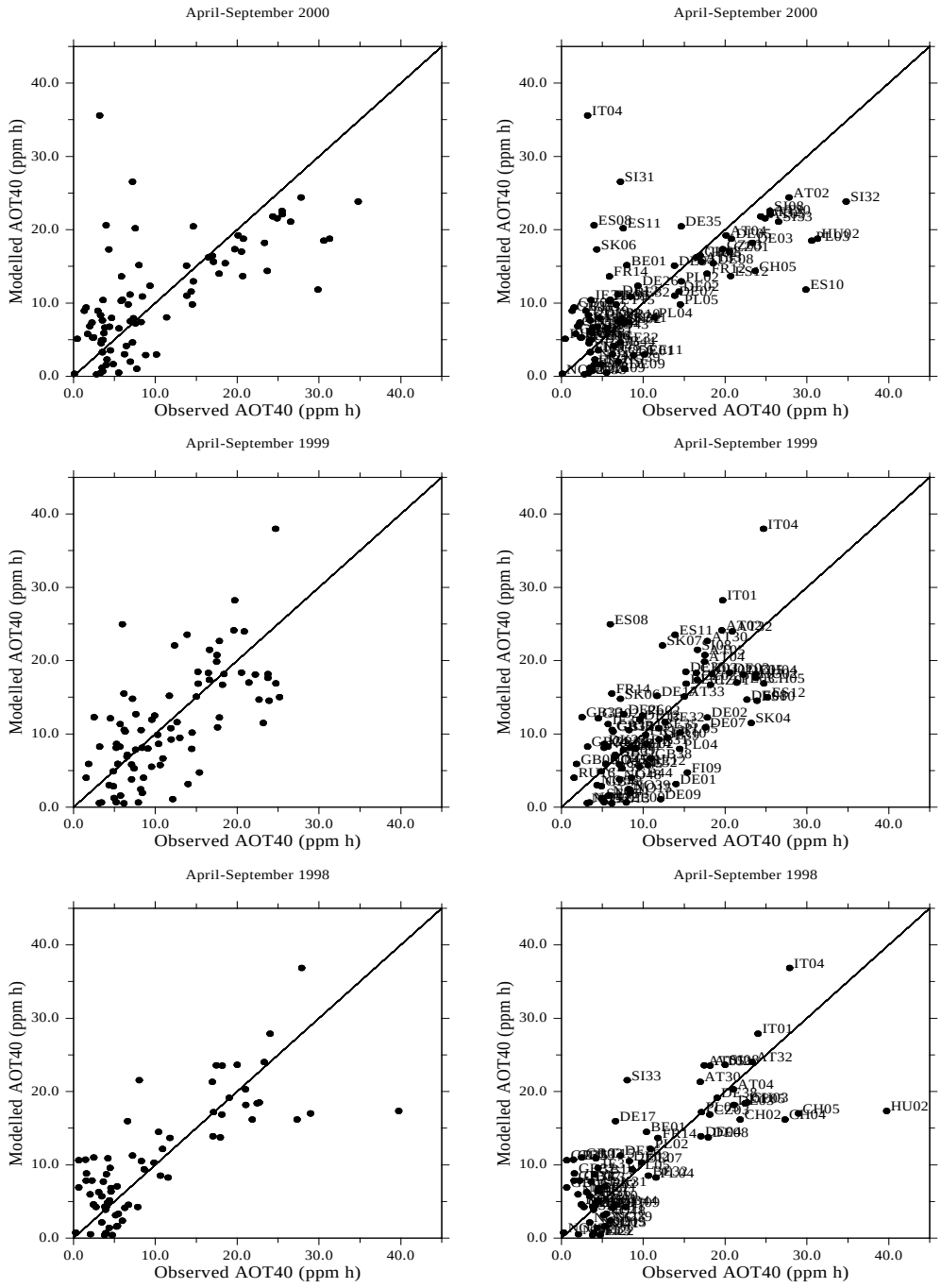

Figure 2.10: Comparison of Observed versus Modelled 6-monthly AOT40, for 1998, 1999 and 2000.

measurements. However, even including these outliers in the analysis, the overall mean bias of -17% (for 2000) is very satisfactory.

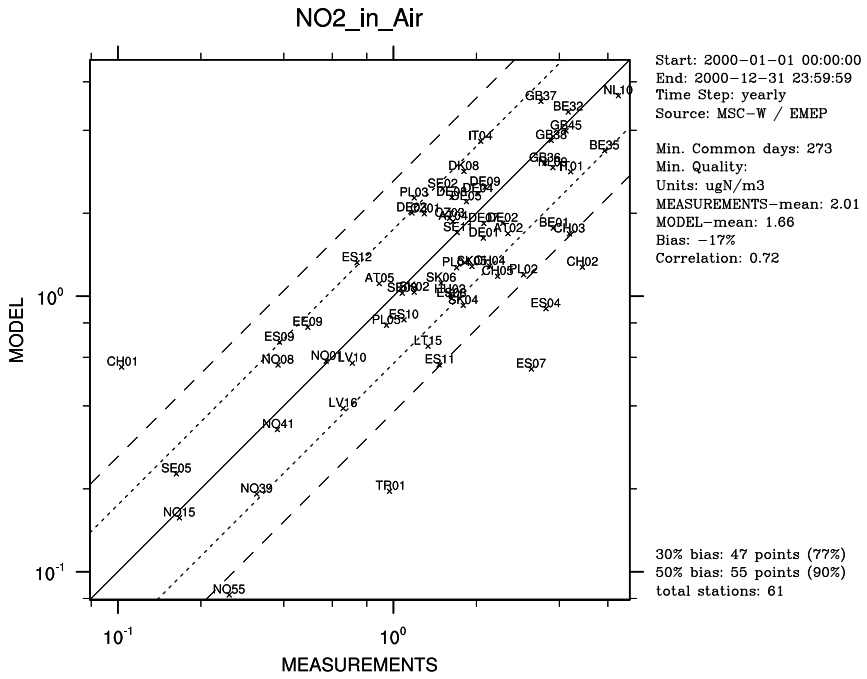

Figure 2.11: Comparison of Modelled versus Observed Annual NO_2 Concentrations, Year 2000.

2.5.2 Regional trends

Figure 2.12 illustrates the development of modelled versus observed monthly average NO_2 concentrations from 1995 to 2000, averaged over 38 European stations. Neither modelled nor observed NO_2 concentration show a clear trend over this period. Over these 38 stations the model underpredicts the observations for all months, with somewhat more underestimation in summertime.

Figure 2.13 presents similar plots, but now by region. The differences between regions are striking. The model performs very well in northern Europe and satisfactorally in western Europe. Underprediction of summertime NO_2 is greatest for eastern European countries. In contrast, the southern European data show large underpredictions in wintertime (only two stations are included here though, due to data-capture and quality limitations). These problems are discussed further in section 2.6.4.

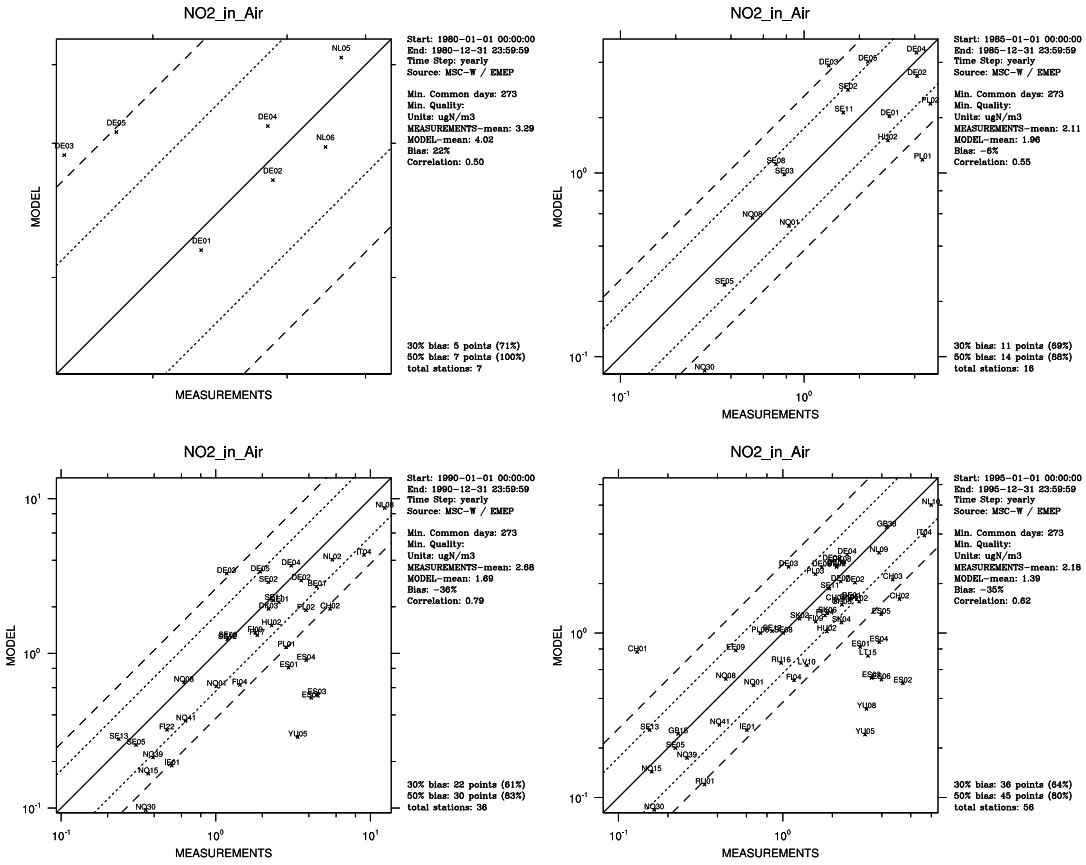

Figure 2.11: Continued, for 1980-1995

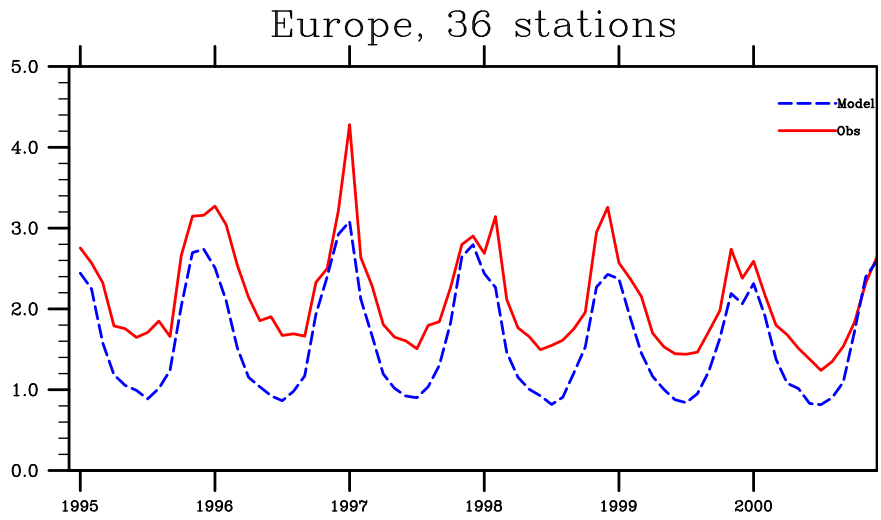

Figure 2.12: Modelled versus Observed NO_2 Concentrations (μg(N) m^{-3}), 1995-2000, for 38 European regions

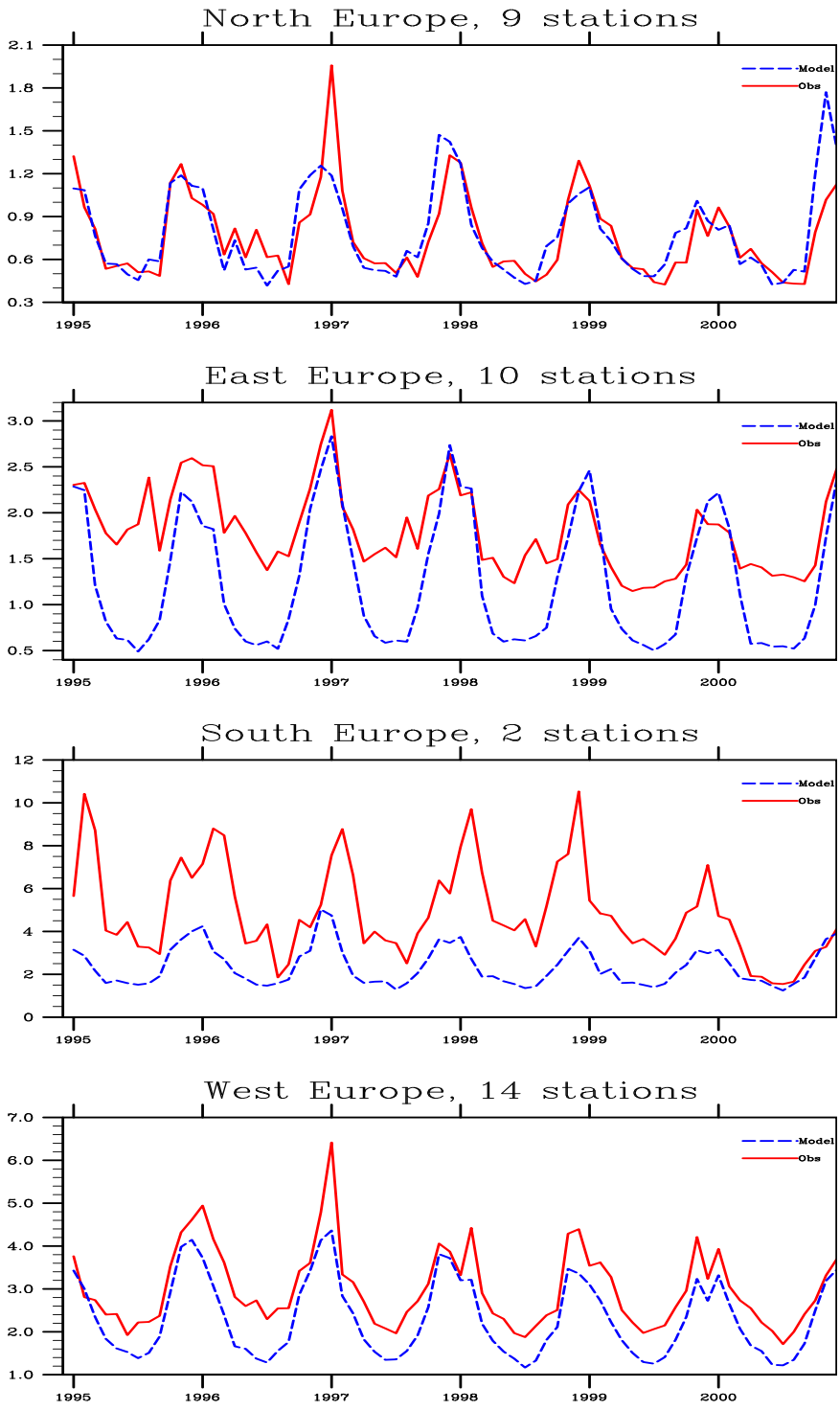

Figure 2.13: Modelled versus Observed NO_2 Concentrations (μg(N) m^{-3}), 1995-2000, for four European regions

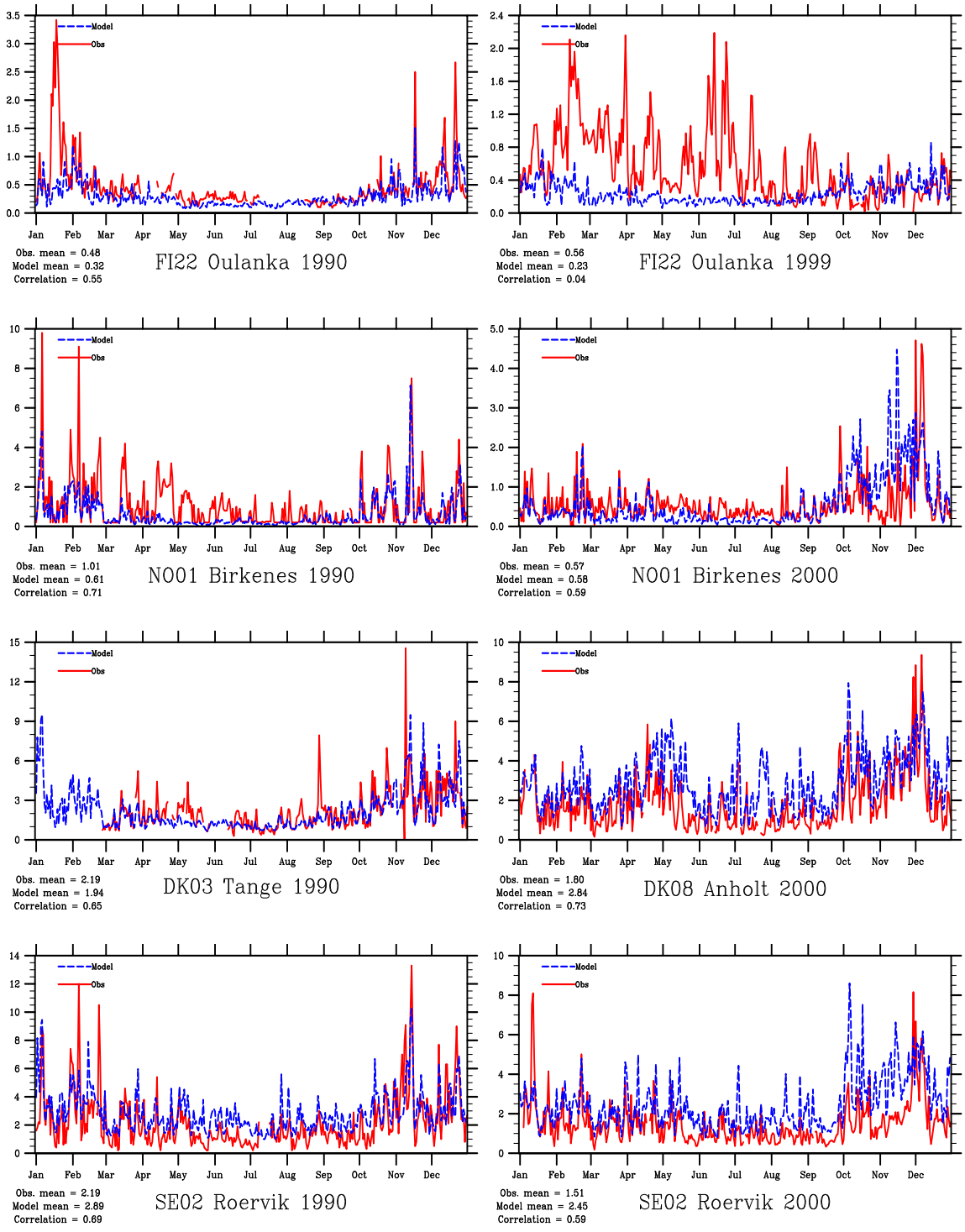

Figure 2.14: Modelled versus Observed Daily Max Ozone (ppb), Nordic Sites, 1990 and 2000 (or 1999 for FI22)

2.6 Time-series for NO_2

2.6.1 Nordic Sites

A number of sites have been operating in the Nordic countries since 1990 and even before. Measurement techniques at these sites have been relatively stable, although Finland changed method in 1995, from manual to automatic methods. Figure 2.14 presents time-series plots of modelled versus observed daily mean NO_2 concentrations for a number of Nordic sites for the years 1990 and 2000. The Nordic sites are characterised by generally low NO_2 levels. The comparison plots show a reasonable agreement at most Nordic sites, with the the clear exception of Oulanka for 1999 which is located in Northern Finland. A possible explanation for this discrepancy is that Oulanka is influenced by nearby sources which are not well reproduced by the model, for example sources in the Kola Peninsula. The results obtained at Osen are also mixed. Results for sites in southern parts of the Nordic region are rather good, for example at Rörvik (SE02) in SE Sweden. Others sites (not shown) such as Aspvreten (SE12) or Utö (FI09) show similarly good results.

2.6.2 Eastern European Sites

Figure 2.15 presents time-series plots of modelled versus observed daily mean NO_2 concentrations for a number of Eastern European sites for the years 1990 and 2000.

These results are very mixed, with the model reproducing observations well for some periods, but then significantly underpredicting in others, especially in summertime. The data quality of the NO_2 measurements in Poland (not PL05) and Slovakia are uncertain, however, because they use non-recommended methods, TGS and gujacol absorption solution respectively.

2.6.3 Central European Sites

Figure 2.17 presents time-series plots of modelled versus observed daily mean NO_2 concentrations for a number of central European sites for the years 1999-2000. Figure 2.16 presents similar plots for two Austrian sites for 2000.

Again the results are mixed. At Payerne (CH02) the model systematically underpredicts NO_2 levels throughout the year. In contrast, results for the other Austrian, German and Dutch sites are reproduced very well. Indeed, NO_2 results for some of these sites are comparable in performance to those shown for ozone. Presumably, Payerne is influenced by some local sources.

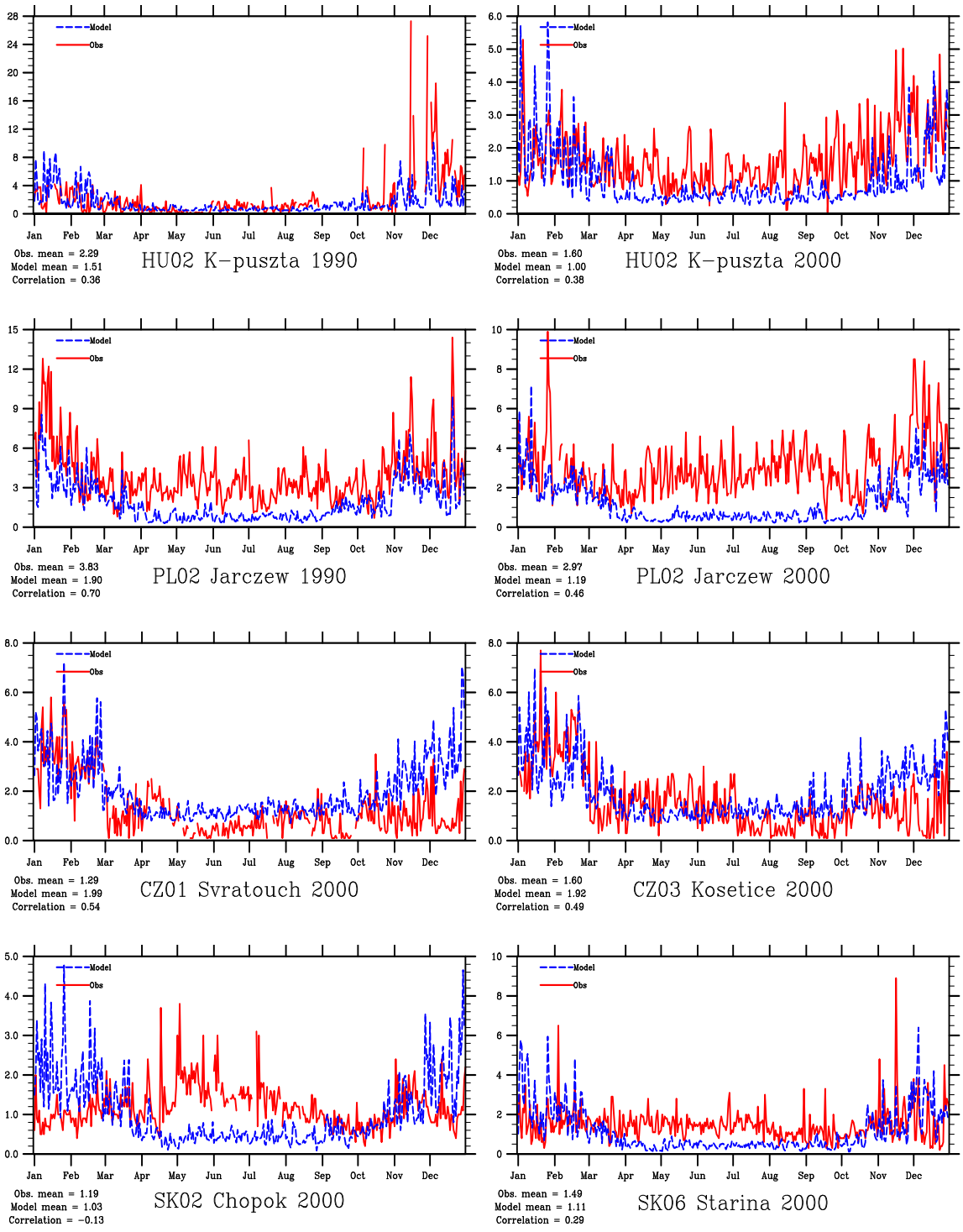

Figure 2.15: Modelled versus Observed Daily Mean NO_2 (μg(N) m^{-3}), Eastern European Sites, 1990 and 2000

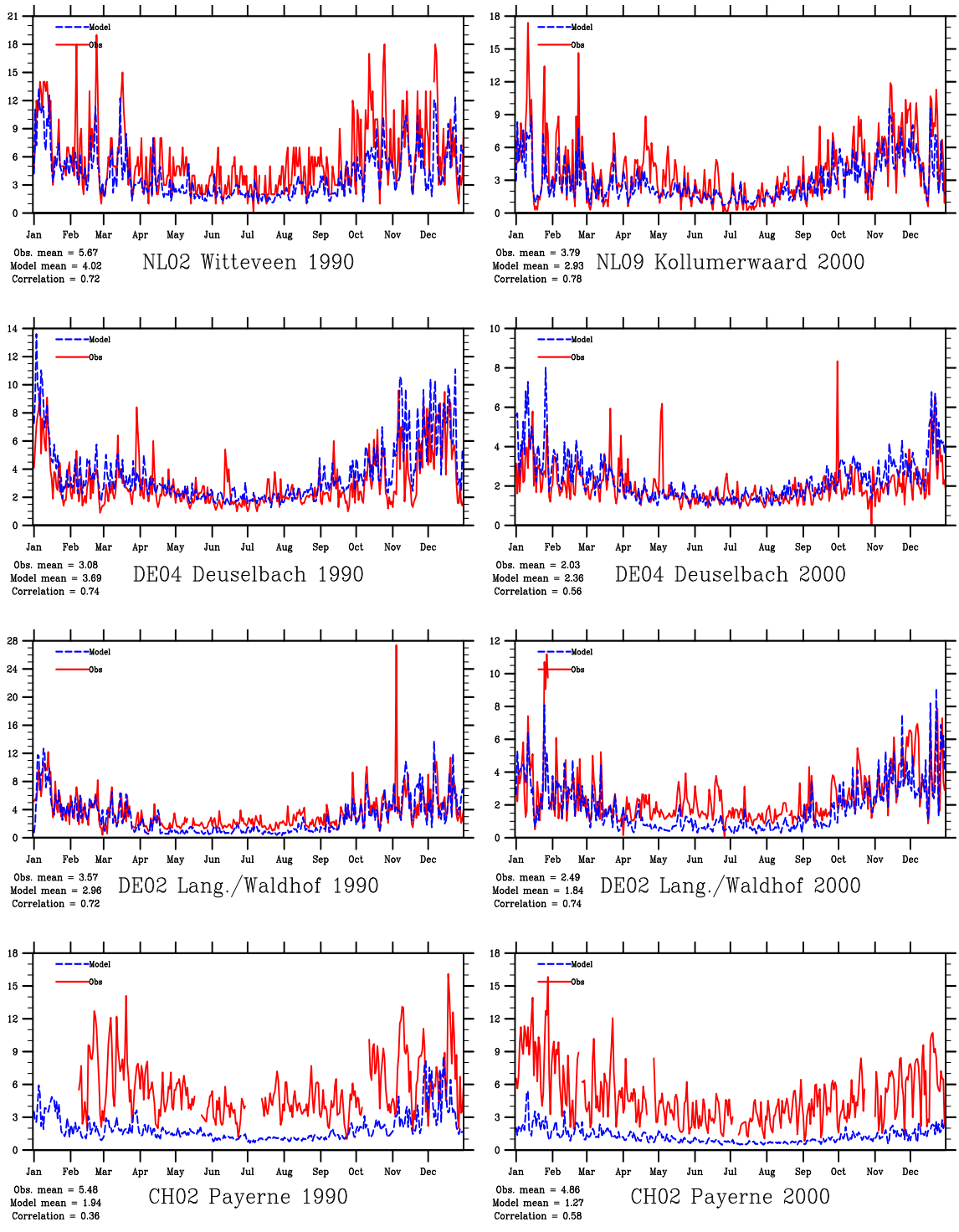

Figure 2.16: Modelled versus Observed Daily Mean NO_2 (μg(N) m^{-3}), Central European Sites, 1990 and 2000

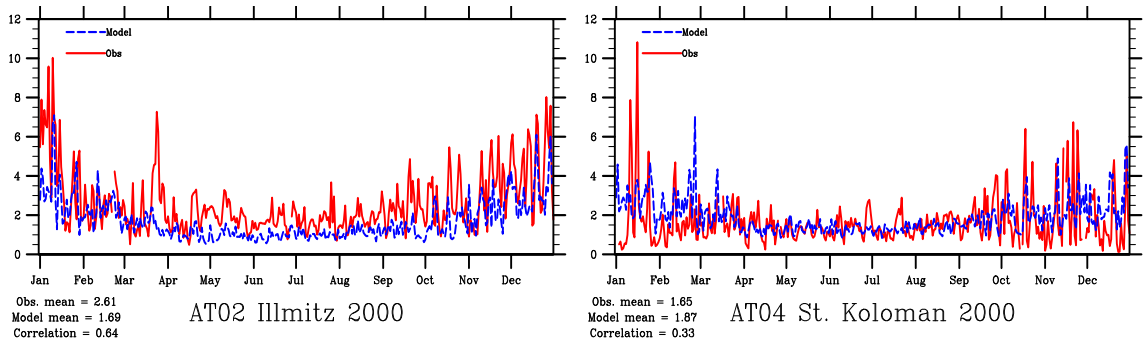

Figure 2.17: Modelled versus Observed Daily Mean NO_2 (μg(N) m^{-3}), Central European Sites, 2000

2.6.4 Mediterranean Sites

Figure 2.18 presents time-series plots of modelled versus observed daily mean NO_2 concentrations for a number of Mediterranean sites for the years 1990 and 1999-2000.

The Spanish and Greek sites show very large discrepancies between the modelled and observed values. Observed NO_2 is often significantly greater than modelled, as illustrated for ES11 (Barcarrota). Results for ES08 (Niembro) shown here are better in summertime, but larger discrepancies were found for the 1999 comparison (not shown). The results for the Italian sites, on the other hand, look quite reasonable in summertime but with underpredictions in the winter months.

Under-prediction of NO_2 at Spanish sites in 2000 can to some extend be explained by the measurement methods being used. In 2000 chemiluminescence monitors were used, and in a field comparison in Spain in 2000, Aas et al. (2002) showed that this method overestimated the concentration by a factor 2 compared to the reference method. Prior to 2000, the data quality of the NO_2 measurements in Spain was even worse, when TEA methods were used. Aas et al. (2002) showed that the TEA method gave 10 times higher concentrations than the reference method, and the correlation was also poor. The 2000 data is thus better, but even this shows significant positive bias compared to the reference method.

The data quality of the Greek NO_2 measurements is uncertain. They use an absorption technique (TGS) and this may not be sensitive or selective enough. This method is known to have problems with instability at high temperatures and sunlight; in addition, the absorption efficiency may vary with concentrations. In addition there are possibly some local sources of NO_2 around the Greek station Aliartos. Yugoslavia use the same method as Greece and the measurements quality has also been tested in a field comparison in Kleiner Fedtberg (Fähnrich et al.(1993),). The measurements give a large positive bias compared to the reference method.

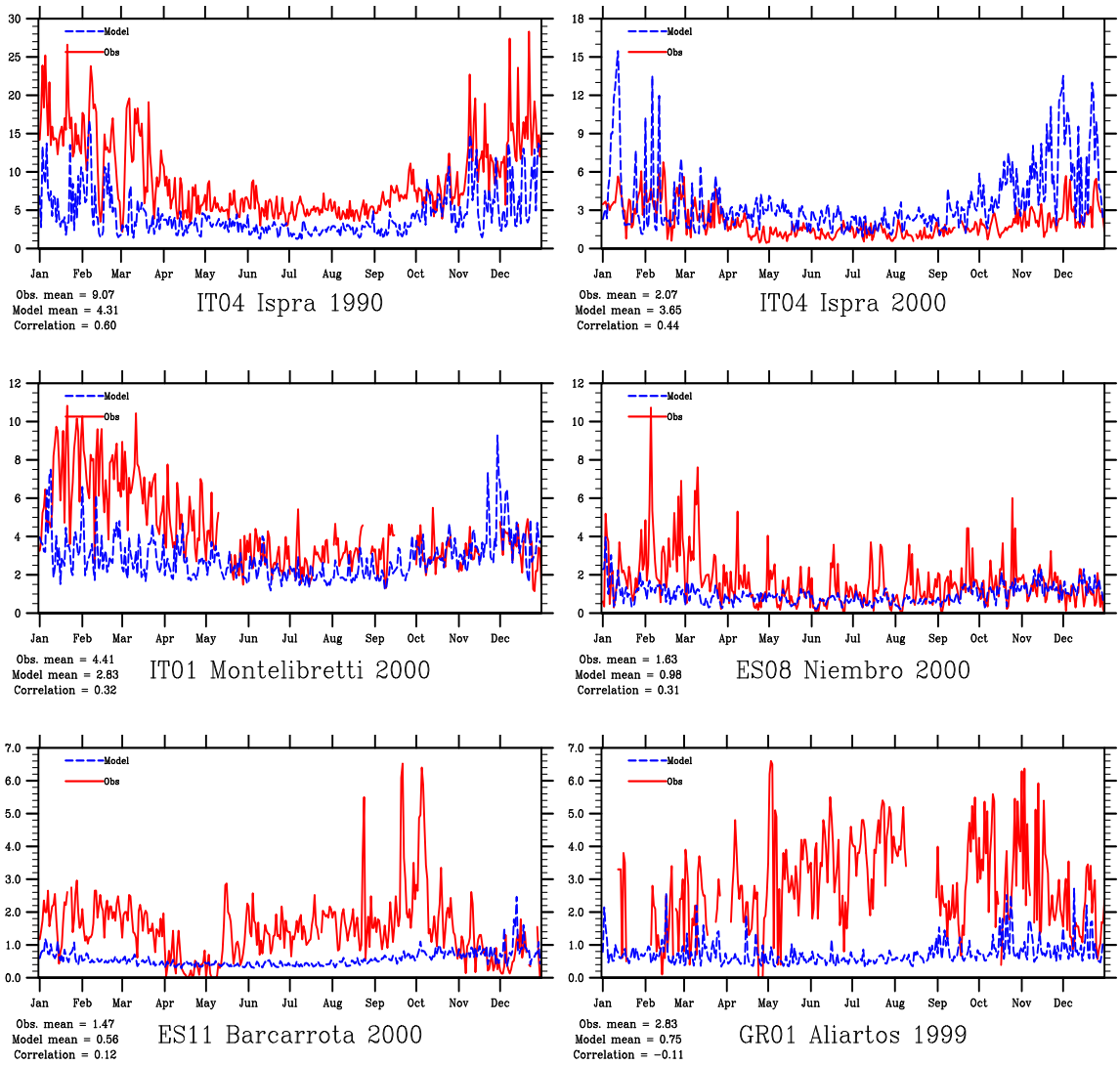

Figure 2.18: Modelled versus Observed Daily Mean NO_2 (μg(N) m^{-3}), Mediterranean Sites, 1990, 1999 and 2000

Finally, it should be stressed that a major problem with use of NO_2 data for model evaluation is that the data quality of the EMEP NO_2 measurements are varying. There are several methods used, such as different absorption solution, chemiluminescence monitors and the recommended impregnated glass sinter method (EMEP(1996),). Some of the absorption techniques are not suitable at EMEP sites due to instability, interferences and poor absorption efficiency. Certain absorbents may react to temperature and sunlight which may partly explain some of the poor correlations in summertime. The chemiluminisence monitors may work at some sites, but it is in general not recommended due to low sensitiv-

ity and relatively demanding maintenance with frequent calibration etc. However, the monitor has high time resolution and is useful at sites measuring ozone, but the quality of these data should be checked by doing a field comparison with the reference method.

2.7 Formaldehyde

Figures 2.19-2.20 present time-series plots of modelled versus measured concentrations of formaldehyde in 2000 at eight sites, Utø, Birkenes, Zingst, Waldhof, Schmucke, Brotjacklriegel, Kosetice and Donon. Figures 2.19 includes two plots for Waldhof, since parallel analyses of carbonyls were carried out there in 2000 by UBA and NILU, respectively, and the model comparison with each of these two time-series are given. As noted in (Jonson et al.(2002)), UBA started their carbonyl measurements in the last months of 1999 and were in a development phase by the beginning of 2000. The measurement data from the German sites should be analysed with this in mind.

Compared to the similar study in (Jonson et al.(2002)), applying earlier model versions (rv1.1 and rv1.2β), the model performance as measured by the linear correlation coefficient, r, is clearly improved for all the sites with formaldehyde measurements. Table 2.3 shows the correlation coefficients and the ratio of the modelled annual average values versus observed (M/O). For Waldhof, Schmucke, Kosetice and Donon correlation coefficients above 0.7 were found for the new model version.

At the same time, the new model version gives generally higher formaldehyde concentration than version rv1.2β. For some sites this improves the agreement with observations, whereas for other sites it leads to a larger discrepancy. However, the model/observed ratio is within 50% for all but one site. The exception is Brotjacklriegel, and the explanation may be related to the fact that this is a mountain site (1016 m asl.). Also for Birkenes a marked bias is found between the measurements and the model calculations in July-October.

There have been a number of changes which might cause these differences between model versions, including changes in landuse data (and hence biogenic emissions), deposition schemes, boundary conditions, and emissions treatment. A more extensive study is needed to shed light on the reasons for the variations in model performance for formaldehyde. More years with monitoring data are needed to evaluate the quality and accuracy of the measurement data compared with the model performance.

Code	Station	rv1.1		rv1.2β		rv1.7	
		M/O	r	M/O	r	M/O	r
FI09	Utø	2.08	0.05	1.26	0.00	1.00	0.12
NO01	Birkenes	2.18	0.15	1.44	0.38	1.99	0.42
DE02	Waldhof (NILU)	1.54	0.33	1.01	0.52	1.50	0.72
DE02	Waldhof (UBA)	1.12	0.33	0.73	0.44	1.10	0.63
DE08	Schmucke	1.18	0.45	0.80	0.64	1.18	0.72
DE09	Zingst	1.27	0.45	0.75	0.37	1.03	0.49
DE05	Brotjacklriegel	3.13	0.43	2.15	0.56	3.60	0.61
CZ03	Kosetice	1.36	0.51	0.95	0.60	1.46	0.71
FR08	Donon	1.41	0.57	0.94	0.71	1.33	0.79

Table 2.3: Comparison of modelled versus observed ratios (M/O) of HCHO concentrations, and correlation coefficients (r), year 2000. Comparisons are shown for current model version (rv1.7) and for versions reported in (Jonson et al.(2002)).

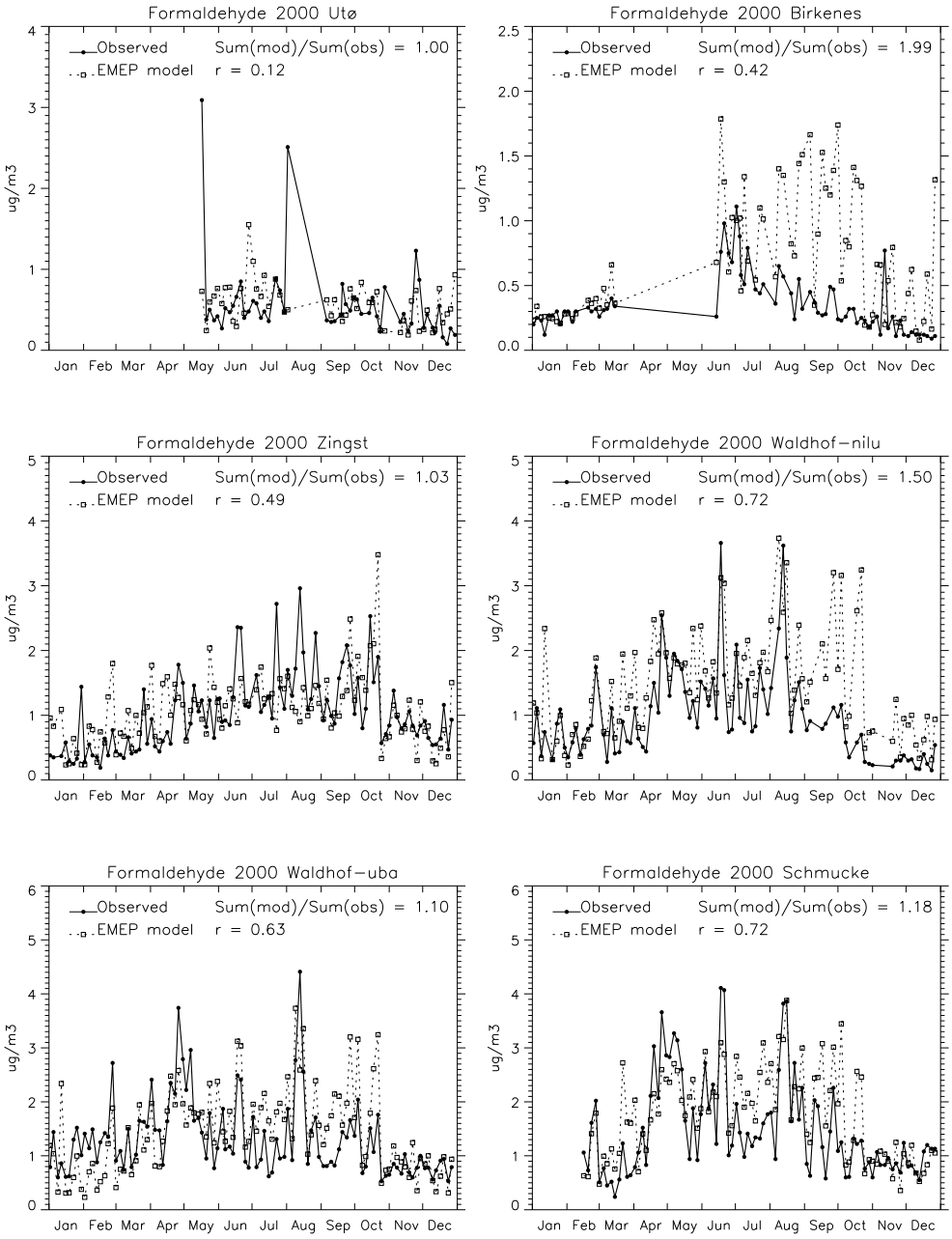

Figure 2.19: Comparison of modelled versus observed HCHO concentrations, year 2000.

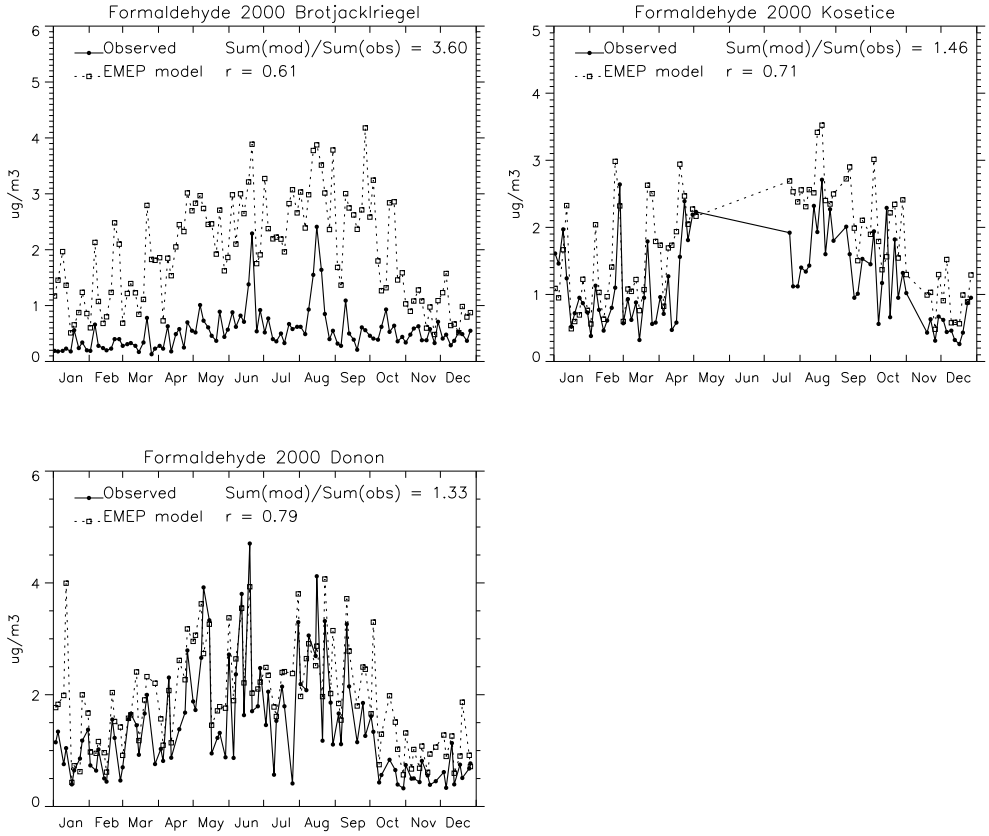

Figure 2.20: Comparison of modelled versus observed HCHO concentrations, year 2000.

2.8 Conclusions

This chapter has presented an evaluation of the new EMEP MSC-W Eulerian model, for ozone, NO_2 and formaldehyde. The analysis has focused on comparisons against recent measurements (2000), but with some results for 1990 and for NO_2 as far back as 1985. One reason for the focus on recent years is that we expect emission inventories to be most accurate for this period – an essential prerequisite for assessing model performance. The later years also have a much greater number of available measurements, especially for ozone. This allows us to examine the model's performance in almost all European countries - a major improvement on earlier comparisons.

Space requirements have allowed us to analyse only a small proportion of sites and data here, but plots for all sites and also for other years will be made available on the EMEP web-site, http://www.emep.int.

Main Conclusions

- The model is found to perform rather well for ozone across most parts of Europe.

- Seasonal cycles of ozone are reproduced with good accuracy, and correlation coefficients (from comparison of daily maximum values over the year) are usually better than 0.7 or 0.8 at the majority of sites.

- In Northern and North-Western Europe ozone is well reproduced at almost all stations. This good agreement is very encouraging given that these sites span more than 20° of latitude, from around 45° N to more than 65° N.

- In Eastern and south eastern Europe ozone is reproduced well at many, but not all, sites. The reasons for the discrepancies between modelled and observed values are unclear, since sites in the same region seem to show quite different results.

- In Southern Europe results are more mixed. Ozone is reproduced well at sites in Italy, southern France and Spain (for the more recent Spanish sites). Modelled ozone values are lower than observed values at sites in Malta and Greece, which may indicate that assumed background ozone values in this region are too low.

- Frequency distributions were calculated for four years from 1997 to 2000. For most years the modelled and observed frequency distributions match rather well. The shapes and peaks of the distributions are reproduced to a satisfactory degree, although the model has a clear tendency to a narrower distribution.

- Concerning time-trends, there seems to be little change in model performance over the years. The year-to-year variation (e.g. from 1997 to 1998) is larger than the variations seem from 1990 to 2000, and it would seem that model performance is thus comparable over the 10-year period.

- The modelled AOT40 values also correlate well with observed values, although, as expected, the scatter is significant. AOT40 is not a robust indicator of model performance though, so these results should be interpreted with care.

- Results for NO_2 are much more mixed. For Northern and Western Europe the model performs satisfactorally. For some sites (e.g. in Germany, Netherlands), the model performance approaches that obtained for ozone. In other parts of results results range from good to very poor. In most cases where discrepancies occur, the observed values are much higher than the modelled values.

- A major problem with use of NO_2 data for model evaluation though is that the data quality of the EMEP NO_2 measurements are varying. There are several methods used, some of which are not recommended and/or require careful field comparison with the reference method. Certain absorbents may react to temperature and sunlight which may partly explain some of the poor correlations in summertime.

- For HCHO we have compared the new model both to measurements at eight sites, and to earlier model versions (rv1.1 and rv1.2β). The model performance as measured by the linear correlation coefficient, r, is clearly improved for all the sites with the new model.

- At the same time, the new model version gives generally higher formaldehyde concentrations than version rv1.2β. For some sites this improves the agreement with observations, whereas for other sites it leads to a larger discrepancy. However, the average model/observed ratio is within 50% for all but one site.

- A more extensive study is needed to shed light on the reasons for the variations in model performance for formaldehyde. More years with monitoring data are needed to evaluate the quality and accuracy of the measurement data compared with the model performance.

The model version used here, revision rv1.7, has undergone a number of changes compared to the versions reported earlier in (Jonson et al.(2002)). The current version, documented in detail in (Simpson et al.(2003)) shows significantly improved performance for ozone compared to the earlier reported revisions of the

EMEP model (revisions 1.1 and 1.2β, Jonson et al., 2002), to the earlier MACHO model (Simpson and Jonson(1998),), or to the Lagrangian model (Simpson et al.(1998),Simpson(1993),). Although model improvements will still be sought, and model evaluation will continue, the new model performs in a very satisfactory manner and seems a worthy successor to the earlier EMEP models.

Chapter 3

Model performance for Particulate Matter

Svetlana Tsyro

This chapter presents results on the modelling of Particulate Matter (PM) at EMEP/MSC-W. It presents results from two models of different purpose and complexity level that presently operate at MSC-W: the EMEP Eulerian Unified model (mass model) and the research aerosol dynamics model (UNI-AERO).

The chapter starts with a short description of the models focusing mainly on differences in their formulation causing the differences in modelling results. PM_{10} and SIA concentrations from the Unified and aerosol model to are compared with observations in the EMEP and AIRBASE networks. Due to limitations in the availability of measurement data for PM, the present study of model performance focuses in the years 1999 and 2000. Furthermore, we present an evaluation of UNI-AERO with respect to $PM_{2.5}$, aerosol chemical composition and particle numbers from national networks and research campaigns. Finally, recommendations on the information and data needed for further models development and evaluation are identified.

3.1 Differences in model formulations

The EMEP Unified model is an aerosol mass model that describes the emission, chemical transformation, transport and removal by dry and wet deposition for Secondary Inorganic Aerosols (SIA), i.e. sulphate (SO_4), nitrate (NO_3) and ammonium (NH_4), and Primary Anthropogenic Particles, i.e. $PPM_{2.5}$ and coarse PPM. It distinguishes fine and coarse particles. The model calculates mass concentrations of the aerosol components and $PM_{2.5}$and PM_{10}. The Unified model was used this year for calculating the source-receptor relationship for SIA, PM2.5 and PM10. The model deals with bulk aerosol and does not account for aerosol dynamics. This is justified by comparison with the aerosol dynamic module where

we find that the inclusion of aerosol dynamics processes has little effect on the aerosol mass.

The EMEP research aerosol model, UNI-AERO, resolves particle size distribution with four monodisperse modes and accounts for aerosol dynamics (Pirjola et al.(2003), Pirjola and Kulmala(2000)). It describes the aerosol chemical composition with 7 components: SIA as SO4, NO3 and NH4, primary anthropogenic compounds as organic carbon (OC), elemental carbon (EC) and mineral dust, and natural PM as sea salt. UNI-AERO calculates size distribution of particle number and mass and aerosol chemical composition in addition to aerosol mass. At present aerosol mass is presented as $PM_{2.5}$ and PM_{10}, but the model can calculate other ranges as for instance PM_1. The aerosol dynamics model is still under development and verification. It is used for testing new parameterisations and also to study the effect of different aerosol processes on aerosol concentrations and sensitivity of results to the uncertainties in input parameters and assumptions involved.

A detailed description of the models is given in the EMEP/MSC-W Report 1, Part I. Here, differences in model formulations, process descriptions and derived differences in the models results are underlined.

Emissions. Calculations of PM concentrations have been performed with the EMEP Unified and aerosol models for 1999 and 2000, using emissions of SO_2, NO_x, NH_3 and NMVOC for correspondent years reported in (V. Vestreng and H. Klein(2002)) and emissions of primary $PM_{2.5}$ and coarse PM in 1995 from the TNO inventory. Emissions are treated in a similar way in both models, except for primary PM that in the aerosol model requires the additional formulation of assumptions on the size of the aerosol and their chemical composition as elemental carbon, organic carbon or mineral dust.

Chemistry. The EMEP Unified model includes a complete SOx-NOx-NHy and photo-oxidant (ozone) chemistry, while UNI-AERO is presently built up on the simplified SOx-NOx-NHy chemistry of the Acid deposition model (UNI-ACID). In the Unified model, concentrations of OH and H_2O_2, which are the main oxidants for SO_2 to SO_4,are calculated, while in UNI-AERO a simple function is used to describe the diurnal variation of OH concentrations, and monthly averaged concentrations of H_2O_2 are taken from the Unified model calculations. In nitrogen chemistry, monthly averaged concentrations of O_3 for oxidation NO to NO_2 in the aerosol model derived from the Unified model calculations, while OH and CH_3COO_2 are tabulated. In the present calculations, the same equilibrium model EQSAM for aerosol/gas fractioning of nitrate and ammonium has been used in both models. In UNI-AERO, EQSAM has also calculated the mass of water associated with aerosol. In section 3.1, preliminary results with a new EQSAM version, which also accounts for Na and Cl from sea salt spray, are

presented.

Aerosol dry deposition. The same scheme for aerosols dry deposition has been used in the Unified and the aerosol dynamics model. The differences in calculated dry deposition velocities result from different description of the aerosol size distribution. The Unified model distinguishes only between fine and coarse particles, for which constant diameters of 0.3 and 4 μm respectively have been assumed based on observed typical values. Those diameters have been used to calculate dry deposition velocities for fine and coarse aerosols. Instead, UNI-AERO distributes aerosols between four size modes, i.e. nucleation, Aitken, accumulation, and coarse. Aerosols in each mode are allowed to grow or shrink as the result of gases condensation/evaporation, particle coagulation and absorption/evaporation of water. Particle size has been calculated at each time-step and the actual diameters have been used to calculate dry deposition velocities.

Aerosol wet scavenging. The same scheme for particle wet scavenging has been used in both models. In the Unified model different scavenging efficiencies have been applied to fine and coarse particles, while in UNI-AERO different scavenging efficiencies have been used for particles in four size modes. It is worth mentioning that the same scavenging efficiencies have been used for fine particles in the Unified model and accumulation mode particles in UNI-AERO, and for coarse aerosols in both models. Since particles from accumulation and coarse size modes account for most of the total mass, it is expected that wet scavenging will affect little the differences between the results from the two models.

In this way, we intended to achieve as similar as possible calculation of dry deposition and wet scavenging in the two models.

Sea salt. The EMEP Unified model does not include at the moment any natural source for PM, not even sea salt. Before implementing sea salt in the EMEP Unified model, a parameterisation for sea salt spray generation and transport was included and tested in the aerosol dynamics model. Sea salt contributes to the fine and particularly to the coarse aerosol mass and its importance is largest in coastal areas, especially in winter months. After some further verification of sea salt with the aerosol model, sea salt will also be implemented in the Unified model.

In the models $PM_{2.5}$ and PM_{10} mass is presently calculated as:

$PM_{2.5}$ = SO_4 + fine NO_3 + NH_4 + primary $PM_{2.5}$ (+ fine sea salt in UNI-AERO)

PM_{10} = $PM_{2.5}$ + coarse NO_3+primary coarse PM (+ coarse sea salt in UNI-AERO)

A crude preliminary parameterisation has been used in the Unified model to describe the formation of coarse NO_3 from HNO_3. In section 3.4, a test version

of the aerosol model is presented, which calculates formation of coarse NO_3 on sea salt aerosols.

Differences between the PM_{10} mass calculated by the two models are presented in Figure 3.1. The red curve shows the monthly variation of PM10 from the EMEP Unified model (UNIF), the mass model. The results from the aerosol model are given in the blue curve (AERO).

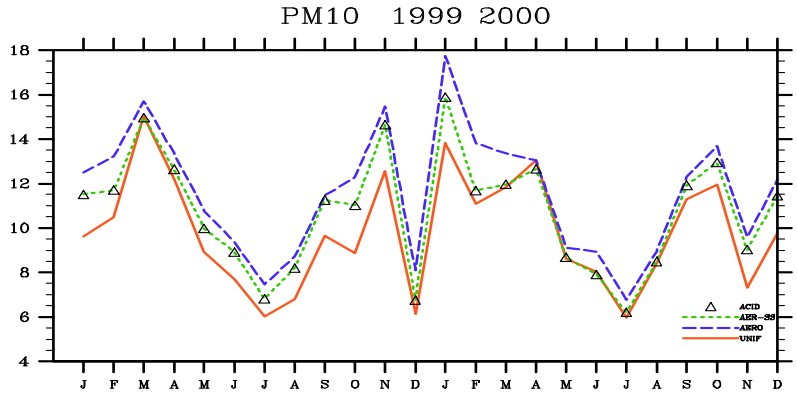

Figure 3.1: Monthly series of PM_{10} concentrations in 1999-2000 calculated with the Unified model (UNI, in red), aerosol dynamics model (AERO, in blue) and acid deposition model (ACID, in diamonds) and PM_{10} with subtracted sea salt mass from the aerosol model (AER-SS, in green). See text for discussion.

To understand better the origin of differences between the two curves, results from two sensitivity tests are shown. The green curve shows PM10 as calculated by the aerosol model without sea salt (AER-SS). The diamonds show the results from a mass model run with the same chemistry as used in the aerosol research model (ACID).

The largest differences are due to differences in the chemistry and to the inclusion of sea salt. The green curve (AER-SS) shows that the effect of sea salt is particularly important in winter and spring. Differences between the blue curve, PM_{10} from the Unified model (UNIF), and the green curve (AER-SS) show the effect of chemistry. The rather close coincidence between (AERO-SS) from the aerosol model and PM_{10} from the acid deposition model (ACID) indicates a little effect of aerosol dynamics on the PM_{10} concentrations.

The distribution of $PM_{2.5}$ and PM_{10} concentrations in 2000 calculated with the Unified model is presented in Figure 3.2(a). Figure 3.2(b) shows the relative differences between $PM_{2.5}$ and PM_{10} concentrations calculated with the aerosol model and the Unified model. Due to the contribution of sea salt aerosols, the overall PM_{10} concentrations from UNI-AERO are higher than PM_{10} from the Unified model. The relative differences between PM_{10} concentrations from two models are within 10 % in the most continental regions, reaching 20-40 % in England and Northern Europe. Sea salt aerosol contributes less to the fine particle

mass, thus $PM_{2.5}$ from UNI-AERO is in general 5 to 10 % larger (up to 20 % at the coasts) than $PM_{2.5}$ from the Unified model. Noticeably, in some areas, in particularly in Mediterranean region, more $PM_{2.5}$ is predicted with the Unified model because of larger concentrations of SO_4 and thus NH_4 calculated for those areas. This is probably because of more effective oxidation of SO_2 to SO_4 in the Mediterranean region due to larger concentrations of OH calculated in the Unified model compared with the tabulated OH in the aerosol model (see Chapter 4 in EMEP Report 1 and 2/2002). The distributions of SIA (the sum of SO_4, NO_3 and NH_4) and primary PM_{10} in 2000 from the Unified model are shown in Figure 3.3.

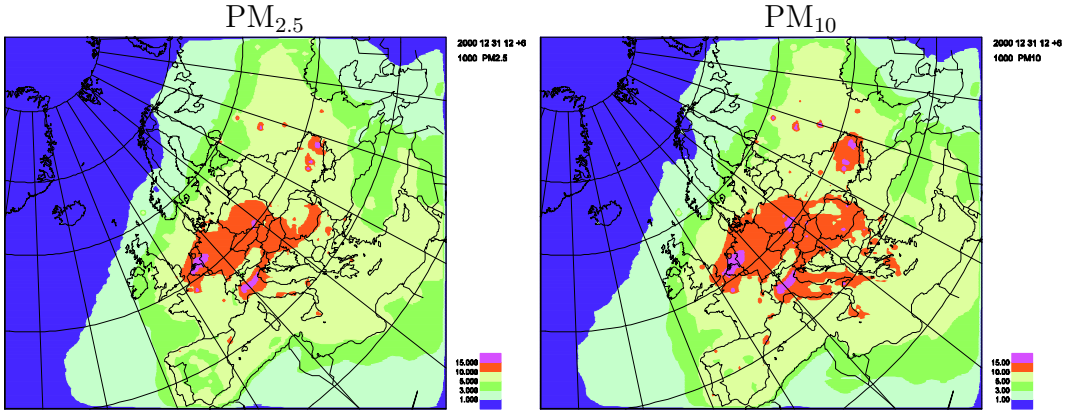

(a)

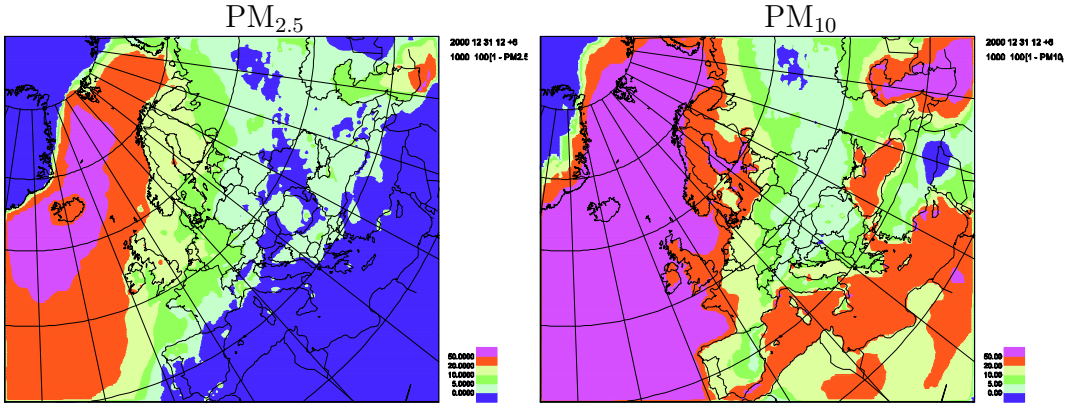

(b)

Figure 3.2: $PM_{10}$and $PM_{2.5}$ concentrations in 2000 calculated with the Unified model (a) and (b) the relative differences (in %) in PM_{10} and $PM_{2.5}$ calculated with the aerosol model and the Unified model.

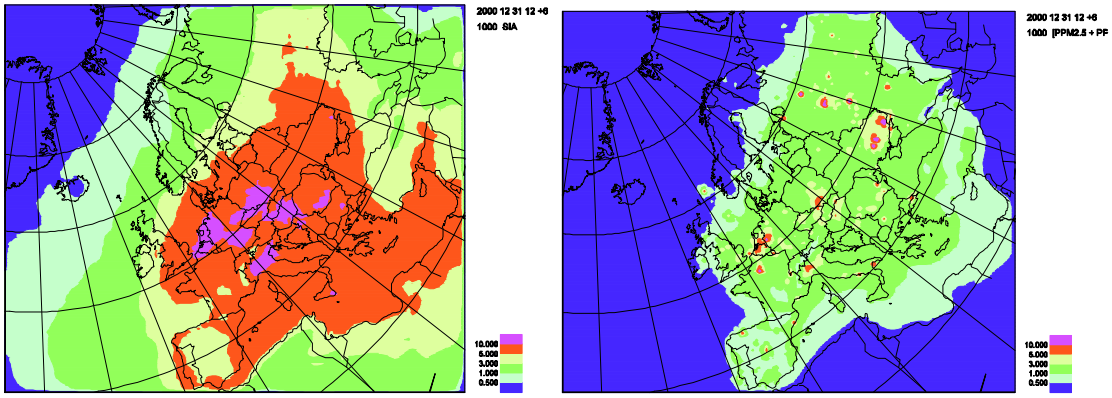

Figure 3.3: Concentrations of secondary inorganic aerosol (SIA) and primary PM in 2000 calculated with the Unified model.

In summary,

- the main reasons for differences in $PM_{2.5}$ and PM_{10} concentrations calculated with the Unified and aerosol model are 1) a more comprehensive chemical scheme in the Unified model and 2) accounting for sea salt aerosol in the aerosol model.
- as a result of the combined effect of these differences in model formulation, the aerosol model predicts larger PM_{10} concentrations than the Unified model. On the other hand, it calculates higher $PM_{2.5}$ in Central and Northern Europe, but lower $PM_{2.5}$ in the Mediterranean area. The differences in $PM_{2.5}$ are largely within 10 % and in PM_{10} are largely within 20 %. Along the Atlantic coast, where contribution of sea salt can be significant, the differences can reach 20 and 50 % respectively.
- aerosol dynamics appears to have very small effect on the $PM_{2.5}$ and PM_{10}mass concentrations.

3.2 Model validation of PM_{10} mass concentrations

3.2.1 Yearly averaged PM10 mass concentrations

Validation with EMEP measurements

Modelled mass concentrations of PM_{10}, SIA and the aerosol individual components, SO_4, NO_3 and NH_4, have been compared for 1999 and 2000 with measurements available from the EMEP network. Table 3.1 summarizes the statistical parameters (mean values, biases and correlation coefficients) of the comparison.

It is important to point out that because not all components were measured concurrently at the same stations, the verification of PM_{10}, SIA and the individual components SO_4, NO_3 and NH_4has been based on different sets of EMEP stations. Therefore conclusions made for any component are only indicative for explaining the other components. This should be considered when co-analysing verification results of the individual components.

Component	**Number of sites**	**Obs**	**Unified model**			**UNI- AERO**		
		Mean (μg/m^3)	**Mean** (μg/m^3)	**Bias** *) (%)	**Corr.**** spatial daily	**Mean** (μg/m^3)	**Bias** *) (%)	**Corr.**** spatial Daily
SO_4	75	2.11	1.97	-6	0.76 0.37	2.07	-2	0.69 0.33
NO_3	20	2.00	3.37	68	0.75 0.45	3.51	73	0.79 0.48
NH_4	25	1.00	1.46	46	0.77 0.46	1.61	60	0.77 0.47
SIA	12	6.34	7.77	22	0.79 0.50	8.43	33	0.75 0.44
PM_{10}	13	14.29	9.81	-31	0.38 0.43	11.60	-18	0.57 0.50

Table 3.1: Statistical parameters of the verification of the Unified and the aerosol model with EMEP measurements in 1999-2000

*) Relative bias calculated as (Model-Obs)/Obs * 100%

**) The upper number is the spatial correlation between observed and modelled yearly averages. The lower number is the daily correlation between all daily data for all stations.

Only 8 German and 5 Swiss EMEP stations reported PM_{10} concentrations in 1999 and 2000. Compared with EMEP measurements, the Unified model underestimates the 1999-2000 averaged PM_{10} concentrations by 31%. This un-

derestimation was expected as some main aerosol components, i.e. Secondary Organic Aerosols (SOA), sea salt and re-suspended mineral dust, was not incorporated in the Unified model. Even so, at some stations (Figure 3.4), PM_{10} is either overestimated (CH01, DE3, DE05) or only slightly overestimated (CH04 and CH05) by the model. All those stations are located over 1000 m, and CH01 (Jungfraujoch) at as high as 3573 m and are in the free troposphere a large part of the year, and practically all winter. Among the possible reasons for model PM_{10} overestimation at those sites could be the inaccuracy in free tropospheric boundary conditions and the coarse topography resolution in the model.

The correlation coefficient between calculated and monitored PM_{10} concentrations$_{\text{averaged}}$ for 1999-2000 is 0.38, and the temporal correlation for daily PM_{10} is 0.43. Separate analyses for Germany and Switzerland has revealed that the low annual correlation between modelled and measured PM_{10} is in fact due to results for German stations, while the correlation for Swiss sites is quite high (0.83). The model performance at German stations is dominated by DE01, DE02, DE07 and DE09 sites, which are strongly affected by the sea salt aerosols (see discussion below on Figure 3.6). At Swiss sites, where the sea salt influence is insignificant, the EMEP Unified model shows higher spatial correlations.

Figure 3.4 indicates that the Unified model tends to predict smaller regional gradients of PM_{10} than observed. PM_{10} measured at German and Swiss (excluding CH01) sites ranges between ca. 8 and 23 $\mu g/m^3$, while calculated PM_{10} varies only between 8.5 and 12.5 $\mu g/m^3$. The model reproduces rather well the measured gradients of other verified aerosol components, i.e. SO_4,NO_3 and NH_4 (see also Chapter 1 in this report), and SIA (Table 3.1). Not accounting for SOA, sea salt and re-suspended mineral dust by the Unified model can be pointed out as one of the reasons for under-predicting the PM_{10} gradients. On the other hand, uncertainties in the spatial distribution of primary PM emissions would also affect the results.

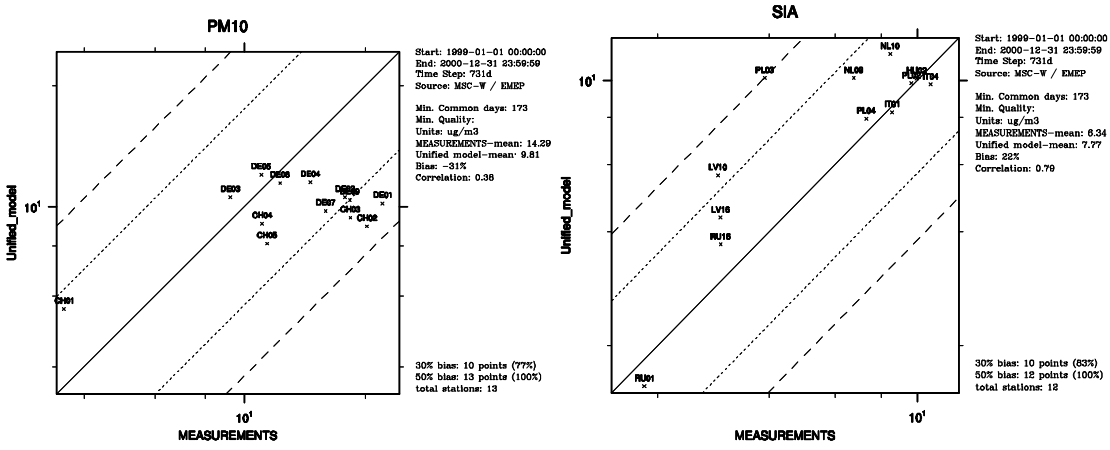

Figure 3.4: Scatter plots of 1999-2000 averaged PM_{10} and SIA calculated with the Unified model vs. monitored at EMEP sites

The correctness of predicted PM_{10} depends on the accurate calculation of each PM_{10} component. To verify SIA concentrations EMEP stations with concurrent measurements of SO_4, NO_3 and NH_4 have been selected. Only 12 such stations were found in 1999 and 13 stations in 2000 (Figure 3.4). Measured SIA concentrations are overestimated by the Unified model by 22 %, and the correlation coefficients is quite high (0.79). The statistics of verification of SO_4, NO_3 and NH_4 can be found in (Table 3.1). The major components of primary PM in the model, i.e. mineral dust, organic (OC) and elemental (EC) carbon, are not monitored at EMEP stations, therefore their verification is not feasible. Summarising the above, underestimation of PM_{10} by the Unified model is apparently due to not including in the model all main aerosol components, partly compensated by the overestimation of SIA concentrations.

To analyse the effect of sea salt in the calculations, results have been carried out for PM_{10} with the **aerosol dynamics model**, UNI_AERO, also for 1999 and 2000. As shown in Figure 3.5(a), the results with the research aerosol model agree better with measurements than results from the Unified model, showing the underestimation of 18 % and correlation coefficient of 0.57. Better correspondence of PM_{10} concentrations from UNI-AERO with observations is attributed to the model accounting for sea salt. To illustrate this statement, the sea salt mass has been subtracted from PM_{10} concentrations calculated by the aerosol model. Figures 3.5(b-d) show the results from this test on calculated PM_{10} at German stations. Here, the scatter plots for PM_{10} from the Unified model (Figure 3.5(d)) is compared with scatter plots for PM_{10} from the aerosol model including (Figure 3.5(b)) and excluding (Figure 3.5(c)) sea salt mass.

These results indicate that sea salt contribution in UNI-AERO has improved the average spatial correlation of PM_{10}. However this statement needs to be confirmed with a broader range of observations from other regions than Central Europe.

Validation with AIRBASE data

Model calculated PM_{10} concentrations in 2000 have been compared with measurements at rural sites available from the **AIRBASE** data-system (Figure3.6) and the results of verification are summarised in Table 3.2.

Both models underestimate the annual mean measured PM_{10} concentrations. The underestimation of PM_{10} by the Unified model is larger than by the aerosol model, as it was explained before, due to the contribution of sea salt to PM_{10} in the aerosol model. It is interesting to note that the level of systematic underestimation is of the same order (-31%) as with the EMEP stations, probably because the stations, although different, are also situated in Central Europe. Again, as with the EMEP stations, the models tend to under predict the regional gradients of observed PM_{10}.

For this dataset, PM_{10} concentrations from the Unified model have been found

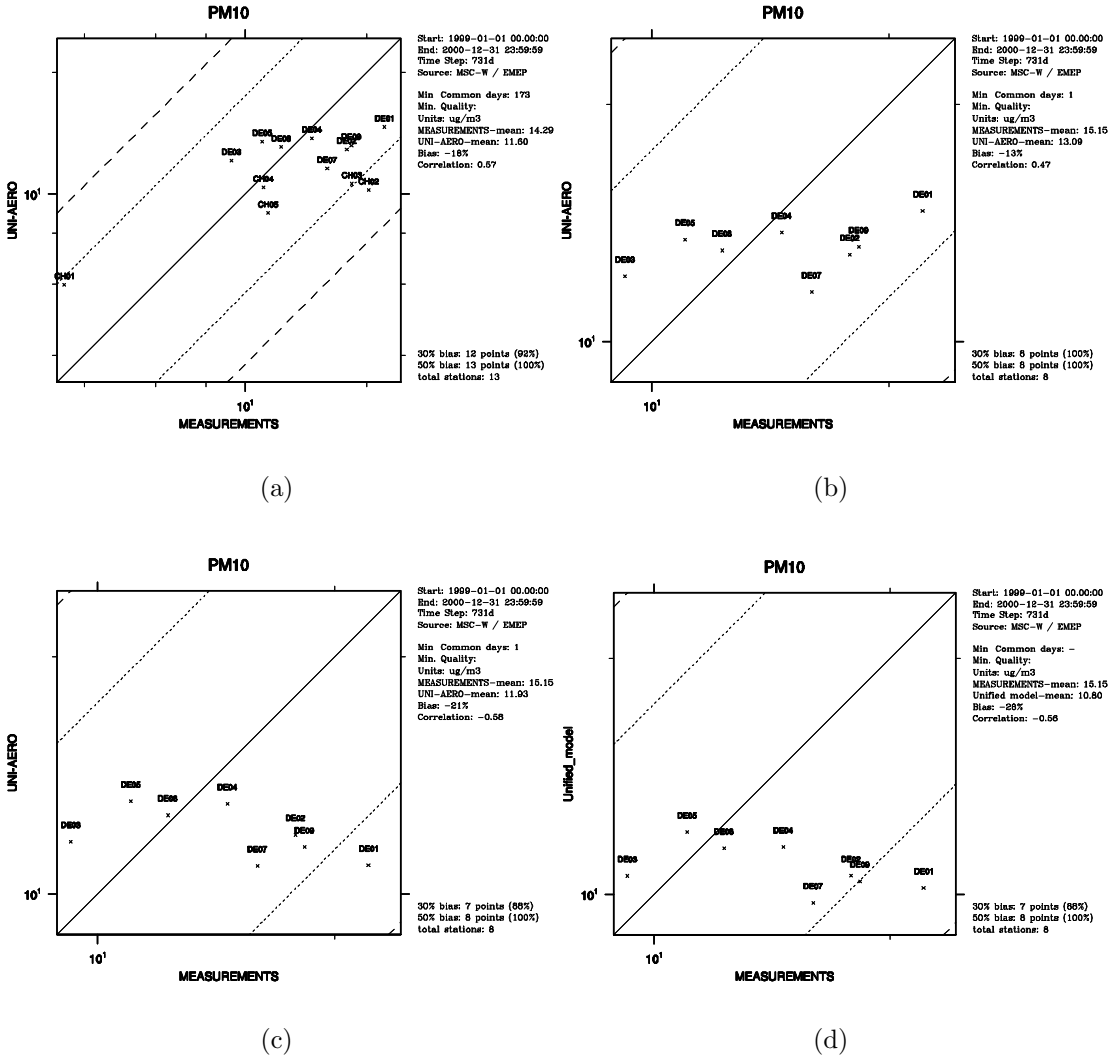

Figure 3.5: Scatter-plots of averaged for 1999-2000 modelled vs. monitored at EMEP sites PM_{10}concentrations: a) PM_{10} from the aerosol model for all stations, b) PM_{10} from the aerosol model for German sites only, c) PM_{10} with subtracted sea salt mass from the aerosol model for German sites, and d) PM_{10} from the Unified model for German sites only.

to correlate better with measurements than results from the aerosol model. The respective spatial correlation coefficients are 0.73 and 0.67. If we subtract sea salt mass from PM_{10} calculated by UNI-AERO the spatial correlation increases from 0.67 to 0.72. Contrary to the results from EMEP stations, accounting for sea salt in the aerosol model seems to decrease PM_{10} correlation with AIRBASE observations. This is probably due to the particular position of the individual stations in the AIRBASE network. Verification for the individual countries has shown that

Area	Number of sites	Obs	Unified model			UNI- AERO		
		Mean ($\mu g/m^3$)	Mean ($\mu g/m^3$)	Bias (%)	Corr. spatial aver.	Mean ($\mu g/m^3$)	Bias (%)	Corr. spatial aver.
All	49	22.19	12.81	-41	0.73	14.76	-33	0.67
CZ	20	21.52	13.38	-37	0.70	14.30	-33	0.67
NL	8	31.93	16.25	-49	0.74	20.50	-35	0.81
DE	10	17.17	11.78	-31	0.48	13.57	-20	0.56

Table 3.2: Statistical parameters for verification of the Unified and the aerosol model with AIRBASE measurements in 2000

PM_{10} fromUNI-AERO correlates with measurements better than PM_{10} from the Unified model in the Netherlands and Germany, where the contribution of sea salt affects the PM_{10} gradients the most.

The spatial correlation for individual countries is of the same level (0.7-0.8) as for EMEP stations except for Germany, where the AIRBASE network doesn't show the anti-correlations between modelled and observed values that were discussed in the previous section. Again, the position of the stations is determinant for the results.

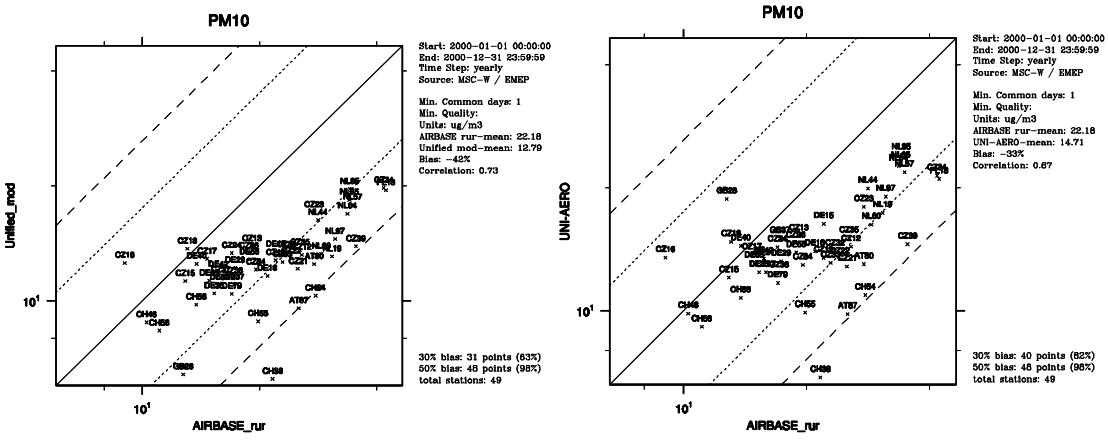

(a) (b)

Figure 3.6: Scatter plots for PM_{10} in 2000 calculated with the Unified model (a) and the aerosol model (b) vs. AIRBASE measurements.

Daily correlations for PM_{10}mass concentrations

In this section, the model's ability to reproduce observed daily variation of PM_{10} concentrations is evaluated against available EMEP and AIRBASE data at individual stations. Adequate description of both the temporal variation of emissions and the chemical transformations of emitted species is a necessary prerequisite for the model to reproduce the observed daily variations of PM concentrations. Daily time series of model calculated PM_{10} have been compared with observations at EMEP stations in 1999 and 2000 and at AIRBASE sites in 2000 (see examples in Figure 3.7). The statistical parameters of the comparison are summarised in Tables 3.3 and 3.4.

			1999			**2000**	
Sites		Obs. mean	Model mean	Correlation	Obs. mean	Model mean	Correlation
CH01	Jungfraujoch	3.77	5.55	0.14	3.38	5.60	0.04
CH02	Payerne	20.59	9.02	0.50	19.80	8.87	0.60
CH03	Taenikon	18.79	8.99	0.50	17.90	9.80	0.47
CH04	Chaumont	12.07	9.40	0.41	10.25	8.81	0.40
CH05	Rigi	11.79	7.86	0.42	11.03	8.36	0.37
DE01	Westerland / Wenningsted	23.54	9.82	0.24	20.49	10.61	0.54
DE02	Langenbrögge / Waldhof	19.11	9.90	0.60	16.52	11.22	0.65
DE03	Schauinsland	8.10	10.07	0.34	10.49	11.08	0.21
DE04	Deuselbach	14.42	11.46	0.57	14.81	11.55	0.57
DE05	Brotjacklriegel	10.53	11.55	0.41	11.51	12.46	0.27
DE07	Neuglobsow	14.57	9.13	0.54	17.37	10.39	0.64
DE08	Schmöcke	12.50	10.80	0.52	12.06	12.13	0.45
DE09	Zingst	17.02	9.82	0.57	19.64	11.00	0.70

Table 3.3: Verification of daily PM_{10} concentrations at EMEP stations in 1999 and 2000: calculated with the Unified model and measured annual means and daily correlation coefficients.

As expected, the Unified model underestimates the overall annual mean PM_{10} concentrations, except for a few elevated sites in Germany and Switzerland. Just to remind, the underestimation by the Unified model of PM_{10} is because the model does not take into account secondary organic aerosol, sea salt and re-suspended mineral dust.

The correlation between modelled and measured daily PM_{10} is rather good. For EMEP stations, the daily correlation coefficients are around 0.5-0.7. Lower correlations (0.2-0.4) are observed at elevated stations. The lowest correlation

is found for CH01 (Jungfraujoch) which is located at 3573 m height. Among AIRBASE sites, the best correlation between calculated and measured PM_{10} are found at Dutch, British (0.6-0.8) and German (0.4-0.6) stations. The correlation coefficients are lower in Czech (0.25-0.50) stations, while at Swiss and Austrian stations the correlation are rather varying, with lower correlation at elevated sites (unfortunately, information on the elevation of AIRBASE sites were not available to MSC-W).

Sites	Obs. mean	Model mean	Correlation	Sites	Obs. mean	Model mean	Correlation
AT80	27.66	12.50	0.48	DE35	15.33	10.47	0.50
AT87	25.22	9.59	0.29	DE40	13.81	12.52	0.46
CZ33	22.92	12.67	0.24	DE18	20.97	11.64	0.57
CZ36	18.79	13.35	0.60	DE55	18.89	12.87	0.50
CZ39	35.33	13.90	0.23	DE65	14.91	11.32	0.50
CZ16	9.04	12.60	0.29	DE29	17.35	12.22	0.57
CZ12	25.68	13.23	0.39	DE42	15.69	11.92	0.56
CZ15	12.92	11.29	0.28	DE31	15.76	11.03	0.53
CZ32	23.49	13.44	0.24	DE79	17.01	10.45	0.60
CZ84	19.58	12.11	0.55	NL97	31.26	14.53	0.53
CZ21	25.09	12.15	0.48	NL44	28.26	16.31	0.70
CZ17	14.70	12.91	0.37	NL65	34.03	18.44	0.73
CZ38	17.14	11.47	0.47	NL85	34.12	19.64	0.72
CZ13	19.15	13.94	0.42	NL60	28.83	13.31	0.68
CZ37	15.92	11.55	0.46	NL57	34.71	17.87	0.77
CZ18	13.08	13.72	0.45	NL04	33.63	16.95	0.67
CZ24	16.99	13.37	0.49	NL19	30.72	13.08	0.68
CZ22	24.11	12.93	0.40	PL18	42.19	19.49	0.30
CZ23	27.58	17.08	0.45	CH46	10.28	8.81	0.40
CZ19	22.02	12.81	0.39	CH54	27.85	10.35	-0.17
CZ34	41.68	19.80	0.48	CH55	19.85	8.87	0.60
CZ35	25.41	13.63	0.51	CH56	11.09	8.37	0.17
GB28	12.77	6.45	0.59	CH38	21.64	6.27	0.37
GB37	17.24	11.05	0.63	CH58	13.80	9.80	0.39

Table 3.4: Verification of daily PM_{10} concentrations at AIRBASE sites 2000: calculated with the Unified model and measured annual means and correlation coefficients

Examples for modelled and measured PM_{10} daily time series at sites in different countries are given in Figure 3.7. The daily series of PM_{10} calculated with the Unified and aerosol model (UNI-AERO) for British and Dutch sites located close to the sea coast illustrate the effect of sea salt. It can be seen that accounting

for sea salt aerosol in UNI-AERO improves (increase towards the measurements) PM_{10} values in especially winter months.

The Unified model captures fairly well the measured PM_{10} daily variability, at least in central Europe. It seems to underestimate the measured PM_{10} concentrations more in late spring and summer than in other seasons. The seasonality of model performance will be further discussed in section 3.2.2.

A very distinct episode with rather high PM_{10} levels was registered at the Czech station in May-June 2000, which the model has failed not predicted. To explain this PM_{10} episode we would need to know what specific components in PM_{10} were responsible for the high PM_{10} concentrations. No measurement of the aerosol chemical composition was available at that site, and the only aerosol measurements available in Czech Republic in 2000 were NO_3 and NH_4 concentrations at EMEP stations CZ01 and CZ03. Scatter plots for NO_3 and NH_4 at those stations do not exhibit any distinct episodes for those components. The most resembling episode we have found is NO_3 fall at CZ03 (Kosetice) on July 1. The closest German station, Deuselbach (see Figure 3.7), does not exhibit any such PM_{10} episode either. The likely reason the enhanced up to 50-60 $\mu g/m^3$ PM_{10} concentrations at CZ13 is thought to be some local sources (e.g. a large source of dust). Measurements on aerosol chemical composition would provide a desirable basis for analyses of such emission episodes and for identification of possible problems in the model.

Concluding, chemical analyses of particle composition and the mass balance should complement the PM_{10} measurements in order to identify the sources of particulate matter and to facilitate the interpretation of model verification and thus the improvement of aerosol modelling.

Frequency distribution of aerosol mass concentrations

The frequency distributions of modelled and measured PM_{10} daily concentrations at 13 EMEP sites for the period of 1999-2000 are compared in Figure 3.8(a, b). The Unified model manages to reproduce differences in the observed frequency distributions between 1999 and 2000. In both years, the model over-estimates the occurrence of PM_{10} concentrations lower than 10-12 $\mu g/m^3$, while the number of days with larger PM_{10} concentrations is under-predicted. In contrast, the model over-predicts the low SIA concentrations and under-predicts high concentrations (Figure 3.8(d)). That means the contribution of SIA in fact improves PM_{10} concentrations. It is expected that inclusion in the model of sea salt, re-suspended dust and SOA will improve the calculated frequency distribution curve towards higher PM_{10}.

Figure 3.8(c) compares the frequency distribution of model calculated PM_{10} concentrations with AIRBASE data. Also here, low PM_{10} concentrations below 10-12 $\mu g/m^3$ are over-predicted, while larger PM_{10} values are under-predicted.

In summary,

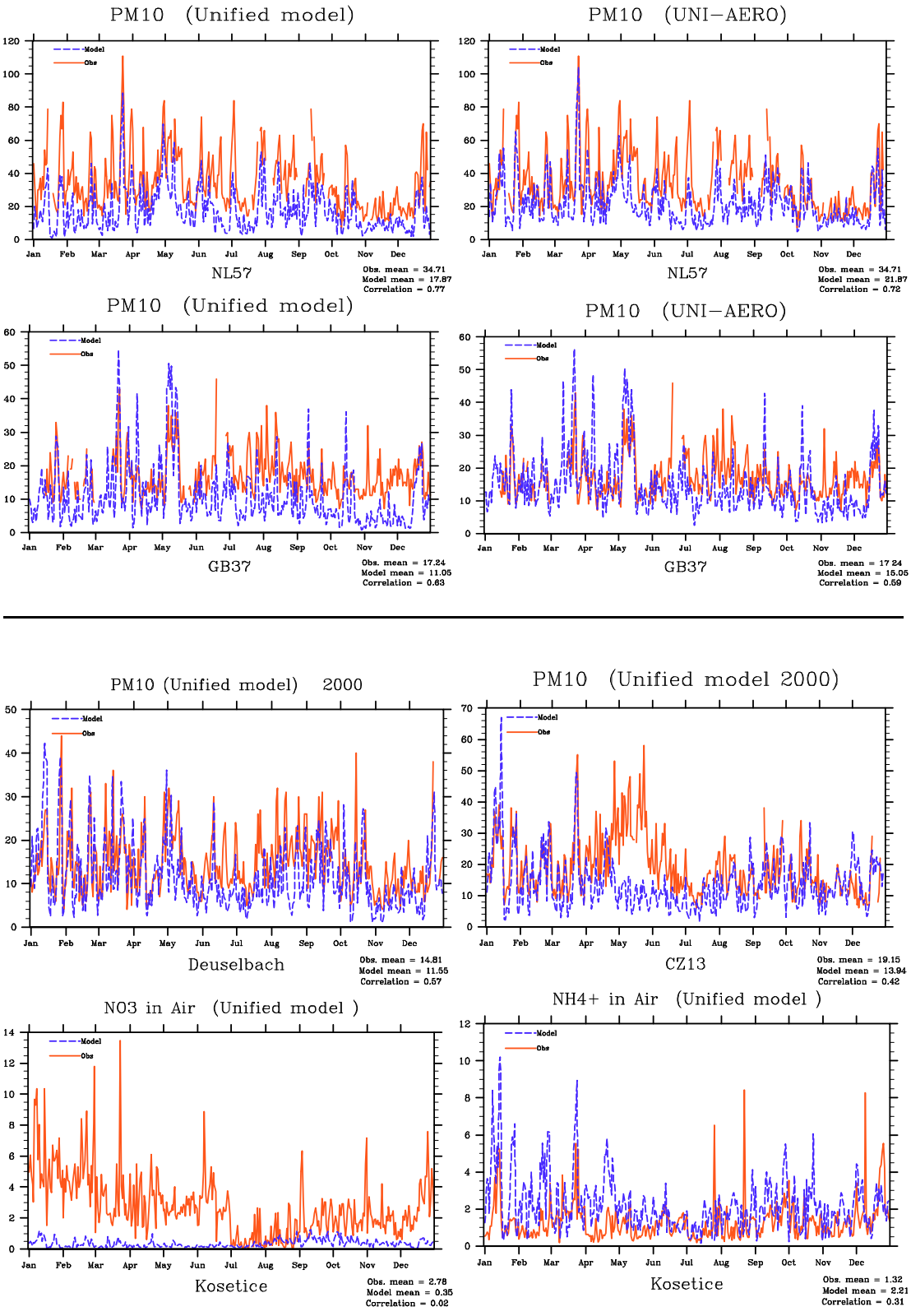

Figure 3.7: Examples of daily series of PM_{10} concentrations at AIRBASE and EMEP stations (see discussion in the test). Model in blue, measurements in red curve.

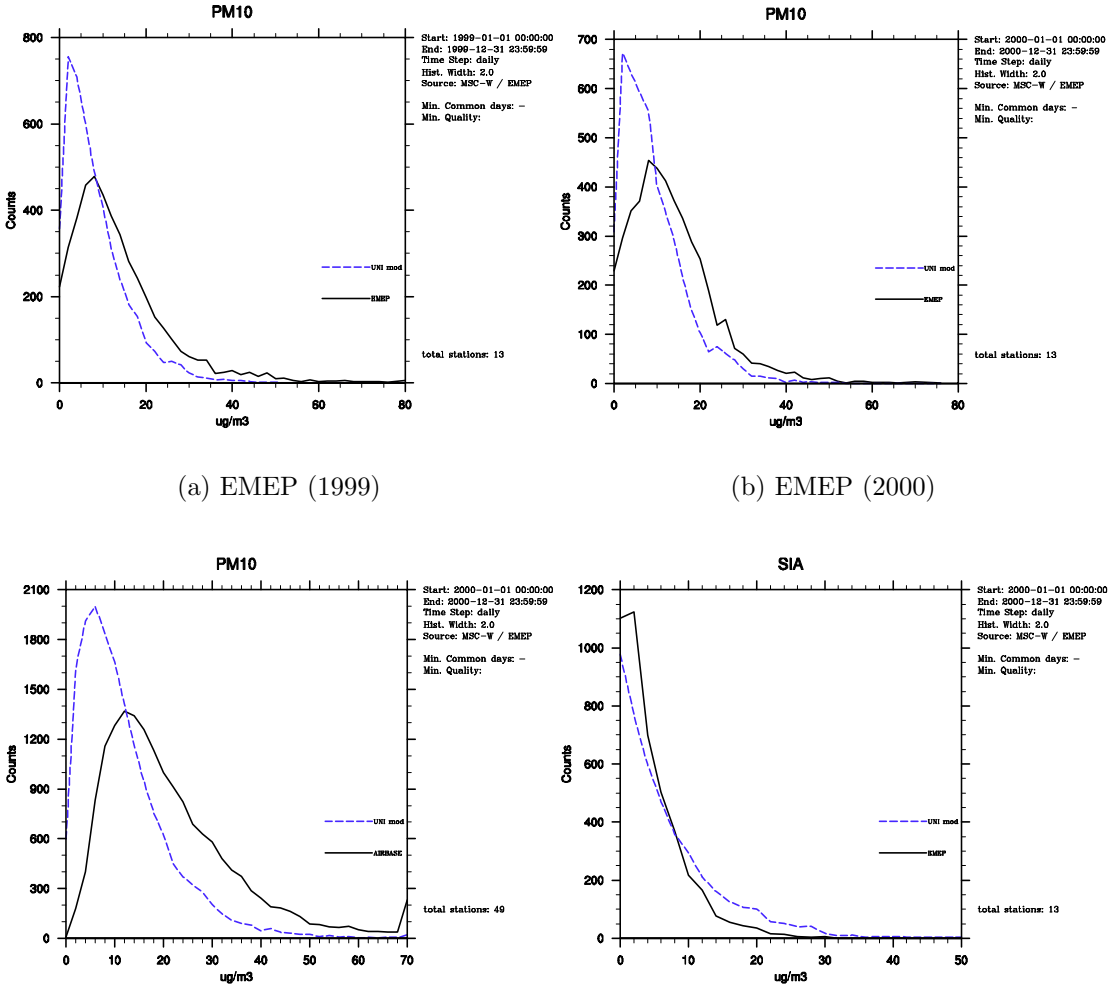

(a) EMEP (1999)

(b) EMEP (2000)

(c) AIRBASE (2000)

(d) EMEP (2000)

Figure 3.8: Frequency distributions of PM_{10} calculated with the Unified model vs. (a) EMEP data in 1999, (b) EMEP data in 2000, (c) AIRBASE data in 2000, and (d) calculated and EMEP measured SIA concentrations: model – dashed blue line, observations – solid black line.

- Both models underestimate the measured PM_{10} concentrations and calculate smaller PM_{10} regional gradients the observed. Accounting for sea salt in UNI-AERO improves partly the level of PM_{10} concentrations and the large scale gradients of PM_{10}

- PM_{10} concentrations from the Unified model correlate better with the measurements in the areas with dominant anthropogenic pollution due to the better chemical scheme. PM_{10} from the aerosol model correlates better with

observations at the sites where the influence of sea salt is significant.

- Modelled frequency distributions of PM_{10} are shifted towards the lower values compared with the observations. Implementation of sea salt, resuspended dust and SOA in the Unified model is expected to improve the modelled PM_{10} frequency distribution.

3.2.2 Seasonal variability of PM_{10}mass concentrations

EMEP sites. Table 3.5 summarizes the statistical parameters of comparison between the Unified model calculations and EMEP measurements in different seasons in 1999 and 2000. It is interesting to notice that measured PM_{10} seasonal concentrations do not exhibit any significant common feature for both years. A small PM_{10} maximum appears to take place in spring, while lower seasonal PM_{10} concentrations are found in winter and summer in 1999 and summer and autumn in 2000. The Unified model predicts greater PM_{10} seasonal variation than the measurements indicate, with the highest PM_{10} occurring in spring (in 1999) and winter (in 2000) and the lowest PM_{10} in summer. The largest underestimation of PM_{10} concentrations by the Unified model is found in summer (45-47 %) and the smallest in winter (16-21 %). This is because the model overestimation of NO_3 and NH_4 in winter (ref. Chapter 1 in this report) increases PM_{10} winter concentrations.

Both calculations and measurements show maximum SIA concentrations in winter (2000) or spring (1999) and minimum SIA in summer. The difference is on the magnitude of the seasonal variations. Calculated seasonal variability of SIA has a pronounced amplitude, while the observed PM_{10} varies rather little with seasons.

AIRBASE data. Compared with AIRBASE observation data at 49 rural sites, the Unified model underestimates PM_{10} concentrations the most in summer (by 51 %) and the least in winter (by 32 %). As a result, the model predicts greater seasonal variability of PM_{10}than observed, especially the difference between winter and summer concentrations is overestimated. The correlation between calculated and measured PM_{10} is highest in summer (0.59) and lowest in winter (0.39). As no measurements of the individual aerosol components have been available for those sites, it is rather difficult to interpret the results.

Monthly variation of PM_{10} is to a large degree governed by the seasonal variation of emissions of both aerosol gaseous precursor and primary particles from different sectors. Averaged over the available stations, the calculated PM_{10}show a general agreement with the observed monthly variation of PM_{10}. PM_{10} concentrations appear to have two maxima: in spring (March-April) and in early autumn (September), and two minima: in summer (June) and late autumn (November-December). As it was expected, both models underestimate the monitored PM_{10} concentrations.

		1999					2000				
Com-po-nent	Season	Number of sites (CH, DE)	Mean obs (μg/m^3)	Mean model (μg/m^3)	Bias (%)	Corr.	Number of sites (CH, DE)	Mean obs (μg/m^3)	Mean model (μg/m^3)	Bias (%)	Corr.
PM_{10}	Year	13	14.37	9.49	-33	0.32	13	14.25	10.15	-28	0.44
	winter	13	13.03	10.15	-21	0.38	13	15.17	12.59	-16	0.32
	Spring	13	16.22	12.06	-25	0.57	13	15.35	11.19	-26	0.54
	summer	13	13.08	6.84	-47	0.36	13	13.67	7.45	-45	0.47
	autumn	13	15.20	10.28	-31	0.41	13	13.52	10.27	-23	0.57
SIA	Year	12	7.01	7.50	7	0.69	13	5.43	7.86	45	0.75
	winter	12	7.46	9.08	22	0.41	13	6.35	9.14	44	0.58
	Spring	12	8.71	9.85	13	0.45	13	5.44	8.72	61	0.50
	summer	12	6.16	5.63	-8	0.57	13	4.78	5.81	22	0.71
	autumn	12	7.04	7.43	6	0.59	13	5.40	7.83	25	0.51

Table 3.5: Statistical parameters of verification of PM_{10} and SIA from the Unified model with EMEP measurements in 1999 and 2000

Com-po-nent	Season	Number of sites	Mean obs (μg/m^3)	Mean model (μg/m^3)	Bias (%)	Corr.
PM_{10}	year	49	22.19	21.81	-41	0.73
	winter	46	23.20	15.59	-32	0.39
	spring	49	24.04	14.19	-40	0.55
	summer	49	20.28	9.79	-51	0.59
	autumn	49	21.14	12.51	-40	0.44

Table 3.6: Statistical parameters of verification of PM_{10} calculated by the Unified model with AIRBASE data in 2000

The underestimation of $PM_{10}$by the models is smallest in winter, except for December 1999. In general, the model underestimation of PM_{10} concentrations is larger in the warm period than in the cold period. In autumn and winter months, both models calculate too high NO_3 and NH_4 concentrations compared with measurements, which partly compensate for the aerosol mass not being accounted for in the models ("better results for the wrong reason"). In summer, calculated NO_3, NH_4 and $SO_4$are closer to the observations (ref. Chapter 1, this report). Given the reasonable SIA prediction for the warm season, the model larger underestimation of PM_{10} is thought to be due to the omitted contribution of re-suspended dust (SOA is less important then). Another source of uncertainties in calculated PM_{10} is the emissions of primary PM and their temporal variation. Furthermore, aerosol dry mass has been used to compare with observations, while the measured PM_{10} mass can contain up to 25-30 % of residual aerosol associated

water.

Finally, SO_4 calculated with a full photo-oxidant chemistry in the Unified model agrees much better with the measurements. Therefore in future we intend to use the photo-oxidant chemical scheme also in the aerosol dynamics model.

Figure 3.9 compares monthly time series of model calculated PM_{10} concentrations with AIRBASE measurements in 2000. Averaged over 49 sites, monthly series of PM_{10} calculated by the Unified and the aerosol dynamics models capture quite well the observed pattern of PM_{10} monthly variation. Both, model and observations exhibit three PM_{10} maximum: in December-January, April and October and minimum in June-July and November. The models underestimate the measured PM_{10} concentrations by ca. 30-50 %. The effect of sea salt contribution to PM_{10} in UNI-AERO is to increase PM_{10} concentrations mainly in winter and autumn. The high PM_{10} in January calculated with UNI-AERO is probably due to the overestimated NO_3 and NH_4 concentrations.

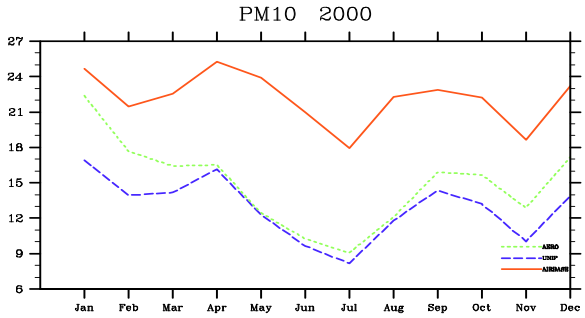

Figure 3.9: PM_{10} monthly series in 2000 calculated by the Unified and aerosol models and measured at AIRBASE rural sites (averaged over 49 sites). Here, Unified model – blue, aerosol model – green, measurements – red line.

Regional differences in PM_{10} seasonal variation Figure 3.10 exemplifies the variability of patterns of PM_{10}seasonal variation in different countries. Modelled and measured monthly series of PM_{10} concentrations are plotted separately for German and Swiss EMEP stations in 1999-2000 and for Czech, Dutch and British AIRBASE rural sites in 2000. The common for all countries is the more or less pronounced PM_{10} maximum in March-April and minimum in June-July. For all countries except the Great Britain, another PM_{10} maximum can be identified in September–October. It has been found rather encouraging that the model manages to capture the most of observed features in PM_{10} seasonal variability.

Rather distinctive monthly variations of PM_{10} concentrationsare found at Dutch and particularly at British stations. In the Netherlands, peaks in PM_{10} observed concentrations in March, May and September could be due to the enhanced ammonium and dust concentrations associated with farming activities. The model captures well the variation of measured at Dutch sites PM_{10} except

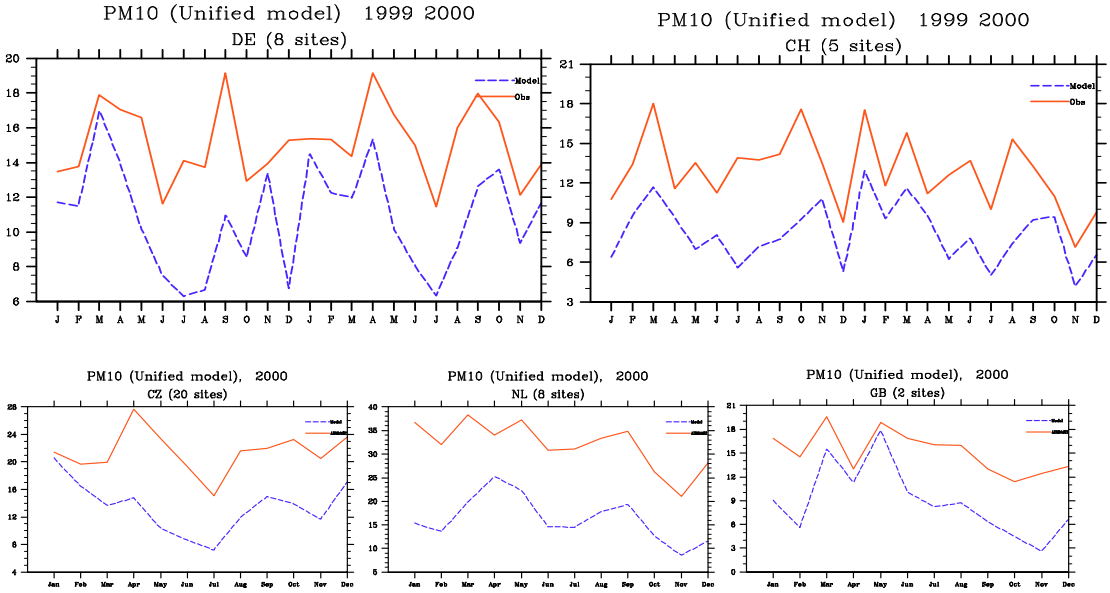

Figure 3.10: PM_{10} monthly series in different countries calculated with the Unified models and measured. Here, Unified model – blue, measurements – red curve.

in spring, when the model predicts PM_{10} maximum in April. This is consistent with the seasonal variation of agricultural emissions from GENEMIS employed in the model. Wind blown dust has not been calculated by the model. These disagreements between calculated and observed PM_{10} implies that the seasonal variation of agricultural emissions in the model is not quite accurately described. In any case, since PM_{10} is a rather complex pollutant, analyses of all individual components is needed in order to identify the source of disagreement between the model and observations in each specific case.

Seasonal frequency distributions of PM_{10} concentrations

In all seasons, the Unified model systematically over-predicts the number of days with PM_{10} concentrations below 8-10 $\mu g/m^3$ and under-predicts the number of days with higher PM_{10} concentrations compared to observations at EMEP stations (examples are given in Figure 3.11 for the year 2000) and in AIR-BASE (see examples in Figure 3.13). The best correspondence between modelled and observed PM_{10} frequency distribution is found in winter and autumn (Figures 3.11(a) and 3.11(d)). Analyses of frequency distributions of SIA has shown that in these seasons, SIA concentrations exhibit just the opposite, i.e. under-prediction of the lower concentrations and under-prediction of the higher concentrations (Figures 3.12(a)). This suggests that in cold seasons we obtain results of PM_{10} closer to the measurements for the wrong reason, i.e. due to overestimating SIA. In spring (Figure 3.11(b)), the model calculates narrower

than observed PM_{10} frequency distribution, predicting too many days with PM_{10} lower than $10\mu g/m^3$. The disagreement between model results and measurements is especially large in summer (Figure 3.11(c)), when the calculated frequency distribution of PM_{10}concentrations is distinctly shifted towards the lower values.

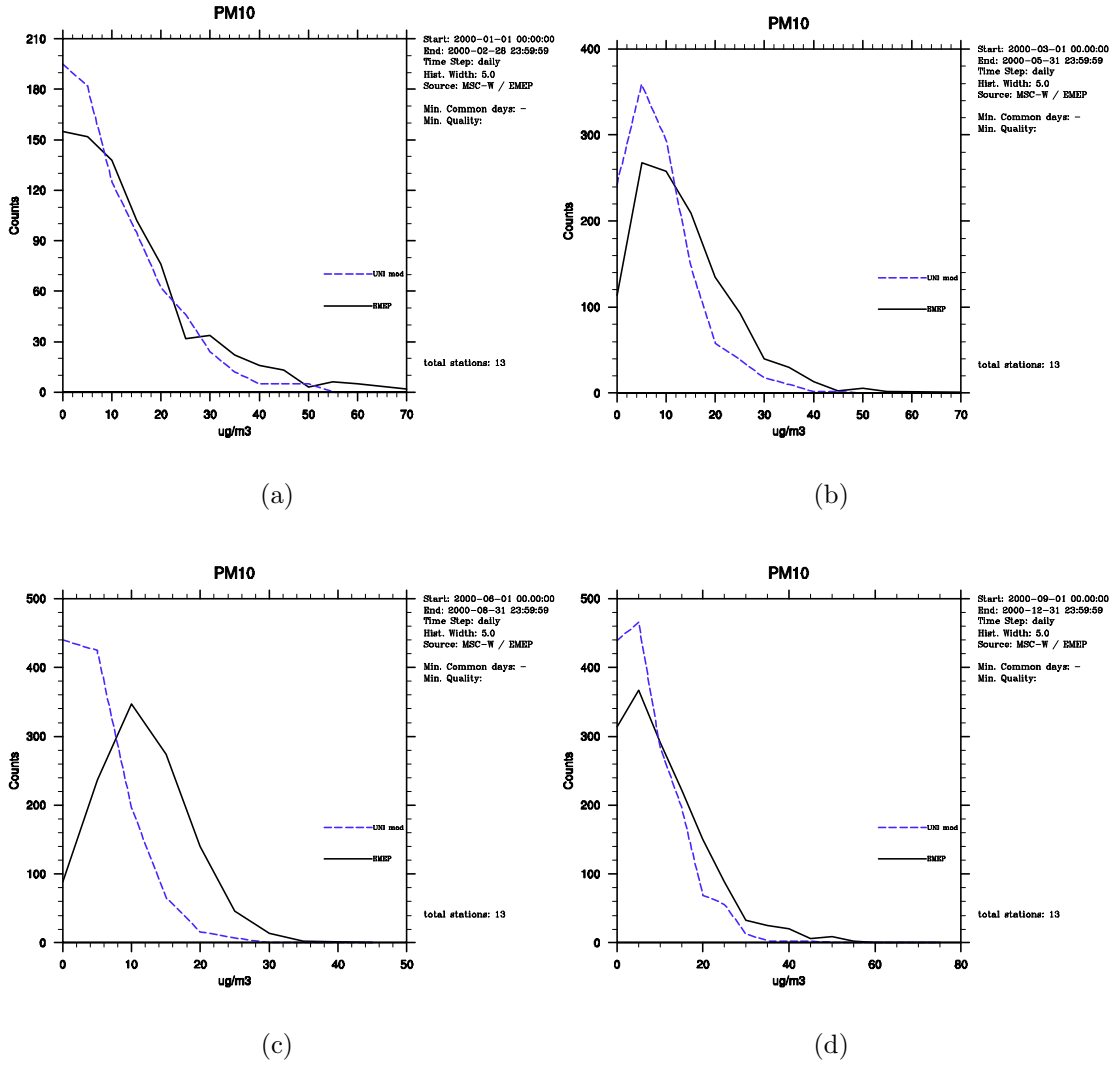

Figure 3.11: Frequency distributions for PM_{10} concentrations in 2000 calculated with the Unified model (dashed blue curve) and measured (solid black curve) at EMEP stations (5 Swiss and 8 German sites).

As we already discussed above, the main reason for the model under-prediction of high PM_{10} concentrations is because the Unified model does not account for all aerosols components. In cold seasons, the missing contribution from SOA and sea salt aerosol in the areas affected by marine air masses is believed to be important. In spring and summer, wind eroded and re-suspended mineral dust is believed

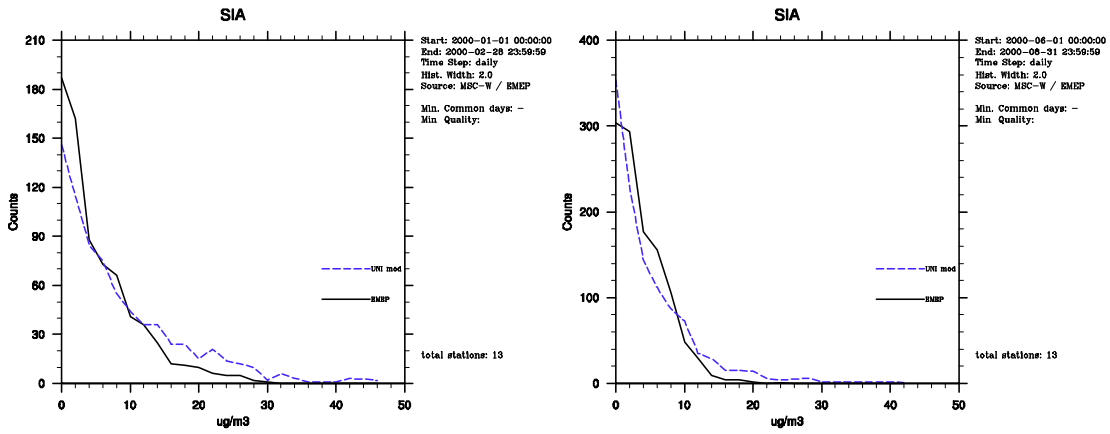

Figure 3.12: Frequency distributions for SIA concentrations in 2000: calculated with the Unified model (dashed blue curve) and measured (solid black curve) at 13 EMEP stations.

to be a significant contributor to the particle mass and likely responsible for the enhanced PM_{10} concentrations and high PM_{10} episodes. The same conclusions are drawn from comparison with AIRBASE site in 2000 (as shown in Figure 3.13).

Regional differences in the PM_{10} frequency distribution

Although all available stations are situated in Central Europe, it is still interesting to compare frequency distributions of PM_{10} concentrations in 2000 for different available countries, e.g. Austria (2 sites), Germany (8 sites) and Switzerland (5 sites). For these countries, the model calculates quite similar shapes for the PM_{10}frequency distribution, while the observed frequency distributions are rather different (Figure 3.14). The best correspondence between the modelled and the observed PM_{10}frequency distribution are seen for German stations. At Austrian sites, measurements exhibit a considerably broader PM_{10}frequency distribution than the model calculates. The model predicts PM_{10} concentrations to be within 20 $\mu g/m^3$most days of the year and a very few days with PM_{10} exceeding 25 $\mu g/m^3$. According to the monitoring data, PM_{10} concentrations from 10 to 35 $\mu g/m^3$ have approximately the same occurrence frequency. Without knowing the sources contributing to PM concentrations in the region it is rather difficult to interpret the disagreement between the model and observations.

Observed PM_{10}frequency distribution at Swiss sites looks different from German and Austrian observations, with the maximum frequency for days with PM_{10} below 1-2 $\mu g/m^3$. This is probably due to the contribution of very low PM_{10} winter concentrations at elevated Swiss sites. In winter, when those sites are often or all the time in a free troposphere and inversions prevent the transport of pollutants from the boundary layer upward, very low PM_{10} is often measured. This is particularly pronounced for CH01 (Jungfraujoch) located at 3573 m above MSL,

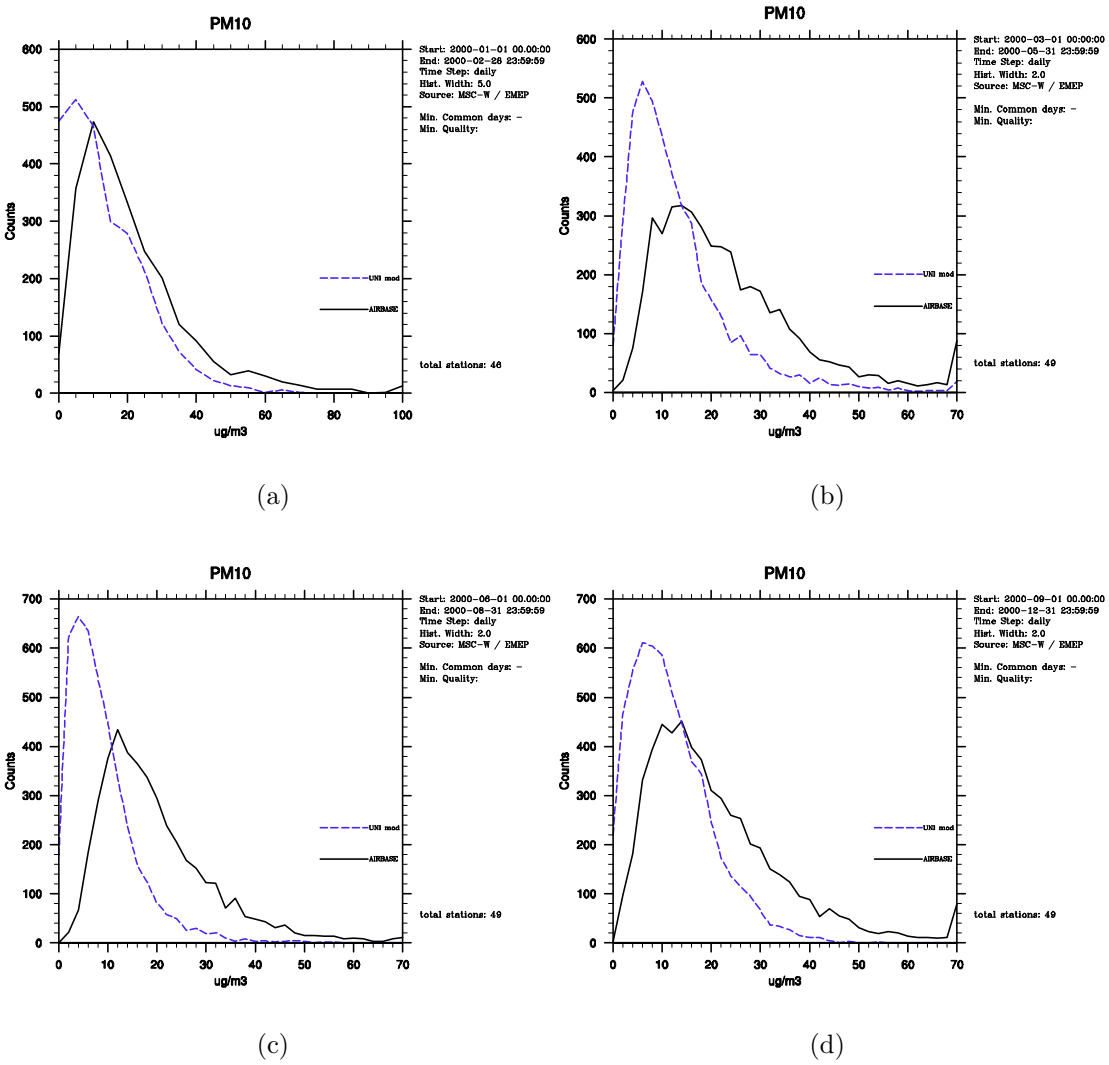

Figure 3.13: Frequency distributions for PM_{10} concentrations in 2000 calculated with the Unified model and measured at AIRBASE rural sites (49 sites): model – dashed blue curve, observations – solid black curve.

where PM_{10} concentrations in winter hardly exceed 5 $\mu g/m^3$ (Figure 3.14(d)). The model calculates much broad winter PM_{10} frequency distribution, predicting too few days with low PM_{10} and also occurrence of quite high PM_{10}. In warm seasons, these sites are within the mixed boundary layer, and the correspondence between modelled and measured PM_{10} frequency distribution is better. This suggests that it would be useful to have better observed information on the vertical profiles of aerosols and their gaseous precursors.

Summing up, the best agreement between PM_{10} frequency distribution calculated with the Unified model and measurements is found in winter and are

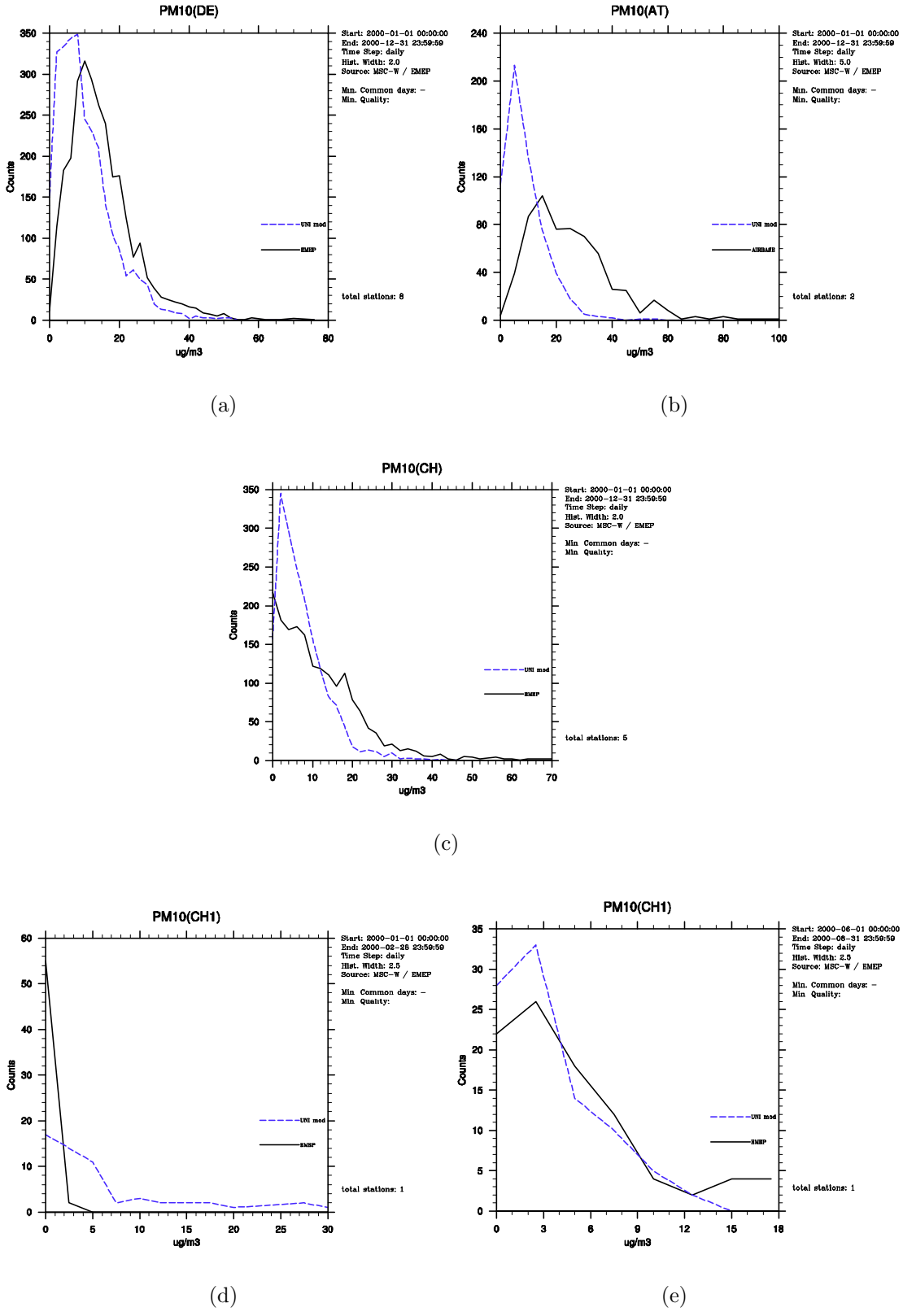

Figure 3.14: Frequency distributions for PM_{10} in 2000 calculated with the Unified model vs. EMEP measurements at German (a) and Swiss (b) sites, and at CH01 in winter(c) and summer (d). Model – dashed blue line, observations – solid black line.

likely due to the model overestimation of SIA (more precisely NO_3 and NH_4). In the other seasons, especially in spring and summer, calculated PM_{10} frequency distributions are narrower the measured ones and shifted towards the lower concentrations. In those seasons, the contribution of re-suspended and wind blown mineral dust to PM_{10} can be important. These discrepancies are expected decrease/vanish when the model will have incorporated all main aerosol component.

3.3 Validation of PM_{10} vs $PM_{2.5}$ mass concentrations

Rather little monitoring data is available for verification of $PM_{2.5}$ concentrations. Here, we compare model calculated PM_{10} and $PM_{2.5}$ with measurements at two Austrian and one Swedish site.

PM10 and PM2.5 daily series. PM_{10} and $PM_{2.5}$ measurements data from the Austrian AUPHEP project was kindly forwarded to MSC-W by IIASA. AUPHEP is a research project of the Clean Air Commission of the Austrian Academy of Science together with a number of other Austrian institutions. The first site, AU01, is located in a residential area of Wien affected by traffic ("urban background"). The second site, AU02, is rural, with some influence of traffic (Streithofen). The measurement period was from 1.06.1999 to 31.05.2000. PM_{10} and $PM_{2.5}$ mass was continuously monitored with TEOM and measured with High-Volume Filter-Samplers. In this report, we consider PM_{10} and $PM_{2.5}$ concentrations determined with a gravimetric method because gravimetric methods are recommended for use in the EMEP monitoring network. The gravimetric method gives typically larger PM mass then TEOM due to the residual aerosol water, and also because of losses of volatile NH_4NO_3 and organic matter in TEOM.

Daily time series of calculated and measured PM_{10} and $PM_{2.5}$ are presented in Figure 3.15. Model calculated and measured PM_{10} and $PM_{2.5}$ are in a rather good agreement at both urban and rural site. The correlation coefficients vary from 0.57 to 0.68 for PM_{10} and from 0.60 to 0.67 for $PM_{2.5.}$

Larger model underestimation of the measured PM_{10} concentrations than $PM_{2.5}$ concentrations indicates that there is too little mass of coarse particles in the Unified model. As it was already pointed out, such important contributors of coarse particles as re-suspended and wind blown dust, which can be important both in the city and the countryside, are not presently accounted for in the Unified model. Underestimation of coarse mass could also be due to too efficient removal of coarse particles in the model by dry deposition.

The model appears to perform better for the period from January to May 2000 than for the period from June to December 1999. In the latter period, the model underestimation of both PM_{10} and $PM_{2.5}$ is larger. Noticeable, the model predicts a period with rather low PM_{10} and $PM_{2.5}$ concentration from December 1999 till mid-January 2000, while the measured concentrations in the same period were at the highest. Interpretation of this episode requires additional information on possible sources, perhaps local, of higher observed concentrations (e.g. increased house heating due to low ambient temperatures).

A rather good correspondence between model calculated and measured PM_{10} and $PM_{2.5}$ (Figure 3.16) also implies that calculations from the Unified model can

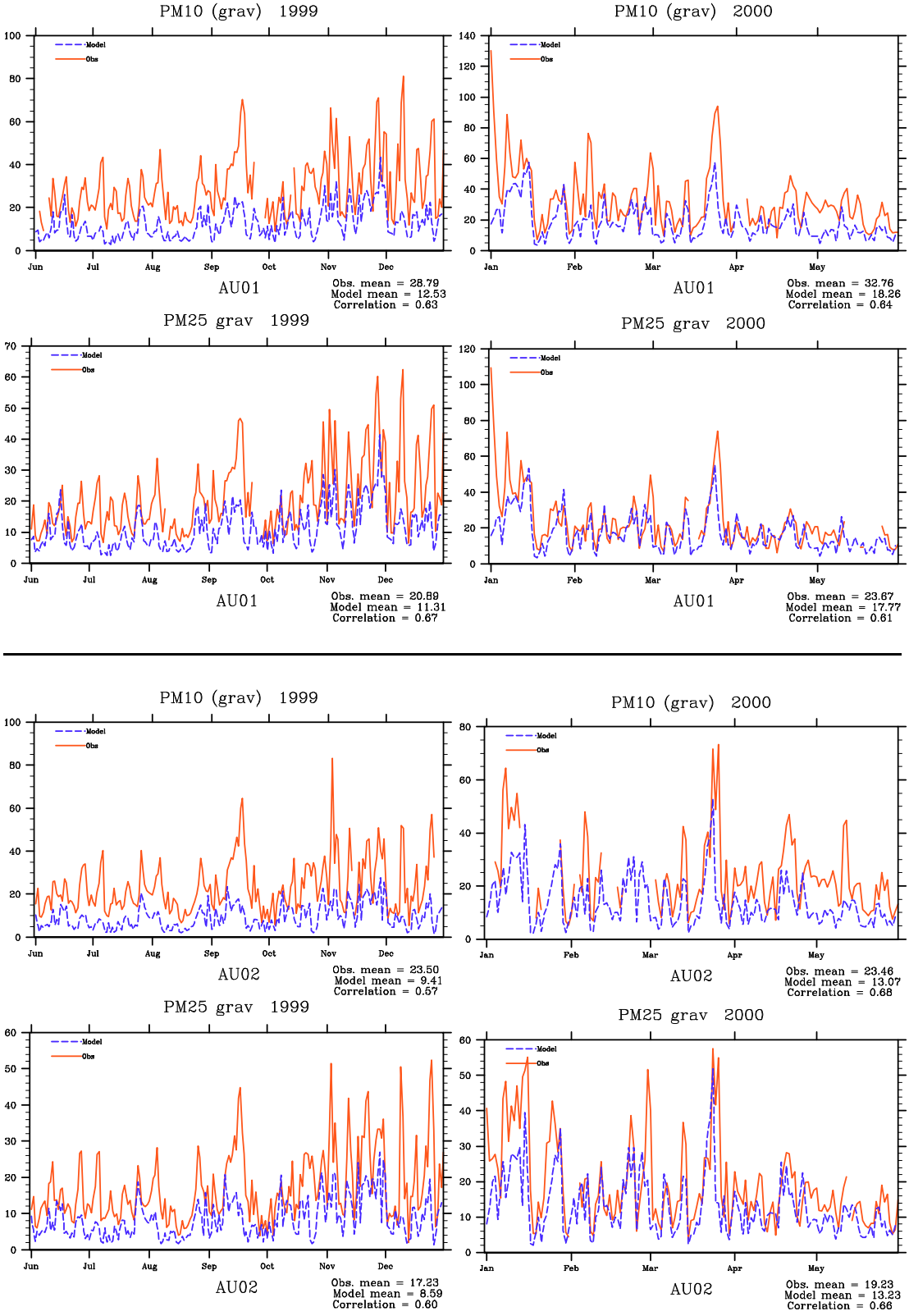

Figure 3.15: Daily time series of PM_{10} and $PM_{2.5}$ concentrations calculated with the Unified model (blue dashed curve) and measured (red solid curve) at Austrian sites.

be used as a first estimate of the PM concentrations in the urban background (see also section 3.6).

PM10 and PM2.5 hourly series with UNI-AERO. Figure 3.17 compares calculated and measured hourly time series of PM_{10} and $PM_{2.5}$ concentrations in June-December 2000 at Aspvreten (SE12), Sweden. Both PM_{10} and $PM_{2.5}$ are underestimated by the model from June to September, while in November-December calculated and measured concentrations are very similar. The correlation coefficients are 0.37 for PM_{10} and 0.4 for $PM_{2.5}$, which are not so bad for hourly PM concentrations. Also here, the model predicts too little of coarse aerosol mass as the model underestimate PM_{10} greater than $PM_{2.5}$.

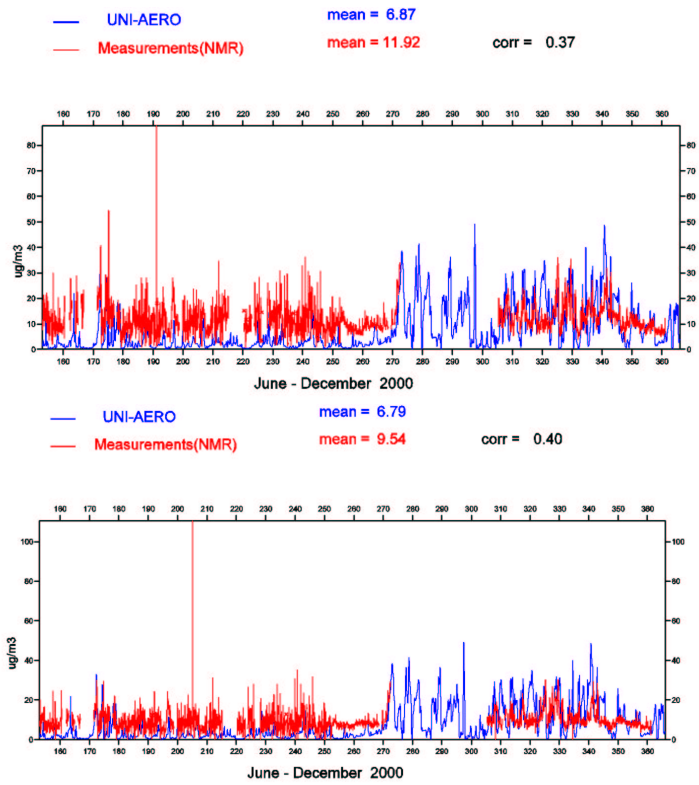

Figure 3.16: Hourly timeseries of PM_{10} and $PM_{2.5}$ concentrations: calculated with the Unified model and measured at Aspvreten, Sweden (NMR Aerosol project).

In Figure 3.17, the geographical variability of fraction of fine particles in the PM_{10} mass calculated with the aerosol model is compared with $PM_{2.5}/PM_{10}$ ratios from (Putaud et al.(2002)). Consistent with the results above, the model tends to calculate higher $PM_{2.5}/PM_{10}$ ratios than it was observed. Large fractions of coarse particles calculated at Sevettijarvi and Skreadalen are due to the contribution of sea salt aerosols. Incorporation in the model of re-suspended min-

eral dust will increase the mass of coarse PM and thus is expected to improve the $PM_{2.5}/PM_{10}$ ratios.

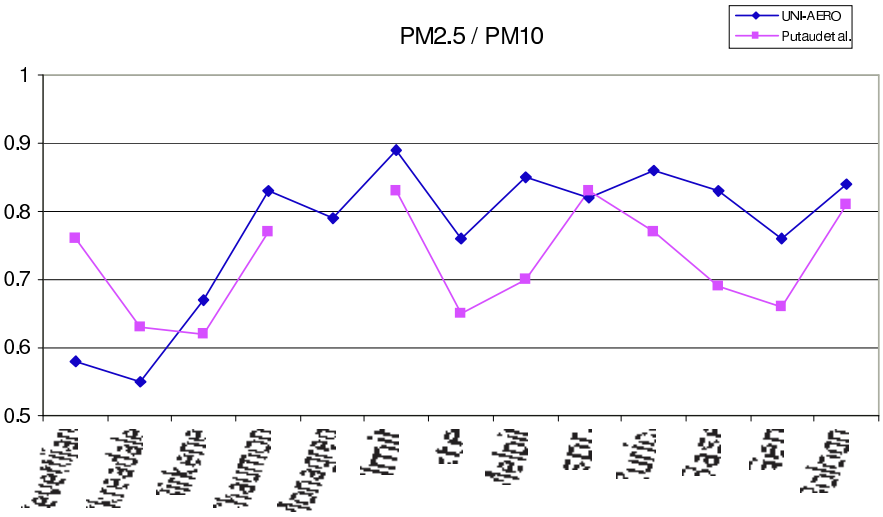

Figure 3.17: $PM_{2.5}/PM_{10}$ ratios calculated with the aerosol model vs. measurements from (Putaud et al.(2002))

3.4 Model validation of aerosol chemical composition

In this section, we present a further evaluation of the aerosol dynamics model with respect to particle chemical composition. As indicated before, appropriate measurement data for verification of the individual PM_{10} chemical components is an essential prerequisite for analyses and improvement of the model calculations of particulate matter.

3.4.1 Recent development of the aerosol model

In the following verifications, results from a new version of the aerosol model, different from the version used for comparison with the Unified model, will be presented. As it was explained in the section 3.1, one of the purposes of the aerosol model is testing new parameterisations. The most recent model development was implementation of an upgraded gas/particle equilibrium model EQSAM ((Metzger et al.(2002b)) and *pers. commun.*). This new EQSAM version was extended to include Na and Cl from sea salt spray, so that a thermodynamic equilibrium of SO_4-NO_3-NH_4-Na-Cl-H_2O system is considered. Compared to the previous version implemented presently in the Unified model, in the latest EQSAM calculations a few parameterisations, e.g. calculation of the aerosol molalities and the solute activity coefficients, were improved. In the aerosol model, inclusion of sea salt in the gas/aerosol partitioning calculations means that in addition of fine NO_3 associated with ammonium nitrate (NH_4NO_3) there is formation of coarse NO_3 on the sea salt aerosols ($NaNO_3$). Coarse NO_3 particles have much larger dry deposition velocities and are removed from the air more efficiently. Since a part of HNO_3condenses on sea salt aerosols, less of it will be available to form fine NO_3.

Very first model tests have given promising results. Concentrations of NO_3, NH_4 and HNO_3 in 2000 calculated by the research aerosol model with new EQSAM compare much better with measurements (Figure 3.18). A large improvement of the predicted NO_3 and NH_4 aerosols is undoubted. Still found overestimation of NH_4 needs to be further analysed. More testing of the new equilibrium model EQSAM and further analyses of results are still needed. Therefore, model calculations presented in the following sections should be considered preliminary.

3.4.2 Phenomenological aerosol chemical composition

Particulate matter is not a single pollutant, but a complex of many pollutants. To be capable of predicting $PM_{2.5}$ and PM_{10} adequately, the model should calculate all aerosol components accurately. In section 3.2, modelled concentrations of

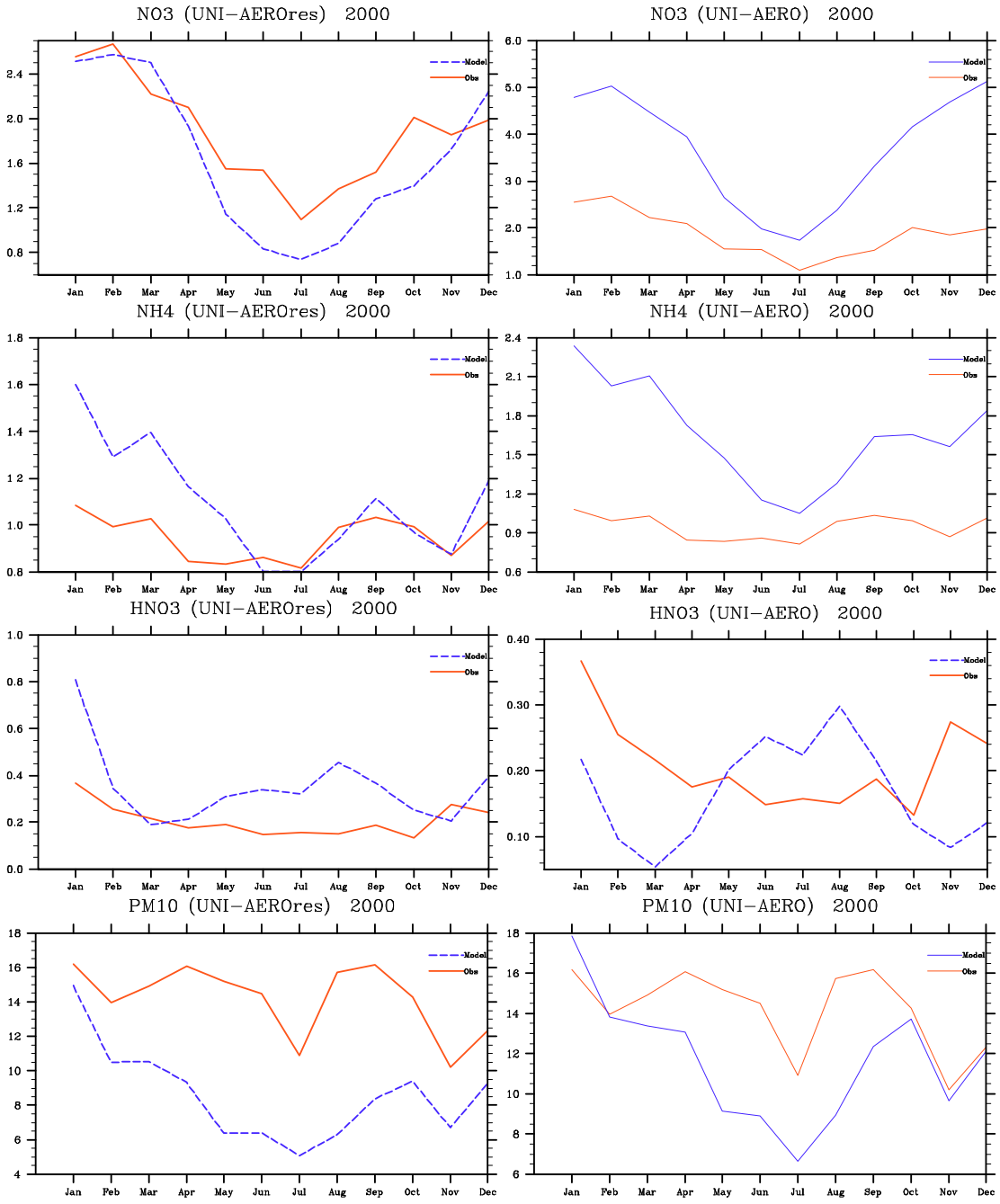

Figure 3.18: Monthly series of NO_3, NH_4, HNO_3 and PM_{10} in 2000 calculated with the aerosol model with new (UNI-AERORes) and old (UNI-AERO) equilibrium scheme EQSAM drawn against measurements at EMEP sites (20 sites for NO_3, 27 sites for NH_4 and 9 sites for NHO_3): model – dashed blue curve, measurements – solid red curve.

PM_{10}, SO_4, NO_3 and NH_4 were compared with measurements from the EMEP network. However, as concurrent measurements of the aerosol components and PM_{10} at the same stations were not available, verification of the aerosol chemical composition was not possible.

In this section, model predicted chemical composition of PM_{10} in 2000 is compared with the results from work by (Putaud et al.(2002)). In this work, aerosol measurement data collected in Europe during the last 10 years were synthesized and analysed. Measurements analysed by the authors is not continuously monitoring data, but rather measurements from various research projects. The data was collected in different years and during different time periods. The sampling technique and the methods of chemical analyses applied in different campaigns could also differ. Uncertainties in comparing the datasets arising from all those differences are discusses in (Putaud et al.(2002)). Measurement sites (Figure 3.19) were classified as natural background, rural, near-city, urban, and kerbside. Table 3.7 gives an overview over the sites selected for comparison, their location, category, and the period when measurements were taken.

Uncertainties in the determination of major inorganic species and total carbon was estimated to be within ±10 %, in the determination of OC - within ±25 %, and uncertainties in mineral dust concentrations was as large as 100 %.

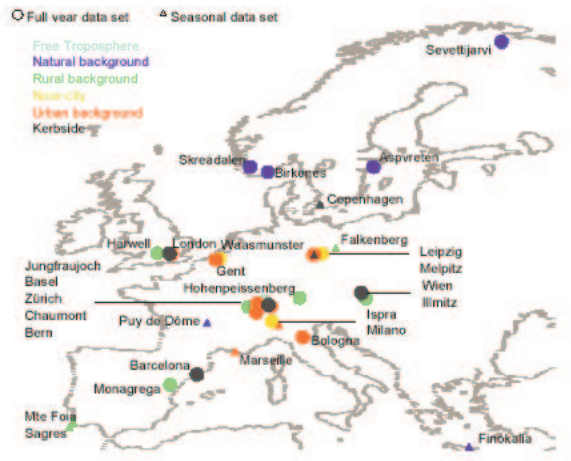

Figure 3.19: The location and classification of measurement sites from (Putaud et al.(2002)).

Figure 3.20 shows the annual average contribution of the individual aerosol components to the PM_{10} mass from (Putaud et al.(2002)) and calculated for 2000 with the EMEP aerosol dynamics model. To provide consistent comparison, we have disregarded the sites where not all components were measured. To ease the comparison the unaccounted aerosol mass was excluded from measured PM_{10}

Site	Latitude	Longitude	Altitude	Category	Period
Sevettijarvi (FI)	69.35	28.50	130	Natural	Nov 93 – Dec 96
Skreadalen (NO)	58.82	6.72	465	Natural	Feb 91 – Feb 96
Aspvretren (SE)	58.80	17.40	20	Natural	Jan 00 – Dec 00
Birkenes (NO)	58.38	8.25	190	Natural	Feb 91 – Feb 96
Melpitz 99-01 (DE)	51.53	12.93	86	Near-city	Dec 99 – Nov 01
Waasmunster (BE)	51.12	4.08	20	Near-city	Jul 94 – Nov 95
Illmitz (AT)	48.23	16.36	117	Rural	Oct 99 – Oct 00
Basel (CH)	47.53	7.58	316	Urban	Jan 98 – Mar 99
Chaumont (CH)	47.05	7.58	1136	Rural	Jan 98 – Mar 99
Ispra (IT)	45.82	8.63	209	Near-city	Feb 00 – Dec 00
Milano-Bresso (IT)	45.53	9.20	130	Urban	May 98 – Jun 98
Bologna (IT)	44.53	11.29	88	Urban	Jan 00 – Dec 00

Table 3.7: Sites description and measurement period (from (Putaud et al.(2002))).

concentrations. Kerbsides have not been considered as the model is not expected to resolve in such a small scale.

It is seen in Figure 3.20 that despite some disagreements, the models prediction of the PM_{10} chemical composition is not so far off compared with the observations. The aerosol model overestimates the contribution of secondary inorganic aerosols (SIA), especially NO_3. The overestimation by the model of NO_3 and NO_4 were discussed earlier in this chapter.

The general model underestimation of the contribution of organic matter is largely because only primary anthropogenic organic carbon has been presently included in UNI-AERO. However, it may also be due to the uncertainties associated with model assumptions on the chemical composition of primary $PM_{2.5}$ and coarse PM emission as no information on the chemical speciation of PM emissions was available to MSC-W. For each emission source, primary $PM_{2.5}$ and coarse PM emissions have been distributed between OC, EC and mineral dust. The same assumptions on chemical characteristic of emissions were applied for all countries.

If we consider mineral dust, given that only anthropogenic dust is included in the model, calculated contribution of mineral dust to PM_{10} is unexpectedly large in Zurich and Basel, and particularly Illmitz. This can also be a consequence of the uncertainties in chemical composition of PM emissions. Smaller contributions of dust at Monagrega can be explained by a significant source of re-suspended dust in Spain, which has not been accounted for in the model. The same reason, re-suspension of dust from roads, could cause too low dust contribution in Bologna calculated by the model. Summarizing, the prediction by the aerosol model of PM_{10} chemical composition is quite reasonable given all complicity and uncertainties involved in the aerosol modelling. The importance of

adequate information on the chemical speciation of PM emissions is crucial for accurate calculation of particle composition.

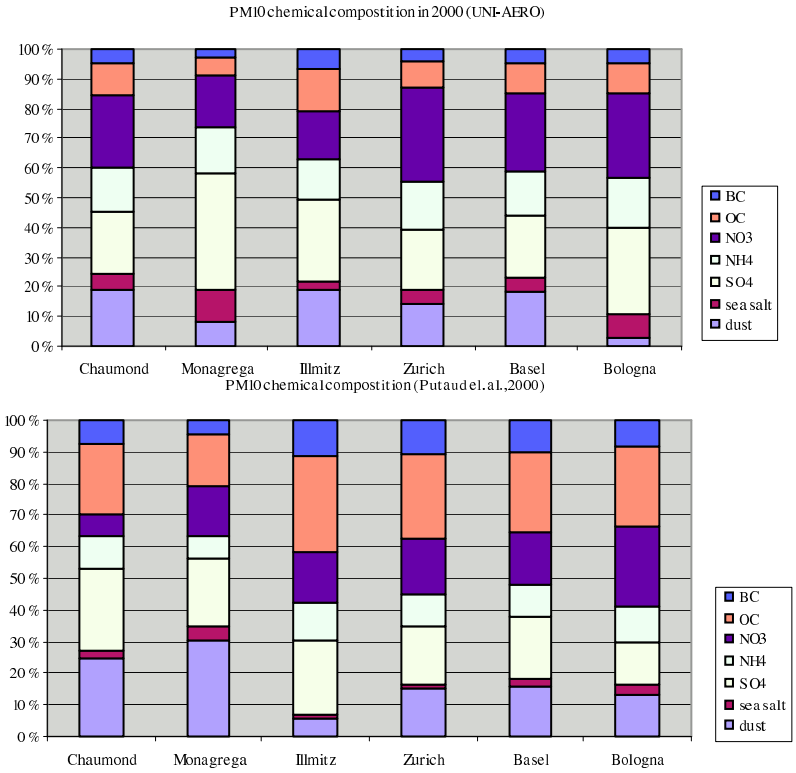

Figure 3.20: Fractional contribution of the aerosol components to PM_{10} as calculated with the aerosol model and constructed by (Putaud et al.(2002))

Figures 3.21 compare modelled and measured chemical composition of PM_{10} at natural background, rural, near-city and urban sites. Here, unaccounted aerosol mass is included in the measured PM_{10} concentrations. In addition to not analysed components, the unaccounted mass may contain residual water associated with aerosol or non-C atoms associated with organic aerosol, or could be due measurement artefacts (e.g. volatilization of NH_4NO_3 and organic aerosols). As it was described above, UNI-AERO does not account for SOA and re-suspended and wind blown mineral dust. Anthropogenic mineral dust, primary OC and EC originates in the model from primary PM emissions. The overall impression from the graphs in figure 3.21 is that with some exceptions, the chemical composition of aerosol calculated with UNI-AERO reasonably agrees with the measurements.

For background sites, the model underestimates anthropogenic aerosols, SO_4, NH_4 and BC (OC was not measured at those sites), while calculated and observed NO_3 is quite similar. The differences between predicted and measured PM_{10} concentrations seem to be due to the model underestimation of SO_4, NH_4 and also

due to the unaccounted mass in measurements. It should be noted that the measurements at those sites are from the early 1990's, while the model calculations are for 2000. During the late 1990's, SO_x emissions were reduced by ca. 40 % inevitably resulting in the lower concentrations of SO_4 and consequently of NH_4. Concentrations of anthropogenic mineral dust from the model are consistently lower than the measured mineral dust mass. Sea salt is predicted quite well for Sevettijarvi and Birkenes, but overestimated at Skredalen, indicating that more verification of modelled sea salt with measurements is needed.

At rural sites, modelled SIA (except for NO_3 in Chaumond) and sea salt concentrations agree quite well with the measurements. As expected, calculated OC and dust (except for Illmitz) is underestimated since only an anthropogenic fraction of these components is was included in the calculations. Model overestimation of mineral dust at Illmitz could be either due to the rather large uncertainties in measurements of mineral dust or due to the assumptions concerning the chemical composition of primary PM emissions (e.g. more of the emitted $PM_{2.5}$ mass should be distributed to OC and EC and less to dust). The latter emphasizes the importance of information on the chemical speciation of PM emissions for accurate modelling of aerosol chemical compositions.

At near-city sites, chemical characterisation of measured aerosol is incomplete. Lower calculated concentration of SO_4 at Wassmunster compared with the measurements is probably because the measurements were taken in 1994-1995, when the European SO_2 emissions were 20-25 % (up to 40-50 % in the major emitters Germany and the United Kingdom) larger than in 2000. Relatively much mineral dust calculated by the model compared to the measurements could be a joint effect of the uncertainties in chemical speciation of PM emissions in UNI-AERO and measurements. Calculated SIA, BC and dust is in a good agreement with the observations at Melpitz and Ispra. Rather high concentrations of organic matter measured in Ispra could be due to SOA or biogenic aerosols not included in the model.

At urban sites Zurich and Basel, the model predicts quite accurately concentrations of SIA, which is controlled largely by the long-range transport. However, the model systematically underestimates BC and especially OC. The latter is probably because only primary OC is calculated in the model, while the contribution of SOA can be considerable in cities.

Summarising, compared with aerosol measurements from (Putaud et al.(2002)) the aerosol model manages to give a realistic description of the aerosol chemical composition. The main causes for discrepancies between calculated and measured aerosol chemical composition are the following:

- measurement artefacts (evaporation of volatile NH_4NO_3 and organic aerosols, aerosol associated water)
- effect of meteorology (measurements were taken in different years while the model calculations are for the meteorological conditions of 2000)

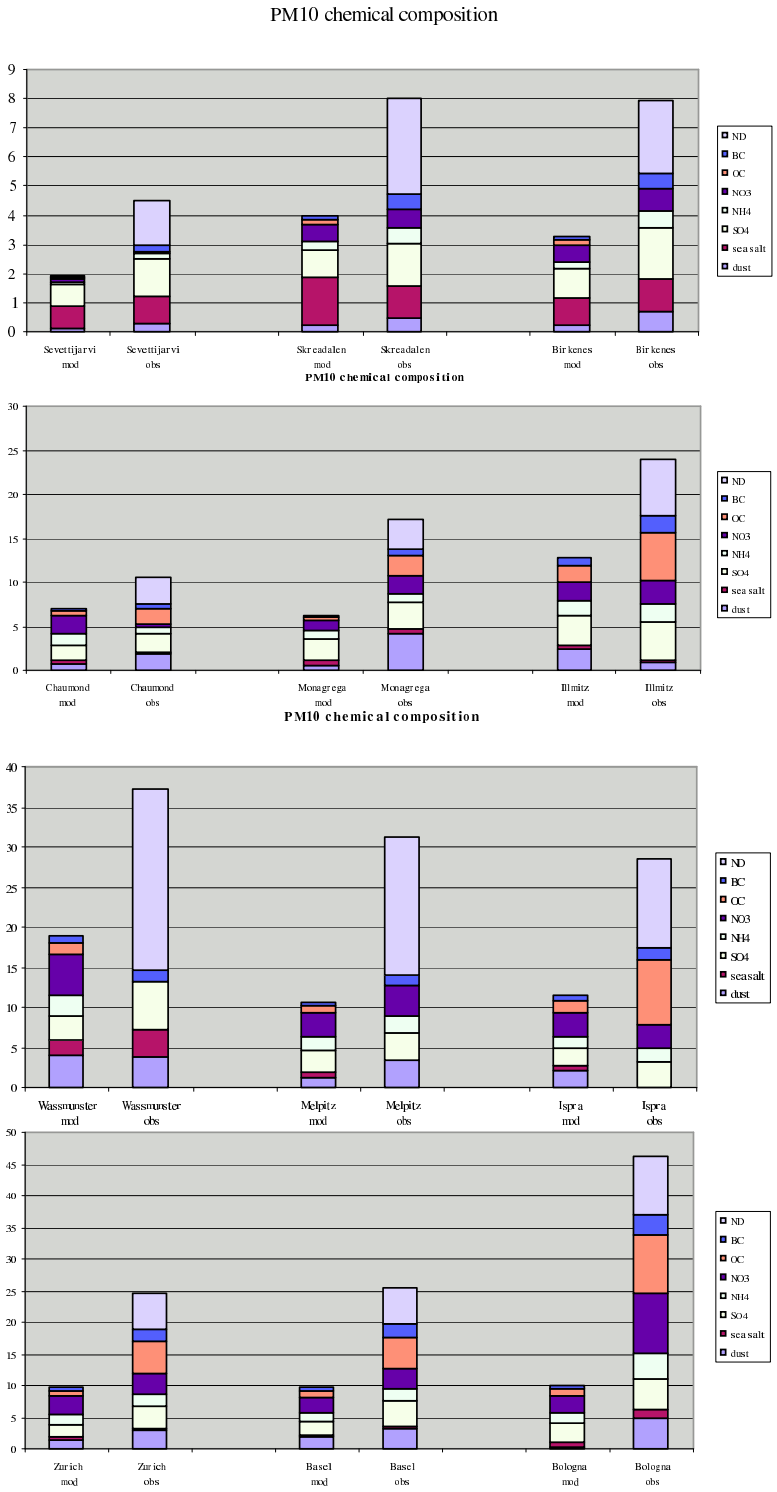

Figure 3.21: Chemical composition of PM_{10} calculated with the EMEP aerosol model and presented in (Putaud et al.(2002))

- SOA and re-suspended and wind eroded mineral dust were not included in the model calculations
- assumptions on the chemical composition of PM anthropogenic emissions in the model as no appropriate information was available to MSC-W. The information on the chemical speciation of PM emissions is crucial for adequate modelling of the aerosol chemical composition

3.5 Model validation of particle number concentration

Very limited measurement data on the particle number concentrations is available. Here, we present comparison of model calculated particle number with the measurements from the Austrian AUPHEP research project (see section 3.3) and the Aerosol project of the Nordic Council of Ministers.

3.5.1 Hourly particle numbers, background sites

Measurement data on the hourly particle number concentrations at four Nordic sites was made available to MSC-W within a framework of the Nordic Council of ministers Aerosol project. A network of Nordic stations running advanced particle measurements was established within the Swedish ASTA research program in close co-operation with University of Helsinki.

The measurements provided to MSC-W were collected during the period 1.06.2000-31.12.2000 at Hyytiälä (a boreal forest site in Central Finland), Pallas and Värriö (north of Finland), and Aspvreten (SE12, Sweden) (Tunved et al.(2003),). The data received includes hourly averaged particle number for in four size bins from 0.003 to 0.5 μm. Figures 3.22 and 3.23 give some examples on comparison between modelled and measured number concentrations of Aitken (diameters of 0.02–0.1gμm) and "small" accumulation (diameters of 0.1–0.5gμm) particles.

The comparison shows a rather poor correlation and even anti-correlation for Aitken mode between calculated and measured hourly particle numbers when the whole period is considered (Figure 3.22(a)). Correlation coefficients at those four sites are between -0.14 and -0.01 for Aitken particles and between 0.08 and 0.27 for accumulation particles. Figure 3.22(a) (run 1) shows that the model underestimates the number concentrations, in particular for Aitken particles.

Sensitivity test of calculated particle numbers to the size distribution of PM emissions. Since no information of the size distribution of primary PM emissions was available to MSC-W, preliminary rough assumptions were made in the aerosol model to distribute $PM_{2.5}$ mass emissions between the Aitken and the accumulation modes and to derive the number emissions from mass emissions. The same assumptions were applied for all countries and all types of emission sources. To study the effect of size distribution of $PM_{2.5}$ emissions on number concentrations another model run (run 2) with different emission size distribution has been performed. The differences in size distribution applied to $PM_{2.5}$ emissions in run 1 and run 2 are the following:

- $PM_{2.5}$ mass emissions are distributed between Aitken and accumulation modes as 0.15 to 0.85 in run 1 and as 0.20 to 0.80 in run 2

- diameter of emitted Aitken particles is 0.03 μm in run 1 and 0.02 μm in run 2
- diameter of emitted accumulation particles is 0.05 μm in run 1 and 0.03 μm in run 2

Thus, more particles in both accumulation and especially Aitken mode were emitted in run 2 than in run 1.

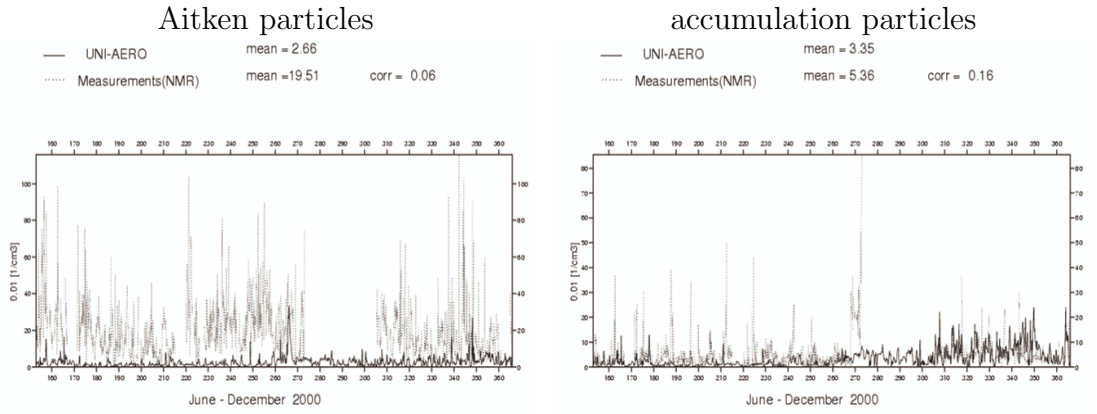

(a) Run1

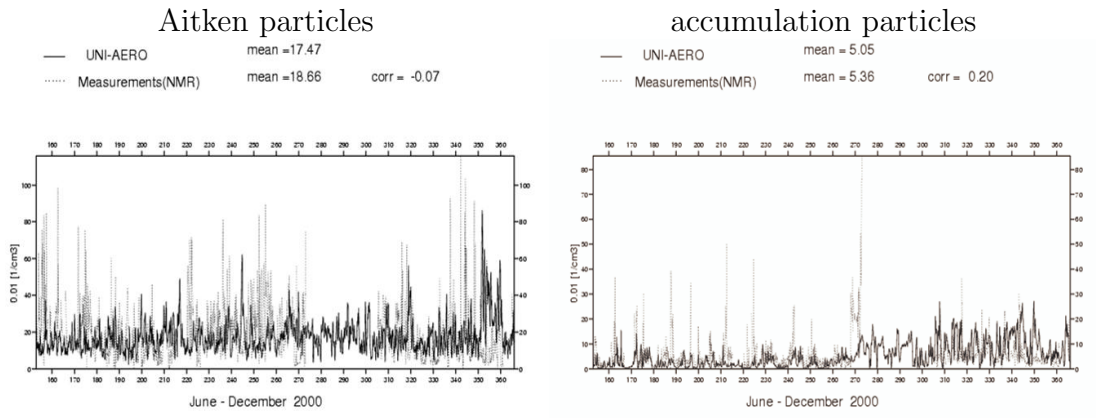

(b) Run2

Figure 3.22: Time series of hourly number concentrations of Aitken and accumulation particles at Aspvreten (SE12) in June-December 2000. Run 1 and run 2 corresponds to different size distributions of primary PM emissions (see explanation in the text); NMR Aerosol project

The effect of emissions size distribution on the calculated particle numbers can be seen when comparing results presented in Figure 3.23(a) and 3.23(b). Mod-

elled number concentrations have increased and become closer to the measurements. We can conclude that size distribution of particle emissions determines the particle number concentrations and therefore should be accurately described in the model. On the other hand, emissions size distribution was found to have insignificant effect on PMmass.

Analyses of hourly series of particle number for individual months has shown a large variation in the model performance. For instance, the monthly correlation coefficients for Aitken particles range from -0.2 to 0.5, and for accumulation particles - between -0.2 to 0.6 (see some encouraging results in Figures 3.23). In general, the aerosol model calculates a smoother series of particle number, governed by the "smooth" temporal variation of model emissions. The hourly variations in particle number are probably affected much by aerosol dynamics processes. Noticeably, the model manages to hit a number of episodes with high particle number concentrations, though it often underestimates the peak values. Those short term episodes are likely due to the effect of local particle sources, not described in the model. This is especially pronounced for Aitken particles, and we shall suggest one feasible explanation for that.

New Aitken particles either directly emitted by natural and anthropogenic sources or produced due to the growth of nucleation particles. Nucleation particles (with diameters less than 0.02 μm), formed by nucleation of H_2SO_4, coagulate very rapidly to the Aitken particles, thus increasing the Aitken mass, but not changing the Aitken number. However, newly formed nucleation particles also grow by coagulation with each other and condensation of H_2SO_4 and organic vapours. If there is sufficient amount of condensable vapours the nucleation particles can reach the Aitken size, increasing the number of Aitken particles.

We have selected several different periods Hyytiälä measurements with and without nucleation events (Kulmala and K. Hameri(2000),) from and compared calculated and measured Aitken numbers for those days. The results are visualised in Figure 3.24. In the upper panels, the observed time evolution of particle number size distributions is shown (red to brown colours mean high concentrations). The lower panels, present modelled and measured number of Aitken particles for the same periods.

In Figure 3.24(a), formation of new particles with diameters 3 nm and their further growth is clearly seen (at least 7 nucleation events within two weeks). The agreement between calculated and measured Aitken numbers in those days is poor. High peaks in the measured Aitken number well correspondent with those nucleation events, while the model does not predict those episodes. This could be either because the model fails to predict the nucleation events or because there is too little condensable vapours in the model so that the nucleation particles would not grow fast enough to the Aitken mode, but rather get scavenged by coagulation. Model ability to prediction the occurrence of nucleation needs further evaluation. As to the former reason, organic vapour, which is believed to be often the major source for new particle growth is not included in the present

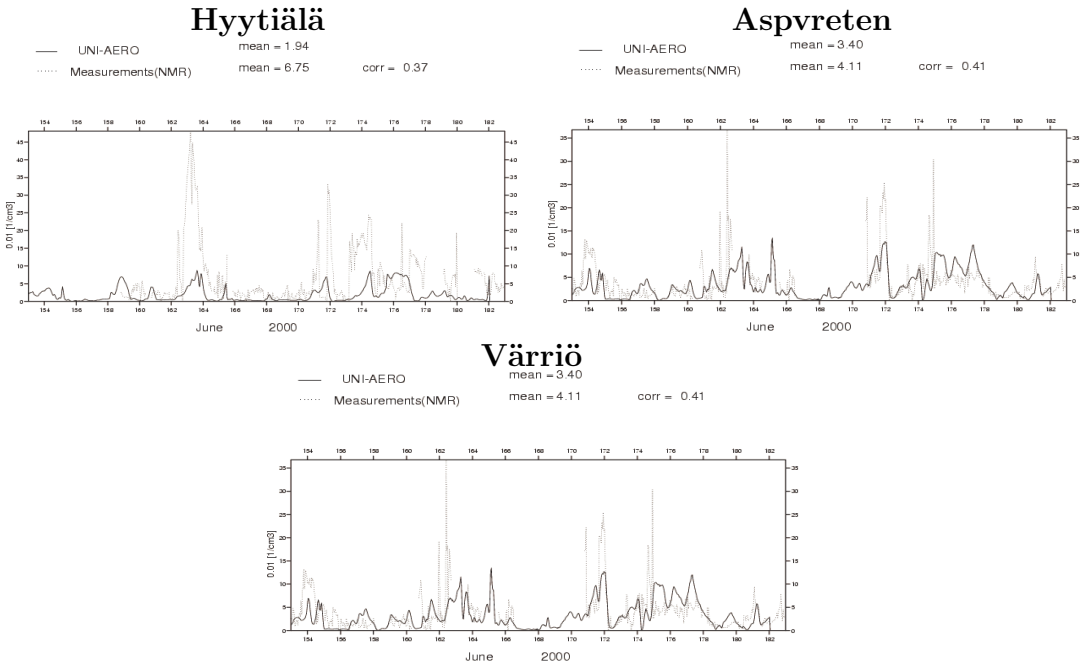

(a) Accumulation mode particles

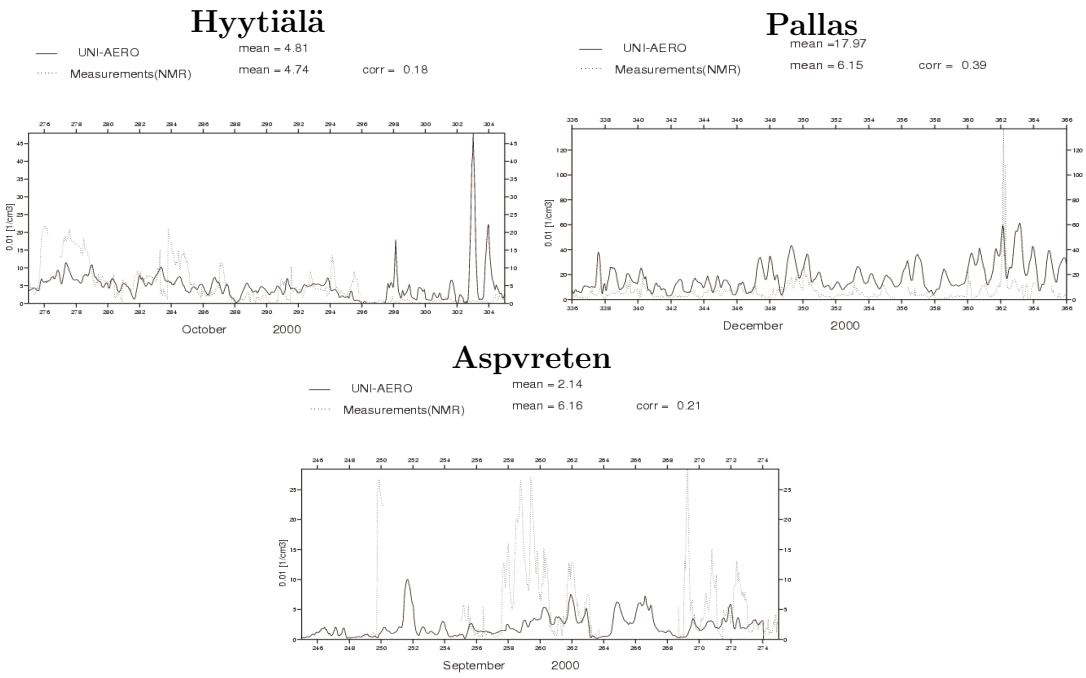

(b) Aitken mode particles

Figure 3.23: Hourly series of calculated and measured particle number concentration in different months (some encouraging examples)

version of aerosol model. Coupling the aerosol model with the photo-oxidant chemistry will provide condensable organic vapour for the particle growth. Figure 3.24(b) illustrates a period without nucleation events, when particle number is rather determined by emissions and transport. Then, agreement between the model and measurements is much better.

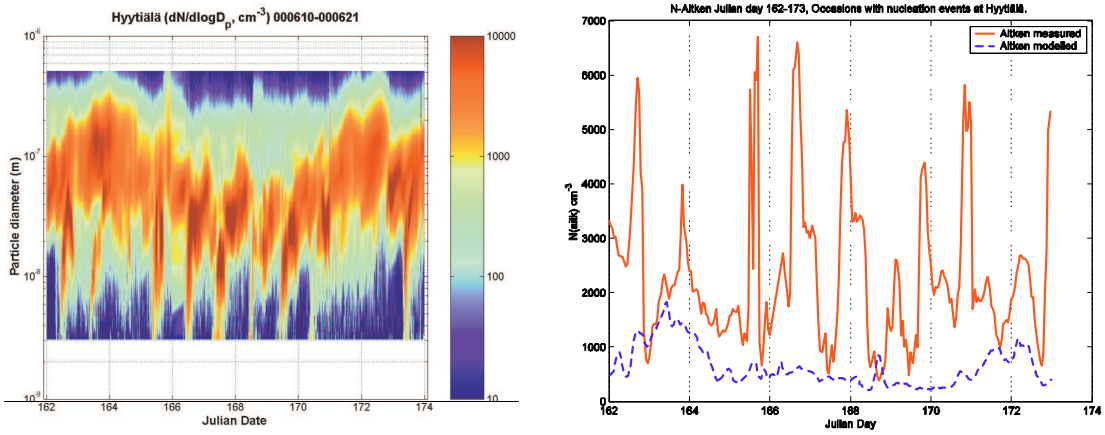

(a)

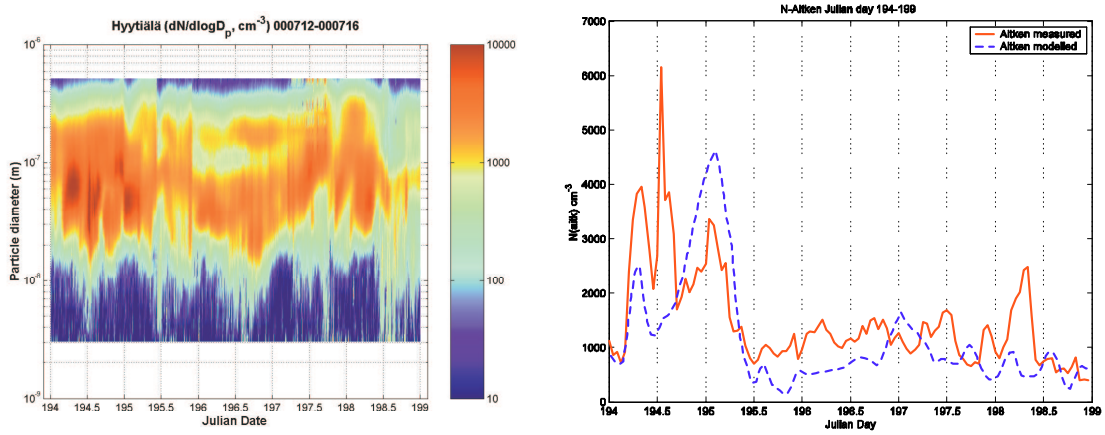

(b)

Figure 3.24: Time evolution of particle number size distributions (upper panels) (Kulmala and K. Hameri(2000),) and calculated and measured hourly series of Aitken numbers (lower panels) for periods with and without nucleation event . Hyytiälä, Finland: (a) June 10-22, 2000, (b) July 12-17, 2000

Summarising the above, the uncertainties in modelling of particle nucleation in regional models are still quite large. Therefore, the model will inevitably

under-predict local short-term episodes with high particle numbers associated with nucleation events. However after the nucleation burst, number of particles falls very rapidly back to some "average" level due to their fast coagulation. Then, the model in principle should be able to give reasonable predictions for that "average" number level, providing the use of adequate information on the size distribution and temporal variation of primary PM emissions.

3.5.2 Daily averaged particle number concentrations

Model calculated and measured daily series of particle total number concentrations at two Austrian sites are shown in Figure 3.25(a) and 3.25(b). Reminding, AU01 was located in a residential area in Wien with traffic influence and AU02 was a rural site. Although modelling of the particle number includes a great deal of uncertainty, the model results are quite encouraging. Modelled particle number concentrations correlate reasonably well with the measurements. The correlation coefficient is lowest at AU2 in 2000. Closer analysis reveals that this is due to the disagreement between the model and observations in May-April 2000. Then the model fails to reproduce the measured episodes with very high particle numbers in May 2000 and enhanced number concentrations in April 2000. If we consider only the period from 1 January to 31 March 2000 the correlation is noticeably better (Figure 3.25(c)).

For both sites, the calculated particle numbers are smaller compared to the measurements. Unlike aerosol mass, total number concentration is determined by the number of smallest particles and hence strongly effected by aerosol dynamics. The major uncertainties in modelled particle number concentrations are thought to be due to the uncertainties in size distribution of emissions of primary PM. Since no information on the size distribution of emitted particles was available, assumptions were made in the aerosol model to distribute particles between different size modes and to derive number emissions from the mass emissions.

To test the sensitivity of particle numbers to emission size distribution, the model has been run with the following changes compared with the results shown in Figure 3.25(a, b):

- $PM_{2.5}$ mass distribution between Aitken and accumulation mode was changed from 0.18/0.82 to 0.20/0.80
- emitted Aitken particles had the same size of 0.03 μm in both runs, while accumulation particles were smaller in the second than in the first run, i.e. 0.2 μm in diameter instead of 0.3 μm.

Due to these changes, the number of emitted both Aitken and accumulation particles has increased. Consequently, the particle total number concentrations have increased by ca. 10 % (Figure 3.25(d)).

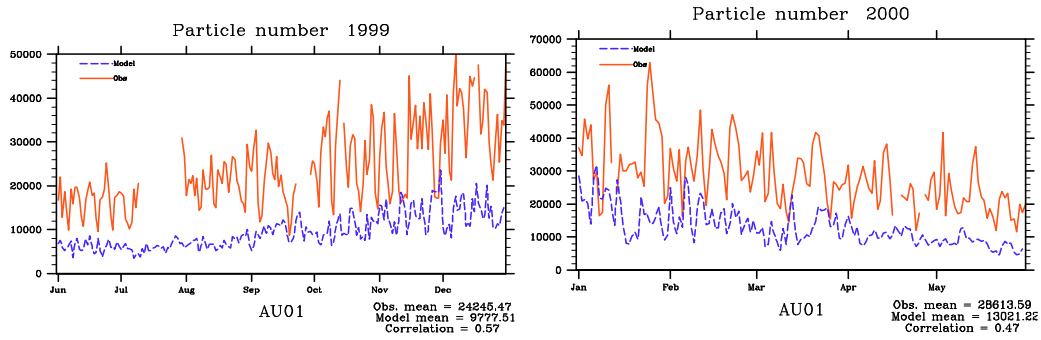

(a)

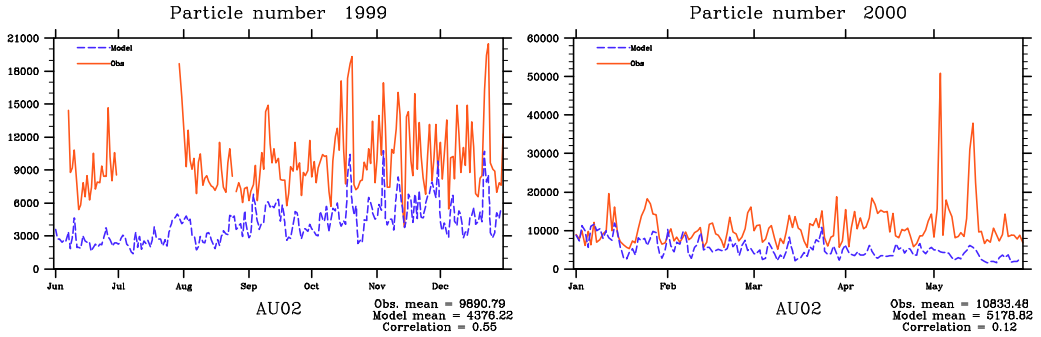

(b)

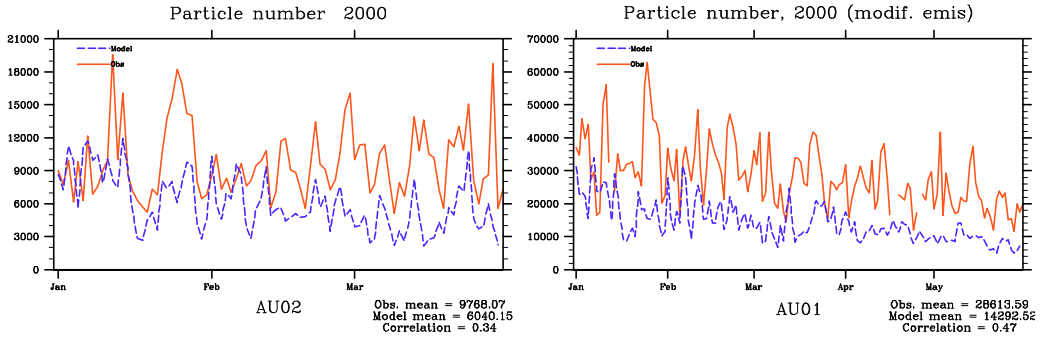

(c) (d)

Figure 3.25: Daily time series of particle total numbers: at Austrian sites (a) AU01 and (b) AU02 in June-December 1999 and January-May 2000, (c) at AU02 in January-March 2000, and (d) at AU01 with different assumption on the size distribution of PM emissions (see in the text).

3.6 Different model performance for rural and urban sites (AIRBASE)

The EMEP Unified model was designed to calculate the background concentrations. However, the health damaging effect of aerosols is largest in urban areas, where the most of population resides. Therefore it is interesting to evaluate how the model performs in urban areas. Annual mean PM_{10} concentrations calculated with the EMEP Unified model have been compared to the annual mean PM_{10} measured at rural and urban sites in 2000 available from AIRBASE. Measured annual mean PM_{10} concentrations were derived based either on daily or hourly measurements.

Figure 3.26 shows that modelled PM_{10} concentrations are correlated quite well with the PM_{10} measured at rural sites, with correlation coefficients of 0.72 for sites with daily measurements and 0.81 for sites with hourly measurements. The Unified model underestimates PM_{10} concentrations by 42-44 %. As expected, for urban sites the correlation is lower (0.33 for daily measurements and 0.14 for hourly measurements), and the model underestimation of PM_{10} is larger (54-55 %) than at rural sites.

These results confirm again that the Unified model manages quite well to predict the large-scale gradients of PM_{10}. Whereas, given the model's resolution of 50x50 km^2, its ability to accurately account for the local scale effects of urban emissions and meteorology is inherently limited. Reasons for model underestimation of PM_{10} were discussed in the previous sections. Here we can see that on the annual basis the underestimation by the Unified model of PM_{10} concentrations in urban sites is only 10 % larger than in rural sites. This result is not surprising as a considerable amount of measurements evidences the presence of a large regional element in the PM concentrations in cities. Model calculation of PM concentrations is expected to further improve when all major aerosol components are accounted for in the model. Therefore, results from the Unified model can be used in studies of the population long-term exposure to PM in background urban areas.

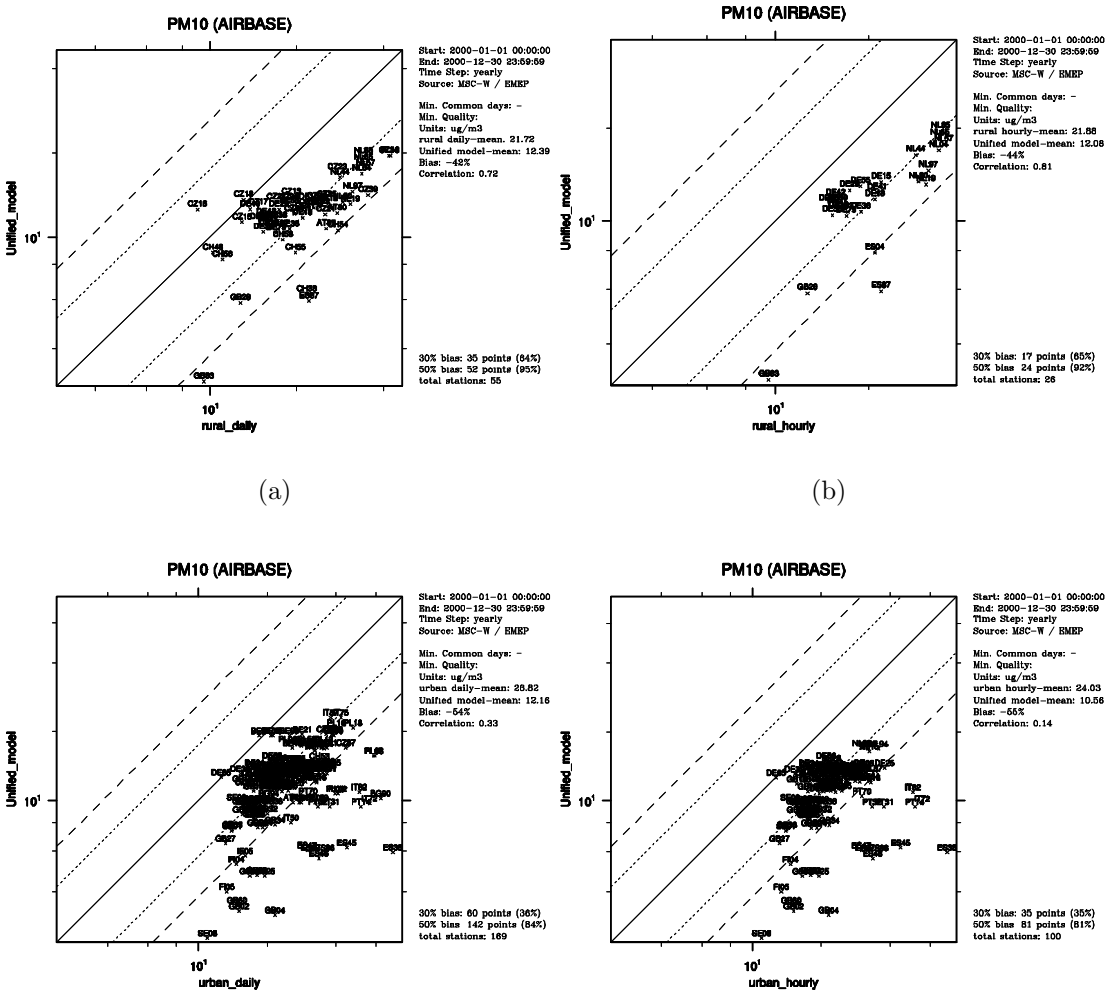

Figure 3.26: Scatter plots of annual mean PM_{10} in 2000: calculated with the Unified model vs. measured at AIRBASE sites: rural with a) daily measurements and b) hourly measurements, and urban with c) daily measurements and d) hourly measurements.

3.7 Summary and conclusions

In this chapter, calculations of particulate matter performed with two models developed at MSC-W were presented. The EMEP Eulerian Unified model deals with bulk aerosol, considers fine and coarse particles and does not account for aerosol dynamics. The Unified model was used this year for calculating the source-receptor relationships for Secondary Inorganic Aerosols (SIA), PM2.5 and PM10. The EMEP research aerosol model, UNI-AERO, accounts for aerosol dynamics and calculates size resolved aerosol mass and number concentrations. UNI-AERO is used for testing new parameterisations, aerosol process analyses and the sensitivity tests of model results to the uncertainties and assumptions involved.

The main reasons for current differences in PM calculated with the Unified and aerosol model are: 1) a more comprehensive chemical scheme in the Unified model and 2) accounting for sea salt aerosol in the aerosol model. Calculations of dry and wet removal in the models were brought to be as similar as possible. Then, aerosol dynamics appears to have a rather small effect on calculated $PM_{2.5}$ and PM_{10}concentrations.

Comparison of calculated PM distributions over Europe has shown that the aerosol model predicts higher PM_{10} and in general higher $PM_{2.5}$, except for the Mediterranean region (effect of chemistry).

- The largest differences on the resulting PM concentrations is due to chemistry and accounting for sea salt, while aerosol dynamics has much smaller effect on the aerosol mass

- The differences in $PM_{2.5}$ concentrations are largely within 10 % and in PM_{10} concentrations are largely within 20 %. Along the Atlantic coast, the differences can reach 20 and 50 % respectively due to the effect of sea salt.

Model results have been verified with available measurements from EMEP monitoring network and AIRBASE data. The spatial and temporal correlation between calculated and measured concentrations of all secondary inorganic aerosols and their sum, is relatively high (0.4-0.7 for spatial correlations in Central Europe, 0.4-0.5 for daily correlations). PM_{10} concentrations from the Unified model correlate better with the measurements in polluted areas due to better description of chemistry in the model. On the other hand, correlation between $PM_{10}$from UNI-AERO and measurements is better in the regions affected by sea salt. The models manage to capture reasonably well the observed monthly variations of PM_{10}.

The Unified model underestimates the observed PM_{10} concentrations (generally between 30-50%) because secondary organic aerosol (SOA), sea salt and re-suspended and wind eroded mineral dust was not accounted for in the present

calculations. Tests with UNI-AERO have shown that accounting for sea salt improves both the concentration level and the large scale gradients of PM_{10}. The work on implementing wind blown dust in the aerosol model is in progress. After necessary testing and verification of sea salt and mineral dust with the aerosol model these aerosols will be also included in the Unified model.

The **main conclusions** based on the analyses and evaluation of model results are:

- comparison between the Unified and aerosol model and verification of results with observations justifies the use of the EMEP Unified model for calculating PM mass

- for calculations of particle numbers, as well the size distribution of aerosol mass and number, the aerosol dynamics model will be used.

The aerosol model has also been used for testing new aerosol parameterisations prior their implementation in the Unified model. A new upgraded equilibrium model EQSAM, which also includes Na and Cl from sea salt spray has recently been implemented in UNI-AERO. First results on NO_3 and NH_4 look quite promising, but more tests are still needed.

The aerosol model has been further verified with respect to aerosol chemical composition and particle number concentrations. Comparison with measurements from (Putaud et al.(2002)) has shown that except for some discrepancies the aerosol model manages to give a realistic description of the chemical composition of aerosol at sites ranging from natural background to urban. The main reasons for discrepancies between predicted and observed aerosol chemical composition are 1) not accounting for SOA and re-suspended mineral dust in the model, 2) assumptions made on the chemical speciation of primary PM emissions, 3) measurement artefacts, and finally 4) that the measurements were collected in different years between 1991 and 2000, while model calculations were made for 2000.

Particle hourly number concentrations have been compared with measurements at four Nordic sites. Sensitivity tests have shown the importance of adequate description of the size distribution of primary PM emissions for reasonable prediction of particle numbers. Sound parameterisation of the aerosol dynamics is an essential prerequisite for the model to capture the observed variations in particle number concentrations. Good correlations have been found for daily total number concentrated with UNI-AERO and measured at two Austrian sites.

Summarising, the results of comparison of aerosol chemical composition and particle numbers predicted by the EMEP aerosol model with observations are rather encouraging. However, further verification of parameterisations and process analyses are needed to assure improvement in the model performance with respect to particle number concentrations.

Closing the chapter on PM modelling in EMEP, we would like to emphasize that there is an urgent need for appropriate information on the chemical composition and the size distribution of primary PM emissions. For model validation, more PM measurements covering different geographical regions are required. Since many sources contribute to the PM mass, measurements of $PM_{2.5}$ and PM_{10} should as far as possible be supplemented with analyses of the aerosol chemical composition. This is an essential request in order to facilitate further model development, verification and improvement.

Bibliography

[Aas et al.(1999)] Aas, W. , Hjellbrekke, A-G. , Semb, A. , and Schaug, S. , 1999, Data quality 1997, quality assurance and field comparisons., EMEP CCC Report 6/1999, Norwegian Institute for Air Research, Kjeller.

[Aas et al.(2000)] Aas, W. , Hjellbrekke, A.-G. , Semb, A. , and Schaug, J. , 2000, Data quality 1998, quality assurance, and field comaprisons, EMEP/CCC Report 6/00, The Norwegian Institute for Air Research, Kjeller, Norway.

[Aas et al.(2002a)] Aas, W. , Hjellbrekke, A-G. , Manø, S. , S, Schaug. , Solberg, S. , and Uggerud, H.Th. , 2002a, Data quality 2000, quality assurance and field comparisons, Norwegian Institute for Air Research, Kjeller. EMEP/CCC-Report 3/2002.

[Aas et al.(2002b)] Aas, W. , Hjellbrekke, A-G. , Manö, S. , Schaug, S. , Solberg, S. , and Uggerud, H. Th. , 2002b, Data quality 2000, quality assurance and field comparisons., EMEP CCC Report 3/2002, Norwegian Institute for Air Research, Kjeller.

[Aas et al.(2003)] Aas, W. , Hjellbrekke, A-G. , Schaug, S. , and Uggerud, H. Th. , 2003, Data quality 2001, quality assurance and field comparisons., EMEP CCC Report 6/2003, Norwegian Institute for Air Research, Kjeller.

[Andersen et al.(1999)] Andersen, H.V. , Hovmand, M. F. , Hummelshój, P. , and Jensen, N.O. , 1999, Measurements of ammonia concentrations, fluxes

and dry deposition velocities to a spruce forest 1991-1995, *Atmospheric Environment*, 33, 1367–1383.

[Cape and Leith(2002)] Cape, J. N. and Leith, I. D. , 2002, The contribution of dry deposited ammonia and sulphur dioxide to the composition of precipitation from open gauges., *Atmospheric Environment*, 36, 5983–5992.

[EMEP(1996)] EMEP, 1996, EMEP Manual for sampling and chemical analysis, Norwegian Institute for Air Research, Kjeller. EMEP/CCC-Report 1995, last revision in 2001. Online at http://www.nilu.no/projects/ccc/manual/index.html.

[Erisman et al.(2001)] Erisman, J. W. , Hensen, A. , Fowler, D. , Flechard, C. R. , Grüner, A. , nd J. H. Duyzer, G. Spindler , Weststrate, H. , Römer, F. , Vonk, A. W. , and Jaarsveld, H. V. , 2001, Dry deposition monitoring in europe, *Water, Air and Soil Pollution, Focus*, 1, 17–27.

[Fagerli(2002)] Fagerli, H. , 2002, Sensitivity Tests, In EMEP MSC-W Report 1&2/2002, Transboundary Acidification, Eutrophication and Ground Level Ozone in Europe. EMEP Summary Report 2002. Norwegian Meteorological Institute, Oslo, Norway.

[Fähnrich et al.(1993)] Fähnrich, B. , Hanssen, JE. , and Nodop, K. , 1993, Comparison of measuring methods for Nitrogen Dioxide in Ambient Air, Norwegian Institute for Air Research, Kjeller. EMEP/CCC-Report 3/93.

[Fowler et al.(2001)] Fowler, D. , Sutton, M. A. , Flechard, C. , Cape, J. N. , Storeton-West, R. , Coyle, M. , and Smith, R. I. , 2001, The control of SO_2 dry deposition on to natural surfeces by NH_3 and its effects on regional deposition, *Water, Air and Soil Pollution*, 1, 39–48.

[Fuhrer and Achermann(1994)] Fuhrer, J. and Achermann, B. , editors, *UN-ECE Workshop on critical levels for ozone, 1-4*

November 1993, Bern. Swiss Federal Research Station for Agricultural Chemistry, 1994.

[Hass et al.(2003)] Hass, H. , van Loon, M. , Kessler, C. , Stern, Rainer , Matthijsen, J. , Sauter, F. , Zlatev, Z. , Lagner, J. , Foltescu, V. , and Schaap, M. , 2003, Aerosol Modelling: Results and Intercomparison from European Regional-scale Modeling Systems, A contribution to the EUROTRAC-2 subproject GLOREAM.

[Jonson et al.(1998)] Jonson, J. E. , Tarrasón, L , Sundet, J.K. , Berntsen, T. , and Unger, S. , 1998, The Eulerian 3-D oxidant model: Status and evaluation for summer 1996 results and case-studies, In *Transboundary photo-oxidant air pollution in Europe.* EMEP/MSC-W Status Report 2/98, The Norwegian Meteorological Institute, Oslo, Norway.

[Jonson et al.(2002)] Jonson, J.E. , Fagerli, H. , Simpson, D. , Anderson-Sköld, Y. , and Ukkelberg, Å , 2002, Model Evaluation, In EMEP MSC-W Report 1&2/2003, Transboundary Acidification, Eutrophication and Ground Level Ozone in Europe. EMEP Summary Report 2002. Norwegian Meteorological Institute, Oslo, Norway.

[Kulmala and K. Hameri(2000)] Kulmala, M. and K. Hameri, eds. , 2000, Biogenic Aerosol Formation in the Boreal Forest (BIOFOR), Report series in Aerosol Science.

[Metzger et al.(2002a)] Metzger, S. M. , Dentener, F. J. , Jeuken, A. , , Krol, M. , and Lelieveld, J. , 2002a, Gas/aerosol partitioning 2. global modeling results, *J. Geophys. Res.*, 107, No. D16, ACH 17.

[Metzger et al.(2002b)] Metzger, S. M. , Dentener, F. J. , Lelieveld, J. , and Pandis, S. N. , 2002b, Gas/aerosol partitioning 1. a computionally efficient model., *J. Geophys. Res.*, 107, No. D16, ACH 17.

[Nemitz et al.(2000)] Nemitz, E. , Sutton, M. A. , Gut, A. , José, R. S. , Husted, S. , and Schjoerring, J. , 2000, Sources and sinks of ammonia within

an oilseed rape canopy, *Agrid. Forest Meteor.*, 105, 385–404.

[Pirjola and Kulmala(2000)] Pirjola, L. and Kulmala, M. , 2000, Aerosol dynamical model MULTIMONO, *Boreal Environ. Res.*, 5, 361–374.

[Pirjola et al.(2003)] Pirjola, L. , Tsyro, S. , Tarrasón, L. , and Kulmala, M. , 2003, A monodisperse aerosol dynamics module, a promising candidate for use in long-range transport models: Box model tests, *J. Geophys. Res.*, 108, No. D9, doi:10.1029/2002JD002867, 2003.

[Putaud et al.(2002)] Putaud, J.-P. , Van Dingenen, R. , Baltensperger, U. andBrüggemann, E. , Charron, A. , Faccini, M.-C. , Decari, S. , Fuzzi, S. Gehrig, R. , Hansson, H.-C. , Harrison, R.M. , Jones, A.M. , Laj, P. , Lorbeer, G. , Maenhaut, W. , Mihalopoulos, N. , Müller, K. , Palmgren, F.K. , Querol, X. , Rodriguez, S. , Schneider, J. , Spindler, G. , ten Brink, H. , Tunved, P. , Tørseth, K. , Weindartner, E. , Weindensohler, A. Wählin, P. , and Raes, F. , 2002, European Aerosol Phenomenology. Physical and chemical characteristics of particulate matter at kerbside, urban, rural, and background sites in Europe., Ispra, European commission, Joint Research Centre (EUR 20114 EN); http://ies.jrc.cec.int/Download/cc.

[Simpson and Jonson(1998)] Simpson, D. and Jonson, J.E. , 1998, Comparison of Lagrangian and Eulerian models for the summer of 1996, In EMEP MSC-W Report 2/98, Part III Transboundary photooxidant air pollution in Europe. Calculations of tropospheric ozone and comparison with observations. Norwegian Meteorological Institute, Oslo, Norway.

[Simpson et al.(1998)] Simpson, D. , Altenstedt, J. , and Hjellbrekke, A.G. , 1998, The Lagrangian oxidant model: status and multi-annual evaluation, In EMEP

MSC-W Report 2/98, Part I Transboundary photooxidant air pollution in Europe. Calculations of tropospheric ozone and comparison with observations. Norwegian Meteorological Institute, Oslo, Norway.

[Simpson et al.(2003)] Simpson, D. , Fagerli, H. , Jonson, J.E. , Tsyro, S. , and Wind, P. , 2003, The EMEP Unified Eulerian Model. Model Description, EMEP MSC-W Report 1/2003, Norwegian Meteorological Institute, Oslo, Norway.

[Simpson(1992)] Simpson, D. , 1992, Long period modelling of photochemical oxidants in Europe. Calculations for July 1985, *Atmospheric Environment*, 26A, No. 9, 1609–1634.

[Simpson(1993)] Simpson, D. , 1993, Photochemical model calculations over Europe for two extended summer periods: 1985 and 1989. Model results and comparisons with observations, *Atmospheric Environment*, 27A, No. 6, 921–943.

[Smith et al.(2003)] Smith, R. , Fowler, D. , and Sutton, M. A. , 2003, The external surface resistance in the EMEP Eulerian model, unpublished.

[Sutton et al.(1995)] Sutton, M. A. , Burkhart, J. K. , Guerin, D. , and Fowler, D. , 1995, Measurements and Modelling of Ammonia Exchange over Arable Croplands, In, Heij, G.J, Erisman, J.W. (Eds.), Acid Rain Research: Do We Have Enough Answers? Elsevier, Amsterdam.

[Tunved et al.(2003)] Tunved, P. , Hansson, H.-C. , Kulmala, M. , Aalto, P. , Viisanen, Y. , Karlsson, H. , Krinsson, A. , Swetlicki, E. , Dal Maso, M. , Ström, j. , and Komppula, M. , 2003, A one-year study of the nordic aerosol., *J. Atmos. Chem. Phys. Discuss.*, 3, 2783–2833.

[Tuovinen(2000)] Tuovinen, J.-P. , 2000, Assessing vegetation exposure to ozone: properties of the AOT40 index and modifications by deposition modelling, *Environmental Pollution*, 109, 361–372.

[V. Vestreng and H. Klein(2002)] V. Vestreng and H. Klein, 2002, Emission data reported to UNECE/EMEP: Quality assurance and trend analysis & Presentation of WebDab, Technical Report Note 1/2002, Meteorological Synthesizing Centre - West, Norwegian Meteorological Institute, Oslo, Norway.